TRIMMING FAT UPON INFECTION: PROTEOLYTIC DEMYRISTOYLATION AS A NOVEL BACTERIAL PATHOGENIC STRATEGY

APPROVED BY SUPERVISORY COMMITTEE

Neal Alto, Ph.D.

Yuh Min Chook, Ph.D.

Kim Orth, Ph.D.

Joachim Seemann, Ph.D.

DEDICATION

Significant achievements such as a Ph.D. degree are gained through the years of hard work that requires commitment as well as support of the people that surround you. I would like to thank everyone who guided and helped me on my way to this day. Yegor Yegorov, MD/Ph.D., and Valeriy Mamaev, Ph.D, were my first mentors and contributed a lot to my present and future achievements. I am thankful to Hava Vishnyakova, Ph.D., who readily spent her time on my first scientific training. I am grateful to Felix Yarovinsky, MD, for the productive time I spent in his laboratory and the experience I gained.

My achievements during graduate school would not become possible without support and inspiration from my mentor Neal Alto, Ph.D. These were four wonderful years of experience and fun in his laboratory. I want to thank Neal and all the people that I had a pleasure to work with.

I acknowledge my dissertation committee members, Joachim Seemann, Ph.D., Kim Orth, Ph.D, and Yuh Min Chook, Ph.D., for the valuable inputs and critique they provided.

Family support is critical if you want to fly high. For their neverending support, I am grateful to my wife Anna Kuchina, Ph.D., my parents Sergey and Elena Burnaevskiy, and my brother Igor Burnaevskiy. Finally, I thank my good friend P.P. Corella for all the fun and joy.

TRIMMING FAT UPON INFECTION: PROTEOLYTIC DEMYRISTOYLATION AS A NOVEL BACTERIAL PATHOGENIC STRATEGY

by

NIKOLAY BURNAEVSKIY

DISSERTATION / THESIS

Presented to the Faculty of the Graduate School of Biomedical Sciences

The University of Texas Southwestern Medical Center at Dallas

In Partial Fulfillment of the Requirements

For the Degree of

DOCTOR OF PHILOSOPHY

The University of Texas Southwestern Medical Center at Dallas

Dallas, Texas

December, 2014

Copyright

by

Nikolay Burnaevskiy, 2014

All Rights Reserved

TRIMMING FAT UPON INFECTION: PROTEOLYTIC DEMYRISTOYLATION AS A NOVEL BACTERIAL PATHOGENIC STRATEGY

Publication No. _____

Nikolay Burnaevskiy, Ph.D.

The University of Texas Southwestern Medical Center at Dallas, 2014

Supervising Professor: Neal Alto, Ph.D.

Host-pathogen interaction is a complex process that involves an array of molecular tools on both sides of the conflict. In the light of growing antibiotics resistance, understanding of virulence factors utilized by pathogenic bacteria is crucial for developing better treatment for infectious diseases. *Shigella spp* are food-borne bacterial pathogens and are one of the leading causes of bacterial dysentery worldwide. Similarly to other gram-negative pathogens, *Shigella* injects effector proteins into an infected cell to control its responses. Dedicated type III secretion system delivers more than twenty effectors which highjack normal cell signaling by modulating activity of host proteins. By interfering with immune signaling, cytoskeleton, and other pathways, effector proteins promote survival of the bacterial pathogen. Inability to secrete effectors severely attenuates *Shigella spp*, pointing to the crucial role of these proteins in pathogenesis. Therefore, gaining an insight into the

mechanism of action of secreted effectors may hold a key to better understanding and treatment of infectious diseases. Here I characterized the *Shigella flexneri* secreted virulence factor IpaJ. I found that IpaJ is a cysteine protease with novel specificity. IpaJ cleaves a myristoylated amino-terminal glycine of host proteins and therefore irreversibly delipidates them. Although IpaJ can target multiple host proteins, it strongly favors members of ADP-ribosylation factors family (ARF) and related ARF-like (ARL) proteins. By inactivating ARF and ARL proteins, IpaJ disrupts the Golgi structure and prevents secretion through general secretory pathway. I also found that by blocking protein export from the endoplasmic reticulum, IpaJ suppresses the activation of immune signaling pathways.

In summary, I characterized a novel virulence factor of *Shigella spp*, IpaJ. I have shown that IpaJ promotes bacterial pathogenesis and therefore may be of potential interest for therapeutic interventions. The biochemical analysis of the enzyme provides the first look at the mechanism of substrate recognition and highlights the potential use of IpaJ as a research tool to study protein N-myristoylation and the mechanisms of membrane trafficking.

TABLE OF CONTENTS

CHAPTER ONE 1

BACTERIAL PATHOGENS MANIPULATE INFECTED HOST CELLS 1

THE GOLGI FUNCTION IN HEALTH AND DISEASE 3

THE GOLGI REGULATION BY BACTERIAL PATHOGENS 5

CHAPTER TWO 10

INTRODUCTION 10

RESULTS 10

Shigella effector proteins IpaJ and VirA disrupt the Golgi 10

Identification of the catalytic triad and potential targets of IpaJ 11

IpaJ removes N-myristoyl glycine of ARF1 13

ARF1 is a physiological substrate of IpaJ 16

CONCLUSIONS 21

MATERIALS AND METHODS 49

Plasmids and cloning 49

Bacterial infection of cultured cells 50

Gene disruption in *Shigella* 52

IpaJ bioinformatics 53

Recombinant protein expression and purification 53

Cell transfections, microinjections and fluorescence microscopy 54

Galactose-induced yeast growth inhibition and Yeast multicopy suppressor screen 55

Top-Down Mass Spectrometry 56

Labeling N-myristoylated proteins by Click Chemistry and in vitro cleavage reaction 57

CHAPTER THREE 59

INTRODUCTION 59

RESULTS 61

IpaJ cleaves diverse proteins *in vitro* 61

IpaJ is highly specific in the context of infection. 63

Recognition of myristoyl-glycine allows broad specificity of IpaJ *in vitro* 64

IpaJ is an ARF/ARL substrate of bacterial origin. 68

ARF6 is not a substrate of IpaJ. 71

CONCLUSIONS 72

MATERIALS AND METHODS 93

Plasmids and cloning 93

In vitro cleavage of proteins and in-gel fluorescence 93

Bacterial infection of cultured cells 94

Proteomic Identification of Alk-12 Labeled Proteins 94

Synthesis of the acylated peptides 96

Peptide cleavage 97

Recombinant protein purification and *in vitro* binding 97

In vitro cleavage of recombinant ARF1 98

CHAPTER FOUR 100

INTRODUCTION 100

RESULTS 100

IpaJ and VirA promote *Shigella* virulence and suppresse cytokine secretion 100

Differential effect of IpaJ and VirA on STING signaling 102

CONCLUSIONS 105

MATERIALS AND METHODS 118

Shigella infection studies in mice: 118

hGH trafficking assay 118

Bacterial infection of cultured cells 119

RNA isolation and qRT-PCR analysis 119

Fluorescent microscopy 119

CHAPTER FIVE 121

CONCLUSIONS AND FUTURE DIRECTIONS 121

BIBLIOGRAPHY 309

PRIOR PUBLICATIONS

Burnaevskiy N, Fox TG, Plymire DA, Ertelt JM, Weigele BA**,** Selyunin AS, Way SS, Patrie SM, Alto NM. Proteolytic elimination of N-myristoyl modifications by the Shigella virulence factor IpaJ. Nature. 2013, 496(7443): 106-109.

Benson A, Murray S, Divakar P, **Burnaevskiy N**, Pifer R, Forman J, Yarovinsky F. Microbial infection-induced expansion of effector T cells overcomes the suppressive effects of regulatory T cells via an IL-2 deprivation mechanism. J Immunol. 2012 Jan 15;188(2):800-10.

Egorov EE, Moldaver MV, Vishniakova KhS, Terekhov SM, Dashinimaev EB, Cheglakov IB, Toropygin IIu, Iarygin KN, Chumakov PM, Korochkin LI, Antonova GA, Rybalkina EIu, Saburina IN, **Burnaevskiĭ NS**, Zelenin AV. Enhanced control of proliferation in telomerized cells. Ontogenez. 2007 Mar-Apr;38(2):105-19

LIST OF FIGURES

FIGURE 1. *SHIGELLA* DISRUPTS THE GOLGI STRUCTURE AND FUNCTION 22

FIGURE 2. *SHIGELLA* EFFECTORS IPAJ AND VIRA DISRUPT THE GOLGI MORPHOLOGY 23

FIGURE 3. IDENTIFICATION OF IPAJ AND VIRA AS EFFECTORS THAT INHIBIT THE GOLGI STRUCTURE AND FUNCTION 25

FIGURE 4. *SHIGELLA ΔIPAJ/ΔVIRA* EXHIBITS NORMAL BEHAVIOR INSIDE THE INFECTED CELLS. 27

FIGURE 5. THE IPAJ FAMILY 28

FIGURE 6. IPAJ BELONGS TO THE C39-FAMILY OF CYSTEINE PROTEASES AND TARGETS ARF-FAMILY GTPASES 29

FIGURE 7. COMPLEMENTATION OF THE *SHIGELLA ΔIPAJ/VIRA* MUTANT STRAIN 30

FIGURE 8. ARF1 AND ARF2 ARE POTENTIAL SUBSTRATES OF IPAJ..... 31

FIGURE 9. IPAJ DOES NOT REGULATE THE GUANINE-NUCLEOTIDE EXCHANGE CYCLE, SUBSTRATE BINDING OR GTPASE ACTIVITY OF ARF1 32

FIGURE 10. IPAJ CLEAVES THE N-MYRISTOYLATED GLYCINE OF LIPIDATED SUBSTRATES 34

FIGURE 11. IDENTIFICATION OF THE GLYCINE-2 CLEAVAGE SITE ON ARF1 BY TOP-DOWN MASS SPECTROMETRY 35

FIGURE 12. THE ARF1 “MYRISTOYL SWITCH” 38

FIGURE 13. METABOLIC LABELING CONFIRMS DEMYRISTOYLATION OF HOST PROTEINS BY IPAJ 39

FIGURE 14. IPAJ CLEAVES DIVERSE N-MYRISTOYLATED PROTEINS 41

FIGURE 15. IPAJ RELEASES ARF1-GTP FROM THE GOLGI MEMBRANES 42

FIGURE 16. SUBCELLULAR LOCALIZATION OF N-MYRISTOYLATED GRASP65 PROTEINS DURING *SHIGELLA* INFECTION……43

FIGURE 17. IPAJ C64A LOCALIZES ON THE GOLGI IN ARF-DEPENDENT MANNER 45

FIGURE 18. THE CELLULAR ACTION OF IPAJ PHENOCOPIES BREFELDIN A 47

FIGURE 19. IPAJ CLEAVES THE MAJORITY OF MYRISTOYLATED PROTEINS IN VITRO 74

FIGURE 20. IPAJ HAS LIMITED NUMBER OF SUBSTRATES DURING INFECTION 76

FIGURE 21. FREE MYRISTIC ACID DOES NOT INHIBIT IPAJ CLEAVAGE OF N-MYRISTOYLATED ARF1 78

FIGURE 22. IPAJ DOES NOT CLEAVE NON-MYRISTOYLATED ARF1 80

FIGURE 23. CLEAVAGE OF THE ACYLATED PEPTIDES 83

FIGURE 24. N-TERMINI OF THE IPAJ SUBSTRATES 85

FIGURE 25. IPAJ BEHAVES AS AN ARF SUBSTRATE 86

FIGURE 26. IPAJ PREFERENTIALLY CLEAVES ARF1 IN THE ACTIVE CONFORMATION 88

FIGURE 27. ARF6 IS SELECTIVELY PROTECTED FROM IPAJ CLEAVAGE 89

FIGURE 28. IPAJ CO-LOCALIZES WITH AND CLEAVES ARF1, ARF5 AND ARL1 91

FIGURE 29. IPAJ AND VIRA ARE ESSENTIAL FOR OPTIMAL *SHIGELLA* VIRULENCE 107

FIGURE 30. IPAJ ACTIVITY MASKS STING ACTIVATION 109

FIGURE 31. IPAJ SUPPRESSES STING-DEPENDENT PRODUCTION OF IFN-B 110

FIGURE 32. IPAJ PREVENTS PROTEIN EXIT FROM THE ER 111

FIGURE 33. *LISTERIA* SECRETING IPAJ OR VIRA DISRUPTS THE GOLGI 113

FIGURE 34. SECRETION OF IPAJ PREVENTS STING TRANSLOCATION INDUCED BY *LISTERIA* INFECTION 114

FIGURE 35. SECRETION OF IPAJ SUPPRESSES IFN-B PRODUCTION UPON *LISTERIA* INFECTION 116

FIGURE 36. SUBSTRATES RECOGNITION BY IPAJ AND C39 PEPTIDASES 125

LIST OF TABLES

TABLE 1 127

LIST OF APPENDICES

APPENDIX A 128

APPENDIX B 211

APPENDIX C 238

LIST OF DEFINITIONS

ARF - ADP-ribosylation factor

ARL – ARF-like protein

BFA - brefeldin ACAD – conditional agglomeration domain

CFU – colony forming units

EHEC – Enterohemorrhagic *Escherichia coli*

EPEC – Enteropathogenic *Escherichia coli*

ER – endoplasmic reticulum

GAP - GTPase activating protein

GEF – guanine nucleotide exchange factor

GFP – green fluorescent protein

GSP – general secretory pathway

GTPase – guanosine triphosphatase

hGH – human growth hormone

IpaJ – invasion plasmid antigen J

LCV – *Legionella* containing vacuole

MHCI - major histocompatibility complex ISCV – *Salmonella* containing vacuole

T3SS – type three secretion system

TNF - tumor necrosis factor

CHAPTER ONE
Introduction

Bacterial pathogens manipulate infected host cells.

Survival of microbial pathogens during infection relies on their ability to evade immune recognition and to establish a replicative niche inside the host organism. To survive, pathogens evolve numerous solutions to adapt to the host environment. For instance, many gram-negative pathogenic bacteria such as *Shigella spp.*, *Yersinia spp.*, and *Salmonella spp.*, utilize a dedicated type III secretion system (T3SS) to deliver specialized effector proteins into the infected host cell (Alto & Orth, 2012). These effectors promote bacterial infection by subverting crucial cellular systems including immune responses, cytoskeleton and membrane trafficking.

T3SS is a complex needle-like structure composed of approximately 20 proteins. It projects from the bacterial surface and reaches the host target cell. Bacterial effectors are then transported through the hollow 'tube' directly into the host cell through the pores formed by the needle of the T3SS (Burdette & Vance, 2013). These secreted effectors utilize various strategies to manipulate host signaling, including mimicking the function of the host proteins and altering the post-translational modifications of the host proteins. For instance, Map effector from the enteropathogenic *Escherichia coli* (EPEC) was found to induce formation of filopodia through the activation of Cdc42 GTPase, a crucial regulator of the active cytoskeleton (Alto et al., 2006; Kenny et al., 2002). Further studies had shown that Map

mimics a guanine exchange factor, an upstream activator of the Cdc42, thereby exploiting the host mechanism of the protein activation (Huang et al., 2009). Another layer of the sophisticated mechanism of Map action is reported by Orchard et al., who uncovered that the protein participates in a positive feedback loop which amplifies the initial nucleation of the actin fibers (Orchard et al., 2012).

Manipulation of the host small GTPases through the molecular mimicry is a recurring theme in the bacterial pathogenic strategies. YopE from *Yersinia pseudotuberculosis* has GTPase activating protein (GAP) activity toward GTPases of the RhoA family (Black & Bliska, 2000; Von Pawel-Rammingen et al., 2000). Host cell GAPs inactivate the GTPases by catalyzing hydrolysis of the bound GTP molecule to the GDP, thereby turning off the GTPase. YopE uses molecular mimicry and, similarly to the host GAPs, provides a critical arginine residue that assists in the hydrolysis. By inactivating the host RhoA GTPases, YopE induces the disassembly of the actin cytoskeleton and prevents the phagocytosis of the pathogen.

In addition to mimicry, many effectors manipulate cell signaling by adding or removing the essential post-translational modifications (PTM) of the host proteins. For instance, YopJ effector from *Yersinia spp.* represents a remarkable example of this strategy (Mittal, Peak-Chew, & McMahon, 2006; Mukherjee et al., 2006; Orth et al., 1999). YopJ was found to block MAPK signaling by modifying MAPKKs with an acetyl moiety. This acetylation of serine and threonine residues prevents their normal phosphorylation, thereby inhibiting protein activity. OspF effector from *Shigella* also relies on the post-translational modifications of its substrates and also targets the MAPK signaling pathway. OspF is a

phosphothreonine lyase that irreversibly dephosphorylates a phosphothreonine residue in the activation loop of MAP kinases ERK1 and ERK2 (Li et al., 2007). Through the unique reaction mechanism OspF removes the hydroxyl group from the phosphothreonine, thereby inactivating the MAP kinases that are critical for the immune response activation.

To summarize, the bacterial pathogens secrete effector proteins into infected cells to promote their own survival. These effectors interfere with host proteins in a way that best fits the need of the given pathogen. Depending on the lifestyle of the pathogen, effectors can subvert certain immune responses, affect cytoskeleton or rewire the endomembrane trafficking system. In particular, an attractive target for pathogen intervention due to its role in maintaining host cell homeostasis is presented by the Golgi network, a central hub of the vesicular transport system.

The Golgi function in health and disease

The Golgi apparatus is a highly dynamic cellular organelle and a central hub for vesicular trafficking (Andreeva, Kutuzov, Evans, & Hawes, 1998). Newly synthesized proteins destined for secretion and intracellular membrane organelles emerge from the endoplasmic reticulum (ER) in COPII-coated transport vesicles and merge with an early Golgi compartment, also known as the cis-Golgi network (CGN). After passing the Golgi stacks, the proteins reach the trans-Golgi network (TGN) where they are sorted for delivery to cellular membrane compartments or for secretion. Depending on its purpose and cell type, a protein may be delivered to either plasma membrane, endosomes, lysosomes, or secretory granules. Secreted proteins include cytokines, hormones, and extracellular matrix proteins,

such as collagen, which supports cellular structure and is crucial for intercellular communication. Lysosomal proteins, such as hydrolases, constitute another group of cargo emerging from the trans-Golgi. Defects in proper secretion and lysosomal function underlie immune diseases, diabetes, and cancer (Baay, Brouwer, Pauwels, Peeters, & Lardon, 2011; Castaneda, Lim, Cooper, & Pearce, 2008; Colbert, Matthews, Miller, & Watts, 2009; Jube et al., 2012; Landstrom, Westman, & Borg, 1988). Thus, the Golgi apparatus serves as an essential organelle that mediates cellular trafficking and maintains cellular homeostasis.

Besides being closely involved in maintaining cellular homeostasis, the Golgi participates in the immune response through the secretion of cytokines such as interleukin-6 (IL-6) and tumor necrosis factor (TNF) (Manderson, Kay, Hammond, Brown, & Stow, 2007; Shurety, Merino-Trigo, Brown, Hume, & Stow, 2000). Both proteins are known as critical regulators of anti-microbial defense (McLoughlin et al., 2005; Wajant, Pfizenmaier, & Scheurich, 2003). In addition to the cytokine secretion, the Golgi also participates in the immune signaling by transporting and housing various immune sensors such as Toll-like receptor 4 (TLR4), a major receptor of bacterial LPS. TLR4 binds its agonist on cell surface and is then internalized for degradation and signal termination. At least in some cell types the Golgi apparatus houses a pool of TLR4 molecules that may be used to replenish the surface level of the receptor (Hornef, Frisan, Vandewalle, Normark, & Richter-Dahlfors, 2002; Latz et al., 2002; Wang et al., 2010). It is known that the disruption of the Golgi by the fungal metabolite Brefeldin A (BFA) leads to a decrease in the surface level of the receptor (Wang et al., 2010). TLR9 is an intracellular receptor that passes through the Golgi to the endosomes (Chockalingam, Brooks, Cameron, Blum, & Leifer, 2009) and serves as another innate

immune sensor recognizing a specific bacterial pattern: CpG-rich DNA. Blocking the Golgi with BFA significantly inhibited TLR9-induced NF-κB activation (Chockalingam et al., 2009).

In addition, traffic from ER through the Golgi includes major histocompatibility complex I (MHCI) which is expressed in all enucleated cells and delivers intracellular antigens, products of proteosomal breakdown, to the cell surface. Cytotoxic $CD8^+$ T cells survey the MHCI complex and induce cell death if they recognize the bound antigen as a 'non-self' product. Cells infected with intracellular pathogens expose foreign antigens and are then eliminated. Importantly, inhibition of the Golgi trafficking suppresses the MHCI-mediated antigens presentation (Yewdell & Bennink, 1989). Therefore, the Golgi apparatus functions not only to support the homeostatic state of the cell, but is also tightly involved in the stress response, such as activation of immune signaling.

The Golgi regulation by bacterial pathogens

As an essential regulator of cellular homeostasis, the Golgi appears an attractive target for invading pathogens. Indeed, as described above, the subversion of the normal Golgi trafficking can potentially prevent cytokine secretion, MHCI-mediated antigen presentation, translocation of immune receptors, and delivery of hydrolytic enzymes to lysosomes and phagosomes. Depending of their life cycle, different bacteria can utilize various strategies to inhibit or even remodel membrane trafficking and the Golgi function for their own needs.

A fine example of such species-specific strategy, *Legionella pneumophile* is an intracellular pathogen that persists in the phagosome after phagocytosis and rewires host

vesicular trafficking in a sophisticated way. Its effectors delivered through Dot/Icm type IV secretion system redirect the ER-derived transport vesicles from the Golgi to the phagosome (Ge & Shao, 2011; Isberg, O'Connor, & Heidtman, 2009). As a result of this 'shortcut', default phagosome maturation pathway is bypassed, allowing *Legionella* to turn phagosomes into its replication niche called *Legionella* containing vacuole (LCV). At least two coordinated strategies are involved in the highjacking of the host trafficking system. First, effector SidF is a phosphatidylinositol (PI) phosphatase that localizes to the LCV and converts its constituent lipids PI(3,4,5)P_3 and PI(4,5)P_2 to PI(4)P which is mainly found in the Golgi membrane (Hsu et al., 2012). This mimicry of the lipid composition likely grants LCV the Golgi-characteristic 'immunity' against fusion with lysosomes and helps to recruit the Golgi-associated proteins. Second, at least six secreted effectors of Legionella control the activity of Rab1 GTPase, a master regulator of the ER to the Golgi trafficking. Specifically, one of the effectors, SidM, activates Rab1 by catalyzing nucleotide exchange and by covalently modifying it with AMP-moiety to prevent Rab1 inactivation by GAPs (GTPase activating protein) (Hardiman & Roy, 2014; Machner & Isberg, 2006; Neunuebel et al., 2011). As a result, the Golgi structure is disrupted, and the activated Rab1 is recruited to the LCV. Furthermore, another effector, LidA, specifically binds Rab1 in the active state and prevents its inactivation by GAPs (Machner & Isberg, 2006; Neunuebel, Mohammadi, Jarnik, & Machner, 2012). Together, these activities stabilize Rab1 in the active form. Two other *Legionella* proteins, SidD and LepB, reverse Rab1 overactivation by deAMPylating and promoting GTPase activity, respectively (Ingmundson, Delprato, Lambright, & Roy, 2007; Neunuebel et al., 2011). Altogether, these effectors regulate Rab1 activity in a

coordinated and complex manner to redirect the ER-derived transport vesicles. Additionally, AnkX and Lem3 effectors give *Legionella* another level of control over Rab1. AnkX is an ankyrin repeat protein that transfers a phosphocholine moiety from CDP-choline to Rab1 (Mukherjee et al., 2011). AnkX was shown to prevent the microtubule-dependent vesicle trafficking and induce fragmentation the Golgi apparatus (Pan, Luhrmann, Satoh, Laskowski-Arce, & Roy, 2008). Finally, Lem3 effector is a dephosphocholinase that reverse choline-modification of Rab1 (Tan, Arnold, & Luo, 2011). Thus, a concerted action of Legionella effectors efficiently subverts ER to the Golgi trafficking and establishes a replicative niche for the pathogen.

Similarly to *Legionella*, *Salmonella spp*. establish an intracellular replicative niche inside a vacuolar compartment that undergoes maturation to *Salmonella* containing vacuole (SCV)(Knodler & Steele-Mortimer, 2003). This process depends on *Salmonella*-pathogenicity island-2 (SPI-2) T3SS effector SseG, whose exact function is yet to be identified (Salcedo & Holden, 2003). After migrating to perinuclear region, the majority of SCV become surrounded by the Golgi membranes(Salcedo & Holden, 2003). Interestingly, the Golgi disruption with Brefeldin A inhibits bacterial growth, proving the importance of the normal Golgi function for *Salmonella* replicative niche.

Another pathogenic bacterium, *Chlamydia trachomatis*, also replicates in a vacuolar compartment termed the inclusion and takes advantage of the normal Golgi trafficking for its own growth. Similarly to other intracellular pathogens, *Chlamydia* needs to satisfy its need for nutrients such as lipids, cholesterol, and sphingomyelin, to grow. The parasite was shown to solve this problem by intercepting normal transportation of these nutrients (Carabeo,

Mead, & Hackstadt, 2003; Hackstadt, Rockey, Heinzen, & Scidmore, 1996; Heuer et al., 2009; Rejman Lipinski et al., 2009). Specifically, *Chlamydia* induces the Golgi fragmentation to facilitate nutrient acquisition by the inclusions (Heuer et al., 2009). Disruption the Golgi is induced by a secreted bacterial protease chlamydial protease-like activity factor (CPAF) which cleaves the Golgi matrix protein golgin-84 (Christian et al., 2011; Heuer et al., 2009). The process also requires functional GTPases Rab6, Rab11 and Rab14 (Capmany & Damiani, 2010; Christian et al., 2011; Rejman Lipinski et al., 2009). The fragmented Golgi forms ministacks that supply nutrients, such as ceramide, to the *Chlamydia* inclusions (Heuer et al., 2009). The inhibition of golgin-84 proteolysis rescues the Golgi structure and inhibits *Chlamydia* maturation. Furthermore, fragmentation of the Golgi by the knockdown of the Golgi matrix proteins enhances bacterial maturation (Heuer et al., 2009).

Finally, several secreted effectors of enterohaemorrhagic *Escherichia coli* (EHEC) were found to block the host general secretory pathway (Selyunin et al., 2011). The most potent of those was EspG, a catalytic scaffolding protein that acts simultaneously on ARF1 and Rab1 GTPases, the two critic regulators of the ER-Golgi trafficking (Dong et al., 2012; Selyunin, Reddick, Weigele, & Alto, 2014). By maintaining ARF1 in the active state and inactivating Rab1 GTPase in its vicinity, EspG induces massive Golgi fragmentation and formation of ministacks. As a result, secretion through the Golgi network is potently shut down. In addition, EspG recruits p21-activated kinases, potentially creating novel signaling circuits(Selyunin et al., 2011).

Therefore, as a critical regulator of cellular homeostasis and a central trafficking hub, the Golgi presents an appealing target for bacterial pathogens that, accordingly, adapted to

subvert its function for their own benefit. Reprogramming the Golgi function may provide nutrients and shelter to intracellular pathogens and interfere with innate immune pathways through inhibition of secretion. Hence, a better characterization of the Golgi-pathogens relationship is critical to understand the mechanisms of bacterial infection and to improve treatments of current and emerging bacterial threats.

CHAPTER TWO
Identification and initial characterization of *Shigella flexneri* effector IpaJ

Introduction

The critical role of the Golgi in regulating immune signaling, as well as its targeting by the bacterial effectors , highlights the necessity for better understanding of the Golgi-pathogen interactions. Previously, our laboratory found that *Shigella flexneri* potently disrupts the Golgi structure, but the mechanism was not well understood. I investigated how *Shigella* inhibits the Golgi function and general secretory pathway. A screen of *Shigella* effectors allowed me to identify two proteins, namely VirA and IpaJ, to disrupt the Golgi structure. In my work I primarily focused on identifying the substrates and determining the mechanism of specificity of the previously uncharacterized effector IpaJ.. My results provide an insight into the previously unappreciated pathogenic strategy of *Shigella* and establish a background for a better understanding of the Golgi function and protein-membrane interactions.

Results

(part of this chapter was published previously in research article)

Shigella effector proteins IpaJ and VirA disrupt the Golgi

While seeking to understand how bacterial pathogens regulate the host secretory pathway(Selyunin et al., 2011), I found that *Shigella flexneri* potently inhibited cargo transport through the Golgi apparatus (Figure 1). Further investigation revealed that the Golgi was severely fragmented after *Shigella* infection (Figure 2a). By contrast, neither

Listeria monocytogenes nor *Salmonella typhimurium* disrupted the Golgi, suggesting that *Shigella* has evolved a specific, yet unidentified mechanism to regulate host organelle function.

Shigella infection requires translocation of over twenty bacterial "effector" proteins into host cells through the Mxi-SPA Type III Secretion System (T3SS) (Ashida et al., 2011). Deletion of *mxiD*, a component of the needle complex required for T3SS, eliminated destruction of the Golgi by *Shigella* infection(Figure 2d). To identify the specific effector protein required for this activity, the Golgi morphology was assessed after transient transfection of 20 effector genes. Both IpaJ and VirA induced profound Golgi fragmentation (Figure 2b). However, the other T3SS effector proteins had no discernable effect on the Golgi structure (Figure 3).

Thomas Fox helped me to validate the role of the two identified effector proteins by creating *Shigella* knockout strains lacking ipaJ, virA, or both genes. Comparison of cells infected with *Shigella* Δ*ipaJ* and Δ*virA* gene deletion strains revealed that these mutants induced variable degrees of Golgi disruption (Figure 2c) and abnormal Golgi morphologies (Figure 2d), yet neither mutant alone fully attenuated destruction of the Golgi. By contrast, the Golgi remained intact and functional in cells infected with *ΔipaJ/virA* double mutant strain (Figure 2c). The *Shigella* Δ*ipaJ/virA* strain displayed normal host cell invasion, intracellular replication, and actin-based motility suggesting the Golgi disruption was specifically caused by these effector genes (Figure 4).

Identification of the catalytic triad and potential targets of IpaJ

While VirA was recently shown to inactivate Rab1 GTPase signaling pathways(Dong et al., 2012), additional mechanisms are necessary for the Golgi destruction during *Shigella* infection (Mounier et al., 2012). I therefore focused on IpaJ since its molecular mechanism of action is poorly understood (Buysse, Dunyak, Hartman, & Venkatesan, 1997b; Liu et al., 2002). BLAST database searches identified IpaJ homologs in numerous bacterial species, but this sequence-based alignment did not offer any clues to its function (Figure 5). However, a structural-based bioinformatics analysis performed with assistance of Bethany Weigele revealed that IpaJ is distantly related to the family of putative C39 peptidase-like enzymes (domains of unknown function annotated as DUF3335) (Figure 6a). C39-family members cleave leader peptides from bacteriocins with anti-microbial and quorum sensing activities (Michiels, Dirix, Vanderleyden, & Xi, 2001). Although IpaJ is unlikely to function in these capacities, it harbors the catalytic Cysteine (C), Histidine (H), and Aspartate (D) residues required for peptide bond hydrolysis (Figure 6a). As predicted by this alignment, alanine substitutions at C64, H206, or D218 abolished IpaJ's ability to disrupt the host Golgi morphology in transfection studies (Figure 6b). In addition, complementation of *Shigella ΔipaJ/virA* deletion strain with plasmid expression of IpaJ induced the Golgi disruption phenotype whereas IpaJ C64A, H206A, and D218A had no effect (Figure 7).

Previous studies have shown that IpaJ induces a growth arrest phenotype in yeast (Slagowski, Kramer, Morrison, LaBaer, & Lesser, 2008). Similar growth inhibition was found with IpaJ, whereas yeast grew normally in the presence of IpaJ C64A, H206A, or

D218A catalytic mutants (Figure 8a). Using a multicopy suppressor screen, I identified three distinct genomic loci that, when introduced on high-copy plasmids, suppressed IpaJ activity in yeast. Two loci encoded ARF1p and ARF2p GTPases, and the third loci encoded VPS15p, a phosphatidylinositol (PI) kinase required for yeast vacuole fusion (Herman, Stack, DeModena, & Emr, 1991) (Figure 8b). While these data suggest that IpaJ may regulate several host signaling pathways, I focused my initial efforts on ARF GTPases since these enzymes are master regulators of cargo trafficking through the Golgi apparatus (Kahn, 2009). Overexpression of either ARF1p or ARF2p rescued the yeast growth arrest phenotype, thereby defining ARF GTPases as potential substrates of IpaJ (Figure 8c).

IpaJ removes N-myristoyl glycine of ARF1

ARF1 functionally couples guanine-nucleotide exchange (GDP for GTP) and membrane binding (via *N*-myristoylation) to the recruitment of COPI coat-complex to the Golgi membranes as a key step in vesicle fission (Kahn, 2009). I suggested that IpaJ might prevent the nucleotide exchange cycle of ARF1 or its interaction with the substrates. Together with Andrey Selyunin, we tested the effect of IpaJ on the function of purified ARF1 (Figure 9a). First, recombinant IpaJ was incubated with GST-tagged GDP-ARF1 followed by induction of GTP-nucleotide exchange (Figure 9b). The ability of ARF1 to exchange nucleotide in the presence of IpaJ was assessed by the ability of GST-ARF1 to pull down GGA, a GTP-dependent substrate of ARF1 (Puertollano, Randazzo, Presley, Hartnell, & Bonifacino, 2001) (top panel, experiments 1). IpaJ did not inhibit GTP exchange and GGA binding under these conditions. Second, we tested the ability of IpaJ to compete for substrate

interaction by incubating GST-tagged GTP-ARF1 with GGA in the presence of IpaJ. GST-pulldown experiments indicated that IpaJ did not affect GGA substrate binding under these conditions (top panel, experiment 2). Third, we tested if IpaJ stimulated GTPase activity of ARF1 by first forming complex between GST-tagged GTP-ARF1 and GGA and then adding IpaJ. IpaJ did not induce the release of GGA from ARF1-GTP, indicating that it does not function as a GTPase activating protein (GAP). Therefore, IpaJ had no effect on the guanine-nucleotide cycle or GTPase-dependent interactions of ARF1 *in vitro*.

I therefore searched for IpaJ-induced post-translational modifications on ARF1 in mammalian cells. I collaborated with Daniel Plymire and Steven Patrie to utilize "top-down" mass spectrometry analysis (Kelleher, 2004; Sze, Ge, Oh, & McLafferty, 2002). ARF1 bearing a COOH-terminal Strep affinity tag (ARF1-strep) was expressed in HEK293T cells and purified by Strep-Tactin chromatography. We observed an intact monoisotopic molecular mass of 26,895.95 Da. Subsequent MS/MS resulted in 30 fragment ions that, together, provide an unambiguous assignment of *N*-myristoylated ARF1-strep protein (Figure 10a and Figure 11a). Cellular expression of IpaJ resulted in a 267.22 Da decrease in molecular mass of ARF1-strep, which corresponds closely to the loss of *N*-myristoyl group and the amino-terminal glycine (Figure 10b). Indeed, the MS/MS data supports the conclusion that IpaJ cleaves the amide bond between glycine-2and asparagine-3, liberating the *N*-myristoylated glycine from the ARF1 GTPase domain (Figure 10d and Figure 11b). ARF1 cleavage was not observed in IpaJ C64A treated samples, consistent with the function of IpaJ as a cysteine protease (Figure 10c and Figure 11c).

N-myristoylation is a normally irreversible 14-carbon fatty acid modification of an amino terminal glycine which occurs on approximately 1% of the human proteome (Farazi, Waksman, & Gordon, 2001; Maurer-Stroh et al., 2004). Despite being irreversible, N-myristoylation often serves as a dynamic regulator of a protein activity by undergoing a conformational rearrangement called the myristoyl switch (McLaughlin & Aderem, 1995). The switch consists of the myristoyl group "flipping" between the sequestered and accessible states, allowing protein-protein interactions, allosteric protein activation, or membrane targeting in the exposed (accessible) state. Since the switch is mechanistically linked to the protein conformational changes induced by ligand binding or another PTM, its activation is tightly coupled to the activation of the protein itself (Farazi et al., 2001). This ability to coordinate protein functional state with its localization or substrate recognition makes N-myristoyl an essential element of numerous signal transduction networks. Specifically, N-myristoylation is a critical feature of ARF proteins. As mentioned above, ARF1 is a small GTPase of the ARF family which cycles between the GTP- and GDP-bound states. These cycles of nucleotide exchange are coupled to the conformational rearrangement of the protein that has two major consequences. First, the GTP-bound (active) state allows ARF1 to interact with and recruit its downstream effectors, which I shall term substrates to distinguish from bacterial effector proteins. Together with its substrates, ARF1 promotes formation of the transport vesicles (Donaldson & Jackson, 2011; Kahn, 2009). Second, the binding of GTP activates the myristoyl switch, exposing the acylated N-terminal helix to promote association of ARF1 with the Golgi membrane (Figure 12). Hence, the myristoyl switch provides temporal coordination of the ARF1 localization with the recruitment of the downstream

substrates. By removing the myristoyl group, IpaJ likely disrupts the functional cycle of ARF1. Therefore, the mass-spectrometric analysis has potentially revealed proteolytic demyristoylation as a novel bacterial pathogenic strategy.

To further confirm that IpaJ removes N-myristoyl glycine, I reconstituted the activity of IpaJ *in vitro* (Figure 13a). I utilized a recently developed 'click labeling' method that allows direct visualization of acylated proteins (Charron et al., 2009; Hang et al., 2007; Wilson, Raghavan, Yang, Charron, & Hang, 2011). For click labeling, cells are incubated with azide-myristate, a synthetic analog of myristic acid which is metabolized as the natural fatty acid for protein acylation. A fluorescent tag can be covalently attached to the azide group through the Cu^{2+}-catalyzed cycloaddition reaction, allowing specific labeling of the proteins acylated with azide-myristoyl. HeLa cells were transfected with Arf1-strep and then metabolically labeled with Azide-conjugated myristic acid (Az-myr). Cellular lysates were prepared 16 hours post-transfection and then incubated with 10μM recombinant IpaJ or the catalytically inactive IpaJ C64A mutant. To directly track the N-myristoylation state of purified ARF1, an alkyne-Alexa647 flurophore was covalently attached to Az-myr-ARF1-strep by copper-catalyzed azide-alkyne cycloaddition. In gel fluorescence assays were used to track the N-myristoylation state of Arf1-strep. Incubation of cellular extracts with recombinant IpaJ protein resulted in the demyristoylation of ARF1-strep as assessed by in-gel fluorescence assays (Figure 13b). Consistent with the proposed mechanism, proteolytically inactive IpaJ C64A did not alter the lipidation state of ARF1 under these conditions. Therefore, I found that IpaJ is a cysteine protease that hydrolyses the peptide bond of the N-myristoylated glycine, thereby effectively demyristoylating ARF1.

ARF1 is a physiological substrate of IpaJ

Having established that IpaJ cleaves ARF1, I turned to the previous observation in yeast showing that IpaJ may target multiple host substrates including VPS15p, a lipidated kinase (Herman et al., 1991). Although ARF1 and VPS15p are both *N*-myristoylated on their glycine-2 residue, they do not share any sequence or functional similarity. These observations suggested that IpaJ might cleave a broader range of substrates than initially suspected. To test this hypothesis, I labeled numerous *N*-myristoylated proteins found in HEK293T cells and discovered that a large proportion of these proteins was demyristoylated in IpaJ-treated samples (Figure 13c, arrows). The spectrum of *N*-myristoylated proteins was unaltered by IpaJ C64A mutant, thereby verifying the proteolyticbasis of this reaction. In addition, IpaJ had no effect on either palmitoylation or geranylgeranylation, indicating that the protease specifically cleaves proteins modified by the myristoyl group (Figure 13c).

N-myristoylated proteins share a conserved glycine but their sequences are otherwise highly variable (Figure 14a). To determine how IpaJ recognizes diverse substrates, I generated chimeric eGFP fusion proteins that expressed 10 amino acid leader peptides derived from c-Src, MARCKs, hVPS15 and GRASP65, N-myristoylated proteins involved in cellular growth, signal transduction, autophagosome maturation, and organelle function, respectively (Figure 14a) (Barr, Puype, Vandekerckhove, & Warren, 1997; Kamps, Buss, & Sefton, 1985; Stumpo, Graff, Albert, Greengard, & Blackshear, 1989; Sun et al., 2008). IpaJ cleaved each of these lipid-modified peptides in a reaction requiring its cysteine protease

activity (Figure 14b). The ability of IpaJ to cleave unrelated peptides suggested that the protease might recognize the acylated glycine-2 common to all of its substrates.

Cleavage of numerous N-myristoylated proteins *in vitro* suggested that IpaJ may have many substrates during infection. It is therefore important to determine which proteins are relevant targets of IpaJ. I first investigated whether ARF1 is a physiological substrate of IpaJ. Several lines of evidence indicated that it is ARF1 cleavage that is responsible for the Golgi destruction phenotype observed during infection.

First, I analyzed ARF1 localization during infection. I found that ARF1 was displaced from the Golgi membranes by WT *Shigella* infection but not by *ΔipaJ* single mutant (note that the Golgi is fragmented by VirA in this infection) or *ΔipaJ/ΔvirA* double mutant strains (Figure 15a). Furthermore, when I microinjected recombinant IpaJ into HeLa cells, I noticed that ARF1 was released from membrane just prior to the Golgi fragmentation (Figure 15b). These results suggested that *Shigella* displaced ARF1 GTPase from host membranes as mechanism of the Golgi disruption by IpaJ. However, several *N*-myristoylated proteins reside at the Golgi and are required for its structure and function (Barr, Nakamura, & Warren, 1998; Shorter et al., 1999). *N*-myristoylation of GRASP65 is required for its initial recruitment to the Golgi, where it is subsequently maintained through both lipidation and secondary protein:protein interactions (Bachert & Linstedt, 2010). For example, GRASP65 forms a complex with GM130, and together they maintain the structural organization of the Golgi cisternae (Barr et al., 1998). To determine if *Shigella* also displaces these *N*-myristoylated substrates from the Golgi, I examined the subcellular localization of GRASP65 during *Shigella* infection. As shown in Figure 16a, GRASP65 co-localizes with GM130 at the cis-

Golgi. While *Shigella* infection induces severe the Golgi fragmentation, both GRASP65 and GM130 maintain their membrane association (Figure 16b). These data suggest that IpaJ does not cause the release of *N*-myristoylated GRASP65 from the Golgi as a mechanism of organelle destruction and indicate that ARF1 is released from the Golgi membane prior to at least some other N-myristoylated proteins that regulate the Golgi function.

In addition, the preferred targeting of ARF1 was further supported by the observation that IpaJ C64A localized to the Golgi apparatus whereas neither WT IpaJ nor other catalytic mutants localized to this site (see Figure 6b). These data suggest that IpaJ C64A may function as a "substrate trap" by binding to its host cellular targets in a catalytically inactive complex. To test if IpaJ C64A localized to the Golgi in ARF-dependent manner, I monitored the subcellular distribution of IpaJ C64A in cells treated with Brefeldin A, a fungal metabolite that locks GDP-inactive ARF1 in an unproductive complex with its cellular GEF (Chardin & McCormick, 1999). I had the following rationale behind this experiment: as BFA was titrating away GTP-active ARF1 from the Golgi (by limiting the excess pool of GDP-ARF1 available for activation), IpaJ C64A mutant would be released from membranes in an ARF1 dependent manner. I found that GFP-IpaJ C64A co-localized with mCherry ARF1 at the Golgi in untreated HeLa cells (Figure 17a). Addition of BFA rapidly displaced both IpaJ C64A and ARF1 from the Golgi membranes (Figure 17b). Importantly, GM130, a peripheral membrane protein that associates with the cis-Golgi, was not displaced by BFA. To assure that the loss of IpaJ C64A localization was not due to non-specific changes in the Golgi membrane morphology, I treated cells with Nocodazole, a microtubule depolymerizing agent that potently disrupts ER to the Golgi trafficking. Both IpaJ C64A and ARF1 co-

localized on membranes in Nocodazole treated cells. As expected after microtubule depolymerization, GM130 localized to the Golgi fragments, yet it did not co-localize with IpaJ C64A or ARF1 (Figure 17c). These findings are in agreement the hypothesis that ARF1 is one of the major substrates of IpaJ.

Finally, the essential role of ARF1 cleavage by IpaJ in the Golgi fragmentation is supported by the observation that IpaJ phenocopies the effect of Brefeldin A. In fact, a hallmark of ARF1 disruption by Brefeldin A is the rapid redistribution of the Golgi enzymes to the ER. To determine if IpaJ functions in a similar fashion as BFA, I compared the subcellular distributions of the medial Golgi enzyme *N*-acetylglucosaminyltransferase I (NAGFP) in HeLa cells treated with BFA and in cells infected with *Shigella flexneri*. As expected, BFA induced the redistribution of NAGFP from the Golgi to the ER (Figure 18a). To directly compare this phenotype to bacterial infection, I infected NAGFP expressing HeLa cells with *Shigella* Δ*virA* (a strain that secretes IpaJ), Δ*ipaJ* (a strain that secretes VirA), and the double Δ*ipaJ/virA* deletion mutant. As shown in Figure 18b, NAGFP redistributed to the ER upon Type 3 secretion of IpaJ. The ER redistribution of NAGFP phenocopies BFA, providing support that ARF1 GTPase is a cellular target of the bacterial protease. In contrast, secretion of VirA did not phenocopy BFA treatment consistent with its role as a Rab1 specific GAP (Dong et al., 2012). Importantly, *Shigella* Δ*ipaJ/virA* double mutant had no effect on NAGFP localization. Altogether these observations strongly indicate that ARF1 acts as a physiological target of IpaJ during *Shigella* infection. Therefore, it is the elimination of ARF1 *N*-myristoylation by IpaJ expression that is largely responsible for the Golgi fragmentation induced by *Shigella* infection.

Conclusions

I have determined that *Shigella flexneri* secretes two effector proteins, IpaJ and VirA, which disrupt the Golgi structure. Furthermore, I found that a previously uncharacterized protein IpaJ is a cysteine protease that cleaves the *N*-myristoylated glycine from ARF1. Remarkably, N-myristoylation is a normally irreversible modification, which makes current finding the first instance of protein demyristoylation known to date. Understanding the mechanism of this novel substrate specificity will require detailed characterization of the protease at the biochemical and structural levels, and will allow better insight into the function of N-myristoylation in various contexts of health and disease.

The uncovered activity of IpaJ also reveals an unprecedented pathogenic strategy of demyristoylation. As described above, I found that cleavage of ARF1 during infection had led to the Golgi disruption. However, I also noticed that IpaJ cleaves numerous host cell proteins *in vitro* suggesting that it might have more physiological substrates. Since N-myristoylation regulates the activity of proteins involved in numerous cellular processes, identification of all relevant IpaJ substrates is necessary to understand the mechanism of *Shigella* infection and potentially other bacterial species that possess IpaJ homologs.

Therefore, current findings raise further questions that need to be addressed. How does IpaJ recognize the acylated proteins? Which proteins are cleaved during infection? What determines these physiological substrates? To address these questions, I pursued further biochemical and functional characterization of IpaJ.

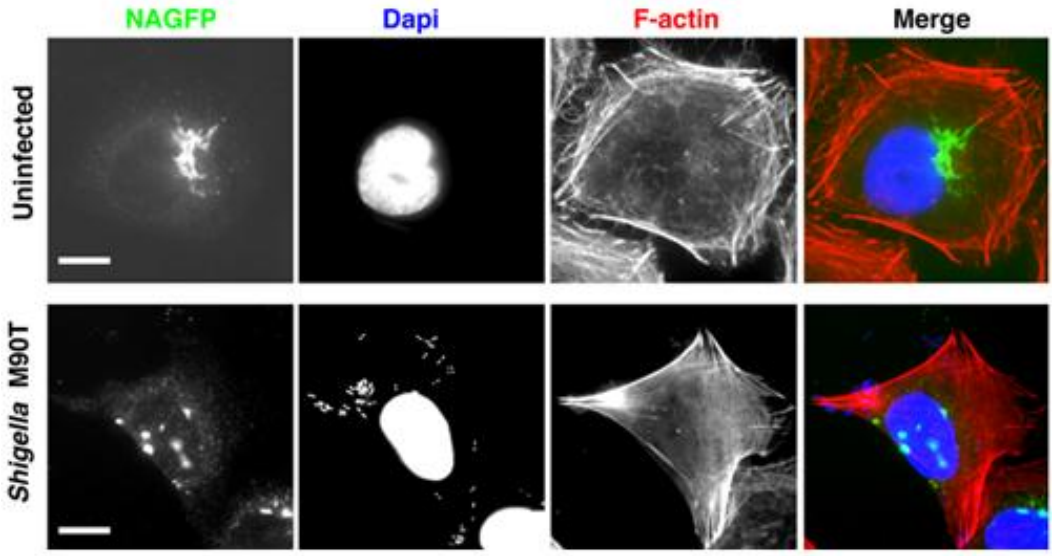

Figure 1: *Shigella* disrupts the Golgi structure and function.

Representative fluorescence microscopy images showing redistribution of the Golgi resident proteins upon *Shigella* infection are presented. To assess the trafficking of enzymes from the endoplasmic reticulum to the Golgi apparatus, I monitored HeLa cells stably expressing green fluorescent protein (GFP) attached to NH_2-terminal retention signal of *N*-acetylglucosaminyltransferase I(Shima, Haldar, Pepperkok, Watson, & Warren, 1997) (HeLa NAGFP). HeLa cells were stimulated for production of NAGFP marker and were infected by wild type *Shigella flexneri*. Infection with *Shigella* results in the inhibition of ER to the Golgi trafficking and redistribution of NAGFP marker into ER/Golgi fragments. Scale bar = 20μm.

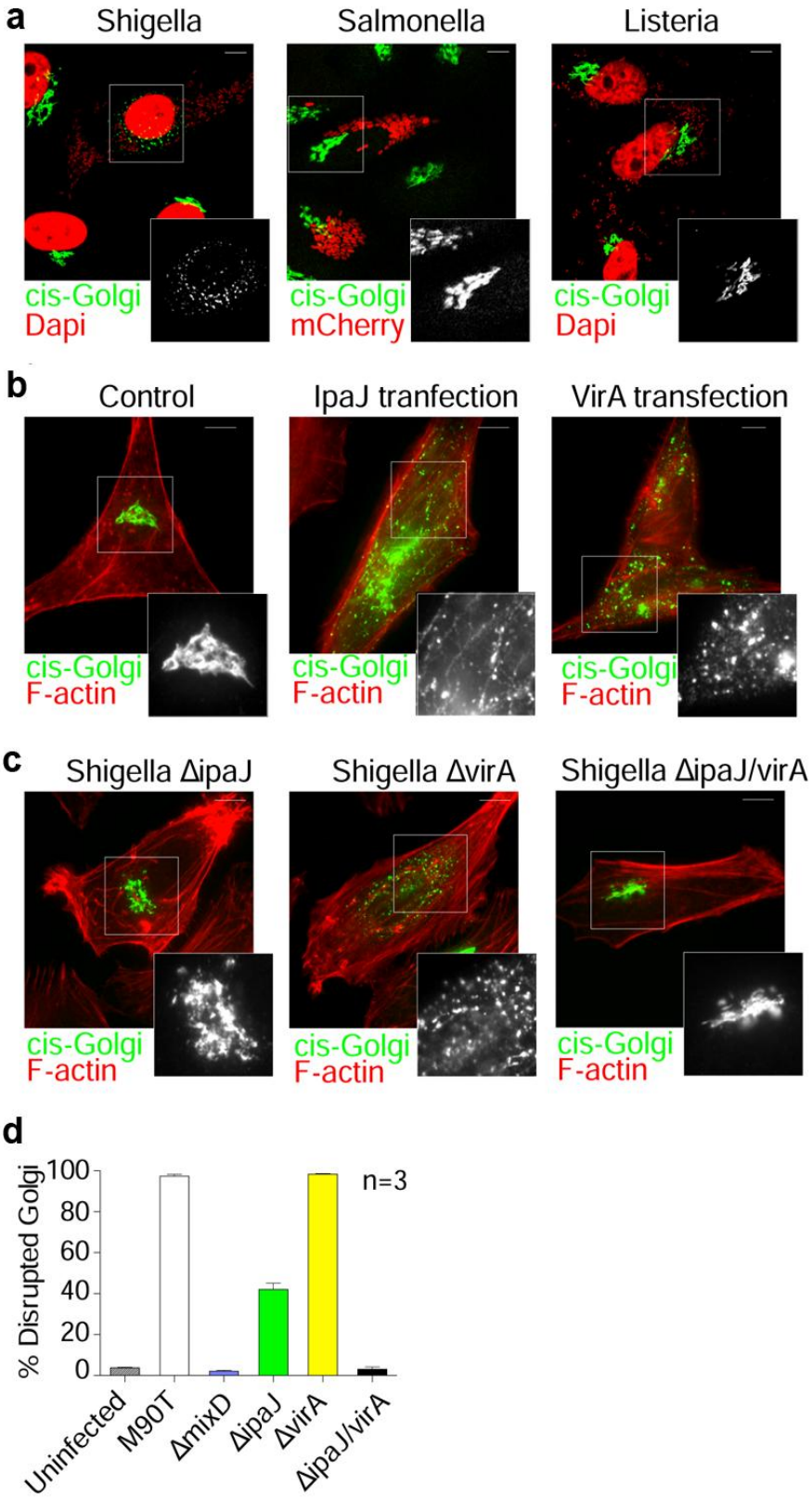
a
Shigella
Salmonella
Listeria
cis-Golgi
Dapi
cis-Golgi
mCherry
cis-Golgi
Dapi
b
Control
IpaJ tranfection
VirA transfection
cis-Golgi
F-actin
cis-Golgi
F-actin
cis-Golgi
F-actin
c
Shigella ΔipaJ
Shigella ΔvirA
Shigella ΔipaJ/virA
cis-Golgi
F-actin
cis-Golgi
F-actin
cis-Golgi
F-actin
d
% Disrupted Golgi
100
80
60
40
20
0
n=3
Uninfected
M90T
ΔmixD
ΔipaJ
ΔvirA
ΔipaJ/virA

Figure 2: *Shigella* IpaJ and VirA disrupt the Golgi morphology.

a. Hela cells were infected with *Shigella, Salmonella* or *Listeria* and the Golgi morphology was assessed with α-GM130 antibodies. *Shigella* and *Listeria were* visualized with Dapi (pseudo-colored red), and *Salmonella* was carrying mCherry-expressing vector (red). Scale bar = 10μm

b. Fluorescence microscopy of HeLa cells transfected with either IpaJ or VirA. Both protein induce fragmentation of the Golgi. The cis-Golgi (GM130, green) and F-actin (red) are shown. Scale bar = 10μm

c. Fluorescence microscopy of Hela cells infected with indicated *Shigella* strains and labeled as in (c).Scale bar = 10μm

d. Graph showing the percent of HeLa cells with disrupted the Golgi morphology in 100 cells infected with either wild-type *Shigella* (M90T) or the indicated mutants. Error bars represent means ± SEM calculated from 3 independent experiments.

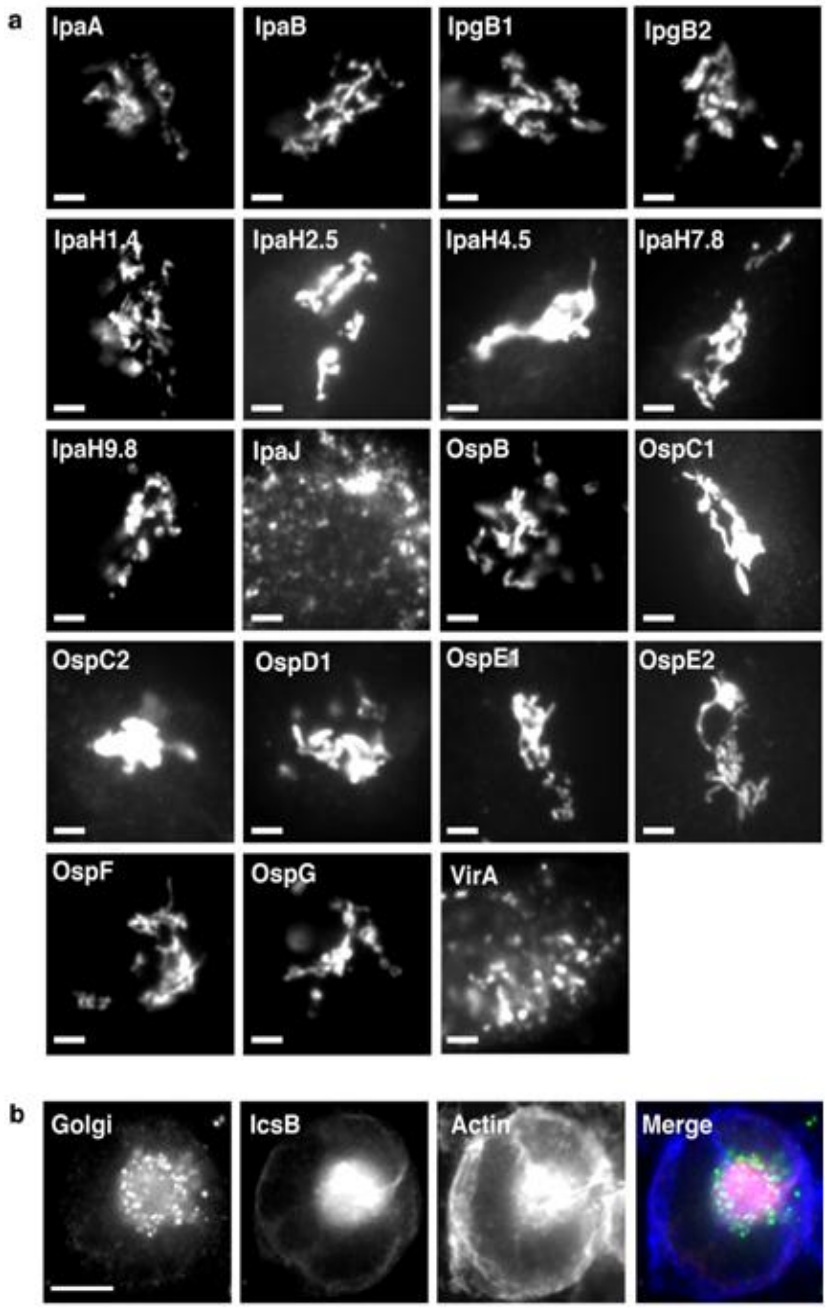

Figure 3: Identification of IpaJ and VirA as effectors that inhibit the Golgi structure and function.

a. HEK293A cells were transfected with *Shigellaflexneri*Type 3 effector proteins and the Golgi morphology was then assayed with fluorescence microscopy. Transfection of IpaJ or VirA resulted in complete disruption of the Golgi whereas 16 other effector proteins had no

effect. IpgD effector did not express in HEK293A or HeLa cells. Cis-Golgi was detected with GM130 antibodies. Scale bar = 5μm.

b. Although IcsB transfection induces the Golgi disruption, my data indicates that this is a non-specific effect. IcsB effector is required for lysis of cell membrane protrusion and facilitates *Shigella*'s intercellular spreading. IcsB is distantly related to and is predicted to share papain-like thiol protease fold with Rho GTPase inactivation domain (RID) of RtxA toxin from *Vibrio cholera(Pei & Grishin, 2009).* Since overexpression of IcsB induces a severe cell rounding phenotype and disappearance of plasma membrane filopodia, the Golgi disruption in this case likely results from non-specific toxicity caused by alterations of the cytoskeleton. Scale bar = 20μm.

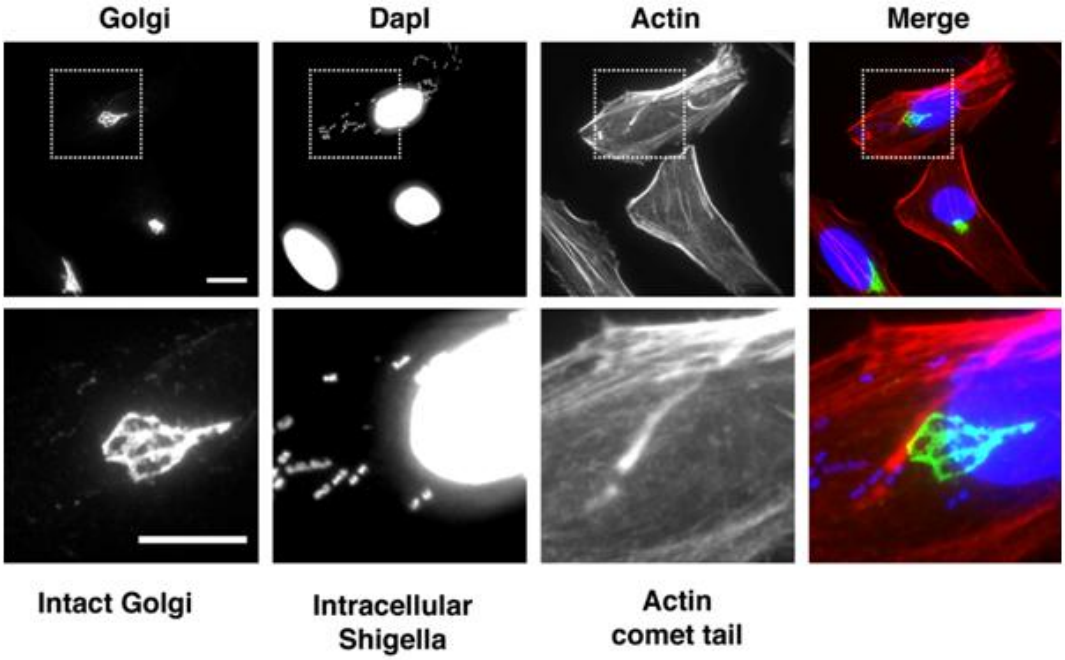

Figure 4: *Shigella ΔipaJ/ΔvirA* exhibits normal behavior inside the infected cells. Fluorescence microscopy showing that *Shigella ΔipaJ/ΔvirA* double knockout strain has no effect on the Golgi morphology. The Golgi ribbon remains intact despite high pathogen burden suggesting that there are no other *Shigella* effectors disrupting the Golgi besides IpaJ and VirA. Double deletion strain exhibits normal intracellular movement evidenced by actin comet tails. These data indicate that Golgi disruption does not result from either high intracellular bacterial replication or intracellular spread, but rather from the specific activities of IpaJ and VirA type 3 effector proteins. *Shigella* was detected by Dapi stain (blue), cis-Golgi was detected with GM130 antibodies (green) and actin was detected by rhodamine-phalloidin (red). Scale bar = 10µm.

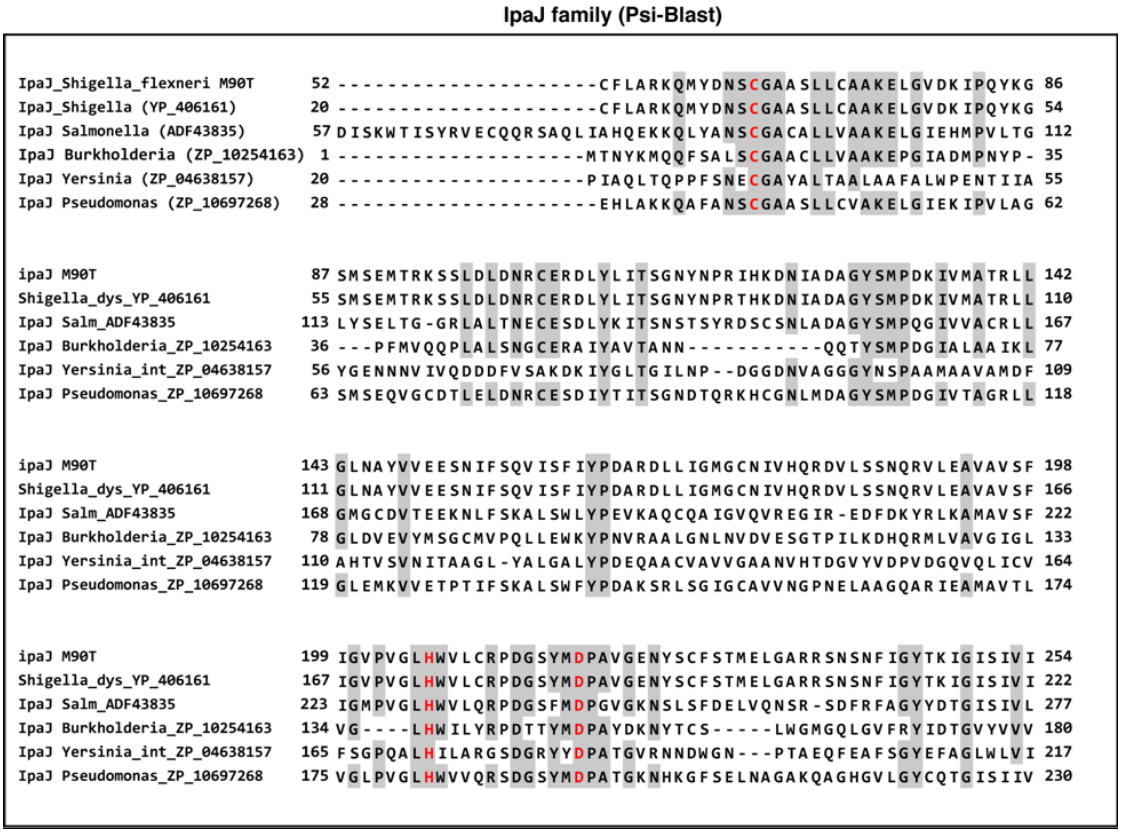

Figure 5: The IpaJ family.

Multiple PSI-BLAST iterations identified bacterial proteins with homology to IpaJ. Six representative family members are shown. Most of the proteins identified are putative and hypothetical proteins with unknown function. IpaJ family includes proteins from *Shigella spp*, *Salmonella spp*, *Burkholderiaspp*, *Yersinia spp*, *Pseudomonas spp*. Invariant Cys/His/Asp residues (see Figure 6a) are colored in red.

a

```
                                   HHHHHHHHHHHH            EEEEEE     EEEEE
IpaJ  NP_085284        56-RKQMYDNSCGAASLLCAAKELG-79  204-GLHWVLCRPDGS----YMDPAV-221
C39L  Q984Z8_RHILO     23-YVQTTPFTCGAACLMMAMSAVK-44  165-VPHWVLAIGDDGDHILIHDPWV-186
C39L  A6WWZ5_OCHA4     23-YVQTTPFTCGAACLLMAFAHHD-44  165-VPHWVLAHGEDGRHILIHDPWV-186
C39L  A0NWQ4_9RHOB     23-YVQTTPFTCGAACLLMSFACLD-44  165-VPHWVLVHDADDRHLIIHDPWL-186
C39L  Q1Q0J2_9BACT     24-YEQTTDFTCGACCLMMAMGRDI-45  166-FPHWVVVTGFDEKYIYVHDPFV-187
C39L  Q0EX59_9PROT     24-YQQTCEFTCGPCCLMMAMANFD-45  166-SPHWVVVSGFDRRFIYIHEPYV-187
C39F  YP_005047809      8-IKQHDITDCGAACLATISRQYG-33   92-LLHYVVIHKITKKEVIVADPAK-113
C1F   AAB02650        150-KNQGSCGSCWAFSAVVTIEGII-171 290-VDHAVAAVGYGPNYILIKNSWG-311
```

b

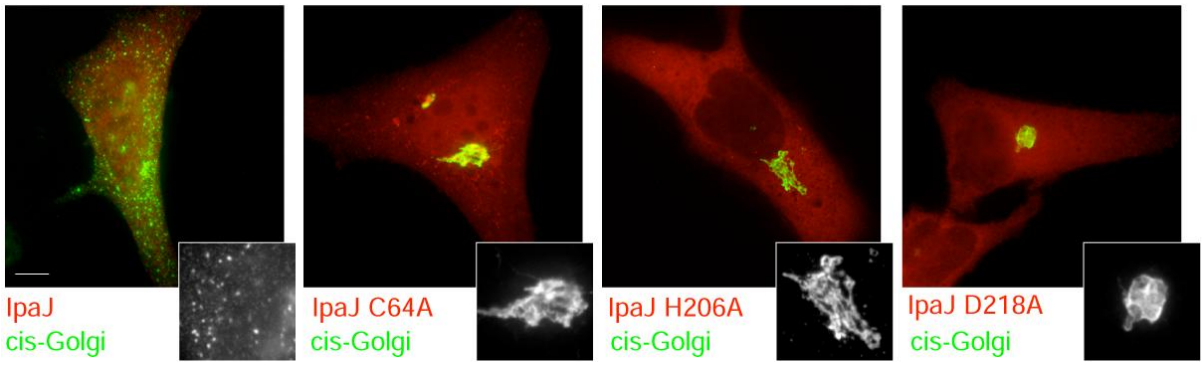

Figure 6: IpaJ belongs to the C39-family of cysteine proteases and targets ARF-family GTPases.

a. Sequence-structure alignment of *S. flexneri* IpaJ with members of C39-peptidase like family identified by HHPred. IpaJ possesses invariant catalytic triad residues Cys64, His206, Asp218 (red). The conserved Gln58, which helps form the oxyanion hole found in many proteases, is shown in green. Invariant residues and core hydrophobic residues found in C39-family are shown in blue and magenta, respectively. Characterized C39-family member (GCN5-acyetyl transferase) and a C1-family member (Papain) are shown.

b. Fluorescence microscopy of Hela cells transfected with the indicated IpaJ mutants. The cis-Golgi (GM130, green) and F-actin (red) are shown. Scale bar = 10μm

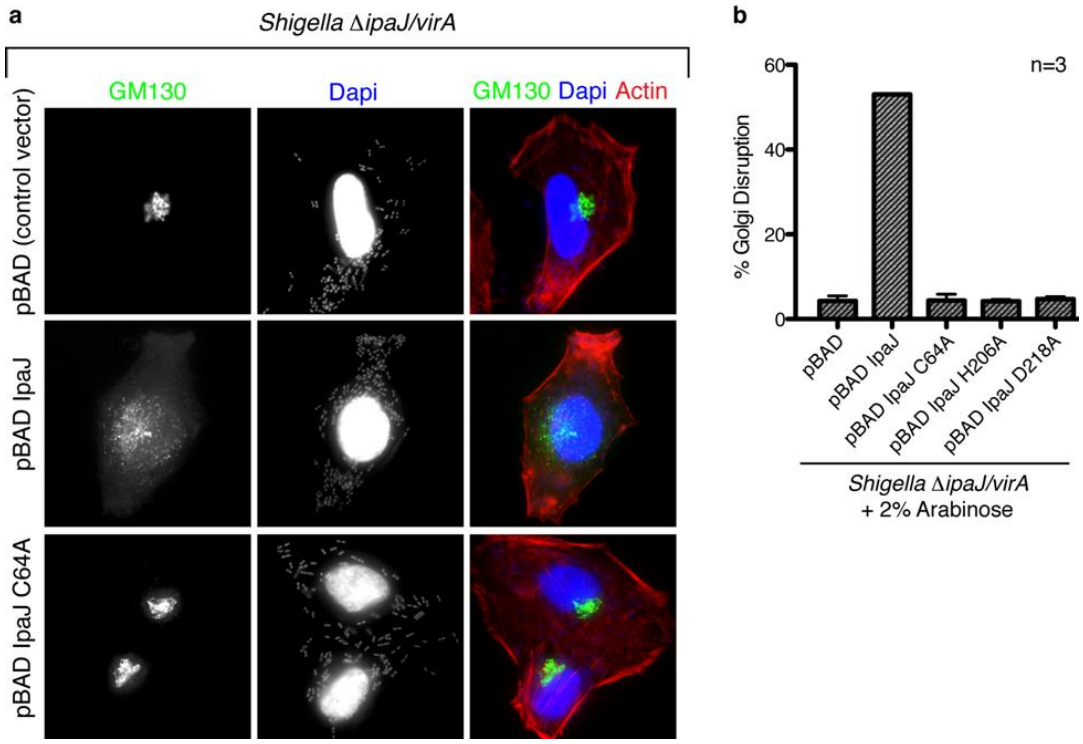

Figure 7: Complementation of the *Shigella*Δ*ipaJ/virA* mutant strain.

a. Fluorescence microscopy of Hela cells infected with *Shigella* Δ*ipaJ/virA* strain harboring control pBAD plasmid, pBAD expressing IpaJ, or pBAD expressing IpaJ C64A as indicated. The Golgi morphology was assessed by visualizing the localization of GM130 (green) in *Shigella* infected cells (Dapi). F-actin is shown (red).

b. Quantification of data presented in a. The graph shows the percentage of HeLacells with the Golgi disrupted after infection with *Shigella ΔipaJ/virA* double mutants complemented with the arabinose inducible pBAD plasmid expressing the indicated protein.

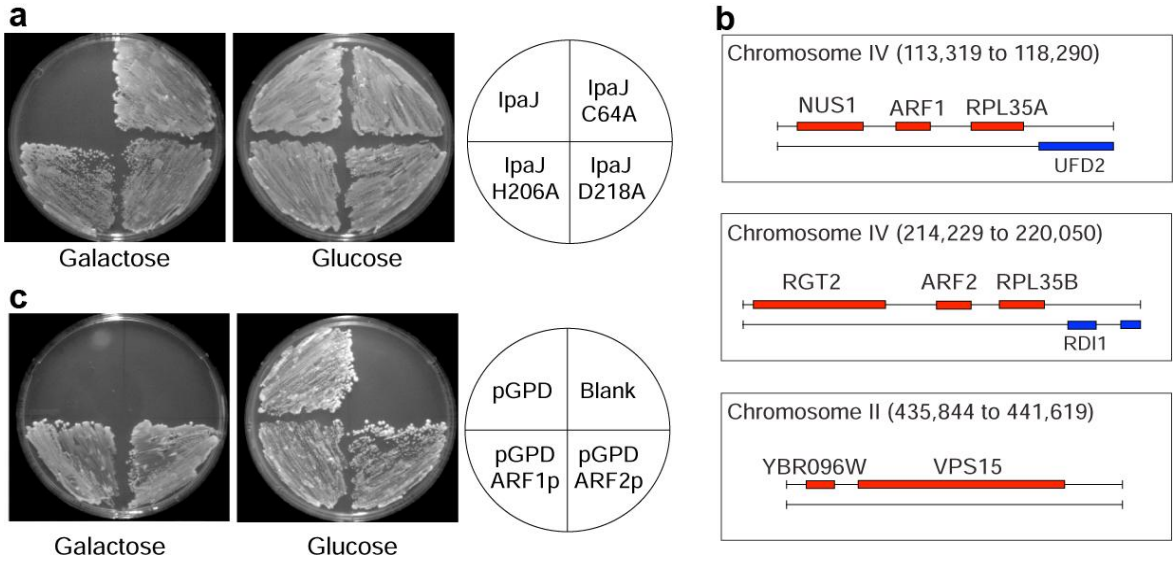

Figure 8: ARF1 and ARF2 are potential substrates of IpaJ

a. IpaJ or its catalytic mutants were expressed from a galactose inducible promoter (pGal413 vector) in yeast and assayed for a growth arrest phenotype on galactose or glucose (control) carbon source.

b. Illustration of the yeast genomic clones isolated from the IpaJ suppressor screen. ARF1p, ARF2p, and VPS15p are highlighted.

c. Yeast strain harboring a galactose inducible IpaJ gene were transformed with a multi-copy vector containing the indicated genes. Yeast were assayed for a growth arrest phenotype on galactose or glucose (control) carbon source.

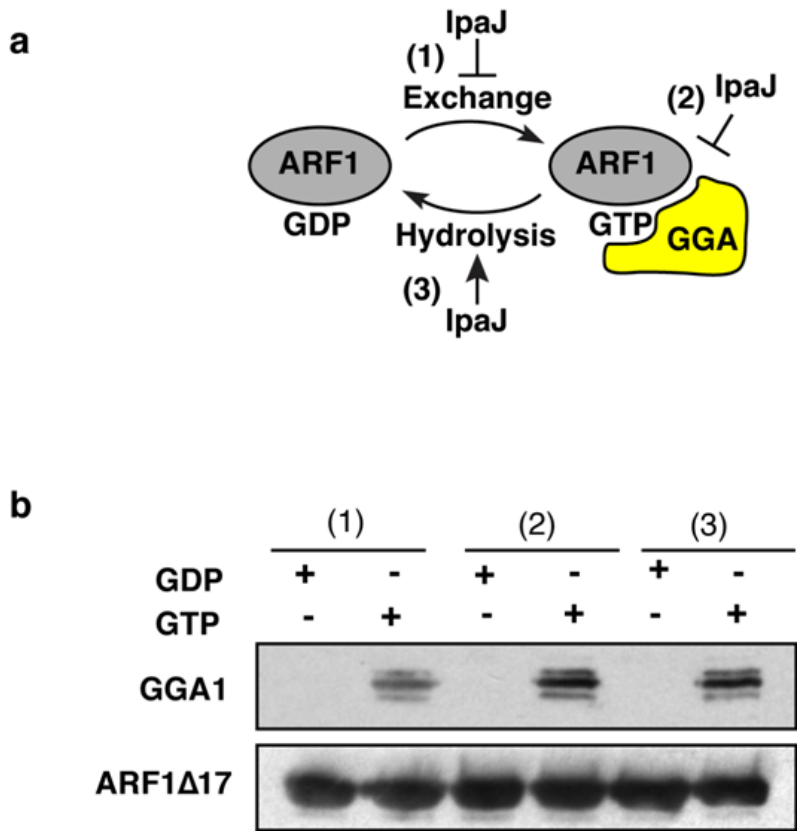

Figure 9: IpaJ does not regulate the guanine-nucleotide exchange cycle, substrate binding or GTPase activity of ARF1.

IpaJ does not regulate the guanine-nucleotide exchange cycle, substrate binding or GTPase activity of ARF1. We performed three different experiments to test the function of IpaJ on the ARF activation and signaling cycle (**a**). First, recombinant IpaJ was incubated with GST-tagged GDP-ARF1 followed by induction GTP-nucleotide exchange (**b**). The ability of ARF1 to exchange nucleotide in the presence of IpaJ was assessed by the ability of GST-ARF1 pulldown GGA, a GTP-dependent substrate of ARF1 (experiment 1). IpaJ did not inhibit GTP exchange and GGA binding under these conditions. Second, we tested the ability of IpaJ to compete for substrate interaction by incubating GST-tagged GTP-ARF1

with GGA in the presence of IpaJ. GST-pulldown experiments indicated that IpaJ did not affect GGA substrate binding under these conditions (experiment 2). Third, we asked if IpaJ stimulated GTPase activity of ARF1 by first forming complex between GST-tagged GTP-ARF1 and GGA and then adding IpaJ (experiment 3). IpaJ did not induce the release of GGA from ARF1-GTP, indicating that it does not function as a GTPase activating protein (GAP). Equal loading of GST-tagged ARF1 (ARF1Δ17 was used as this truncation mutant of ARF1 that harbors an intact GTPase domain) is shown in the bottom panel.

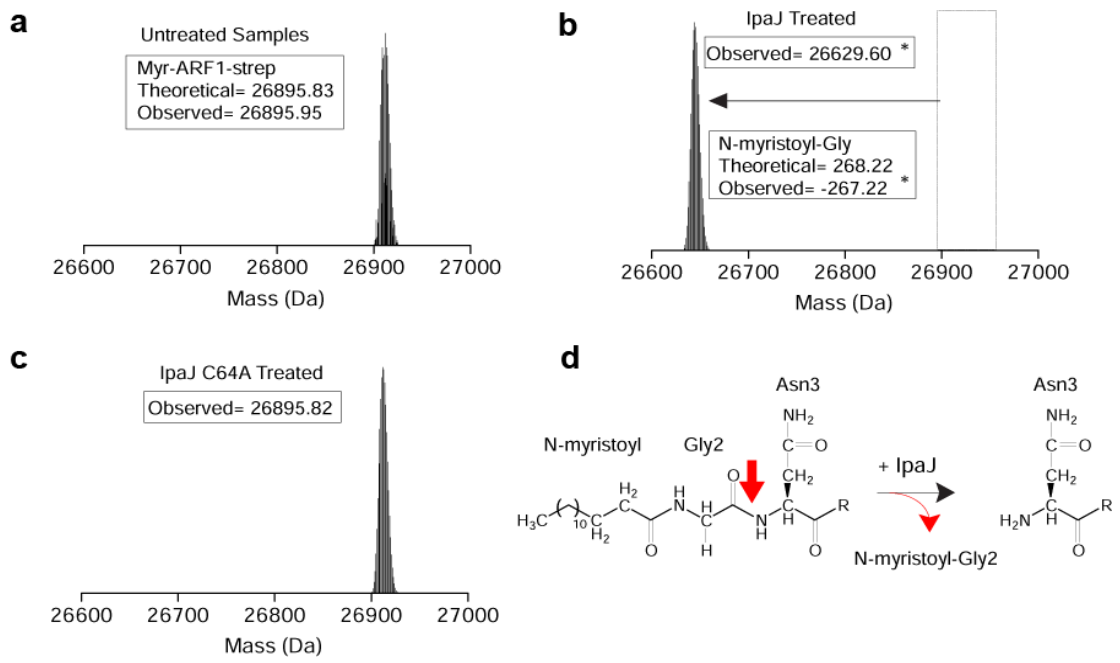

Figure 10: IpaJ cleaves the *N*-myristoylated glycine of lipidated substrates.

ARF1-strep was co-expressed with empty vector or IpaJ (wild type of C64A mutant) in HeLa cells. ARF1 was then purified and analyzed by intact mass-spectrometry.

a-c. Mass spectra of purified ARF1-strep in untreated (a), IpaJ treated (b), or IpaJ C64A treated cells (c) with the observed monoisotopic mass reported with Dalton units. Asterisk represents an observed 1 Da molecular mass shift that is accounted for in MS/MS data (Figure 11).

d. The chemical structure of *N*-myristoylated ARF1 amino-terminus in untreated (left) and IpaJ treated (right) samples. R group following Asn3 denotes ARF1-strep protein residue 4-240.

a

ARF1-strep (untreated sample); 30 fragments, 8 b-ions

```
b1   Myristoyl-
     G-N-I-F-A-N-L-F-K-G-L-F-G-K-K-E-M-R-I-L-M-V-G-L-D-   y215
b26  A-A-G-K-T-T-I-L-Y-K-L-K-L-G-E-I-V-T-T-I-P-T-I-G-F-   y190
b51  N-V-E-T-V-E-Y-K-N-I-S-F-T-V-W-D-V-G-G-Q-D-K-I-R-P-   y165
b76  L-W-R-H-Y-F-Q-N-T-Q-G-L-I-F-V-V-D-S-N-D-R-E-R-V-N-   y140
b101 E-A-R-E-E-L-M-R-M-L-A-E-D-E-L-R-D-A-V-L-L-V-F-A-N-   y115
b126 K-Q-D-L-P-N-A-M-N-A-A-E-I-T-D-K-L-G-L-H-S-L-R-H-R-   y90
b151 N-W-Y-I-Q-A-T-C-A-T-S-G-D-G-L-Y-E-G-L-L-D-W-L-S-N-Q-   y65
b176 L-R-N-Q-K-K-G-G-R-A-D-P-A-F-L-Y-K-V-V-R-Y-P-A-Q-W-   y40
b201 R-P-L-E-G-G-G-G-W-S-H-P-Q-F-E-K-G-G-G-S-G-G-G-S-G-   y15
b226 G-G-S-W-S-H-P-Q-F-E-K-G-P-V                          y1
```

Ion	Observed mass	Theoretical mass	error (ppm)
b29	3329.93	3329.91	4.5
b40	4589.68	4589.66	4.5
b41	4702.76	4702.75	2.1
b42	4801.83	4801.81	2.3
b43	4902.88	4902.86	3.8
b44	5003.91	5003.91	0.5
b45	5117.01	5116.99	3.9
b47	5315.14	5315.09	8.8

Ion	Observed mass	Theoretical mass	error (ppm)
y7	803.42	803.42	-2.4
y8	900.47	900.47	0.7
y9	1037.53	1037.53	3.3
y10	1124.56	1124.56	-1.6
y14	1511.72	1511.72	0.6
y15	1568.74	1568.74	0.3
y16	1655.77	1655.77	0.9
y17	1712.79	1712.79	0.6
y18	1769.82	1769.81	1.4
y19	1826.84	1826.84	1.7
y24	2213.03	2213.03	1.6
y28	2714.22	2714.25	-9.6
y53	5566.72	5566.72	1.4
y62	6521.25	6521.22	4.7
y67	7119.59	7119.53	7.4
y68	7232.63	7232.62	1.5
y69	7418.73	7418.70	4.1
y70	7533.74	7533.72	1.5
y71	7646.82	7646.81	2.0
y72	7703.83	7703.83	-0.4
y73	7832.90	7832.87	3.6
y76	8166.08	8166.04	5.1

b

ARF1-strep (IpaJ); 39 fragments, 12 b-ions

```
     *
b1   N-I-F-A-N-L-F-K-G-L-F-G-K-K-E-M-R-I-L-M-V-G-L-D-A-   y214
b26  A-G-K-T-T-I-L-Y-K-L-K-L-G-E-I-V-T-T-I-P-T-I-G-F-N-   y189
b51  V-E-T-V-E-Y-K-N-I-S-F-T-V-W-D-V-G-G-Q-D-K-I-R-P-L-   y164
b76  W-R-H-Y-F-Q-N-T-Q-G-L-I-F-V-V-D-S-N-D-R-E-R-V-N-E-   y139
b101 A-R-E-E-L-M-R-M-L-A-E-D-E-L-R-D-A-V-L-L-V-F-A-N-K-   y114
b126 Q-D-L-P-N-A-M-N-A-A-E-I-T-D-K-L-G-L-H-S-L-R-H-R-N-   y89
b151 W-Y-I-Q-A-T-C-A-T-S-G-D-G-L-Y-E-G-L-L-D-W-L-S-N-Q-L-   y64
b176 R-N-Q-K-K-G-G-R-A-D-P-A-F-L-Y-K-V-V-R-Y-P-A-Q-W-R-   y39
b201 P-L-E-G-G-G-G-W-S-H-P-Q-F-E-K-G-G-G-S-G-G-G-S-G-G-   y14
b226 G-S-W-S-H-P-Q-F-E-K-G-P-V                            y1
```

Ion	Observed mass	Theoretical mass	error (ppm)
b22*	2508.39	2508.39	-0.9
b24*	2736.51	2736.50	1.2
b26*	2878.59	2878.58	3.8
b27*	2935.62	2935.60	8.1
b32*	3491.96	3491.96	1.2
b39*	4323.45	4323.44	1.1
b40*	4436.53	4436.53	1.7
b41*	4535.61	4535.59	2.8
b42*	4636.66	4636.64	2.8
b43*	4737.70	4737.69	1.7
b44*	4850.79	4850.77	2.6
b227*	25318.75	25319.00	-8.7

Ion	Observed mass	Theoretical mass	error (ppm)
y7	803.42	803.42	-1.8
y8	900.47	900.47	0.9
y9	1037.53	1037.53	1.1
y10	1124.56	1124.56	0.9
y13	1454.70	1454.70	0.4
y14	1511.72	1511.72	0.5
y15	1568.74	1568.74	0.7
y16	1655.77	1655.77	1.5
y17	1712.80	1712.79	1.3
y18	1769.82	1769.81	1.8
y19	1826.84	1826.84	1.4
y23	2084.94	2084.93	2.8
y28	2714.26	2714.25	1.9
y53	5566.73	5566.72	2.1
y67	7119.54	7119.53	1.1
y68	7232.62	7232.62	0.7
y69	7418.70	7418.70	0.0
y70	7533.75	7533.72	3.6
y71	7646.82	7646.81	1.1
y72	7703.82	7703.83	-1.0
y73	7832.86	7832.87	-1.9
y74	7995.94	7995.94	0.6
y101	10990.47	10990.40	3.8
y106	11488.70	11488.70	2.5
y110	11901.86	11901.80	1.6
y175	19639.82	19639.80	3.4
y194	21778.85	21778.80	0.2

c

ARF1-strep (IpaJ C64A); 56 fragments, 18 b-ions

```
b1   Myristoyl-
     G-N-I-F-A-N-L-F-K-G-L-F-G-K-K-E-M-R-I-L-M-V-G-L-D-   y215
b26  A-A-G-K-T-T-I-L-Y-K-L-K-L-G-E-I-V-T-T-I-P-T-I-G-F-   y190
b51  N-V-E-T-V-E-Y-K-N-I-S-F-T-V-W-D-V-G-G-Q-D-K-I-R-P-   y165
b76  L-W-R-H-Y-F-Q-N-T-Q-G-L-I-F-V-V-D-S-N-D-R-E-R-V-N-   y140
b101 E-A-R-E-E-L-M-R-M-L-A-E-D-E-L-R-D-A-V-L-L-V-F-A-N-   y115
b126 K-Q-D-L-P-N-A-M-N-A-A-E-I-T-D-K-L-G-L-H-S-L-R-H-R-   y90
b151 N-W-Y-I-Q-A-T-C-A-T-S-G-D-G-L-Y-E-G-L-L-D-W-L-S-N-Q-   y65
b176 L-R-N-Q-K-K-G-G-R-A-D-P-A-F-L-Y-K-V-V-R-Y-P-A-Q-W-   y40
b201 R-P-L-E-G-G-G-G-W-S-H-P-Q-F-E-K-G-G-G-S-G-G-G-S-G-   y15
b226 G-G-S-W-S-H-P-Q-F-E-K-G-P-V                          y1
```

Ion	Observed mass	Theoretical mass	error (ppm)
b23	2774.63	2774.61	8.2
b25	3002.72	3002.72	-1.5
b26	3073.75	3073.76	-2.1
b27	3144.79	3144.80	-2.4
b29	3329.92	3329.91	2.7
b30	3430.98	3430.96	6.4
b33	3758.20	3758.18	6.9
b34	3921.25	3921.24	3.8
b36	4162.43	4162.42	3.7
b37	4290.52	4290.51	0.5
b40	4589.67	4589.66	2.2
b41	4702.76	4702.75	2.2
b42	4801.82	4801.81	1.7
b43	4902.87	4902.86	1.4
b44	5003.92	5003.91	1.9
b45	5117.00	5116.99	1.4
b49	5485.22	5485.20	4.2
b171	19663.07	19663.20	-7.7

Ion	Observed mass	Theoretical mass	error (ppm)
y7	803.42	803.42	-1.6
y8	900.47	900.47	0.1
y9	1037.53	1037.53	0.8
y10	1124.56	1124.56	0.2
y11	1310.65	1310.64	3.6
y13	1454.70	1454.70	-0.5
y14	1511.72	1511.72	0.1
y15	1568.74	1568.74	0.1
y16	1655.77	1655.77	0.3
y17	1712.79	1712.79	0.8
y18	1769.82	1769.81	0.9
y19	1826.84	1826.84	1.1
y23	2084.94	2084.93	2.0
y28	2714.25	2714.25	1.5
y53	5566.73	5566.72	1.8
y62	6521.25	6521.22	4.9
y66	7032.51	7032.50	0.9
y67	7119.54	7119.53	1.4
y68	7232.62	7232.62	-0.2
y69	7418.70	7418.70	0.0
y70	7533.75	7533.72	2.8
y71	7646.80	7646.81	-1.7
y72	7703.83	7703.83	0.2
y73	7832.88	7832.87	0.4
y74	7995.95	7995.94	2.2
y75	8109.05	8109.02	4.0
y78	8338.10	8338.09	1.6
y79	8425.15	8425.12	2.7
y91	9869.78	9869.79	-1.1
y101	10990.41	10990.40	-1.0
y104	11303.63	11303.60	3.6
y106	11488.69	11488.70	2.3
y107	11619.76	11619.70	4.1
y110	11901.89	11901.80	4.2
y191	21467.48	21467.70	-8.3
y194	21778.92	21778.80	3.8
y207	23250.83	23250.70	3.5
y209	23464.93	23464.90	2.2

Figure 11: Identification of the Glycine-2 cleavage site on ARF1 by top-down mass spectrometry.

The tandem MS/MS fragmentation maps for *N*-myristoylatedARF1 in untreated (**a**), IpaJ treated (**b**), and IpaJ C64A treated (**c**) samples (**left**). Proteins were subjected to online LC-MS and online tandem LC-MS/MS by source-induced disassociation. Two sequence tags, EIVTTI and EGLDWLS, were identified from the ARF1-strep sample MS/MS data. Searching these two sequence tags against the default human top-down protein database (official_human_TD, 117059 basic sequences, 7563274 protein forms) in ProSightPC 2.0TM identified ARF1 with a score of 2.14. ProSightPC 2.0TM was used to assign fragmentation datasets to theoretical ARF1 sequences with < 10 ppm mass accuracy (lists of matching fragment ions are presented in the corresponding Tables). These data provide an unambiguous identification of N-myristoylated ARF1-strep from these samples.

a. The *N*-myristoylated ARF1-strep (untreated sample) had 30 fragments with 8 b-ions showing the myristoyl group being localized to the N-terminal region of the protein.

b. The IpaJ treated ARF1 had 39 fragments with 12 b-ions. These provide an unambiguous assignment of ARF1-strep residues 3-240. Thus IpaJ induces the cleavage between Gly2 and Asn3, thereby liberating *N*-myritoyl glycine from the intact ARF1 protein. The "Δm mode" of ProSightPC 2.0TM facilitated the assignment of a 1 Da change in molecular mass on all b-ionsat the protein N-terminus. Evidence for a 1 Da shift in molecular weight is observed at the intact protein level as well (Figure 10b). I presume that the 1Da shift is caused by adeamidationevent, a known effect of the cysteine protease fold(Schmidt, Selzer, Lerm, & Aktories, 1998), occurring at the amino terminus of the ARF1 protein. Because a similar shift is not observed in untreated (a) or IpaJ C64A treated (b) sample, I assume that ARF1

deamidation is caused by IpaJ activity, yet the location and functional consequences of this event is currently unknown.

c. The myristoylated ARF1-strep (IpaJ C64A sample) had 56 fragments among which 18 b-ions show the myristoyl group being localized to the N-terminal region of the protein.

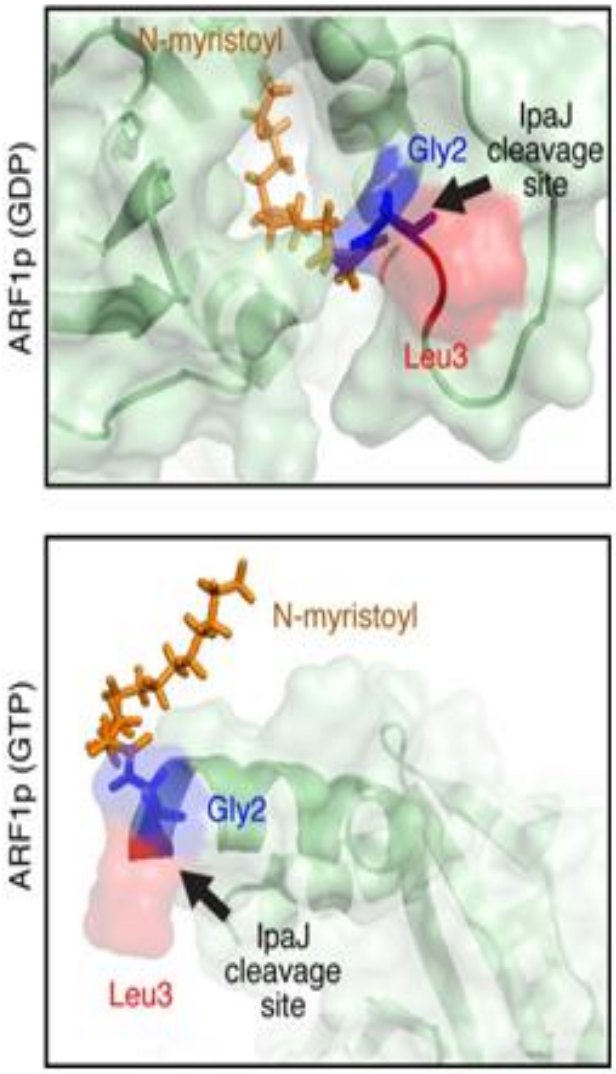

Figure 12: The ARF1 "myristoyl switch".

The structure of yeast *N*-myrisoylated ARF1p in the GDP-inactive conformation (PDB ID: 2K5U) and the GTP-active conformation (PDB ID: 2KSQ). The*N*-myristoyl group is deeply buried in GDP-inactive ARF1p (upper panel) whereas it is extended toward the membranein the GTP-ARF1p structure (lower panel).

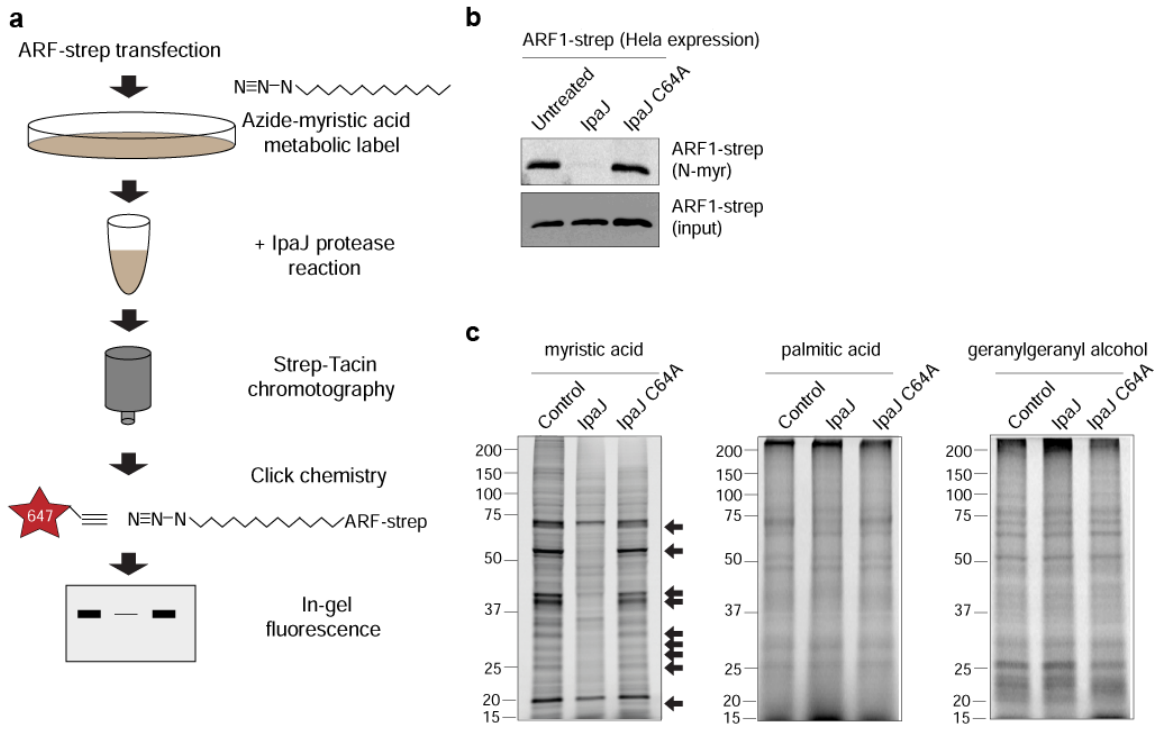

Figure 13: Metabolic labeling confirms demyristoylation of host proteins by IpaJ.

a. Diagram illustrating the procedure to directly visualize the IpaJ-catalyzed loss of myristoyl group. Cells were transfected with ARF1-strep and incubated in a presence of azide-myristic acid. After *in vitro* IpaJ cleavage, ARF1 was covalently attached to Alexa647 through the myristoyl group, purified and visualized in gel.

b. In gel fluorescence assay (top panel) visualizing Alexa647-labeled myristoylated ARF1-strep purified from HeLa cell lysates left untreated or incubated with IpaJ or its catalytic mutant as indicated. The expression levels of Arf1-strep (detected by wesern blot) are shown (bottom panel).

c. In gel fluorescence assay visualizing protein extracts isolated from HeLa cells incubated with azide myristic acid, azide palmitic acid, or geranylgeranyl alcohol azide and

subsequently labeled with Alexa Fluor 647 alkyne by Click chemistry. Arrows indicate proteins that are proteolytically demyristoylated by IpaJ.

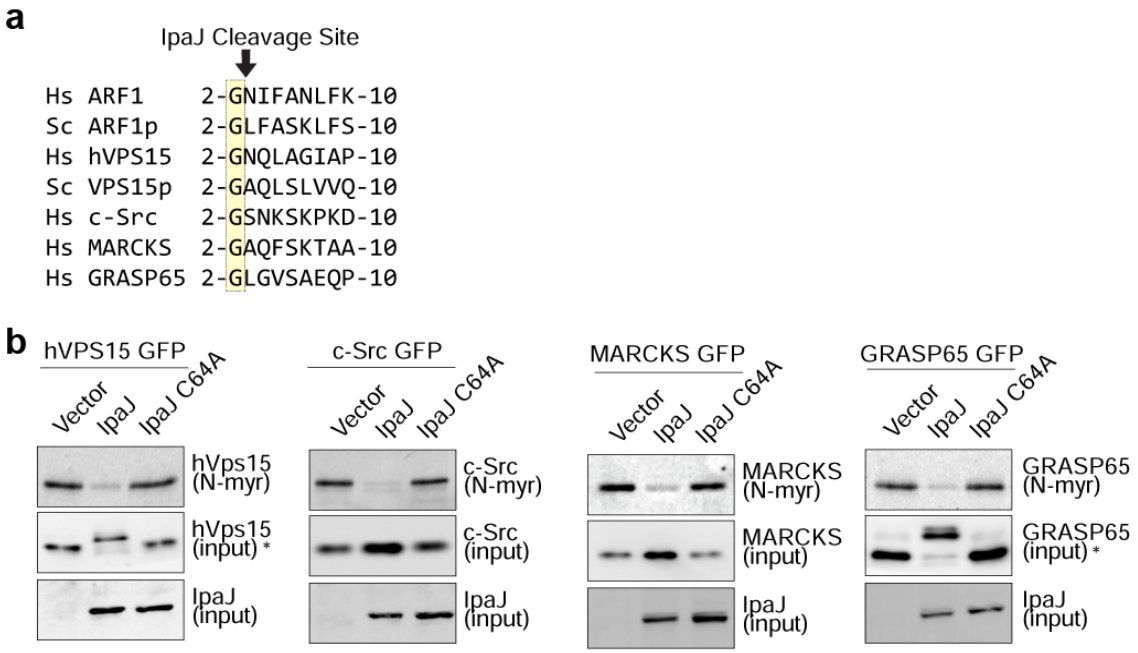

Figure 14: IpaJ cleaves diverse N-myristoylated proteins.

a. Multiple sequence alignment of *N*-myristoylated glycine and downstream sequences from the indicated proteins (*Hs Homo sapiens*; *Sc Saccharomyces cerevisae*). Alignment of the identified potential substrates identified the myristoyl-glycine as the only common motif.

b. In gel fluorescence assay showing myristoylated peptides of the indicated proteins in cells expressing IpaJ or catalytic mutant. The peptide-eGFP and IpaJ inputs are indicated. *Demyristoylation of GRASP65 and hVPS15 resulted in slower mobility of the resulting peptide, potentially due to reduced mobility in SDS-PAGE caused by proteolytic reaction.

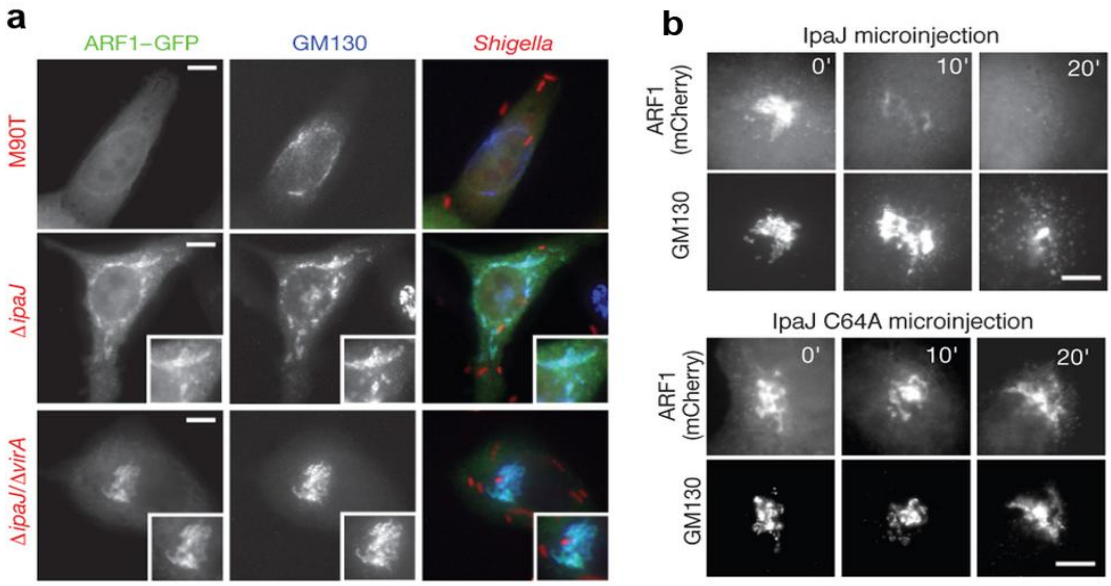

Figure 15: IpaJ releases ARF1-GTP from the Golgi membranes.

a. Fluorescence microscopy showing ARF1-eGFP (green) and the Golgi membranes (blue, GM130) after infection with *Shigella* M90T and the indicated mutants (red; mCherry expressing bacteria). Infection with wild type but not *ΔipaJ* or *ΔipaJ*/*ΔvirA*. *Shigella* results in ARF1 displacement from the Golgi membrane. Scale bar = 10µm

b. To analyze ARF1 liberation from the Golgi by IpaJ, we microinjfected recombinant IpaJ, or IpaJ C64A into HeLa cells. Fluorescence microscopy shows ARF1-mCherry and the Golgi apparatus (GM130) after cellular microinjection over the indicated time period. Scale bar = 10µm

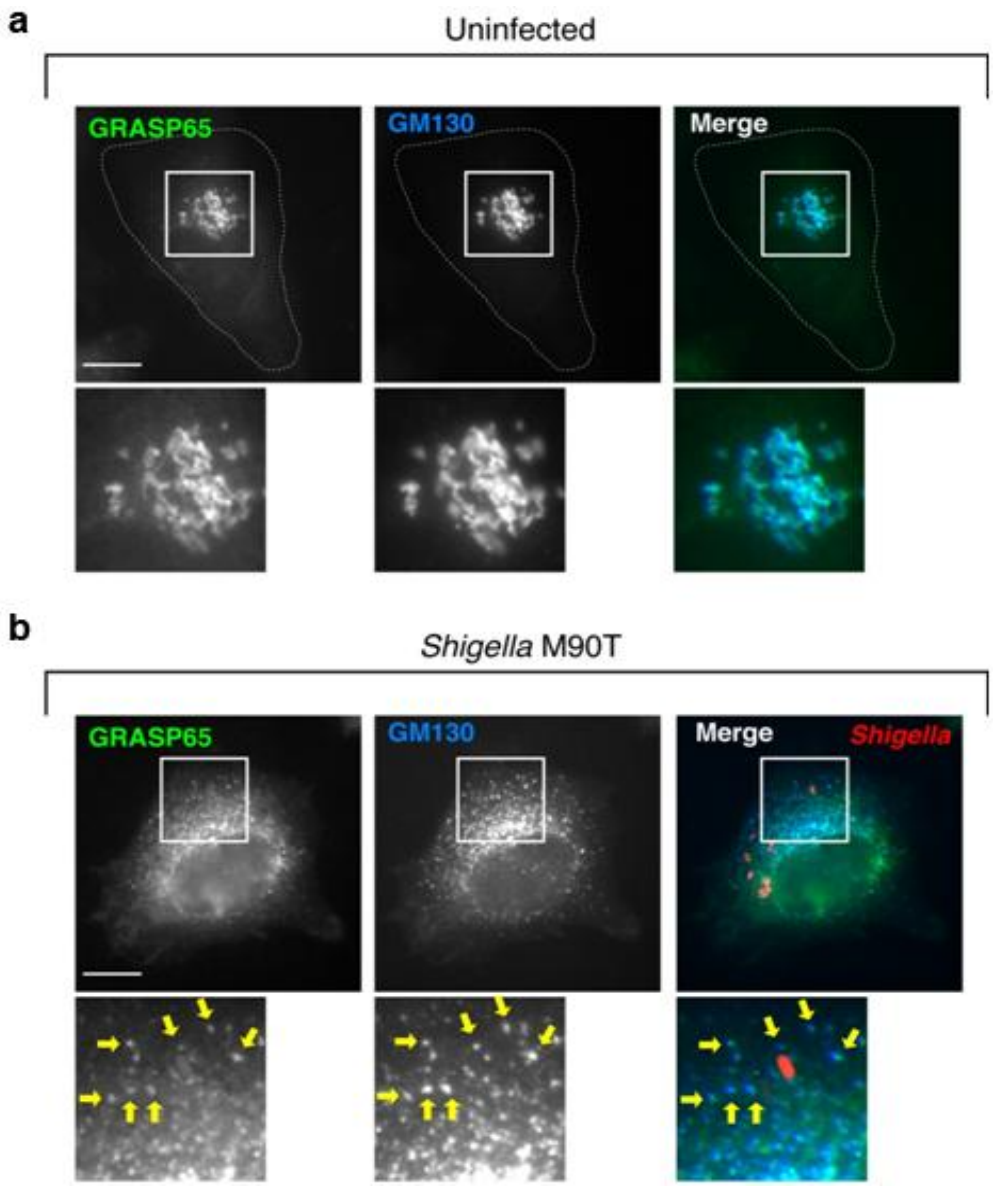

Figure 16: Subcellular localization of *N*-myristoylated GRASP65 proteins during *Shigella* infection.

a. Fluorescence microscopy of GRASP65 (green) and GM130 (blue) in untreated cells. Enlarged regions show the localization of these proteins to the Golgi apparatus.

b. Fluorescence microscopy of GRASP65 (green) and GM130 (blue) in cells infected with WT *Shigella* M90T (red). In contrast to ARF1, GRASP65 was not displaced from the Golgi

membrane upon *Shigella* infection. Enlarged regions show the localization of these proteins to disrupted the Golgi membranes. Scale bar = 10µm.

a Untreated

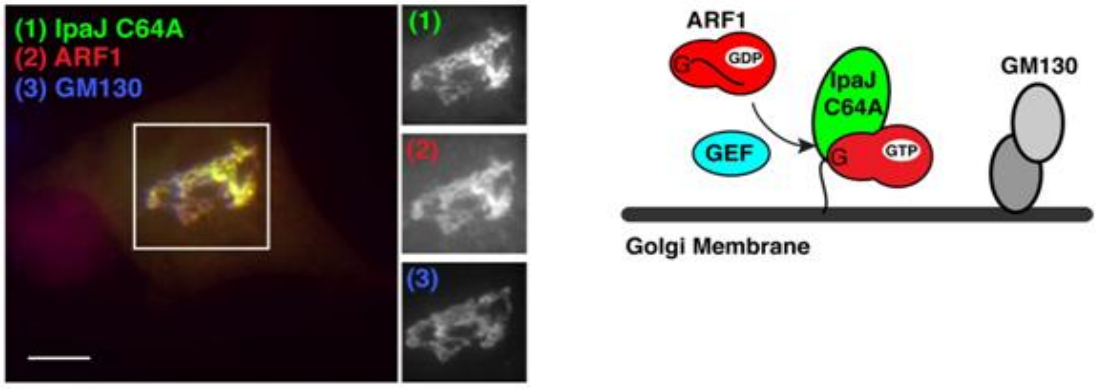

b Brefeldin A

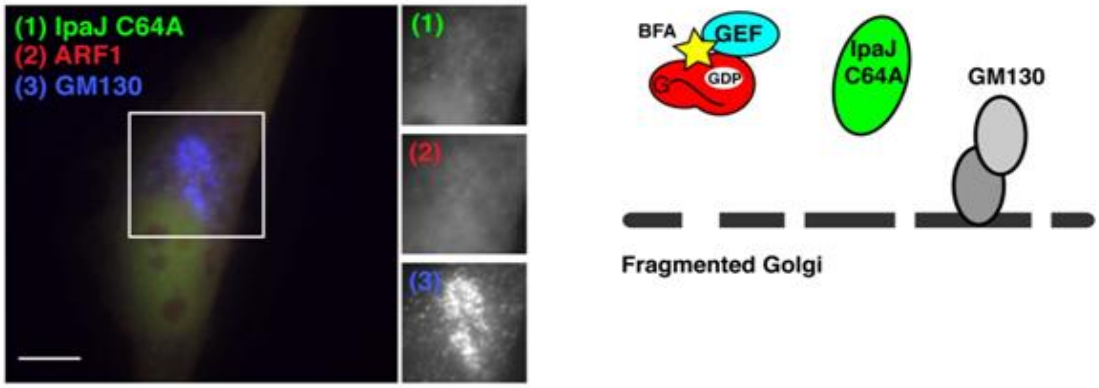

c Nocodazole

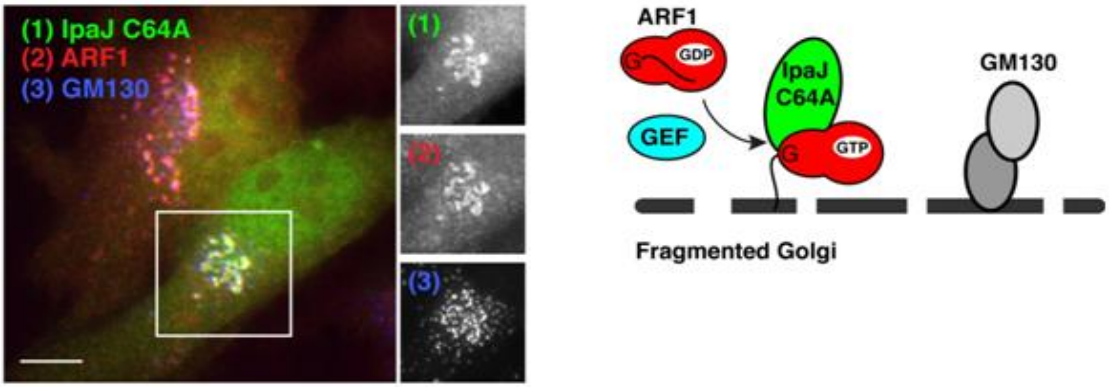

Figure 17: IpaJ C64A localizes on the Golgi in ARF-dependent manner.

a. Fluorescence microscopy of HeLa cells transfected with eGFP-IpaJ C64A (1) and ARF1-mCherry (2). The Golgi apparatus is monitored by immunocytochemistry of GM130, a membrane-associated the Golgi matrix protein (3). An illustration of the natural ARF1 activation cycle at the Golgi is shown. Scale bar = 10µm.

b. Fluorescence microscopy of HeLa cells transfected with eGFP-IpaJ C64A (1) and ARF1-mCherry (2) and treated for 20 minutes with BFA. The Golgi membranes were monitored by immunocytochemistry of GM130, membrane associated the Golgi matrix proteins (3). Also shown is an illustration highlighting the effects of BFA on both ARF1 and IpaJ C64A localization, as well as the Golgi fragmentation. Scale bar = 10µm.

c. Fluorescence microscopy of HeLa cells transfected with eGFP-IpaJ C64A (1) and ARF1-mCherry (2) and treated for 1 hour with Nocodazole (10µg/ml). The Golgi apparatus monitored by immunocytochemistry of GM130, a membrane-associated the Golgi matrix proteins (3). An illustration highlighting the effects of Nocodazole on both ARF1 and IpaJ C64A localization, as well as the Golgi fragmentation, is shown to the right. Scale bar = 10µm.

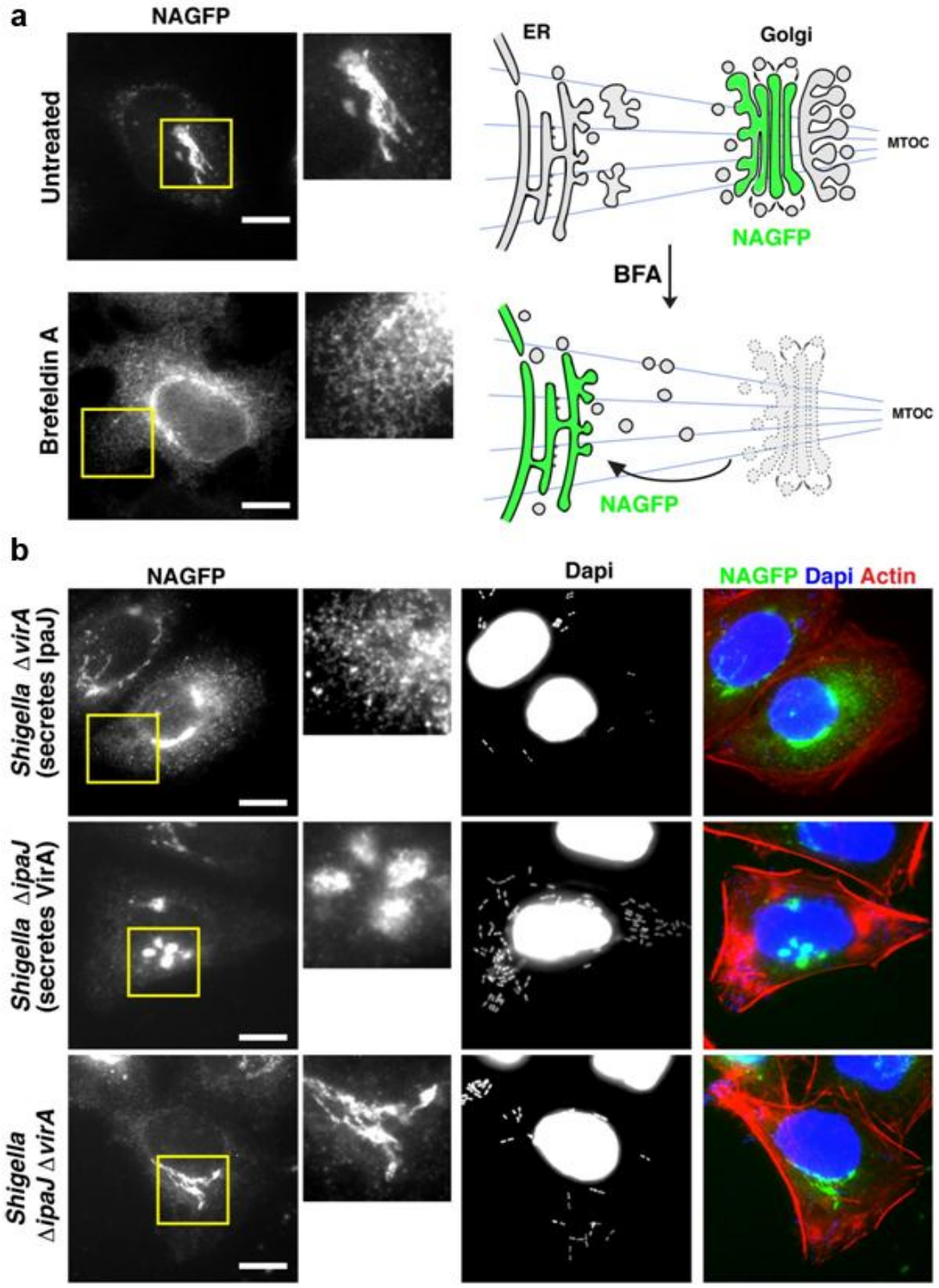
a
NAGFP
Untreated
Brefeldin A
ER
Golgi
MTOC
NAGFP
BFA
MTOC
NAGFP
b
NAGFP
Dapi
NAGFP Dapi Actin
Shigella ΔvirA (secretes IpaJ)
Shigella ΔipaJ (secretes VirA)
Shigella ΔipaJ ΔvirA

Figure 18:The cellular action of IpaJ phenocopies Brefeldin A.

a. Fluorescence microscopy of NAGFP (green) in untreated (upper image) and BrefeldinA (lower image) treated cells. Enlarged regions show the clear Golgi and ER morphologies, respectively. Cartoon diagram (right panel) shows the expected localization of NAGFP before (upper diagram) and after (lower diagram) BFA treatment. Under normal conditions NAGFP resides in the medial Golgi compartment. Cellular treatment with BFA induces its redistribution into the Endoplasmic Reticulum (ER).

b. NAGFP (green) expressing HeLa cells were infected with the indicated mutant *Shigella* strains for 4 hours and visualized by fluorescence microscopy. Importantly, NAGFP redistributes to ER in *Shigella* Δ*virA* infected cells, a gene deletion mutantt hat secretes IpaJ (enlarged image). The ER distribution of NAGFP induced by IpaJ phenocopies BFA treatment (compare to **a**). To compare the Golgi disruption phenotype caused by IpaJ to that of VirA, I examined the localization of NAGFP in cells infected with *Shigella* Δ*ipaJ*,a gene deletion mutant that secretes VirA. NAGFP formed large membrane aggregations in *Shigella*Δ*ipaJ* infected cells (enlarged image). This phenotype did not resemble BFA, which is consistent with the function of VirA as a Rab1 specific GAP(Dong et al., 2012).In control experiments, I found that *Shigella* Δ*ipaJ/virA* double mutant had no effect on NAGFP localization. The merged image shows NAGFP (green), Dapi (blue, shows both Hela nuclei and *Shigella* DNA), and F-actin (red, Rhodamine-phalloidin).

Materials and methods:

Plasmids and cloning:

Bacterial effector genes were PCR amplified from *Shigella flexneri* M90T and cloned into pEntr/D, generating a Gateway™ compatible entry clone (Invitrogen) according to manufacturer recommendations. Twenty *Shigella flexneri* effectors were cloned into pEntr/D vector: IpaA: AAK18443.1, IpaB: AAK18446, IpaH1.4: AAK18594.1, IpaH2.5: AAK18367, IpaH4.5: AAK18395, IpaH7.8: AAK18394.1, IpaH9.8: AAK18544, IpaJ: AAK18440, IpgD: AAK18452, IcsB: AAK18450, OspB: AAL72323.1, OspC1: AAL72322.1, OspC2: AAW64906, OspD1: AAW64782, OspE1: AAW64916, OspE2: AAW64805, OspF: AAW64770, OspG: NP_085391, VirA: AAK18501. For mammalian expression the effectors were then recombined into modified pcDNA3.1 vector carrying NH_2-terminal eGFP or mCherry in frame with the Gateway cassette (Gateway™ vector conversion system, Invitrogen). For bacterial expression50 amino acid NH_2-terminal deletion of IpaJ (IpaJΔ50; residues 51-259) was cloned in frame into pGEX-4T1 (GST-tag) (Amersham), yielding intact catalytic domain of IpaJ COOH-terminally fused to GST-tag. NH_2-terminal deletion of ARF1 (ARF1Δ17; residues 18-181) was PCR subcloned into pGEX-4T1 vector. Human GGA1 (GAT domain, residues 76-215) was PCR amplified and cloned in frame into pET28b-MBP-His vector. For complementation of *Shigella flexneri* knockout strains *ipaJ* was PCR amplified and cloned into pBad/Myc-His vector to be expressed under arabinose-inducible promoter. *mcherry* was expressed from the *rpsD* promoter in pDP151 vector in *Shigella strains*. For galactose-induced yeast expression, *ipaJ* was recombined from pEntr/D into

Gateway^{TM} compatible pYes-Dest52 vector (Invitrogen) for expression under galactose inducible promoter. Yeast *arf1* and *arf2* (SGD:S000002351, SGD:S000002296) were PCR amplified from Yep13 genomic clones and cloned into p415 vector for yeast expression from a constitutively active promoter (GAPDH). Human full-length *arf1* was cloned in frame into modified pcDNA3.1 vector carrying COOH-terminal mCherry or eGFP. Human GRASP65 was cloned in frame into peGFP-N2 vector. For expression of Strep-tagged full-length human ARF1 in mammalian cells, the *arf1* cDNA (Missouri S&T cDNA Resource Center; #ARF0100000) was first cloned into pEntr/D entry vector. The gene was then recombined into modified pcDNA4T/O vector carrying Gateway^{TM} cassette and two repeats of COOH-terminal Strep-tag (Trp-Ser-His-Pro-Gln-Phe-Glu-Lys, IBA GmbH). For expression of leader peptides bearing myristoylation signal sequences derived from c-Src, MARCKs, hVPS15, and GRASP65, cDNA sequences encoding 10 NH_2-terminal amino acids (see Figure 4A) were cloned into modified pcDNA4T/O vector carrying COOH-terminal GFP and two repeats of Strep-tag. All site-directed mutations were generated using the QuickChange Site-Directed Mutagenesis Kit (Stratagene). Additional primer and plasmid information is available upon request.

Bacterial infection of cultured cells:

For *Shigella* infections, HeLa or HeLa cells stably expressing a green fluorescent protein (GFP) tag attached to the NH_2-terminal Golgi retention signal of *N*-acetylglucosaminyltransferase I(Shima et al., 1997) (NAGFP HeLa), were seeded onto coverslips in 6-wells dishes the day before infection. Sodium butyrate at 5 μM was added to

NAGFP cells after seeding to stimulate production of the Golgi-localized GFP marker(Shima et al., 1997). *Shigella* strains were inoculated from frozen stocks and grown overnight at 30°C in Brain-Heart Infusion media (BHI) (Difco^{TM}, BD Biosciences). Bacteria were then back diluted 1:50 and incubated at 37°C until reaching OD_{600}~ 0.5-0.6. Bacteria were then washed in 1X phosphate buffer saline (PBS) and incubated at 37°C for 15 minutes in 0.003% Congo Red. 20 µl of bacterial suspension was then added to each well of 6-well dish of semi-confluent HeLa or NAGFP cells and centrifuged for 10 minutes at room temperature (1000xg) to facilitate bacterial adherence. The plates were then incubated for 90 minutes at 37°C, 5%CO_2. The media was removed and the wells were washed three times with gentamicin (150 µg/ml) followed by three washes with sterile PBS. Fresh antibiotic-free DMEM was added to each well after that and cells were incubated an additional 2-4 hours (37°C, 5% CO_2). Following incubation, the slides were fixed in 3.7% formaldehyde and prepared for microscopy. The Golgi and F-actin were visualized with anti-GM130 (BD Transduction Laboratories) and rhodamine-phalloidin (Molecular Probes) respectively. For infections with *Shigella flexneri* knockout strains complimented with IpaJ (wild type and C/H/D mutants) overnight bacterial cultures were diluted 1:50 in BHI containing 2% arabinose and incubated until reaching OD_{600}~ 0.5-0.6 as described above. Infections were performed in low glucose media containing 2% arabinose to allow expression of IpaJ from arabinose-inducible promoter. For infections with *Shigella flexneri* strains expressing mCherry ampicillin was added both to BHI and DMEM culture media.

A protocol for *Salmonella* infection of HeLa cells was adapted from previous studies (Steele-Mortimer et al, 1999). *Salmonella typhimurium* was grown overnight at 37°C in a

glass flask with shaking then subcultured (1:30) and grown 3 hours. 1ml was pelleted, suspended in 1X PBS and added dropwise at various concentrations to semi-confluent HeLa cells in low glucose DMEM+10% FBS. Cells were incubated (37°C, 5% CO_2) for 10 minutes, washed three times with PBS, and incubated an additional 15 minutes (37°C, 5% CO_2) in fresh low-glucose DMEM + 10% FBS. Cells were washed again with PBS and incubated in DMEM + 10% FBS + 100 mg/ml gentamicin before fixing with 3.7% formaldehyde at various time points. Cellular phenotypes were visualized as described.

Listeria monocytogenes was grown and prepared for HeLa infection as described (Shiloh et al, 1999). Various concentrations of bacteria were added to semi-confluent HeLa cells in DMEM + 10% FBS from an overnight culture of *Listeria* grown in BHI media. Cells were centrifuged (250xg, room temperature, 5 minutes) and incubated (37°C, 5% CO_2) for 10 minutes, then washed three times with 1X PBS. Fresh media containing 10-mg/ml gentamicin was added and cells incubated an additional 4-6 hours before fixation and visualization.

Gene disruption in Shigella:

The *virA*, *ipaJ* and *mxiD* genes were individually disrupted using the λ red recombinase mediated recombination system (Datsenko & Wanner, 2000). Briefly, a kanamycin resistance cassette flanked with 50 base pairs homologous to the gene of interest (*virA*, *ipaJ* or *mxiD*) was amplified from plasmid DNA (pKD3) (primer sequences are available upon request). PCR products were electroporated into *Shigella flexneri* strain M90T carrying the red recombinase plasmid pKD46. Transformants were selected by growth on LB

agar plates containing kanamycin (50µg/ml) and simultaneously cured of pKD46 by growth at 42°C overnight. The kanamycin resistance gene was eliminated through the introduction of the pCP20 helper plasmid that contains the FLP recombinase. Subsequent curing of pCP20 was carried out by growing strains at 42°C for 5 hours. Disruption of the *virA* and *ipaJ* genes was confirmed through DNA sequencing of the respective genetic loci. To generate the double strain (*Shigella* Δ*virA*/Δ*ipaJ*) the *ipaJ* locus was disrupted from a *Shigella* Δ*virA* strain following the protocol described above.

IpaJ bioinformatics:

HHpred was used to detect known Pfam domains (profile database search used: pfam version: 25.0) with distant structural homology relationships to full length IpaJ (GI:12329066) with default parameter settings (Soding, Biegert, & Lupas, 2005). The DUF3335 (C39-like peptidase family) gave a probability score of 90.0. One hundred proteins in the Pfam database contain this domain. PROMALS3D was used to produce a multiple sequence alignment with the eight IpaJ and one hundred DUF3335 family members to identify invariant catalytic residues and confirm conserved secondary and hydrophobicity patterns(Pei, Kim, & Grishin, 2008).

Recombinant protein expression and purification:

*R*ecombinant proteins (IpaJΔ50, ARF1ΔN17, GGA1$_{76\text{-}215}$) were expressed in BL21-DE3 E. coli strains by induction with 0.4 mM IPTG for 16 h at 18 °C. Pellets were lysed with His buffer (100 mM HEPES, pH 7.5, 300 mM NaCl) or GST buffer (TBS; 50 mM Tris

pH 7.5, 150 mM NaCl, 2 mM DTT) supplemented with protease cocktail (Roche). Proteins were purified with nickel agarose (Qiagen) or glutathione Sepharose (Amersham Biosciences) following manufacturer's instructions. Eluted proteins were buffer exchanged into TBS using concentration centrifugal columns (Millipore), glycerol was added to 15% and the proteins were then stored at −80 °C.

Cell transfections, microinjections and fluorescence microscopy:

HEK293A, HeLa and NAGFP HeLa (see above) cells were transfected using FuGene6 (Roche) and incubated for 16–18 hours. For expression of Strep-tagged proteins HEK293T were transfected using calcium phosphate and incubated for 18-24 hrs. Equal amounts of DNA were used for co-transfection. Cells were then lysed (lysis buffer: 20 mM Tris HCl pH 7.5, 1.5 mM $MgCl_2$, 350 mM NaCl, 0.5% NP-40, 5% glycerol) and sonicated for 5 seconds. The lysate was then clarified by centrifugation (15,000xg, 10 minutes) and applied to Strep-Tactin Superflow Plus resin (Qiagen). After incubation (90 minutes, $4^{O}C$) the column was washed 3 times (washing buffer: 20 mM Tris HCl pH 7.5, 1.5 mM $MgCl_2$, 150 mM NaCl, 0.2% NP-40, 5% glycerol) and Strep-tagged proteins were eluted with 2.5 mM desthiobiotin (100 mM Tris·HCl, 150 mM NaCl, 1 mM EDTA, 2.5 mM desthiobiotin, pH8.0). Microinjections of IpaJΔ50 were performed using a semiautomatic InjectMan NI2 micromanipulator (Eppendorf). Recombinant proteins were diluted in 1X Tris buffer saline (TBS) with Cascade Blue (Invitrogen) fluorescent dyes until the final concentration of the protein of 1 mg/ml (21μM). Cellular concentration of microinjected protein was estimated as 1μM. For IpaJ C64A and ARF1 co-localization studies HeLa cells

were treated either with Brefeldin A (2.5 μg/ml) for 20 minutes or with nocodazole (10 μg/ml) for 1 hour before fixation. Immunofluorescence images in all experiments were acquired with Zeiss AxioVert 200 Fluorescence Microscope. F-actin was visualized by rhodamine- or Alexa350-conjugated phalloidin (Molecular Probes), the Golgi was detected by GM130 antibodies (BD Biosciences) and secondary anti-mouse IgG antibodies (Thermo Scientific). NAGFP HeLa cells stimulated for production of GFP marker were additionally stained with anti-GFP antibodies (Clontech) and fluorescein-conjugated anti-rabbit IgG secondary antibodies (Thermo Scientific) to enhance fluorescent signal.

Galactose-induced yeast growth inhibition and Yeast multicopy suppressor screen:

Yeast InvscI strain was transformed with pYes-dest52 (Invitrogen) vector carrying *ipaJ* gene (wild type or C/H/D catalytic mutant) under the GAL1 inducible promoter. Yeast was streaked onto Yc-U agar media containing glucose or galactose and rafinose as carbon source. Yeast was cultured for at 30°C for 3-5 days and the plates were visually inspected for growth. For the yeast multicopy suppressor screen, *ipaJ* gene was stably integrated into Y7092 yeast strain genome (MATα *can1*Δ::STE2pr-Sp_*his5 his3*Δ*1leu2*Δ*0ura3*Δ*0met15*Δ*0 lyp1*Δ) as previously described(Alto & Dixon, 2008). Resulting strain Y7092-IpaJ (MATα *can1*Δ::STE2pr-Sp_*his5 his3*Δ*1leu2*Δ*0ura3*Δ*0met15*Δ*0 lyp1*Δ trp1Δ::GAL1-IpaJ-URA3) is carrying single copy of *ipaJ* gene under control of GAL1 galactose-inducible promoter. Y7092-IpaJ cells were then transformed with *S. cerevisiae* genomic library in the Yep13 vector (ATCC) and transformants were selected for survival on Yc-UL media containing 2% galactose and 1% raffinose as carbon sources. Positive clones were isolated and library

vectors were sequenced. For complementation assay PCR-amplified yeast *arf1* and *arf2* were expressed in yeast under GAPDH promoter (see above).

Top-Down Mass Spectrometry:

Strep-tagged ARF1 protein was co-transfected with IpaJ or control vector. Arf1-strep was purified with Strep-Tactin Superflow Plus column and eluted with 2.5 mM desthiobiotin buffer (see above). Purified Arf1-strep was used for LC-MS/MS analysis.

LC-MS/MS instrumentation and analysis was generally performed as previously described (Roth et al., 2011). Optima® grade solvents and acids (Thermo Scientific, Waltham, MA) were used. RPLC capillary columns were packed in-house to a length of 15 cm with 5 µm diameter C18 Poroshell-300® resin (Agilent Technologies, Santa Clara, CA) in 75 µm I.D. x 360µm O.D. Picofrit® columns (New Objective, Inc., Woburn, MA) with 15 µm I.D. integrated micro-electrospray tips. A capillary column heater (Analytical Sales & Services, Pompton Plains, NJ) was used to maintain the column temperature at 60 °C during analysis. RPLC mobile phase A included 0.025% TFA, 0.3% formic acid and 5% acetonitrile in water. RPLC mobile phase B included 0.025% TFA, 0.3% formic acid and 20% isopropanol in acetonitrile. The elution gradient was 0% B at 0-3 min, 45% B at 3.01 min, and 45-60% B from 3.01-23 minutes. Flow was regulated by an 1100-nano-LC (Agilent, Santa Clara, CA) at a 0.5 µL / min flow rate.

Prior to analysis, the protein was desalted using a C4 ZipTip® (Millipore, Billerica, MA) as described previously and suspended in 0.2% formic acid in water. Approximately 1600 fmole of protein was loaded onto the capillary column per injection. Analysis was

performed on an LTQ Orbitrap XLTM (Thermo Scientific, Waltham, MA) in full MS mode at 60,000 FTMS resolution, 2 microscans, maximum ion accumulation time of 500 ms, scan range from 800-2000 m/z, source induced dissociation = 25 V, tube lens 100 V, capillary voltage 50 V, capillary temperature 275 °C. MS/MS data was collected with the source induced dissociation = 60 V, tube lens 100 V, capillary voltage 50 V, capillary temperature 375 °C. The [M +6H]6+ charge state of ubiquitin was used to tune the mass spectrometer. The "Xtract" function in the XcaliburTM (Thermo Scientific, Waltham, MA) data system with a signal to noise of 3 was used to extract intact protein and fragment masses from the raw spectral data. All fragmentation data presented was the summation of scans across the entire protein elution profile. MS/MS datasets were interrogated with Prosight PC 2.0TM (Thermo Scientific, Waltham, MA). Analysis of the MS/MS data against the known ARF1 sequences without the correct modification state led to few or no b-ion matches. Replicate analysis were performed on each sample and assigned fragment ions were manually validated in raw data.

Labeling N-myristoylated proteins by Click Chemistry and in vitro cleavage reaction:

For metabolic labeling in mammalian cells myristic acid-azide (Invitrogen) was added to the cell cultures 6 hours after transfection at final concentration 10 uM and incubation was continued overnight. Next day Strep-tagged proteins were purified using Strep-Tactin SuperFlow Plus columns (see above). *N*-myristoylated proteins were labeled with Alex Fluor® 647 Alkyne as described above. Column was then washed and proteins were eluted with 2.5mM desthiobiotin elution buffer. Purified proteins were separated on

SDS-PAGE gel and transferred onto nitrocellulose paper (Biorad) for probing with STREPtactin-HRP (Biorad). Fluorescence was analyzed both in SDS-gel and on nitrocellulose paper (collectively "in gel fluorescence"). Expression of IpaJ-GFP (wild type or catalytic mutants) was confirmed by probing cell lysates with anti-GFP antibodies (Clontech) and secondary HRP-anti-rabbit IgG antibodies (Invitrogen). Expression of GRASP65- and hVPS15-GFP chimeric proteins was probed in cell lysate, before protein purification. For *in vitro* cleavage reaction Arf1-Strep transfected cells labeled with myristic acid-azide were lysed and 3µg of recombinant IpaJ Δ50 (wild type or C64A catalytic mutant) were added into 20 µl of the lysate. After incubation at 37°C for 30 minutes, myristoylated Arf1-Strep was labeled and analyzed as described above. For analysis of cleavage of multiple proteins, HEK293T were cultured in the presence of azide-modified moieties (myristic acid, palmitic acid, geranylgeranyl alcohol) according the Click-it® protocol. Cell lysates were incubated with 3ug of IpaJ Δ50 (WT or C64A) for 30 min at 37°C. Proteins containing azide-modified moieties were then labeled with Alex Fluor® 647 Alkyne and purified according for the Click-it® labeling protocol.

CHAPTER THREE
Substrates analysis and biochemical characterization of IpaJ

Introduction

The data described in the previous chapter have revealed the proteolytic demyristoylation of host proteins as a novel mechanism of bacterial pathogenesis. The outcome of this strategy is well exemplified by inhibition of GSP through the cleavage of ADP-ribosylation factor 1 (ARF1), a master regulator of endoplasmic reticulum-Golgi trafficking. The uncovered effect of IpaJ on the membrane trafficking provided the first insight into function of the protease but also raised questions that I aimed to address further. Specifically, I set out to investigate whether IpaJ cleaved other proteins besides ARF1 during infection and how it specifically recognized its substrates.

So far, ARF1 was identified as the only physiological substrate of IpaJ targeted during infection. However, I discovered that IpaJ cleaved numerous N-myristoylated proteins *in vitro* (Figure 12d, 13b). Large number of potential targets suggests that IpaJ might also cleave multiple proteins during infection, thereby affecting multiple host cell processes that are essential for the bacterial survival. The identification, yet incomplete, of all relevant targets of IpaJ would be critical to unravel the pathogenic strategy of *Shigella*.

Besides pointing at novel physiological targets, the ability of IpaJ to cleave numerous N-myristoylated proteins *in vitro* also suggests a unique mechanism of substrate specificity. Interestingly, bioinformatics analysis of secondary structures had assigned IpaJ to a poorly characterized C39 peptidase-like family of domains of unknown function (DUF3335) (Figure

6a). Putative enzymes of this family are found in more than 200 bacterial species including pathogenic *Pseudomonas aeruginosa* and *Vibrio cholera*, but IpaJ remains the only member of this group with confirmed enzymatic activity. Determining the mechanism of IpaJ specificity could shed light on the functions of the entire family, while it is currently unclear how the protease selects N-myristoylated proteins both *in vitro* and during infection.

Therefore, I performed an unbiased survey of the 'myristoylome' profile of host cells and its sensitivity to the IpaJ protease. Metabolic labeling coupled to mass-spectrometric protein identification revealed that the majority of N-myristoylated proteins were indeed cleaved by IpaJ *in vitro*. However, IpaJ demonstrated remarkable specificity in the context of infection, exclusively targeting members of the ARF and ARL families. We also discovered that E3-ubiquitin ligase ZNRF2 constitutes another potential IpaJ substrate *in vivo*. Biochemical studies established that IpaJ behaved as ARF substrate by specifically recognizing ARFs in the active state and interacting with ARFs which were normally utilized to recruit downstream host partners. Therefore, in the present chapter I describe a framework for comparative analysis of cellular 'lipidomes' in various physiological contexts. This approach has revealed remarkable difference in IpaJ substrate specificity *in vitro* and in the context of infection and highlighted its potential use for the wider applications such as studies of N-myristoylated proteins in other systems.

Results
(part of this chapter was published previously in research article)

IpaJ cleaves diverse proteins in vitro

Previously, a yeast genetic screen and infection studies defined ARF1 as one of the major substrates of IpaJ. However, this approach did not address the possibility that IpaJ could cleave other N-myristoylated proteins during infection. To investigate the potential additional substrates of IpaJ, I collaborated with Tao Peng and Howard Hang (Rockefeller University, New York, NY) to establish a system to identify N-myristoylated proteins cleaved by IpaJ. We utilized click-chemistry technique described above (see Chapter 2) to label N-myristoylated proteins and detect them later with fluorescent or affinity tags.

I incubated HeLa cells with alkyne-myristic acid for 18 hrs before the cells were lysed. The clarified lysate was split equally and incubated with either recombinant IpaJ or a mock control (IpaJ storage buffer) to cleave potential substrates (Figure 19a). The acylated proteins in the lysate were then covalently attached to rhodamine-azide and separated on a polyacrylamide gel. Since rhodamine was conjugated to the myristoyl group, I was able to directly visualize the acylated proteins. Comparison of the control and the IpaJ treated sample by in-gel fluorescence confirmed that IpaJ cleaved numerous proteins in this setup (Figure 19b).

I then asked if mass-spectrometry would allow us to identify the substrates of IpaJ. (Figure 19a). To purify acylated proteins for the analysis, I used azido-biotin tag instead of rhodamine. After IpaJ cleavage, the alkyne-myristoyl group was covalently attached to azido-biotin which allowed the enrichment of the acylated proteins on the streptavidin resin. The proteins bound to the resin were then digested with trypsin and the tryptic peptides were

analyzed by mass-spectrometry to quantify the abundance of their parent proteins (Silva, Gorenstein, Li, Vissers, & Geromanos, 2006). Since the biotin tag was attached to the myristoyl group, the relative abundance of the peptides should correlate with the myristoylation status of a given protein after IpaJ cleavage. Therefore, I expected that the proteins cleaved by IpaJ would be underrepresented in the IpaJ-treated sample compared to the control. In total, I identified 102 proteins harboring the N-terminal glycine that represents a potential site for the myristoyl modification (Appendix A). In this proof of principle experiment I focused on the analysis of the proteins for which N-myristoylation was already confirmed previously. I found 45 such proteins including members of ARF family (Appendix A). Mass-spectrometric quantification revealed that the majority of those proteins were underrepresented after incubation with IpaJ, suggesting their cleavage by the enzyme (Figure 19c). Specifically, in agreement with our previous finding that MARCKS and Src were cleaved by IpaJ *in vitro* (Figure 13), both proteins were underrepresented after the IpaJ treatment (Appendix A). Furthermore, we found that 33 out of 45 identified N-myristoylated proteins were reduced at least three-fold in the treated sample (Figure 19c). Remarkably, the list of *in vitro* substrates comprised proteins of diverse molecular functions including kinases, E3 ubiquitin ligases, and α-subunints of guanosine nucleotide-binding proteins (Appendix A). Furthermore, the identified potential substrates were involved in crucial signaling pathways such as apoptosis (apoptosis-inducing factor 2), autophagy (tyrosine-protein kinase ABL1), and immune response (tyrosine-protein kinase Lyn), suggesting that IpaJ could be exploited as a molecular tool to study the role of N-myristoylation in various signaling networks.

In the same experiment I also identified proteins which do not possess a site for the myristoyl modification (Appendix A). A potential explanation for their retention on the resin is that i) they might interact with myristoylated proteins, ii) they might incorporate metabolic derivatives of alkyne-myristoyl, or iii) they could be myristoylated on internal lysine residue, which may not be affected by IpaJ. Nevertheless, consistent with in-gel visualization, the mass-spectrometric analysis confirmed that the majority of identified myristoylated proteins were cleaved by IpaJ *in vitro* proving that this approach can be used to screen for the changes in the myristoylation profile during bacterial infection.

IpaJ is highly specific in the context of infection

After establishing the experimental system to monitor the cellular myristoylome, I asked which proteins are cleaved by IpaJ during *Shigella* infection. To identify the relevant physiological substrates, I labeled HeLa cells with alkyne-myristic acid and infected them with either wild-type or Δ*ipaJ Shigella* strain (Figure 20a). In-gel fluorescence revealed remarkable selectivity of IpaJ in the context of infection. Only one visible band (~20 kDa) had decreased intensity upon infection with wild-type *Shigella*, whereas the Δ*ipaJ* strain had no noticeable effect (Figure 20b). To identify the physiological substrates of IpaJ, we compared the myristoylation profile of HeLa cells after infection with either wild type or the Δ*ipaJ* strain using mass-spectrometry. We specifically focused on the proteins that i) harbored a site for the potential myristoylation (including those known to be modified), and ii) were decreased reproducibly in two experimental repetitions (Appendices B, C). Consistent with the in-gel visualization, we found that only a limited number of proteins were affected by IpaJ during infection (Figure 20c). Specifically, ARF1 decreased upon

infection with the wild type *Shigella* but not Δ*ipaJ* mutant strain. However, ARF1 was not the only substrate, since other ARF isoforms, namely ARF3, ARF4 and ARF5, all decreased reproducibly to the similar extent (Appendices B, C). In addition, IpaJ also targeted the members of the related ARL (ARF-like) family. Specifically, ARL1 was identified as a reproducible hit, and ARL4C, while not recovered after one infection, was found to be affected to a similar extent as ARL1 in the repeated experiment (Appendices B, C). Intriguingly, we also noticed that E3 ubiquitin ligase ZNRF2 was reproducibly and strongly affected by the wild type *Shigella* to the extent of falling below detection limit, while not significantly changed by the Δ*ipaJ* strain (Appendices B, C). To summarize, we found that in contrast to the *in vitro* setting, IpaJ is highly specific in the context of infection. Furthermore, unbiased interrogation of the myristoylome profile revealed several ARF and ARL isoforms as well as an E3 ubiquitin ligase ZNRF2 as potential novel substrates of IpaJ.

Recognition of myristoyl-glycine allows broad specificity of IpaJ in vitro

The ability of IpaJ to cleave many proteins *in vitro* and its remarkable specificity during infection suggested that IpaJ recognized common motifs of all N-myristoylated proteins as well as unique signatures of its preferred substrates. To understand the mechanism of IpaJ substrate specificity, I first asked what common features of the myristoylated proteins are essential for the cleavage by IpaJ. Since the acyl group should be in close proximity to the IpaJ active site and is shared by all identified *in vitro* substrates, it could comprise a part of the motif recognized by IpaJ. To investigate the role the myristoyl group in IpaJ proteolysis, I developed an *in vitro* assay to monitor the cleavage of recombinant myristoylated proteins (Figure 21a).

Full-length ARF1 was co-expressed with the yeast N-myristoyl transferase (yNMT) in *E.coli* BL21 strain in the presence of the azide-myristate resulting in the acylated ARF1. Since *E. coli* does not have endogenous N-myristoylated proteins, ARF1 was the major protein modified with the acyl group by yNMT. Recombinant IpaJΔ50 (truncated amino acids 1-50) was separately expressed in BL21 *E.coli.* Two cell lysates were mixed and incubated together for 30 minutes to allow ARF1 cleavage by IpaJ. After incubation, the myristoylated ARF1 was click-labeled with alkyne-Alexa647® allowing its fluorescent detection (Figure 21a). In-gel visualization revealed that IpaJ cleaved recombinant myristoylated human ARF1 (Figure 21b), therefore defining *E. coli* as a suitable system to assay the IpaJ proteolysis.

After obtaining these data, I asked whether IpaJ simply recognized the myristoyl for cleavage. Therefore, I tested whether soluble myristic acid could inhibit ARF1 cleavage by IpaJ (Figure 21c). I used the same system to express the myristoylated ARF1 in bacteria, but free myristic acid at increasing concentrations was added before mixing of lysates. The demyristoylation of ARF1-His occurred in the presence of wild type IpaJ but not IpaJ C64A mutant (Figure 21c, lane 1, 2, 9). Free myristic acid did not have any effect on ARF1 cleavage by IpaJ, suggesting that IpaJ does not simply recognize long hydrocarbon chains (Figure 21c).

I then tested if N-myristoylation is necessary for substrate cleavage by IpaJ. To this end, I expressed non-acylated ARF1 without yNMT. Recombinant IpaJΔ50 was separately expressed in BL21 *E.coli.* Similarly to the procedure described above, the lysates were mixed and incubated together for 30 minutes at 37^0C. ARF1-His was then purified using Ni-resin

and analyzed by intact protein mass spectrometry (UTSW proteomics core). Full-length ARF1 was identified in the control sample with the mass corresponding closely to the theoretical prediction (Figure 22a, b). However, the analysis of ARF1 after co-expression with IpaJ or IpaJ C64A did not detect any mass change, indicating no cleavage of ARF1 (Figure 22 c, d). Therefore, I conclude that myristoylation is necessary for proteolysis by IpaJ. Even the full-length ARF1, a well-established substrate of IpaJ, could not be cleaved without acylation. Together, these experiments indicate that IpaJ recognizes the myristoyl group, but only in the context of the acylated proteins.

To gain a better insight into the mechanism of recognition by IpaJ, I developed a flexible system to monitor the IpaJ cleavage using short peptide substrates. UTSW protein chemistry technology core synthesized the peptides corresponding to either the myristoylated or cleaved amino-terminal sequence of ARF1 (myr-Gly_2-Glu_{17} and Asn_3-Glu_{17} respectively) (Figure. 23a). Both peptides were also labeled with FITC (fluorescein isothiocyanate) on their C-termini for detection by the size-exclusion fluorescent chromatography. The myr-Gly_2-Glu_{17} peptide had a retention time of 10.8 minutes on the size exclusion column and could be easily distinguished from the Asn_3-Glu_{17} with the retention time of 12.3 minutes (Figure 23b). Therefore, the cleavage of the acylated peptide would result in the decrease of the 10.8 minutes peak and the appearance of the 12.3 minutes peak. As shown in Figure 23b, incubation of the myristoylated peptide with the recombinant IpaJΔ50 resulted in the elution profile indistinguishable from that of the non-acylated form, suggesting that I reconstituted the IpaJ proteolysis in solution. Consistent with the enzymatic mechanism of reaction, IpaJ cleaved an excess of the peptide in a time-dependent manner, while a cysteine mutant of IpaJ

did not have any effect (Figure 23c and 23d). This result indicated that i) I established the system to monitor IpaJ cleavage in solution, and ii) unlike full-length non-myristoylated ARF1, its acylated N-terminal peptide is sufficient to be a substrate of IpaJ.

The ability to manipulate synthetic peptide substrates allowed me to explore the molecular motifs recognized by IpaJ in greater details. I first asked if IpaJ distinguished the myristoyl group over other fatty acyls. In the same ARF1 peptide we substituted 14-carbon myristoyl (C14:0) for 16-carbon palmitoyl (C16:0) or 10-carbon decanoyl (C10:0), which would be impossible to do in the cellular context (Bhatnagar et al., 1998; Bhatnagar et al., 1997). The resulting peptides (palm-Gly_2-Glu_{17} and dec-Gly_2-Glu_{17}) had retention time close to 10.8 minutes, and therefore could be resolved from the non-acylated form and tested in the cleavage assay. As shown in Figure 23b, while IpaJ cleaved the myr-Gly_2-Glu_{17} completely, only small fractions of palm-Gly_2-Glu_{17} and dec-Gly_2-Glu_{17} were deacylated in the same time frame. Therefore, it is likely that IpaJ specifically recognizes 14-carbon myristoyl over other saturated fatty acids of comparable length.

It is interesting to point out that similarly to IpaJ, NMT - the enzyme that catalyzes protein N-myristoylation - is also highly specific for 14-carbon myristoyl over other fatty acyl groups (Bhatnagar et al., 1998; Bhatnagar et al., 1997). I was interested whether the two enzymes shared more similarities in substrate recognition. Specifically, steric hindrance prevents NMT from transferring the myristoyl group to amino acids larger than glycine, thereby making glycine the only residue that can be N-myristoylated. To test if the (acylated) glycine is also critical in the recognition by IpaJ, I used the ARF1 peptide with an N-myristoylated alanine (Figure 23b). Remarkably, size-exclusion chromatography did not

detect any cleavage of this peptide, suggesting that it is glycine that can be accommodated in the active site of the enzyme. Therefore, the myristoyl-glycine motif is required for recognition by IpaJ. Furthermore, close examination of the substrates identified in the *in vitro* screen (Figure 24a) revealed a great diversity in the amino acid content of their N-termini which included polar, charged, or bulky residues and even residues acylated with a large palmitoyl moiety. All these substrates were successfully cleaved by IpaJ *in vitro*, suggesting that IpaJ mostly interacts with the myristoyl-glycine, but not with the rest of N-termini. In agreement with this hypothesis, the N-termini of the identified physiological substrates from the ARF/ARL families also share little sequence similarity (Figure 24b). To test directly if myristoyl-glycine is sufficient for cleavage, I synthesized minimal IpaJ peptide substrate that only included myristoyl-glycine and lysine with attached FITC (myr-Gly-Lys). As a control for cleavage I used the peptide consisting of only lysine residue and the fluorophore (Lys). The myr-Gly-Lys had the retention time of 12 minutes and could be distinguished from Lys peptide (two peaks at 15 and 15.8 minutes) (Figure 23e). Remarkably, incubation of myr-Gly-Lys with IpaJ resulted in a significant decrease of the 12 minutes peak and the appearance of two peaks at 15 and 15.8 minutes (Figure 23e). Therefore, myr-Gly-Lys peptide was successfully cleaved by IpaJ. Although I cannot exclude that IpaJ may still have higher affinity for certain N-terminal sequences, the current results strongly suggest that for the majority of identified substrates, the recognition of the acylated glycine is necessary and largely sufficient for the cleavage by IpaJ.

IpaJ is an ARF/ARL substrate of bacterial origin

The diversity of *in vitro* substrates contrasts dramatically with the small number of proteins affected by IpaJ during infection. Seeking to understand the mechanism of specificity for ARF/ARL proteins, I asked if additional interactions beyond a myristoylated N-terminus recruit IpaJ to its major physiological substrates. In case of ARF1 the acylated N-terminal sequence (residues 2-17 in ARF1) which allows association with the Golgi membranes is followed by a GTPase domain that interacts with ARF regulators and downstream substrates. To test if IpaJ interacts with the GTPase domain, I purified recombinant proteins MBP-IpaJΔ50 (C-terminally fused to maltose binding protein with 1-50 amino acids truncated) and GST-ARF1Δ17 (ARF1 GTPase domain C-terminally fused to glutathion S-transferase). I then analyzed whether IpaJ would co-precipitate with GST-ARF1Δ17 or GST control. I found that IpaJ in fact was pulled down by the GTPase domain (Figure 25a), pointing to their direct interaction and suggesting a mechanism of ARF/ARL preferential targeting by IpaJ. Furthermore, as mentioned previously, ARF proteins cycle between GDP-bound (inactive) and GTP-bound (active) states. It is the active form that is specifically recognized by host substrates of ARF1, such as gamma adaptin ear-containing protein GGA1 (Figure 25b). Intriguingly, I found that IpaJ behaves similarly to the host substrates and specifically interacts with the GTP-bound ARF1 and ARF5 (Figure 25b, c). It is interesting to point out that in the GDP-bound state, which is recognized by IpaJ, the N-terminus of ARF1 is sequestered into a hydrophobic groove and the site of cleavage is likely inaccessible for the protease (see Figure 12). Indeed, I observed only a modest cleavage of a myristoylated GDP-restricted ARF1 mutant *in vitro* (Figure 26), which is likely explained by the poor accessibility of the acyl group in this conformation. As mentioned above, the host

substrates recognize the active membrane-associated ARFs to be properly recruited. Here I uncovered that IpaJ also specifically recognized only GTP-bound ARFs and inactivated it by proteolytic cleavage. Therefore, I conclude that IpaJ functions as an ARF substrate of bacterial origin.

Recognition of the GTP-bound ARFs indicated that IpaJ might interact with the same motifs which are utilized by ARFs host substrates. Specifically, switch I, interswitch, switch II and helix 3 of ARF1 undergo major conformational rearrangements upon guanine exchange, thereby allowing GTP-dependent interaction with downstream targets (Donaldson & Jackson, 2011; Kahn, 2009). To test if IpaJ also recognized these structural elements, I introduced single and double point mutations into these regions and tested interaction of ARF1 mutants with IpaJΔ50. For this analysis I chose to mutate the residues that were previously shown by crystal structures or mutational screens to interact with guanine exchange factors, GTPase activating proteins or downstream substrates POR1, MKLP1, GGA1, LTA1, AP-1, and COP subunits (Table 4) (Goldberg, 1998; Kuai, Boman, Arnold, Zhu, & Kahn, 2000; Kuai & Kahn, 2000; Luo et al., 2005; Ren, Farias, Canagarajah, Bonifacino, & Hurley, 2013; Shiba et al., 2003; Wu, Lu, Hong, & Song, 2004). *In vitro* pulldown experiments revealed that ARF1 double mutants I49T/F51Y, W66H/D72A, and W78C/R79G were significantly impaired in their ability to bind IpaJ, whereas I46D form had increased affinity (Figure 25d). To map the interaction sites more precisely, we made ARF1 forms harboring single mutations and tested them in the same assay. Three mutations - I49T, W66H, and W78C – had abolished the interaction with IpaJ, and D72A had mild effect (Figure 25e). Other ARF1 forms, including I46K (opposite charge with I46D), did not differ

significantly from the wild type protein in this experiment (Figure 25e). The identified critical residues, I49, W66, and W78C belong to switch I, interswitch, and switch II respectively, suggesting that all three elements interact with IpaJ. To summarize, I found that IpaJ specifically recognized active forms of ARFs even without the myristoylated N-terminus. Moreover, IpaJ utilized the same critical motifs of GTPase domain that normally interact with ARFs host substrates.

ARF6 is not a substrate of IpaJ

The unbiased analysis of the myristoylome has implicated ARF6 as the only member of ARF family that is not cleaved efficiently during *Shigella* infection. To get a better insight into the selective protection of ARF6, I first tested its interaction with IpaJ *in vitro*. Surprisingly, and similarly to ARF1 and ARF5, the active ARF6 GTPase domain was able to co-precipitate IpaJ (Figure 27a). Therefore, ARF6 protection cannot be attributed to the inability of IpaJ to bind the GTPase domain. I then compared how the protease could cleave ARF isoforms upon expression in mammalian cells. When expressed alone, ARF1, ARF5, and ARL1 were localized to the Golgi, and ARF6 – near the plasma membrane, consistent with previous reports (Figure 27b, 28a) (D'Souza-Schorey, Li, Colombo, & Stahl, 1995; Peters et al., 1995). Co-expression of IpaJ induced a complete redistribution of ARF1, ARF5 and ARL1 from the Golgi membranes into the cytosol, whereas ARF6 remained highly enriched near the plasma membrane (Figure 27b, 28a), suggesting that a significant fraction of ARF6 is still myristoylated. In-gel fluorescence assay further supported the idea that ARF6 is only partially cleaved upon co-expression with IpaJ (Figure 27c, d). This result was

quite remarkable, since previously I have found that in these conditions IpaJ cut a diverse set of myristoylated proteins (see Figure 19c). Only partial cleavage of ARF6 suggests that in the cellular environment it may be poorly accessible for IpaJ. Indeed, lack of significant interaction with ARF6 is further supported by the observation that a cysteine mutant of IpaJ (IpaJ C64A) is trapped on the Golgi, but not on plasma membrane (Figure 27e, 28b). Furthermore, I noticed that the localization of IpaJ mutant on the Golgi was ARF-dependent, since the ARF inhibitor Brefeldin A rendered IpaJ completely cytosolic (Figure 27e). On top of that, when IpaJ C64A co-localizes with ARF1, ARF1 or ARL1 upon co-expression (Figure 28b). In contrast, I did not observe any enrichment of IpaJ C64A near the plasma membrane even when ARF6 was overexpressed (Figure 27e). Therefore, I found that although IpaJ interacts with ARF6 GTPase domain *in vitro*, ARF6 nevertheless is a poor substrate for the protease. I conclude that efficient cleavage of ARF6 and potentially other proteins is likely limited by other yet to be identified factors, which may include the subcellular localization of the protease or a substrate.

Conclusions

In the current chapter, I gained a deeper insight into the mechanism of *Shigella* infection using unbiased analysis of IpaJ substrates. I found that IpaJ mainly cleaves ARF/ARL GTPases and potentially the ZNRF2 E3-ubiquitin ligase during infection. This specificity was quite remarkable if compared to the list of the identified *in vitro* substrates. It is interesting to point out that I currently analyzed the IpaJ substrates only in one cell type (HeLa). It will be potentially important to test other cell types, such as macrophages, which

participate early in *Shigella* life cycle (Islam, Veress, Bardhan, Lindberg, & Christensson, 1997; Zychlinsky et al., 1996).

I identified the mechanism of substrate selectivity in the context of infection by mapping the IpaJ recognition sites on ARF to the switch I, interswitch, and switch II regions. If ZNRF2, and potentially some other proteins, will be confirmed as a physiological substrate of IpaJ, it will be important to define how they interact with the protease and compare to ARF GTPases. Since bacterial effectors often utilize molecular mimicry, it is possible that IpaJ exploits a structural motif that is shared by different host proteins for interaction with their common partners.

Altogether, these results provide the first insight into the mechanism of IpaJ substrate recognition. This study precedes and facilitates structural characterization of IpaJ that should unambiguously describe how the protease interacts with its substrates.

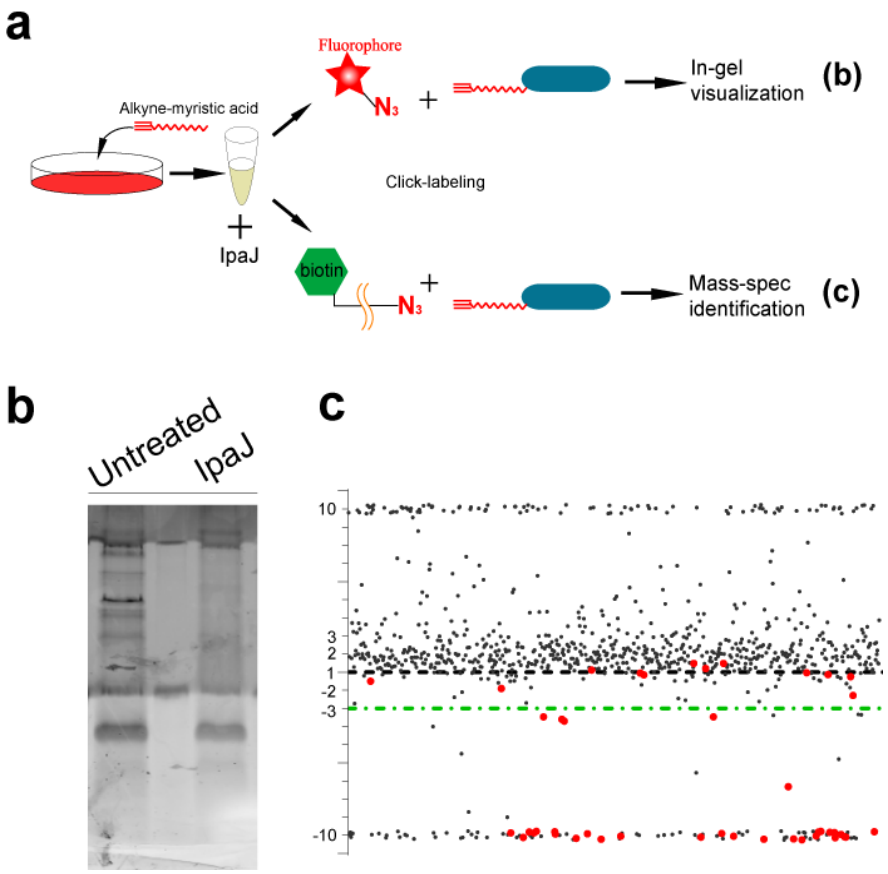

Figure 19. IpaJ cleaves majority of myristoylated proteins *in vitro*.

a. Design of the experiment to analyze protein cleavage by IpaJ *in vitro*. Cells were metabolically labeled with Alk-12. Cell lysate was split equally in two parts which were treated with recombinant IpaJ or mock control (IpaJ storage buffer). Small fractions of the lysates were visualized in gel with rhodamine-azide (Figure 19B). The rest was used to label proteins with azido-biotin tag for purification and mass-spectrometric analysis (Figure 19C).

b. In gel fluorescent visualization of myristoylome profile of IpaJ- and mock-treated HeLa lysates. Dark bands correspond to myristoylated proteins. Cleavage of proteins by IpaJ results in disappearance of the bands.

c. Result of mass-spectrometric analysis. Y-axis shows the ratio of protein abundance in IpaJ-treated sample compared to mock-treated. Proteins that are known to be N-myristoylated are shown in red, the rest are shown in black. Green dashed line marks 3-fold underrepresentation threshold in IpaJ-treated lysates. For convenience more than 10 fold over- or under-representation is shown as approximately 10).

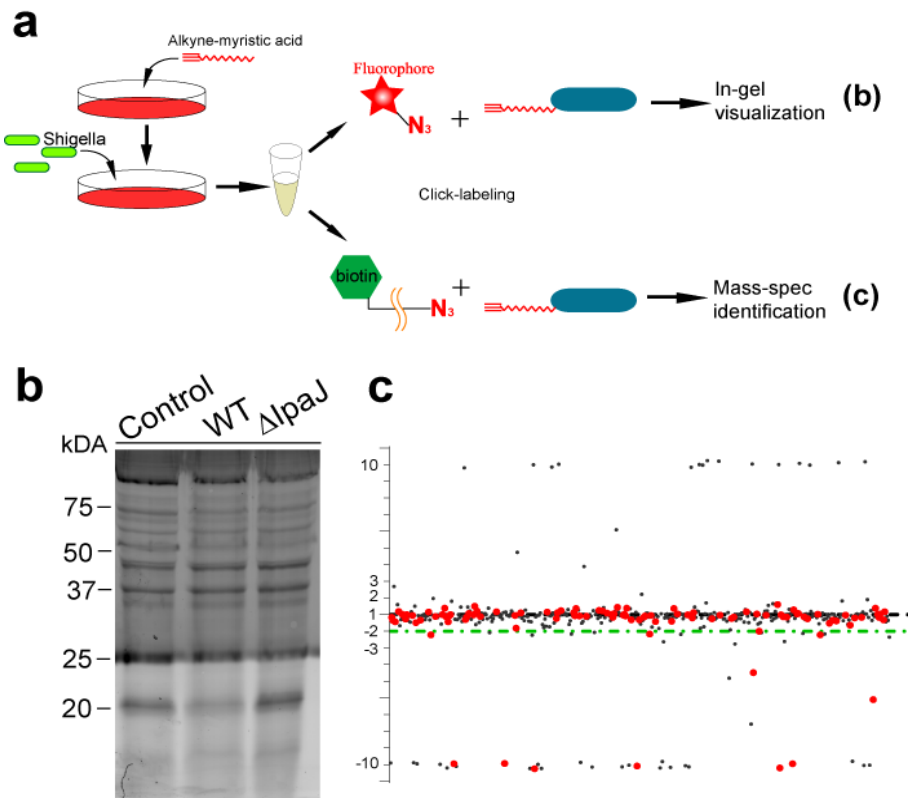

Figure 20. IpaJ has limited number of substrates during infection.

a. Design of the experiment to determine physiological substrates of IpaJ. Cells were metabolically labeled with Alk-12 and infected with wild type of *ΔipaJ* mutant *Shigella flexneri*. Cells were lysed and myristoylated proteins were labeled either with rhodamine-azide for in-gel visualization or with azido-biotin for purification and mass-spectrometric analysis.

b. In-gel visualization of myristoylome profile of non-infected HeLa cells and cells infected with wild type or *ΔipaJ Shigella* strain.

c. Result of mass-spectrometric analysis. Y-axis shows ratio of protein abundance in wild type *Shigella*-infected sample compared to cells infected with *ΔipaJ* mutant. Proteins that

have N-terminal glycine (site of potential N-myristoylation) are shown in red. For convenience more than 10 fold over- or under-representation is shown as approximately 10.

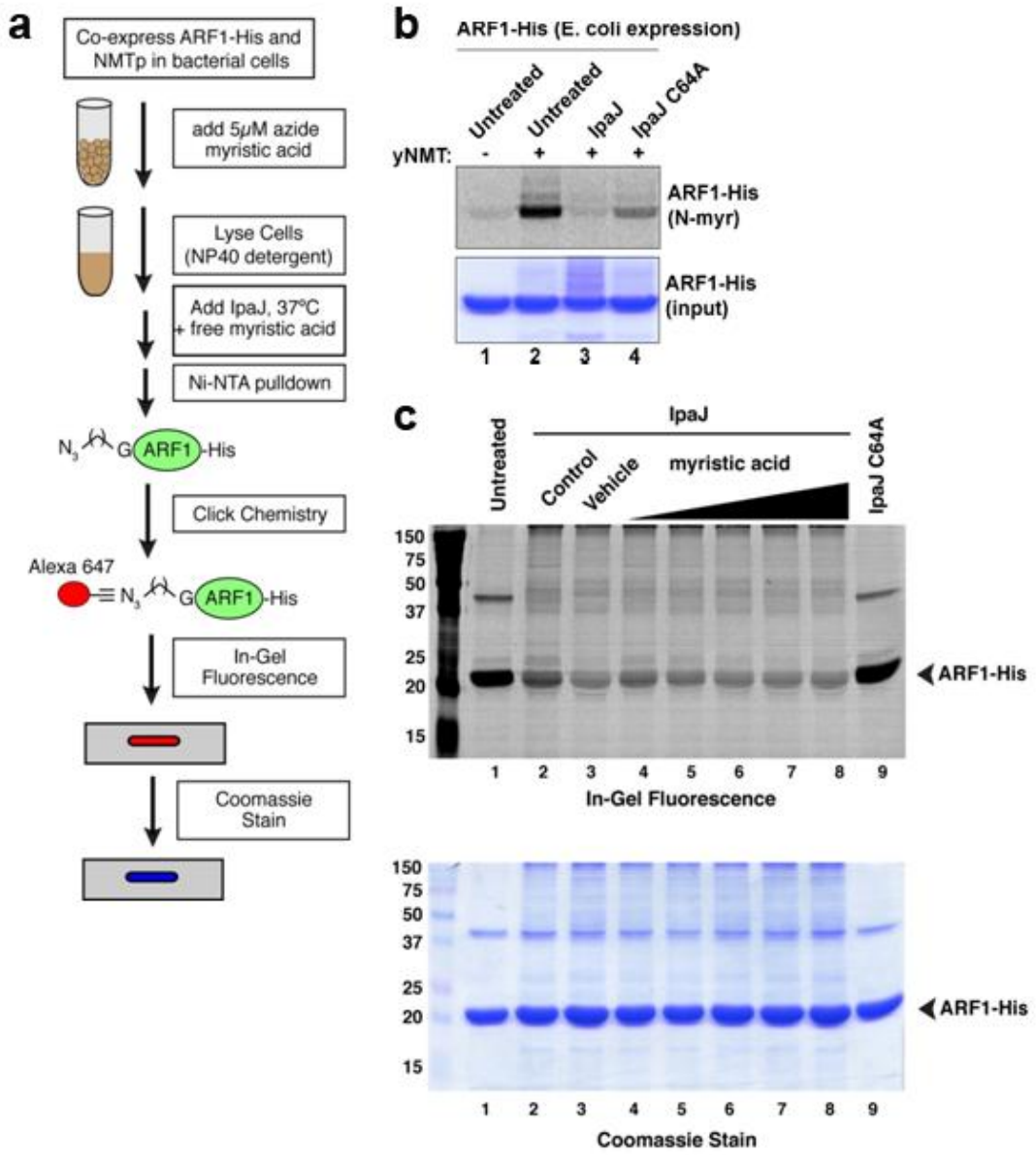

Figure 21: Free myristic acid does not inhibit IpaJ cleavage of *N*-myristoylated ARF1.

a. Diagram illustrating the procedure for the reconstitution of cleavage of myristoylated ARF1-His expressed in BL-21 *E. coli* by IpaJ. Full-length ARF1 was co-expressed with the yeast N-myristoyl transferase (yNMT) in *E.coli* BL21 strain in the presence of the azide-myristate resulting in the acylated ARF1. Recombinant IpaJΔ50 (truncated amino acids 1-50)

was separately expressed in BL21 *E.coli*. Two cell lysates were mixed and incubated together to allow ARF1 cleavage by IpaJ. After incubation, the myristoylated ARF1 was click-labeled with alkyne-Alexa647® allowing its fluorescent detection.

b. In gel fluorescence assay (top panel) visualizing Alexa647-labeled myristoylated ARF1-His isolated from bacteria either not expressing (lane 1) or expressing (lane 2) NMTp. Bacterial cell lysates treated with recombinant IpaJ or IpaJ C64A as indicated. The expression levels of Arf1-His were determined by Coommassie stain.

c. In gel fluorescence assay (top panel) visualizing Alex Fluor® 647 myristoylated ARF1-His isolated from bacteria expressing NMTp. Bacterial cell lysates were left either untreated (lane 1)or were treated with IpaJ(lane2). Neither vehicle control (DMSO) (lane 3) nor free myristic acid (1 nM, 100 nM, 10 uM, 100 uM, 1 mM*, lanes 4-8) inhibited the proteolytic cleavage. *1 mM concentration was beyond the solubility of myristic acid and some precipitate was observed. After the in gel fluorescence, the gel was stained with Coommassie Brilliant Blue to confirm equal protein loading in each reaction.

a Theoretical molecular weight of ARF1-His:

(Met1-end) = 22714.91

(Gly2-end) = 22583.72

(Asn3-end) = 22526.67

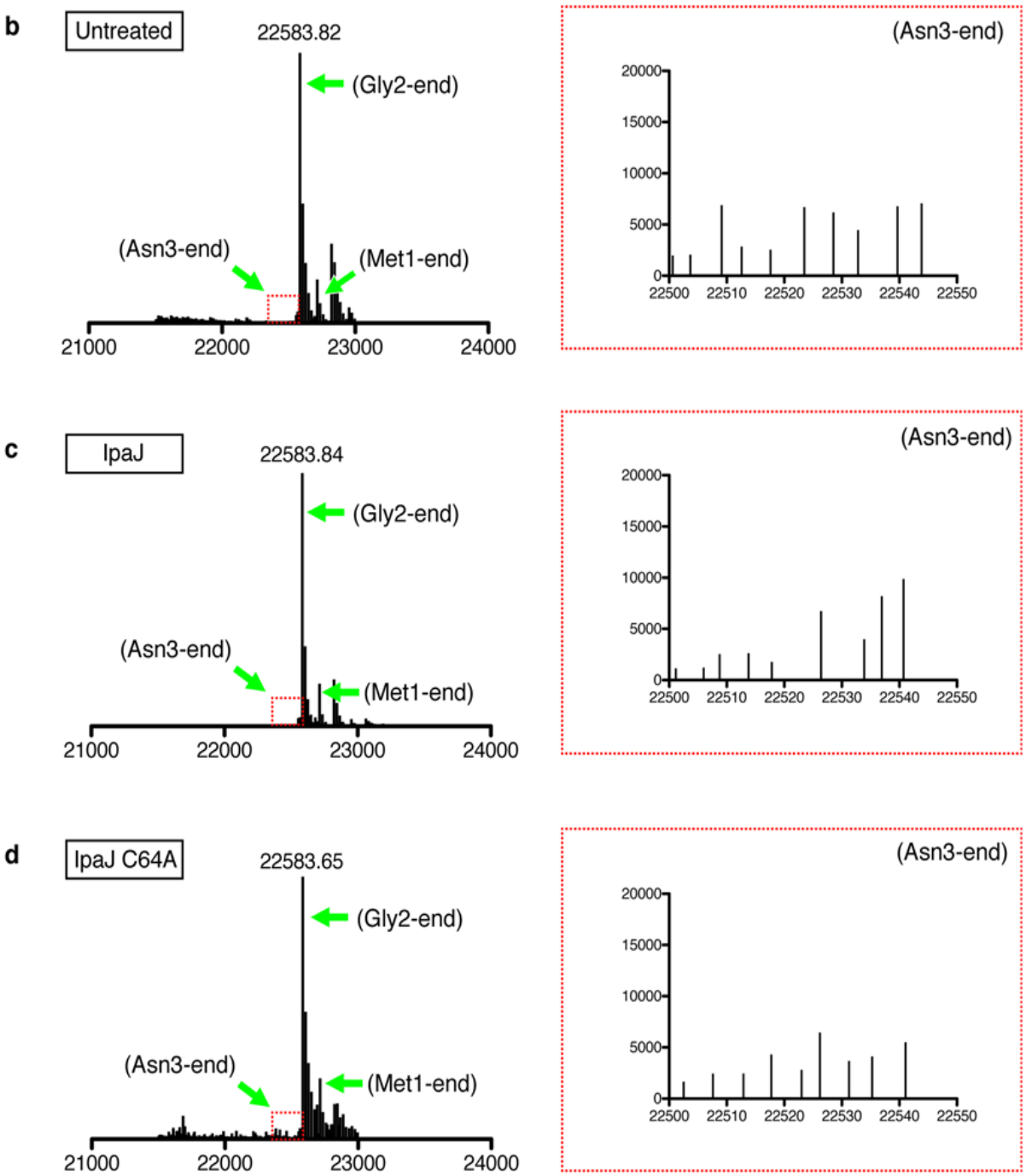

Figure 22: IpaJ does not cleave non-myristoylated ARF1.

The cleavage of ARF1-His was tested as in Figure 21a and 21b (with the exception that *E. coli* was not expressing yeast NMTp and was not exposed to exogenous myristic acid). Lysates of *E. coli* cultures producing full-length ARF1 were co-incubated with *E. coli* lysates producing IpaJ (wild type of C64A mutant) to allow IpaJ-dependent cleavage reaction. ARF1 was then purified using Ni-NTA resin and intact molecular weight was determined by mass spectrometry.

a. Diagram showing the theoretical molecular mass of expected ARF1-His forms purified from *E. coli* cultures. Full-length ARF1 (Met1-end) and ARF1-His processed by methionine aminopeptidase (Glycine2-end) are expected in all samples examined. Cleavage by IpaJ would also remove glycine-2 and expose asparagine-3, therefore producing a shorter form of ARF1 (Asn3-end).

b. *E. coli* cellular extracts expressing ARF1-His were incubated at 37°C for 30 minutes. ARF1-His was subsequently purified on Ni-NTA resin and analyzed by mass spectrometry. As expected, only the peaks representing Met1-end (22714.81) and Gly2-end (22583.83 Da) forms were found and the Gly2-end peak was predominant. No Asn3-end form was found, as shown in the inset (red box). All of the peaks in the red box represent background levels of protein.

c-d. *E. coli* cellular extracts expressing ARF1-His were incubated with the lysate containing IpaJ (**c**) or IpaJ C64A (**d**) protein at 37°C for 30 minutes and subsequently purified on Ni-NTA resin and analyzed by mass spectrometry. Importantly the mass spectrometry profile

was identical to that of untreated samples shown in (**b**). No Asn3-end form was found in either of the treated samples, as shown in the insets. Thus IpaJ requires ARF1 *N*-myristoylation to perform the cleavage reaction.

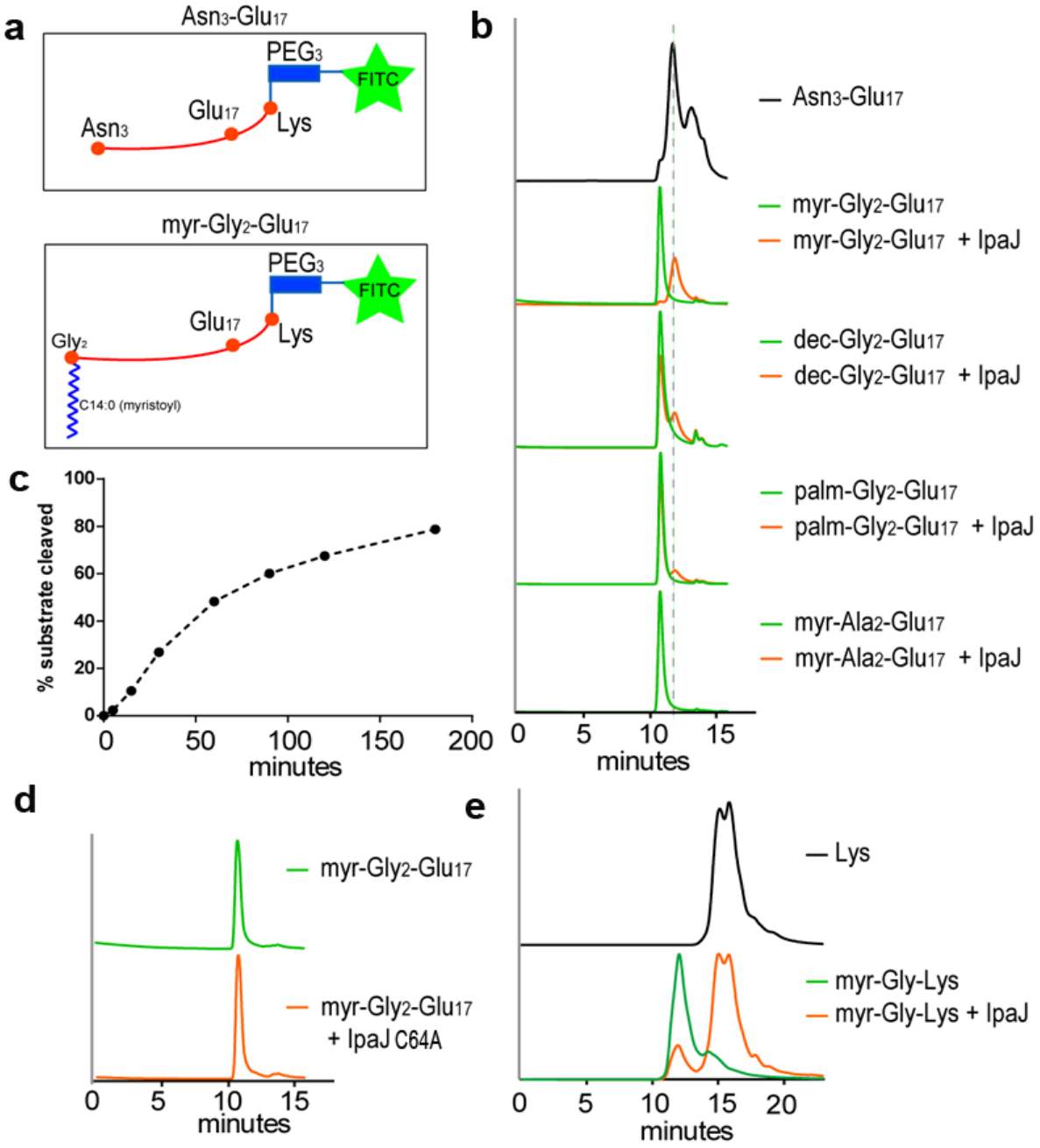
a
Asn3-Glu17
PEG3
FITC
Glu17
Lys
Asn3
myr-Gly2-Glu17
PEG3
FITC
Glu17
Lys
Gly2
C14:0 (myristoyl)
b
Asn3-Glu17
myr-Gly2-Glu17
myr-Gly2-Glu17 + IpaJ
dec-Gly2-Glu17
dec-Gly2-Glu17 + IpaJ
palm-Gly2-Glu17
palm-Gly2-Glu17 + IpaJ
myr-Ala2-Glu17
myr-Ala2-Glu17 + IpaJ
0 5 10 15
minutes
c
% substrate cleaved
100
80
60
40
20
0
0 50 100 150 200
minutes
d
myr-Gly2-Glu17
myr-Gly2-Glu17
+ IpaJ C64A
0 5 10 15
minutes
e
Lys
myr-Gly-Lys
myr-Gly-Lys + IpaJ
0 5 10 15 20
minutes

Figure 23. Cleavage of the acylated peptides.

Schematic diagram of ARF peptides. Peptides harbor the additional C-terminal lysine which was required for the synthesis. FITC was attached to the lysine side chain through polyethylenglycole(n=3).

b. Fluorescent chromatography analysis of peptide cleavage. Acylated peptides (1μM) were incubated for 30 min at 37°C with recombinant MBP-IpaJΔ50 (500 nM) and analyzed with chromatography. Acylated peptides (green) were eluted faster than Asn3-Glu17control (10.8 minutes and 12.3 minutes respectively). Incubation with IpaJ resulted in the appearance of the peak at 12.3 minutes (orange) consistent with the peptides cleavage.

c. Time course of the myr-Gly_2-Glu_{17} cleavage by IpaJ. The peptide (1μM) was incubated with MBP-IpaJΔ50 (50 nM) for indicated time. Areas under the curves were used to quantify peptide form (acylated and cleaved) at each time point

d. Fluorescent chromatography analysis of peptide cleavage by IpaJ C64A. The experiment was performed as in (**b**) with myr-Gly_2-Glu_{17} peptide, but IpaJ C64A was used instead of wild type enzyme.

e. Analysis of minimal substrate cleavage. Myr-Gly-Lys peptide (1μM) were incubated for 30 min at 37°C with recombinant MBP-IpaJΔ50 (500 nM) and analyzed with chromatography. The myristoylated peptide was eluted faster (12 minutes) (green) than Lys peptide (two peaks at 15 and 15.8 minutes) (black). Cleavage of the myr-Gly-Lys resulted in a decrease of the peak at 12 minutes and appearance of the two peaks at 15 and 15.8 minutes (orange).

a

```
2-GCIKSKGKD-10    Lyn
2-GSQVSVESG-10    AMID
2-GAKQSGPAA-10    ZNRF2
2-GSNKSKPKD-10    Src
2-GAQFSKTAA-10    MARCKS
2-GQSQSGGHG-10    PSMC1
2-GCCYSSENE-10    LAMTOR1
2-GCTLSAEDK-10    Gαi3
2-GNAAGSAEQ-10    FMNL1
2-GAAHSASEE-10    Tescalcin
```

b

```
2-GNIFANLFK-10   ARF1
2-GNIFGNLLK-10   ARF3
2-GLTISSLFS-10   ARF4
2-GLTVSALFS-10   ARF5
2-GGFFSSIFS-10   ARL1
2-GNISSNISA-10   ARL4C
```

Figure 24. N-termini of the IpaJ substrates.

a. Multiple sequence alignment of *N*-myristoylated glycine and downstream sequences from selected identified *in vitro* substrates. The alignment revealed a great sequence diversity of substrates' N-termini. Positively charged residues are labeled with green, negatively charged – with red. Blue-colored cysteines are palmitoylated.

b. Multiple sequence alignment of *N*-myristoylated glycine and downstream sequences from the identified ARFs and ARLs substrates. Positively charged residues are labeled with green.

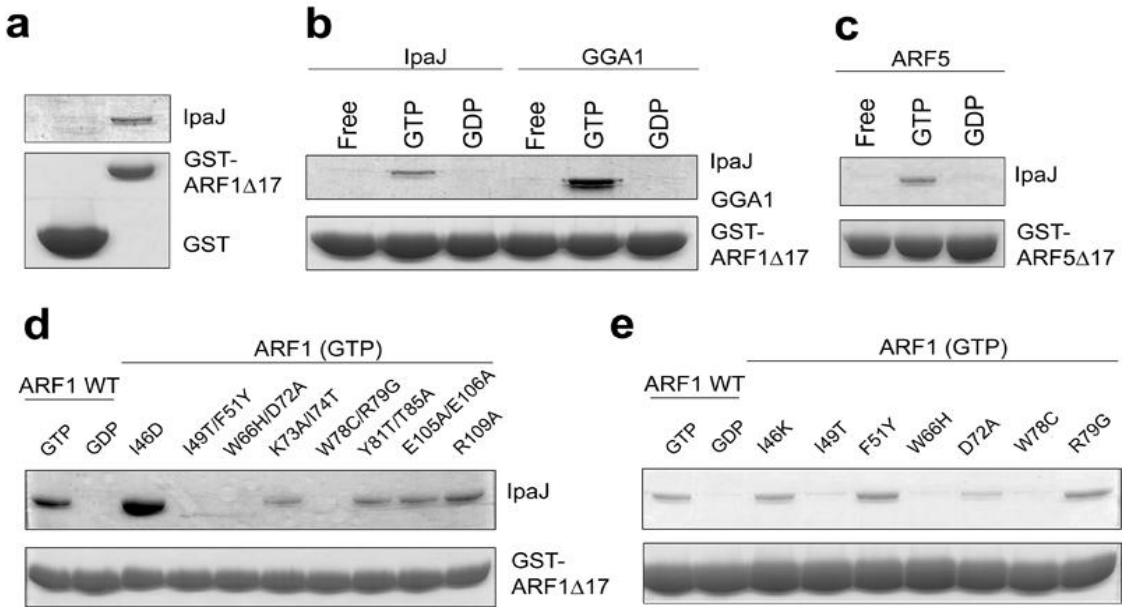

Figure 25. IpaJ behaves as an ARF substrate.

a. IpaJ co-precipitates with GST-ARF1 but not with GST. Recombinant MBP-IpaJΔ50 (625 μg) was incubated with GST-ARF1Δ17 or GST (125 μg) and glutathione-agarose beads for 1hr at 4°C. After washes proteins were eluted with 10mM glutathione and separated on SDS PAGE.

b. IpaJ specifically interacts with active form of ARF1. GST-ARF1Δ17 was subjected to *in vitro* nucleotide exchange for GTP or GDP or rendered nucleotide-free. The protein was tested for interaction with MBP-IpaJΔ50 as in (**a**). GAT domain of GGA1 (625 μg), a natural ARF1 substrate, was used as a positive control.

c. IpaJ specifically interacts with active form of ARF5. GST-ARF5Δ17 was subjected to *in vitro* nucleotide exchange for GTP or GDP or rendered nucleotide-free. The protein was tested for interaction with MBP-IpaJΔ50 as in (**a**).

d. Mutational analysis of ARF1-IpaJ interaction sites. GST-ARF1Δ17 mutants containing indicated single and double amino acid substitutions were nucleotide-exchanged and tested for interaction with MBP-IpaJΔ50.

e. Mutational analysis of ARF1-IpaJ interaction sites. GST-ARF1Δ17 mutants containing single amino acid substitutions were made to confirm the loss of interaction of the respective double-mutants in (**d**). Proteins were nucleotide-exchanged and tested for interaction with MBP-IpaJΔ50.

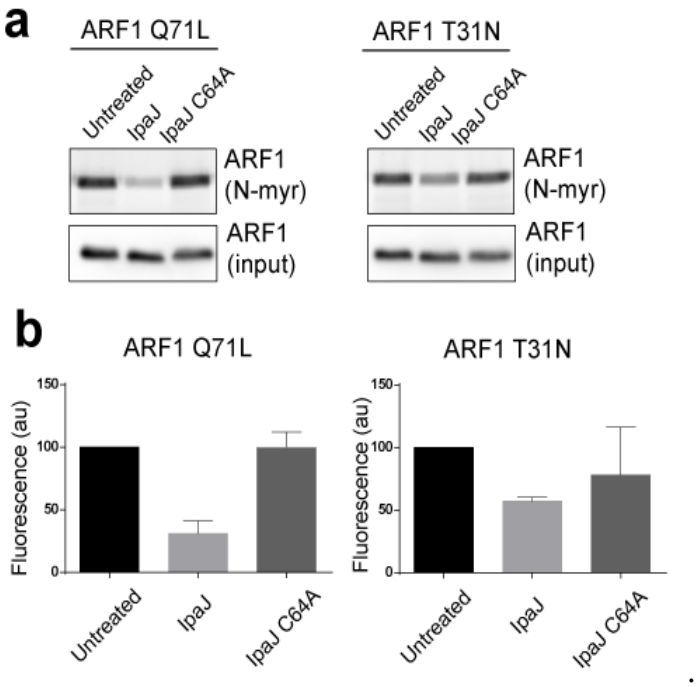

Figure 26. IpaJ preferentially cleaves ARF1 in the active conformation.

a. In gel fluorescence analysis shows myristoylated ARF1 T31N mutant (a GDP-locked mutant) or ARF1 Q71L (a GTP-locked mutant) expressed in HeLa cells and incubated with recombinant IpaJ or catalytic mutant. IpaJ cleaved ARF1-GDP less efficiently than ARF1-GTP. Equal loading of ARF1 (middle panel) was determined by western blot analysis.

b. Quantification of fluorescence in (**a**). Values are presented in arbitrary units (au). Signal of 'untreated' condition is normalized to 100 for both mutants. Fluorescent signal was quantified in three experiment repetitions using ImageJ.

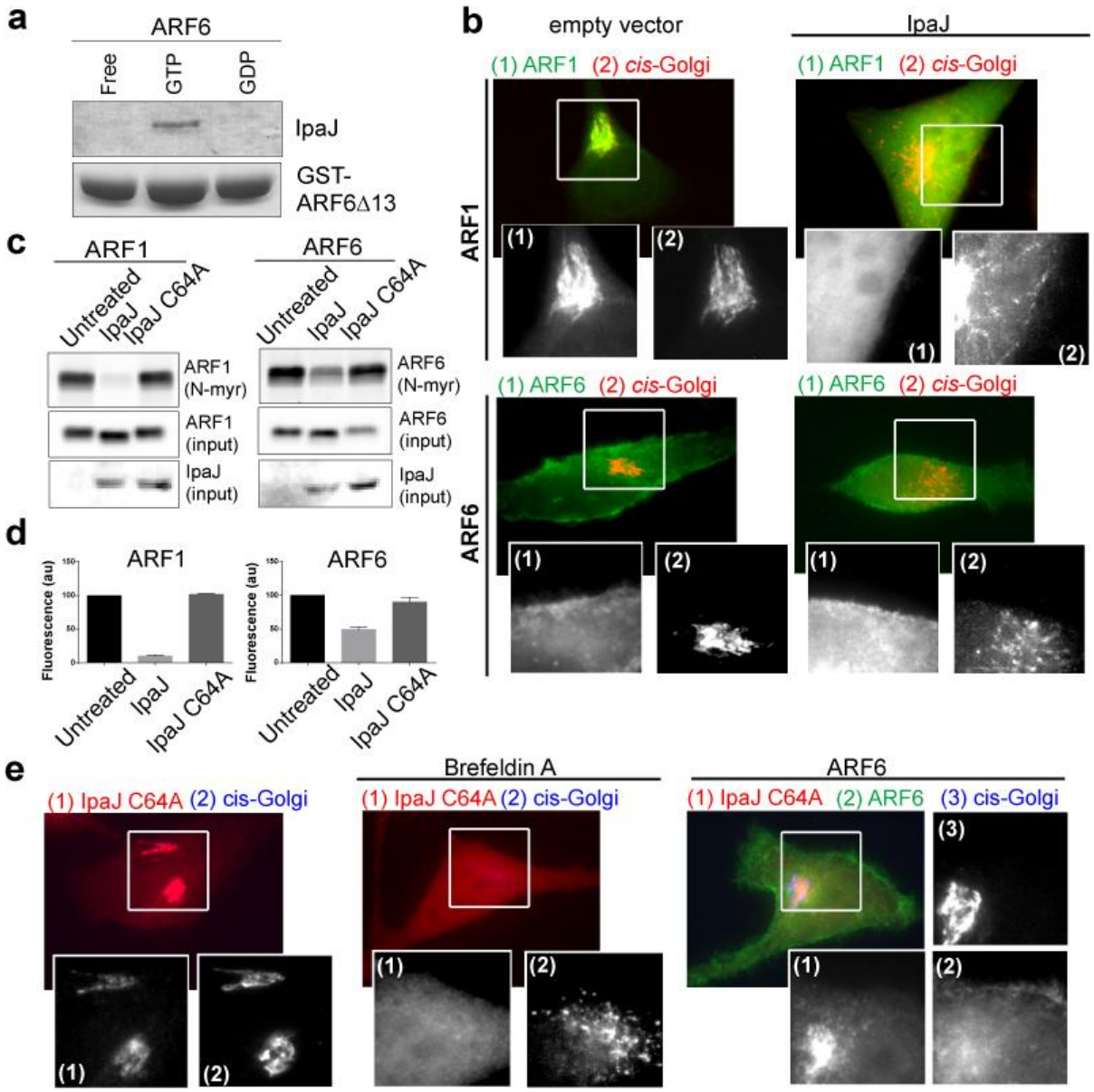

Figure 27. ARF6 is selectively protected from IpaJ cleavage.

a. IpaJ specifically interacts with active form of ARF6. GST-ARF6Δ13 was subjected to *in vitro* nucleotide exchange for GTP or GDP or rendered nucleotide-free. The protein was tested for interaction with MBP-IpaJΔ50 as in Figure 25a.

b. IpaJ cleaves ARF6 only partially upon expression in HeLa cells. ARF1-GFP and ARF6-GFP were co-expressed either with empty vector (control) or with IpaJ-mCherry and their localization was analyzed with fluorescent microscopy. ARF1 localized on the Golgi in control conditions but was rendered completely cytosolic upon co-expressed with IpaJ. ARF6 localized near plasma membrane in control samples and still highly enriched near it upon co-expression with IpaJ suggesting an incomplete cleavage. *Cis*-Golgi was visualized with gm130 antibodies. See also Figure 28a.

c. ARF6 was cleaved less efficiently than ARF1 upon co-expression with IpaJ. In gel fluorescence shows myristoylated ARF1 or ARF6 after co-expression with IpaJ or catalytic mutants as indicated (top panel). Equal loading of ARF1/ARF6 (middle panel) and expression of IpaJ (lower panel) were confirmed by western blot analysis.

d. Quantification of fluorescent signal of ARF1 and ARF6 in (**c**). Values are presented in arbitrary units (au). Signal of 'untreated' condition is normalized to 100 for both proteins. Fluorescent signal was quantified in three experiment repetitions using ImageJ.

e. IpaJ C64A localized on the Golgi but not near plasma membrane. IpaJ C64A – mCherry was expressed in HeLa cells and was visualized using fluorescent microscopy. Unlike the wild type protein, which was cytosolic (see Figure 28b), this mutant localized on the Golgi. Brefeldin A treatment rendered IpaJ C64A cytosolic indicating that its Golgi-association was ARF-dependent. However IpaJ C64A did not show any co-localization with ARF6 and was not enriched near plasma membrane even when ARF6 was overexpressed. *Cis*-Golgi was visualized with gm130 antibodies. ARF6 was a fusion protein with GFP. See also Figure 28b.

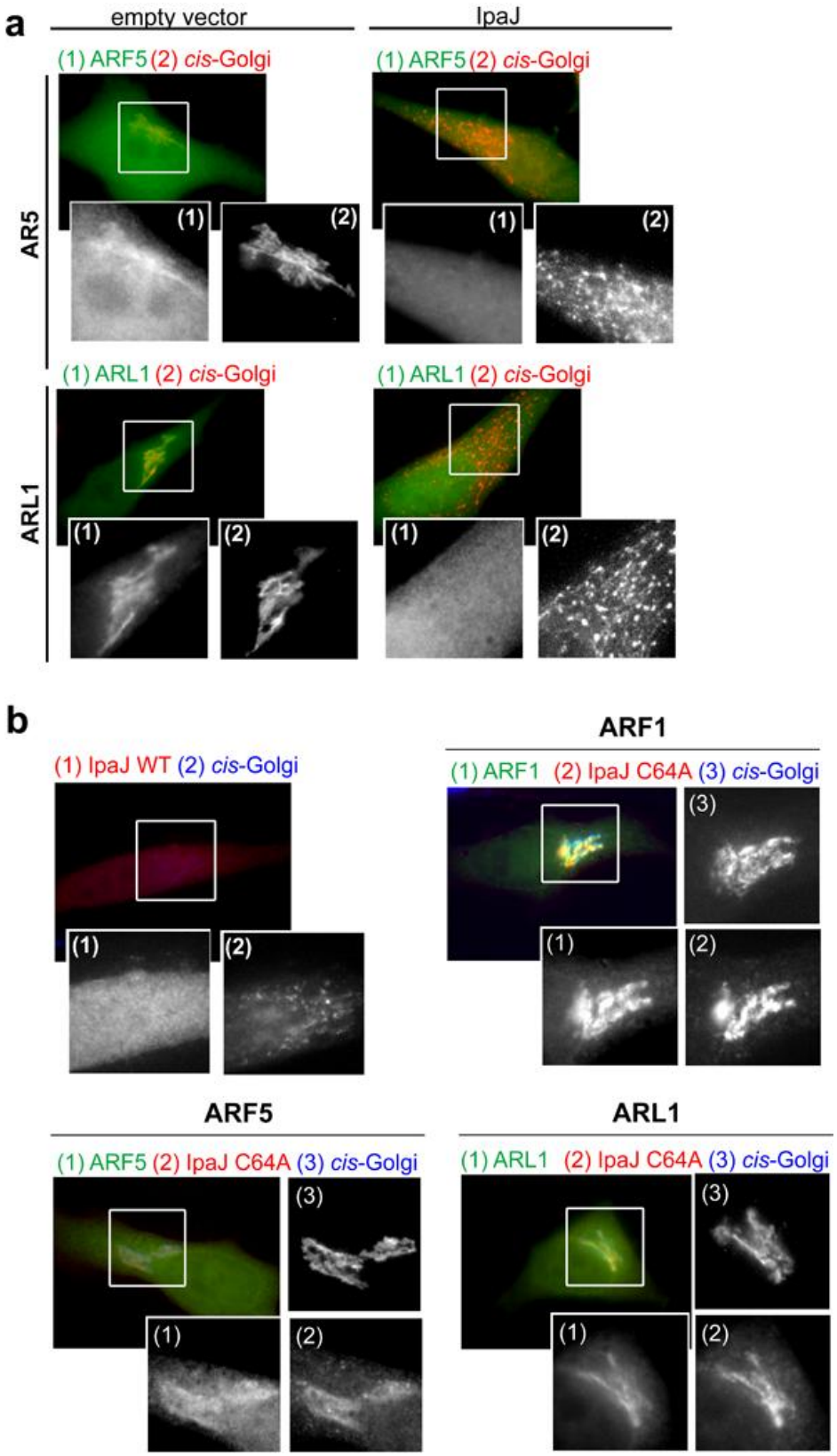
a
empty vector
IpaJ
(1) ARF5 (2) cis-Golgi
(1) ARF5 (2) cis-Golgi
AR5
(1)
(2)
(1)
(2)
(1) ARL1 (2) cis-Golgi
(1) ARL1 (2) cis-Golgi
ARL1
(1)
(2)
(1)
(2)
b
(1) IpaJ WT (2) cis-Golgi
(1)
(2)
ARF1
(1) ARF1 (2) IpaJ C64A (3) cis-Golgi
(3)
(1)
(2)
ARF5
(1) ARF5 (2) IpaJ C64A (3) cis-Golgi
(3)
(1)
(2)
ARL1
(1) ARL1 (2) IpaJ C64A (3) cis-Golgi
(3)
(1)
(2)

.

Figure 28. IpaJ co-localizes with and cleaves ARF1, ARF5 and ARL1.

a. IpaJ cleaves ARF5 and ARL1 upon co-expression in HeLa cells. ARF5-GFP and ARL1-GFP were co-expressed either with empty vector (control) or with IpaJ-mCherry and their localization was analyzed with fluorescent microscopy. Both GTPases localized on the Golgi in control conditions but were displaced into cytosol upon co-expression with IpaJ. *Cis*-Golgi was visualized with gm130 antibodies.

b. Wild type IpaJ is cytosolic (top left panel), but IpaJ C64A mutant is associated with the Golgi and partially co-localizes with ARF1, ARF5 and ARL1.

Methods:

Plasmids and cloning:

IpaJ gene (AAK18440) was PCR amplified from *Shigella flexneri* M90T and cloned into pEntr/D, generating a GatewayTM compatible entry clone (Invitrogen) according to manufacturer recommendations. For mammalian expression the effector was then recombined into modified pcDNA3.1 vector carrying NH2-terminal eGFP or mCherry in frame with the Gateway cassette (GatewayTM vector conversion system, Invitrogen). For bacterial expression 50 amino acid NH2-terminal deletion of IpaJ (IpaJΔ50; residues 51-259) was cloned in frame into pET28b-MBP vector, yielding intact catalytic domain of IpaJ COOH-terminally fused to MBP-6His-tag. NH2-terminal deletion of ARF1 (ARF1Δ17; residues 18-181) was PCR subcloned into pGEX-4T1 vector. Human GGA1 (GAT domain, residues 76-215) was PCR amplified and cloned in frame into pET28b-MBP vector. For co-localization studies full-length ARF1 and ARF5 (Missouri S&T cDNA Resource Center; #ARF0100000, #ARF0500000) were cloned into modified pcDNA3.1 vector carrying COOH-terminal eGFP. For plasma membrane targeting 10 NH2-terminal amino acids of neuromodulin were cloned in front of eGFP in the pcDNA3.1-based vector. ARF1 and ARF5 were then subcloned COOH-terminally to eGFP. Site-directed mutation (IpaJ Cys64Ala) was generated using the QuickChange Site-Directed Mutagenesis Kit (Stratagene).

In vitro cleavage of proteins and in-gel fluorescence:

To assay *in vitro* substrates HeLa cells were plated on 10cm dishes. 20 uM Alk-12 was added into the media for metabolic labeling. For *in vitro* cleavage of ARF1 and ZNRF2,

cells were transfected with respective STREPtag-containing constructs using Lipofectamine® according to manufacturer recommendations 18 hrs before adding alkyne-myristic acid. Next day cells were washed with PBS and fresh media was added containing alkyne-myristic acid. After 24 hrs of metabolic labeling cells were lysed (with 20 mM Tris HCl pH 7.5, 1.5 mM MgCl2, 350 mM NaCl, 0.5% Igepal CA630, 5% glycerol) and protein content was measured by BCA assay. Lysate was incubated with 5 ug of MBP-IpaJd50 (wild type of C64A catalytic mutant) at 37°C for 30 minutes. 100 ug of protein solutions were used for click-labeling with rhodamine-azide as described previously (Charron et al., 2009). The remaining portions of lysates were used for coupling to biotin and mass-spectrometric analysis (see below). Fluorescently labeled proteins were separated on SDS-PAGE and visualized on Typhoon Trio imaging system. ARF-strep fusion proteins were then transferred on nitrocellulose paper for western blot with STREPtactin-HRP.

Bacterial infection of cultured cells:

Infection was performed as described above. For click-labeling cells were lysed in 50 mM TEA (triethanolamine), 4% SDS, 150 mM NaCl, ph7.4. Lysates then were prepared for in-gel visualization or mass-spectrometry as previously described.

Proteomic Identification of Alk-12 Labeled Proteins:

2 mg of protein was clicked with azido-biotin (Click Chemistry tools) for 4 h (1 mM Cu2+, 1 mM TCEP, 200 μM TBTA, 200 μMazido-biotin) at 1mg/ml in 4% SDS. Protein was precipitated using methanol (8 mL), chloroform (3 mL), and water (6 mL) overnight at –20 °C and washed with methanol (5 mL) twice. Protein pellets were dried and resuspendedin

200 μL of 4% SDS. Equal protein amounts were diluted to 2 mg/mL with 50 mM TEA buffer containing 150 mMNaCl at pH 7.4. 60 μL of streptavidin beads (Thermo) were added to each sample and the mixtures were incubated for 1 h at room temperature on a nutating mixer.The beads were then washed three times with 1%SDS (50 mM TEA, 150 mMNaCl, pH 7.4), 5M urea (50 mM TEA, 150 mMNaCl, pH 7.4), and PBS. Centrifugation of the beads between washing steps was carried out (2000 × g, 1 min) to collect the beads. The beads were thenresuspended in 200 μL 25 mM ammonium bicarbonate (ABC), reduced with 10 mM DTT for 30 min, and alkylated with 20 mMiodoacetamidein the dark for 30 min. After that, the beads were washed three times with 200 μL 25 mMABC and suspended in 50 μL of 25 mMABC. 0.5 μg of trypsin was added to each sample and the mixtures were digested at 37 °C overnight. The supernatant was collected, dried on a Speedvac and resuspended in water containing 5% acetonitrile and 1% formic acid for mass spectrometry.

LC-MS analysis was performed with a Dionex 3000 nano-HPLC coupled to an LTQ-Orbitrap ion trap mass spectrometer (ThermoFisher).Tryptic peptide samples were desalted on a trap column following separation on a 12cm/75μm reversed phase C18 column (NikkyoTechnos Co., Ltd. Japan). A 180 minutes gradient increasing from 10% B to% 45% B in 133 minutes (A: 0.1% Formic Acid, B: Acetonitrile/0.1% Formic Acid) were delivered at 200 nL/min. The liquid chromatography setup (Dionex, Boston, MA, USA) was connected to an Orbitrap XL (Thermo, San Jose, CA, USA) operated in top-8-CID-mode with MS spectra measured at a resolution of 60,000@m/z 400. One full MS scan (300–2000 MW) was followed by three data-dependent scans of the nth most intense ions with dynamic exclusion enabled.

Acquired tandem MS spectra were extracted using ProteomeDiscoverer v. 1.4.0.288 (Thermo, Bremen, Germany) and queried against Uniprots complete human database concatenated with common known contaminants (Bunkenborg, Garcia, Paz, Andersen, & Molina, 2010) using MASCOT v. 2.3.02 (Matrixscience, London, UK). Peptides fulfilling a Percolator calculated 1% false discovery rate threshold (Kall, Storey, MacCoss, & Noble, 2008) were reported. For a matched protein, its abundance was calculated based on the average area of the three most abundant peptides (Silva et al., 2006). All LC-MS/MS analysis was carried out at the Proteomics Resource Center at The Rockefeller University, New York, NY, USA.

Synthesis of the acylated peptides:

Peptides were synthesized manually on a scale of 50 micromol using Rink-amide copoly-(styrene-divinylbenzene) resin (Novabiochem, CA) with a substitution value of 0.41 mmol/g, Fmoc protected amino acids and HATU activation in NMP. Single coupling cycles were used throughout with a 10-fold excess of activated amino acid. Removal of the orthogonally protected methyltrityl group was achieved using 1% TFA in dichloromethane (DCM) prior to the addition of Fmoc PEG(n=3)-OH and Fluorescein succinimidyl ester. Final deprotection and cleavage of the peptides from the resins was carried out using 5% triisopropylsilane/95% trifluoroacetic acid (TFA) for 90 mins at room temperature. The crude cleavage mixtures were filtered and peptides precipitated from cold diethyl ether and allowed to air dry. Purification was achieved on either a Vydac C4 or C18 (250x10mm) column using a 120 min gradient of 0% buffer A (water/0.1% TFA) to 100% B

(acetonitrile/0.1% TFA) and 220nm wavelength detection. Purified fractions are combined and lyophilized.

Peptide cleavage:

For enzymatic cleavage myristoylated peptide was incubated with IpaJ in 50 mM Tris ph7.5, 150 mM NaCl, 1 mM MgCl2, 10mM DTT, 0.5% Igepal CA630 at 37°C for indicated amounts of time. Reaction was stopped by addition of methanol with 0.5M HCl. After incubation the solution was centrifuged at 40000g for 30 minutes. The supernatant was used for HPLC gel filtration with TOSOH TSK-GEL® SuperSW3000 column. Area under the peaks was used to quantify the abundance of each peptide form.

Recombinant protein purification and in vitro binding:

Recombinant proteins (IpaJΔ50, IpaJΔ50 C64A, ARF1ΔN17, GGA1$_{76\text{-}215}$) were expressed in BL21-DE3 E. coli strains by induction with 0.4 mM IPTG for 16 h at 18 °C. Pellets were lysed with His buffer (100 mM HEPES, pH 7.5, 300 mM NaCl) or GST buffer (TBS; 50 mM Tris pH 7.5, 150 mM NaCl, 2 mM DTT) supplemented with protease cocktail (Roche). Proteins were purified with nickel agarose (Qiagen) or glutathione Sepharose (Amersham Biosciences) following manufacturer's instructions. Eluted proteins were buffer exchanged into TBS using concentration centrifugal columns (Millipore), glycerol was added to 15% and the proteins were then stored at −80 °C. For *in vitro* nucleotide exchange 60 uM of ARF-GST fusion protein was incubated in TBS buffer with 500 uM GTP or GDP nucleotide, 10 mM of EDTA, 2mM TCEP, 10% glycerol at 37 °C for 1hr. After incubation solution was cooled down on ice for 1 min, mixed with 40 mM of MgCl2 and was spun down

(15000g, 2 minutes). Supernatant containing non-precipitated protein was used for *in vitro* binding assay. ARFs was mixed with MBP-IpaJΔ50 and GST-agarose beads and incubated in the presence of 0.5% Triton X-100 for 1 hr at 4°C. Beads were washed three times with TBS containing 0.5% Triton X-100 and ARF -GST was eluted with 10 mM glutathione. Proteins were boiled with SDS, separated on SDS-PAGE and visualized with coomassie staining.

In vitro cleavage of recombinant ARF1:

E. coli BL-21 cells expressing ARF1-His with or without yeast NMTp were grown overnight at 37°C in LB media. Cultures were diluted 1:50 and incubated at 37°C till reaching OD_{600}~ 0.5-0.6. Myristic acid and azide myristic acid were added at the concentrations 50μM and 5μM respectively and cells were additionally incubated for 30 minutes. Protein expression was then induced with 0.4 mM IPTG and cells were further incubated at 37°C for 3 hrs. We estimated that *N*-myristoylated ARF1 is bound in a GDP:GTP ratio of 1:1 as assessed by GGA binding assays. Expression of IpaJ or IpaJ C64A mutant was performed by the same method without adding myristic acid. ARF1 and IpaJ expressing cells were lysed by 1-minute sonication separately (lysis buffer: 20 mM Tris HCl pH 7.5, 1.5 mM $MgCl_2$, 350 mM NaCl, 0.5% NP-40, 5% glycerol) and the lysates were mixed together and incubated for 30 minutes at 37 ^{o}C. ARF1 was then purified using nickel agarose (Qiagen). *N*-myristoylated proteins were labeled with Alex Fluor® 647 Alkyne using Click-It® reaction buffer kit (Invitrogen) according to instructions with modifications. Specifically, Click-labeling was performed on the proteins still bound to the column. Column was then washed and proteins were eluted with 500 mM Imidazole/100mM HEPES

containing 1% SDS. Myristoylation status was analyzed by in-gel fluorescence and the equal protein load was confirmed by Coommassie stain. For cleavage inhibition free myristic acid or vehicle control (DMSO) was added to bacterial lysate containing ARF1 before adding IpaJ. After cleavage reaction ARF1 was then labeled and purified as described above. To test the cleavage of non-myristoylated ARF1 a similar experimental setup was used with the following modifications: *E. coli* BL-21 cells expressing ARF1-His (in the absence of NMTp or exogenous myristic acid) was purified with Ni-NTA agarose, eluted with 500 mM Imidazole/100mM HEPES, and processed for mass spectrometry.

CHAPTER FOUR
IpaJ and VirA suppress immune signaling and promote *Shigella* infection

Introduction

So far I have found that *Shigella flexneri* secreted effector IpaJ is a cysteine protease that removes N-myristoyl glycine of ADP-ribosylation factors (ARF) and ARF-like proteins (ARL). This results in the Golgi fragmentation, prevention of protein export from endoplasmic reticulum, and suppression of general secretory pathway. In addition, another effector, VirA also disrupts the Golgi structure through inactivation of the Rab1 GTPase. Therefore, inhibition of the Golgi trafficking is a crucial part of *Shigella* infection. But why does *Shigella* need to inhibit membrane trafficking and how important is it for infection? As mentioned above, the Golgi performs essential immune functions by directing transport of cytokines and various receptors. I therefore set up to determine if these processes might be affected by IpaJ and VirA activities.

Results

(part of this chapter was published previously in research article)

IpaJ and VirA promote Shigella virulence and suppress cytokine secretion

Earlier I did not observe any abnormalities in *ΔipaJ* and *ΔvirA Shigella* infection in the context of cell culture. However, if IpaJ and VirA activities results in defects in immune signaling, then *ΔipaJ* and *ΔvirA Shigella* mutants should be less virulent in animal models. Indeed, in a previous study with a limited number of animals the *ΔipaJ* strain demonstrated a slower development of inflammation reaction and a less pronounced inflammatory phenotype

in guinea pig model of keratoconjunctivitis (Buysse, Dunyak, Hartman, & Venkatesan, 1997a). I collaborated with James Ertelt and SIng Sing Way (Cincinnati Children's Hospital Medical Center) to evaluate bacterial replication *in vivo* using an established mouse model of mucosal infection (Way, Borczuk, Dominitz, & Goldberg, 1998). Mice were infected intranasally with $1x10^6$ of wild type or each mutant *Shigella* strain. After 24 hours measured the number of colony-forming units per mouse lung was measured. The number of recoverable bacteria was sharply reduced (by 100-fold, $P < 0.001$) for both *ΔipaJ* and *ΔvirA* strains compared to wild type *Shigella* (Figure 29a). As expected, bacterial replication was further attenuated in the *Shigella* Δ*mixD* mutant lacking all T3SS function (Figure 29a). Taken together, these data demonstrate that two *Shigella* effector proteins, IpaJ and VirA, each harbor the Golgi-disrupting activity, are essential and play non-redundant roles for optimal *in vivo* virulence.

Having established the importance of IpaJ and VirA for the bacterial infection, I asked what specific processes of immune signaling could be affected by these effectors. As mentioned above, secretion of many cytokines is the Golgi-dependent and therefore might be suppressed upon Golgi disruption. To address this possibility, I used a human growth hormone (hGH) secretion assay developed previously (Rivera et al., 2000). This system utilized hGH which is genetically fused to conditional agglomeration domain (CAD). CAD proteins form stable aggregates that cannot be exported from the ER, thereby blocking the secretion of fusion protein. This aggregation can be reversed by the addition of a cell permeable ligand (AP21198) allowing the release of the proteins from the ER and their entry into the secretory pathway. Once inside the Golgi, hGH-CAD fusion protein is cleaved by the

resident enzyme furin at an encoded furin cleavage site. Free hGH is then secreted into the extracellular space (Figure 29b). I co-expressed hGH-CAD with IpaJ or VirA or control plasmid and measured a secreted amount of hormone in the presence of the AP21198 ligand by ELISA. Addition of the ligand to the cells co-expressing hGH and empty plasmid led to a significant increase in the amount of the extracellular hormone (Figure 29b). Co-expression of either IpaJ or VirA, however, resulted in a loss of the extracellular hGH as measured by ELISA (Figure 29b). Therefore, both effector proteins potently inhibit the Golgi-dependent secretion.

Differential effect of IpaJ and VirA on STING signaling

In addition to cytokine secretion, translocation of some immune receptors may also be affected by the Golgi fragmentation. Specifically, STING is a major sensor of cytosolic DNA with crucial role in anti-microbial signaling (Paludan & Bowie, 2013). STING protein resides in the ER, but upon DNA recognition, direct or mediated by its upstream regulators, the receptor translocates to the Golgi and later reaches its final destination at autophagosome-like structures (Ishikawa, Ma, & Barber, 2009; Saitoh et al., 2009). This translocation from the ER to post-Golgi compartments is a hallmark of STING activation (Saitoh et al., 2009). Although it is mostly studied in the context of viral infections, this receptor also mediates the response to *Listeria monocytogenes* and *Mycobacterium tuberculosis* (Hansen et al., 2014; Ishikawa et al., 2009; Manzanillo, Shiloh, Portnoy, & Cox, 2012). It was suggested that STING might respond to other bacterial infections as well, but *Shigella* was never reported to activate this pathway. The discovered effect of IpaJ and VirA on the Golgi trafficking

indicated a possibility that *Shigella* may suppress STING function through these secreted effectors. In collaboration with Nicole Dobbs and Nan Yan (UT Southwestern). I tested if *ΔipaJ* or *ΔvirA* or double knockout *Shigella* strains would activate STING. I used mouse embryonic fibroblasts (MEF) that were stably expressing STING-GFP and infected them with different *Shigella* strains. STING activation was assessed by its exit from the ER. As expected, I only observed minor STING exit from the ER in the cells infected with wild type *Shigella* (Figure 30). Deletion of VirA (*ΔvirA strain)* did not promote STING translocation significantly. However, the receptor reached vesicular structures upon infection with *ΔipaJ* or *ΔipaJΔvirA* strains, suggesting that IpaJ might mask STING activation (Figure 30). To confirm the microscopy study, we measured STING-dependent IFN-β production in primary MEF infected with wild type and mutant *Shigella* strains (Figure 31a). While the cytokine production was stimulated by wild type and *ΔvirA Shigella*, the response to *ΔipaJ* strain was much more pronounced (Figure 31a). In contrast, IpaJ deletion did not have significant effect on the TNF-α cytokine production (Figure 31a). To verify that the IFN-β response was STING-dependent, we repeated this experiment with primary 'Goldenticket' MEF that carry T596A mutation in STING and fail to produce a detectable amount of the protein (Sauer et al., 2011). IFN-β response to both wild type and *ΔipaJ Shigella* was significantly decreased in the mutant cells. Furthermore, we found that *ΔipaJ* strain stimulated production of TNF-α but not of IFN-β, in contrast to the wild type bacteria (Figure 31b). Therefore, I found that *Shigella* infection does induce STING activation, which is masked by the IpaJ activity.

Interestingly, it was only IpaJ, but not VirA, that blocked STING signaling. The two effector proteins have different modes of action and may affect various steps of membrane

trafficking. To better characterize the difference between these two proteins, I utilized the CAD-domains based system. A Golgi resident enzyme 1,4-GGTase was fused to GFP and to CAD, resulting in the fluorescent protein (Golgi-GFP) that normally aggregates in the ER but moves to the Golgi upon addition of the AP21198 ligand, if the trafficking system is functional (Selyunin et al., 2014). I transfected the cells with Golgi-GFP and microinjected either recombinant IpaJ, VirA or vehicle control. Using fluorescent microscopy, I analyzed GFP localization after addition of the ligand (Figure 32). While in VirA-injected cells the fusion protein reached the Golgi remnant (produced by VirA), IpaJ prevented exit of this marker from the ER. The observed phenotype closely resembled the one obtained with STING-GFP (see Figure 30). Therefore, IpaJ and VirA block various steps of protein trafficking, which may explain their differential effects on STING activity. Better characterization of this difference may provide a unique insight into the mechanism of STING function and is a subject of ongoing research (manuscript in preparation).

To further validate the suppression of STING activity by IpaJ, I switched to the *Listeria monocytogenes* model of infection. *Listeria* is known to be a potent inducer of STING signaling, and its mechanism of infection is thoroughly studied (Witte et al., 2012). Using previously developed integration vectors, we introduced IpaJ or VirA into the bacteria by fusing them to the promoter and the first 100 amino acids of actA, *Listeria* effector that polymerizes actin near the bacterial surface allowing intracellular movement and cell-to-cell dissemination of the pathogen (Auerbuch, Lenz, & Portnoy, 2001; Lauer, Chow, Loessner, Portnoy, & Calendar, 2002; Pistor, Chakraborty, Niebuhr, Domann, & Wehland, 1994; Travier et al., 2013).

To confirm that the derived *Listeria* strains secret functional IpaJ and VirA proteins, I first analyzed the Golgi morphology in HeLa cells during infection. As expected, *Listeria*-IpaJ and *Listeria*-VirA deformed the Golgi structure similarly to *Shigella* ΔvirA and ΔipaJ mutants respectively (Figure 33, compare to Figure 2c). I then used these *Listeria* strains to infect the MEF cells expressing STING-GFP. While the parent strain induced the expected STING translocation to post-Golgi compartments, the receptor remained in the ER upon infection with the *Listeria* strain carrying the wild type IpaJ (*Listeria*-IpaJ) (Figure 34). In contrast, the strain carrying VirA did not prevent STING exit from ER (Figure 34). Furthermore, the RT-PCR analysis of infected cells revealed that while TNF-a production was attenuated by both IpaJ and VirA, IFN-β was decreased only when *Listeria* secreted IpaJ (Figure 35). This result demonstrates different effects of the two proteins on immune signaling and defines IpaJ as a potent inhibitor of STING function.

Conclusions

In the present chapter, I determined that IpaJ and VirA promote *Shigella* infection, and deletion of either gene significantly attenuates the bacterial virulence. Furthermore, I found that these two proteins exert overlapping but non-redundant effects on immune signaling. While both proteins potently suppress the Golgi-dependent cytokine secretion, only IpaJ inhibits the activation of the DNA sensor STING. The obtained in this chapter results explain why IFN-β signaling was previously never associated with *Shigella* and highlights the necessity for thorough examination of the signaling pathways that may be actively suppressed by microbial pathogens.

It is likely that other immune signals are also affected by either IpaJ or VirA, or both. These may include trafficking of various receptors and their adaptors as well as MHC-complexes. Identification of the signaling pathways affected during infection will foster the understanding of *Shigella* mechanisms of pathogenesis.

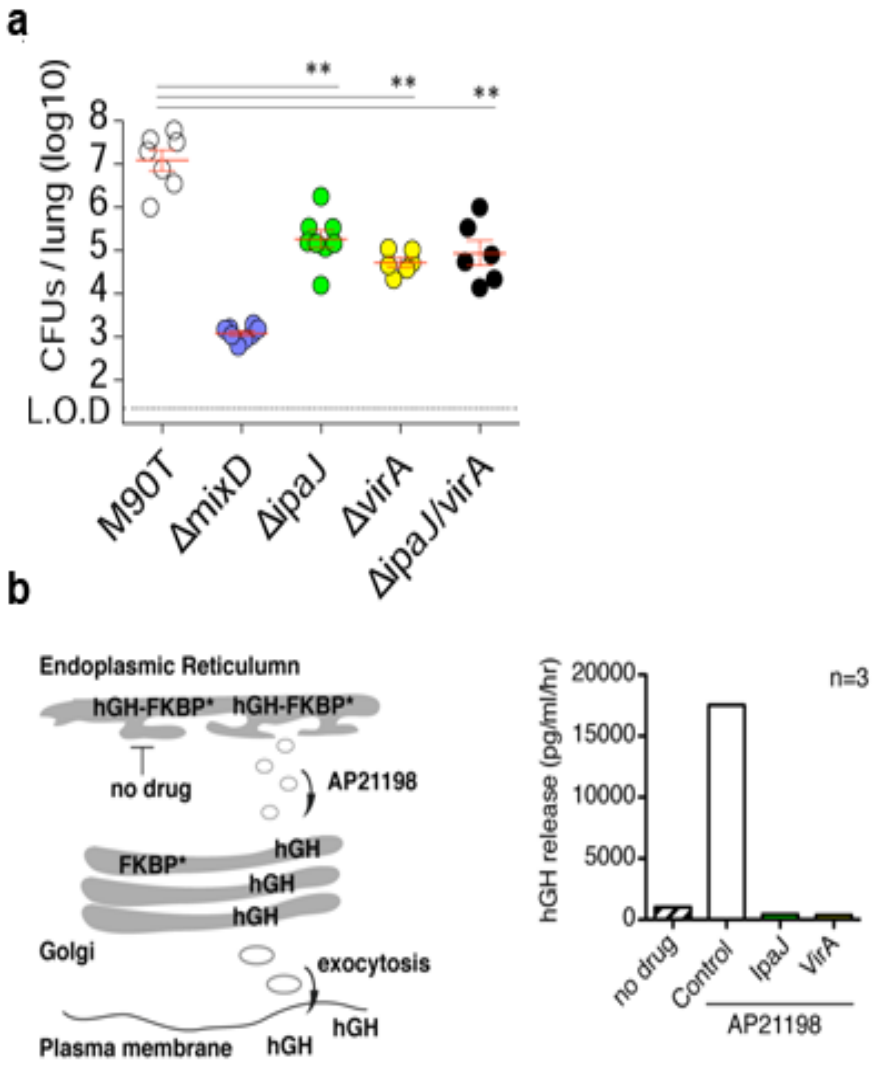

Figure 29. IpaJ and VirA are essential for optimal *Shigella* virulence.

a. Mice were infected intranasally with $1x10^6$ of WT M90T or each mutant *Shigella* strain as indicated. Number of recoverable CFUs per mouse lung 24 hours after intranasal inoculation was analyzed to assay virulence. Limit of detection (L.O.D) for this assay is indicated by the dashed line. Error bars represent geometrical means ± SEM. $^{**}P<0.001$

b. Diagram (left) and Graph (right) showing the amount of human Growth Hormone (hGH) released from Hela cells (after drug addition) transfected with indicated expression plasmids. Cells were transfected with CAD-GFP fusion protein, that aggregated in the ER and could not be released without addition of the AP211198 ligand. Addition of drug allowed the secretion of the protein, which could then be detected by ELISA. Co-expression of IpaJ or VirA prevented protein secretion. Experiments were performed as previously described (Rivera et al., 2000; Selyunin et al., 2011).See extended material and methods for additional experimental details accompanying this figure. Error bars represent means ± SEM.

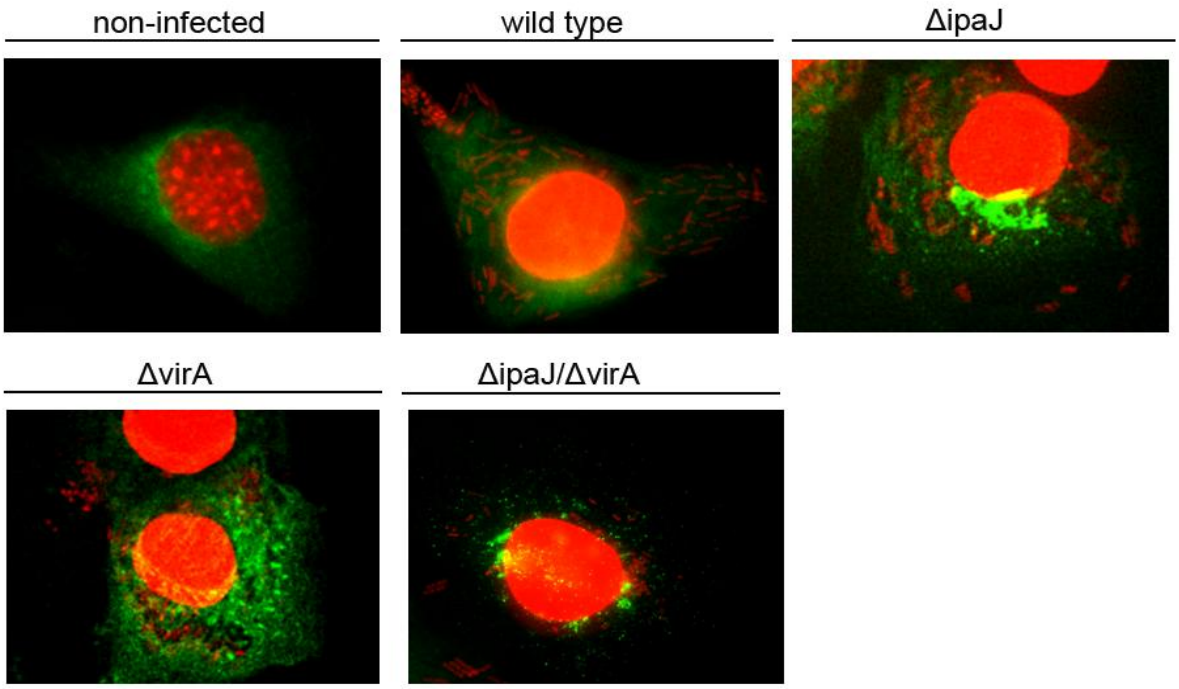

Figure 30. IpaJ activity masks STING activation.

MEF cells expressing STING-GFP were infected with wild type or indicated *Shigella* mutants for 5 hours and analyzed by fluorescent microscopy. STING resided in the ER in non-infected cells and its activation was assessed as its transloction from the ER. Deletion of IpaJ, but not of VirA derepressed STING translocation upon *Shigella* infection.*Shigella* was visulized with DAPI (red). STING-GFP is shown green.

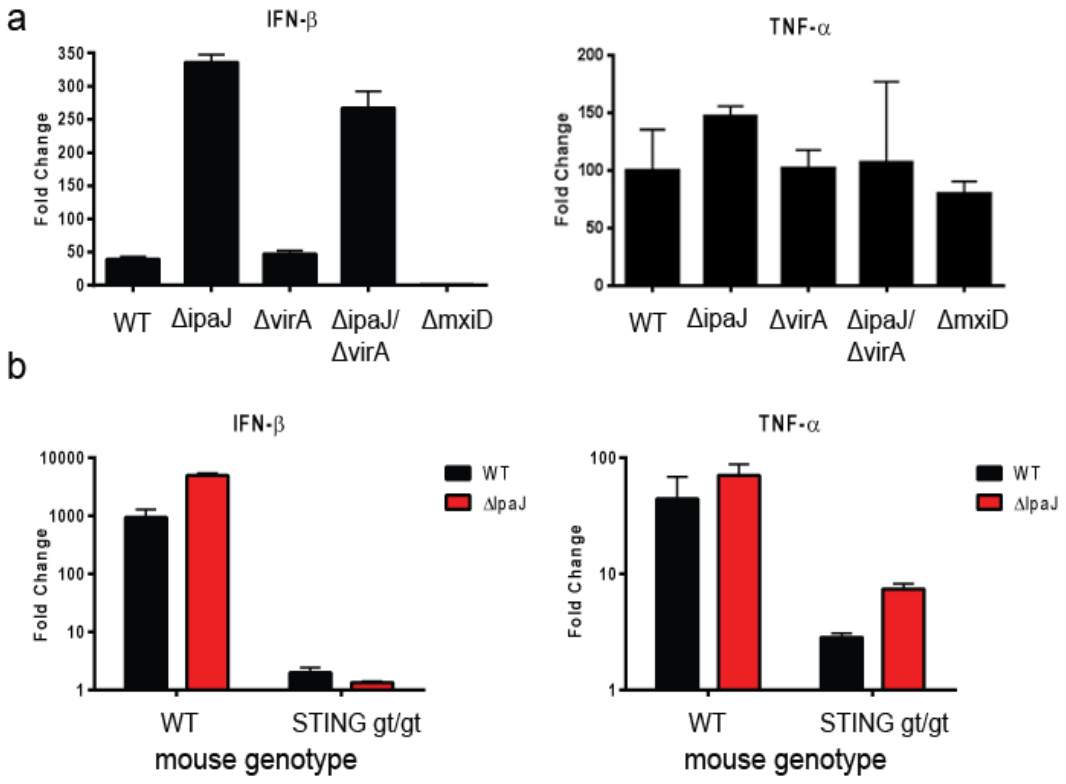

Figure 31. IpaJ suppresses STING-dependent production of IFN-β.

Primary MEF were infected with indicated *Shigella* strains for 8 hours and cytokine production (IFN-β and TNF-α) was analyzed with quantitative RT-PCR. Deletion of IpaJ but not VirA resulted in a marked increase in IFN-β production.

a. Wild type primary MEFs were infected with indicated *Shigella* strains.

b. Wild type or STING Goldenticket primary MEF were infected with wild type (black bars) or ΔipaJ (red bars) *Shigella* strains.

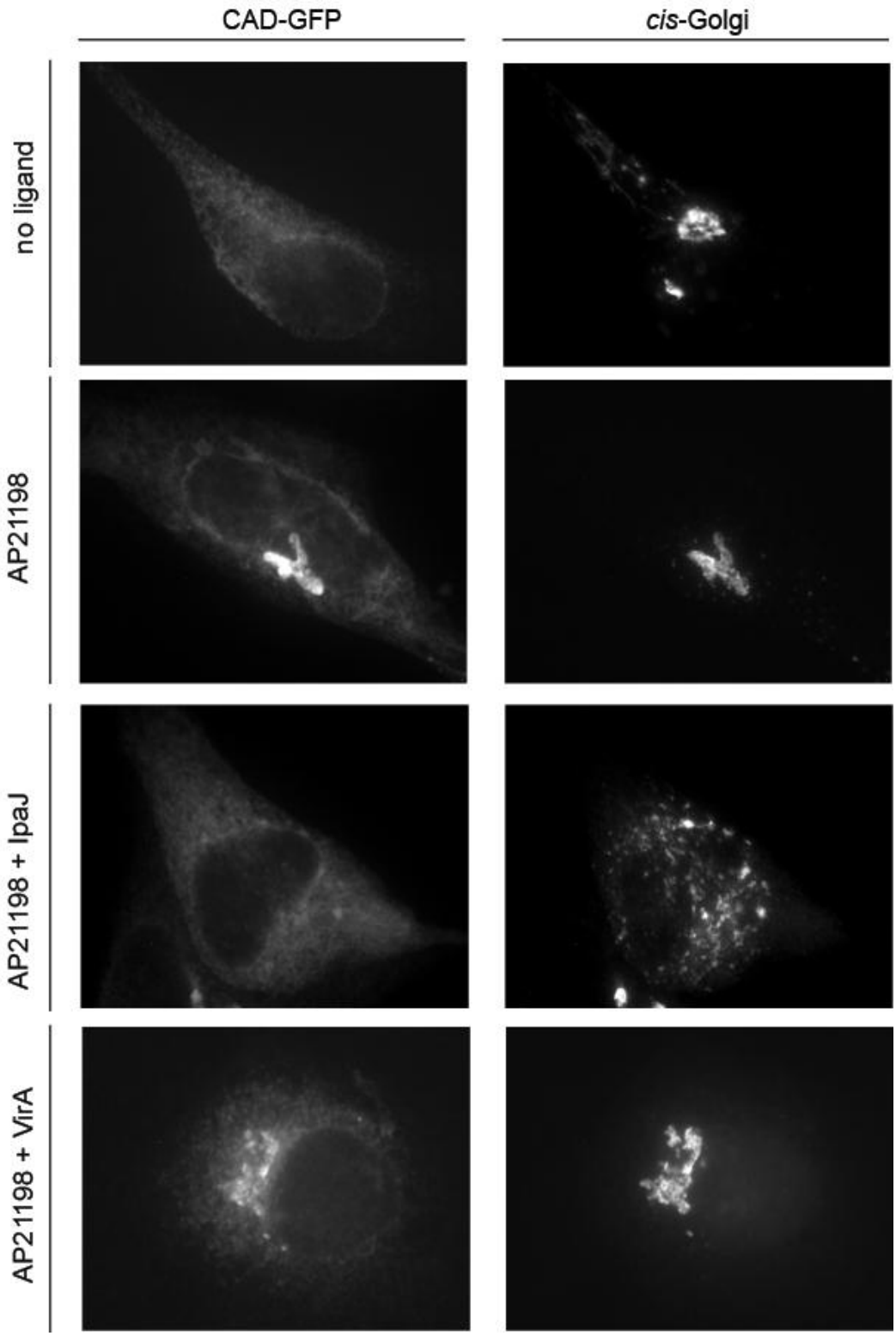
CAD-GFP
cis-Golgi
no ligand
AP21198
AP21198 + IpaJ
AP21198 + VirA

Figure 32. IpaJ prevents protein exit from the ER.

To analyze the effect of IpaJ and VirA on protein trafficking we microinjected recombinant proteins (IpaJ or VirA) into HeLa cells expressing the Golgi-CAD-GFP fusion protein. Addition of AP AP211198 ligand relieved aggregation of CAD domains and allowed fusion protein translocation to the Golgi in the control cells. Microinjection of IpaJ trapped the marker in the ER, however the CAD protein was able to reach post-ER compartment upon microinjection of VirA. cis-Golgi is visualized with α-GM130 antibodies.

Figure 33. *Listeria* secreting IpaJ or VirA disrupts the Golgi.

We adapted *Listeria monocytogenes* to express and secrete IpaJ or VirA (*Listeria*-IpaJ and *Listeria*-VirA strains) through genomic integration of fusion protein with ActA effector of *Listeria*. HeLa cells were infected with *Listeria*-IpaJ or *Listeria*-VirA or parent strain and analyzed with fluorescent microscopy. Parent strain did not have a discernable effect of the Golgi, however expression of IpaJ or VirA resulted in the disruption of the Golgi comparable to that induced by *Shigella* (compare to Figure 2c). *cis*-Golgi was visualized with gm130 antibodies (green), DNA and bacteria were visualized with DAPI staining (red).

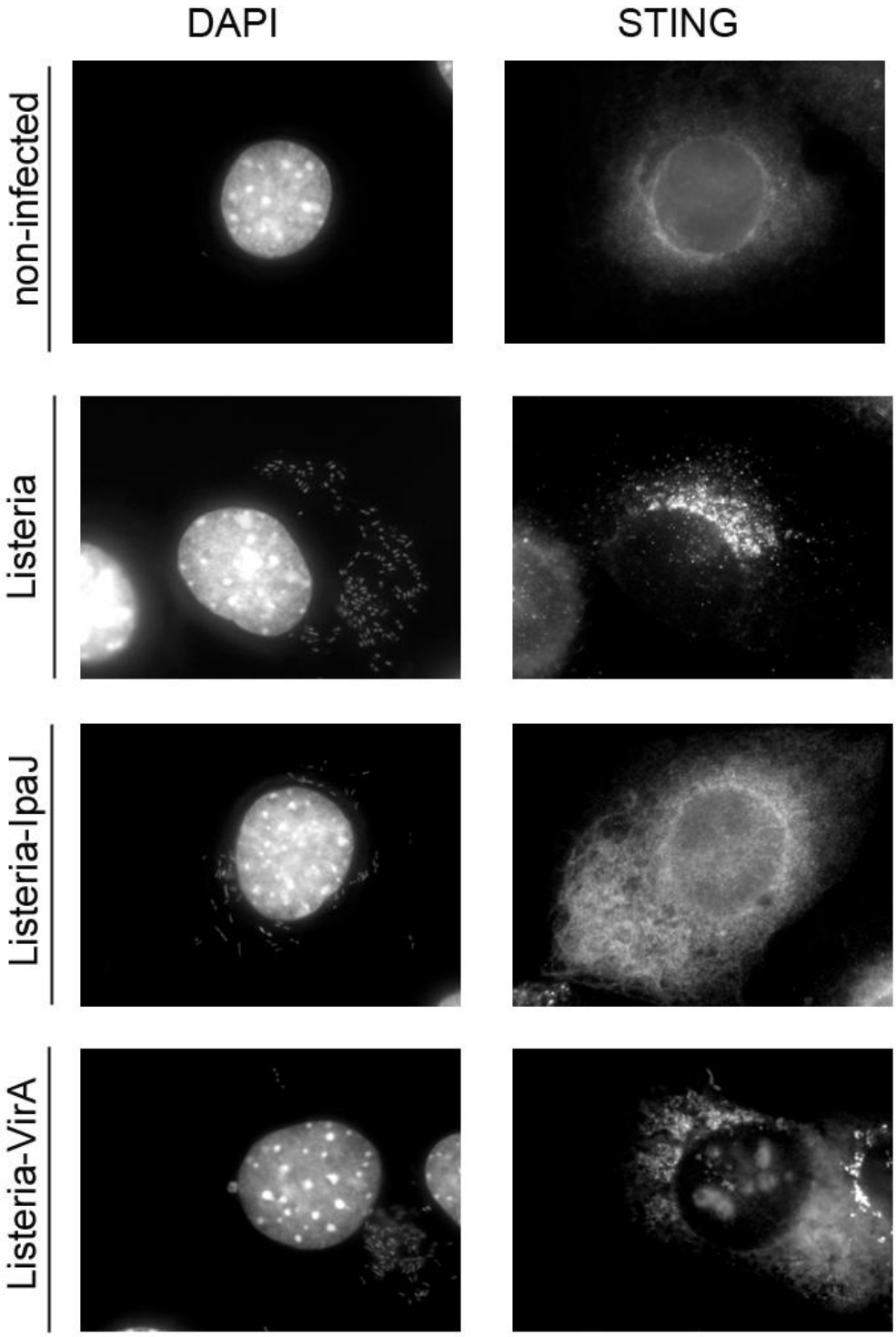
Listeria-VirA
Listeria-IpaJ
Listeria
non-infected
DAPI
STING

Figure 34. Secretion of IpaJ prevents STING translocation induced by *Listeria* infection.

MEF cells expressing STING-GFP were infected with parent *Listeria* strain or Listeria expressing IpaJ or VirA for 4 hours and and analyzed by fluorescent microscopy. STING resided in the ER in non-infected cells and its activation was assessed as its transloction from the ER. While infection with the paretn strain potently induced STING translocation to the endomembrane compartemtns, the receptor remained in the ER upon infection with *Listeria*-IpaJ. Upon infection with *Listeria*-VirA STING reached post-ER endomembrane compartment. *Listeria* was visulized with DAPI.

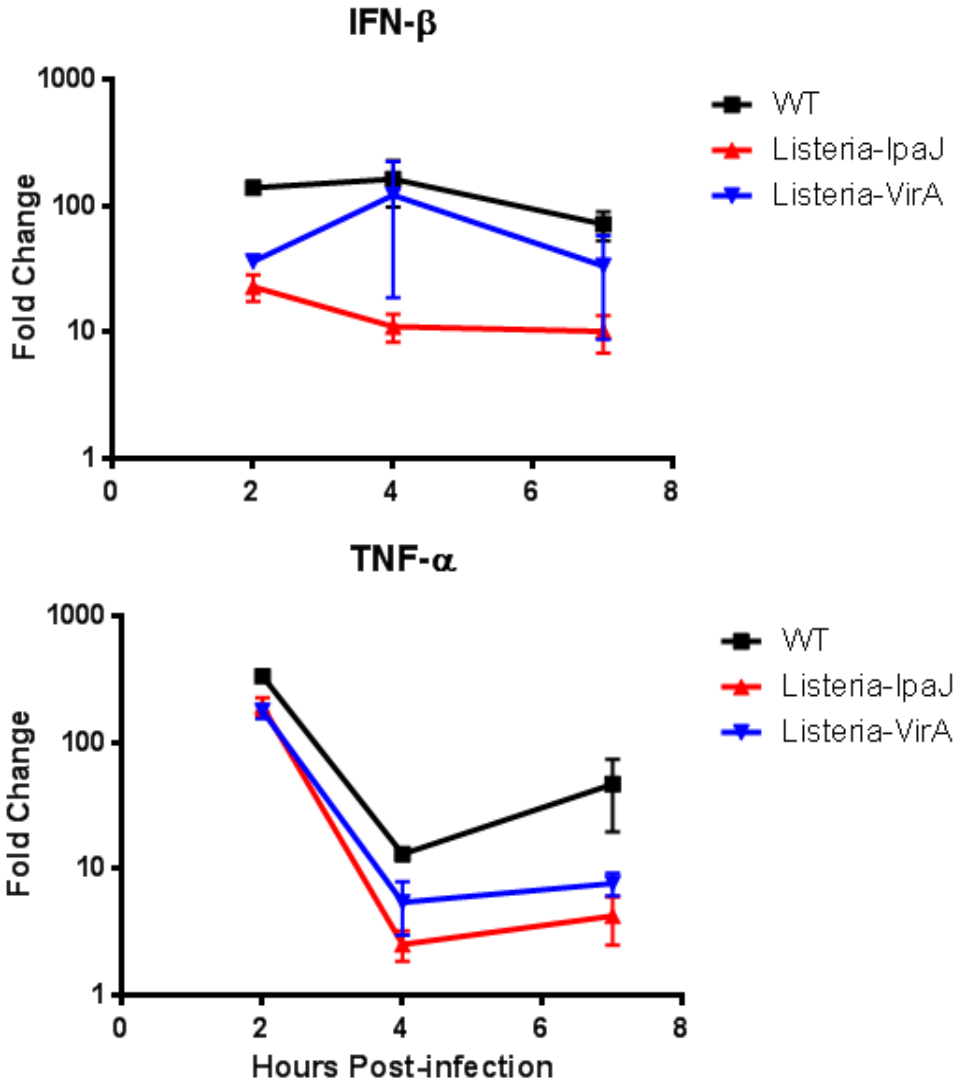

Figure 35. Secretion of IpaJ suppresses IFN-β production upon *Listeria* infection. Primary MEF were infected with indicated *Listeria* strains for indicated amount of time and cytokine production (IFN-β and TNF-α) was analyzed with quantitative RT-PCR. Deletion of IpaJ but not VirA resulted in a marked increase in IFN-β production.

Material and methods

Shigella infection studies in mice:

Female C57Bl/6 mice were purchased from the National Cancer Institute and used between 6-8 weeks of age. For infection, *Shigella flexneri* M90T or mutants were grown and back diluted from the stationary to early log phase growth (OD_{600}~0.1) in BHI media (BD Bioscience) at 37°C, washed and diluted in sterile saline, and administered dropwise (10^6 CFUs in 30 microliters volume) into the external nares of mice anesthetized with ketamine/xylazine as described(Way et al., 1998). At the indicated time points after infection, mice were euthanized, and the recoverable bacterial CFUs enumerated by plating serial dilutions of the lung homogenate on BHI plates. Statistical significance was determined by one-way analysis of variance (ANOVA, P<0.01) Tukey post hoc test. The levels of the TNF-a and IL-6 in the serum and lung homogenate were enumerated using commercially available ELISA reagents (R&D Systems). All experiments were performed under University of Minnesota IACUC approved protocols (S.S.W).

hGH trafficking assay:

As previously described (Rivera et al., 2000; Selyunin et al., 2011), HeLa cells (50% confluence) were transfected with 1 µg of4xFKBP-hGH (Ariad Pharmaceutical, Inc.; http://www.ariad.com/regulationkits;source of material, David Bernstein) and either 0.5µg eGFP–IpaJ, eGFP-VirA or pEGFP control plasmid with Fugene6 (Roche). Sixteen hours later, the medium was replaced with medium containing AP21998 (final concentration, 2 mM) or vehicle control. AP21998 was incubated with the cells for 2 h before the supernatant

was collected. The supernatant was then diluted 100-fold and compared against an hGH standard curve (12.5–400 pg/ml) for the quantification of hGH released using an hGH enzyme-linked ELISA (Roche). For no drug controls, 100% ethanol (2 µl) was incubated with the cells for 2 h.

Bacterial infection of cultured cells:

Shigella infection was performed by the same protocol as described in Chapter 2. *Listeria* infection was performed by a similar protocol with modifications. Bacteria were grown overnight at 30^0C without shaking, washed with PBS and added to mammalian cell culture at MOI~100. Plates were centrifuged at 1000xg for 10 minutes and then incubated at 37^0C. Cells were washed with gentomycin after 90 minutes, fresh antibiotic-free media was added and cell were incubated further for the indicated amount of time. After that cells were washed with PBS containing gentomycin and processed for RNA analysis.

RNA isolation, qRT-PCR analysis and Cytokine detection assay:

Total RNA from cells was isolated using TRI Reagent (Sigma) according to the manufacturer's instructions. RNA quantity and quality were confirmed using a NanoDrop® ND-1000 Spectrophotometer. cDNAs were synthesized from 1 µg total RNA using SuperScript® III First-Strand Synthesis (Invitrogen). Real-time PCR was performed using the Power SYBR Green PCR master mix in an ABI-7500 fast real-time PCR machine (Applied Biosystems) with specific gene primers.

Fluorescent microscopy.

Immunofluorescence images in all experiments were acquired with Zeiss AxioVert 200 Fluorescence Microscope. The Golgi was detected by GM130 antibodies (BD Biosciences)

and secondary anti-mouse IgG antibodies (Thermo Scientific). Cell nuclei and intracellular bacteria were visualized with DAPI.

CHAPTER FIVE
Conclusions and future directions

Many bacterial pathogens utilize secreted effectors to promote their survival and dissemination. Characterization of the secreted effectors reveals common and species-specific strategies of various pathogens and may help to develop better treatments for infectious diseases.

In the current dissertation, I determined that *Shigella flexneri* effector IpaJ is a cysteine protease with a novel specificity toward N-myristoylated proteins. This discovery adds significantly to the small, but increasing number of bacterial proteases that cleave lipidated proteins as a mechanism of microbial pathogenesis (Choy et al., 2012; Shao, Merritt, Bao, Innes, & Dixon, 2002). In addition to IpaJ, other effectors of this group – YopT and RavZ - were also shown to inhibit essential antibacterial activities of the host cell. YopT is secreted by extracellular pathogens *Yersinia spp.* It cleaves the prenylated cysteine of the RhoA family GTPases to disrupt the cytoskeleton and suppress phagocytosis (Shao et al., 2002). C. Roy and colleagues established that RavZ from *Legionella spp.* cleaved phosphatidylethanolamine-modified glycine of ATG8 to prevent destruction of the pathogen by autophagy (Choy et al., 2012). Therefore, “delipidation” of host proteins is an emerging theme in bacterial pathogenic strategies.

The initial observation that *Shigella* disrupts the Golgi structure lead me to the discovery of the IpaJ activity as a cysteine protease. ARF1 was first identified to be one of the major substrates of IpaJ. However, the observed cleavage of a large number of proteins *in*

vitro suggested that the IpaJ protease can also have other targets during infection. Driven by these considerations, I conducted an unbiased survey of the physiological substrates of IpaJ. To my knowledge, it was the first comparative analysis of the protein myristoylation profiles in various cellular conditions. The interrogation of the 'myristoylome' confirmed that IpaJ cleaved diverse proteins *in vitro* and allowed to define a range of the relevant physiological substrates of the protease. I suggest that this approach can be also utilized to analyze various 'lipidomes' in a context of different bacterial infections and other physiological states.

Using the unbiased myristoylome profiling, I expanded the list of IpaJ substrates beyond ARF1. I discovered that several other members of ARF and ARL families were also targeted by the protease. This is consistent with the Golgi phenotype induced by IpaJ, since the knockdown of any single ARF isoform does not affect the morphology of the organelle (Volpicelli-Daley, Li, Zhang, & Kahn, 2005). The Golgi ribbon represents a central hub for protein and lipid trafficking and is also a site of glycosylation and other post-translational modifications (Andreeva et al., 1998; Stanley, 2011). Importantly, different ARF (except for ARF6) and some ARL members function at different compartments of the Golgi (Donaldson & Jackson, 2011). Therefore, by targeting multiple ARF and ARL isoforms, IpaJ likely exerts a complex effect on vesicular trafficking. Why is the disruption of the Golgi trafficking important for *Shigella*? Inhibition of the Golgi function may prevent cytokine secretion and therefore is potentially beneficial for the infection. Furthermore, as *Shigella* is an intracellular pathogen, its presence may be exposed to the immune system by MHC class I – mediated antigen presentation. Since membrane translocation of MHCI receptors is the

Golgi-dependent, (Yewdell & Bennink, 1989), IpaJ may assist in the evasion from immune surveillance. This possibility presents an exciting venue for the future research.

It is interesting to point out that ARF6 was previously implicated in the bacterial uptake by macrophages and also by non-immune cells (Smyth et al., 2012; Zhang, Cox, Tseng, Donaldson, & Greenberg, 1998). If ARF6 is also important for the *Shigella* invasion, it should be selectively protected from IpaJ activity. Indeed, I found that ARF6 was an exception in the ARF family. Although IpaJ interacted with ARF6 *in vitro*, ARF6 was not cleaved upon infection and even co-expression with IpaJ. Further work should reveal the exact mechanism of ARF6 protection from IpaJ.

I aimed to gain a better understanding of how IpaJ recognized its substrates. My results point to a 'dual' interaction mechanism. First, the myristoyl-glycine is recognized by IpaJ and is required for the cleavage. Second, IpaJ specifically interacts with the active GTPase domains of ARF and thus behaves as the ARF substrate. The requirement for the exposed acylated N-terminus and the active conformation of the GTPase suggests that IpaJ cleaves membrane associated ARF/ARL when both criteria are met. However, this plausible hypothesis poses intriguing questions which require further investigation. Specifically, how does IpaJ access the activated ARF/ARL substrates? Our results map IpaJ recognitions sites on switch I, interswitch, and switch II regions of ARFs, which in active state are occupied by the ARFs host substrates. The ability of IpaJ C64A to localize on the Golgi without affecting its morphology suggests that the protease might interact with ARFs non-competitively. However, we cannot exclude that the IpaJ displaces some ARFs substrates thereby partially perturbing the Golgi function. Discriminating between these scenarios will require structural

studies of IpaJ and a kinetics analysis of the ARFs release from the membranes by IpaJ. Successful accomplishment of these goals may provide a critical insight into the mechanism of the coatamer function, which is still poorly understood.

Another question raised by the current findings: how does IpaJ interact with the membrane-embedded myristoyl group of the active ARFs? I propose three potential explanations (Figure 36a). In the first scenario, IpaJ interacts with the acyl group in the membrane. Alternatively, the myristoyl may flip in and out of the membrane, allowing IpaJ to stabilize the "out" state. Yet another potential explanation that I do not rule out here, employs the idea that the membrane-embedded myristoyl group orients the glycine in such a way that its peptide bond can be attacked by IpaJ. Further biochemical and structural characterization of IpaJ will address these possibilities and advance our understanding of the mechanism of membrane association of numerous N-myristoylated proteins.

Finally, my current results presented in this work may provide a hint on the function of the DUF3335 proteins. According to the bioinformatics analysis, IpaJ is structurally related to this family which consists of putative C39-peptidase like enzymes. C39-peptidases are bacterial bacteriocin-processing proteases which cleave their substrates after the double glycine (Havarstein, Diep, & Nes, 1995; Havarstein, Holo, & Nes, 1994). Intriguingly, this motif is identical to a part of the myristoyl-glycine group (Figure 36b). It is interesting to speculate that the members of the DUF3335 family (C39-peptidase like proteins) also recognize similar structures which may include double glycine or modified glycine residue. My findings lay a background from which to explore the function of this large yet uncharacterized family.

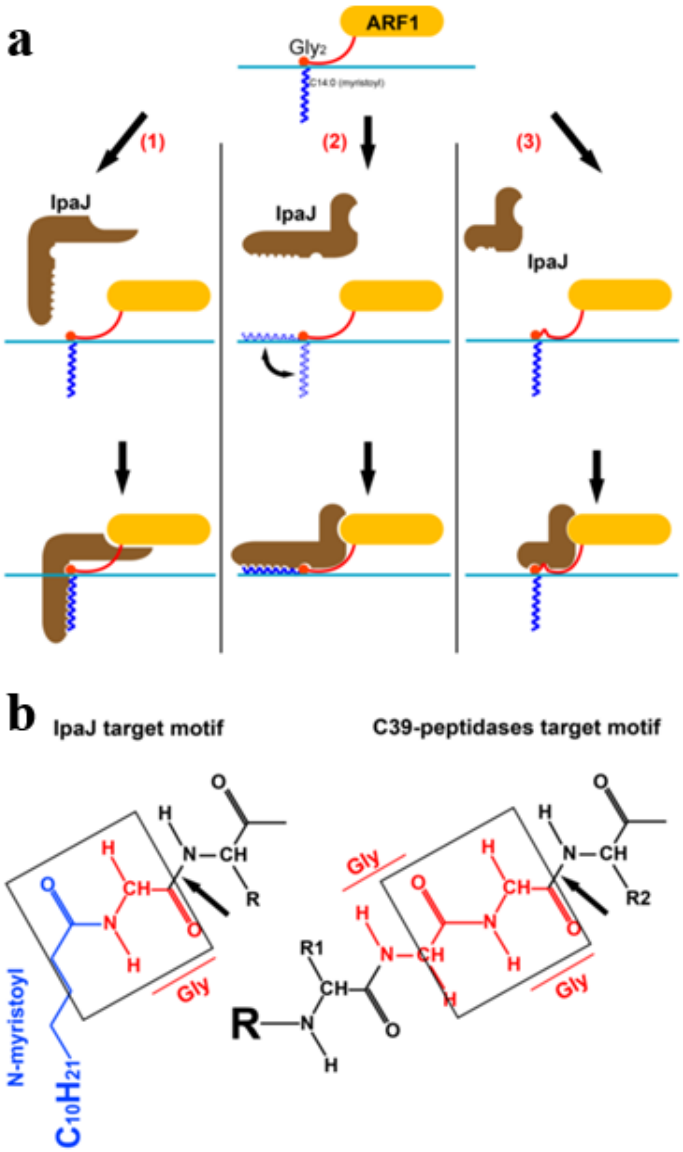

Figure 36. Substrates recognition by IpaJ and C39 peptidases.

a. Three hypothetical models of IpaJ interaction with myristoyl. (1) IpaJ interacts with the acyl group in the membrane. (2) The myristoyl flips in and out of the membrane allowing IpaJ to stabilize the "out" state. (3) The critical role of myristoyl for IpaJ is to orient the glycine in a way that its peptide bond can be attacked.

b. Comparison of the target motifs on IpaJ C39 peptidases. IpaJ recognizes myristoyl glycine. C39 peptidases cleave bacteriocin precursors after Gly-Gly pair. Black frame

encloses identical signatures in both targeted motifs. Arrows indicate cleavage sites. Glycines are marked with red, myristoyl group – with green.

TABLE 1
ARF1 mutatons used for IpaJ binding analysis

Mutation	ARF1 region
I46D	switch 1
I46K	switch 1
I46A	switch 1
I49T	switch 1
F51Y	switch 1
W66H	interswitch
D72A	switch 2
K73A	switch 2
I74T	switch 2
W78C	switch 2
R79G	switch 2
Y81T	switch 2
T85A	switch 2
E105A	helix 3
E106A	helix 3
R109A	helix 3

APPENDIX A
Abundance of the proteins upon IpaJ cleavage in vitro

Proteins with N-terminal glycine

Accession	Description	Control	IpaJ-treated	ratio	N-myristoylation confirmed
A8MUB1	Tubulin alpha-4A chain OS=Homo sapiens GN=TUBA4A PE=2 SV=1 - [A8MUB1_HUMAN]	1.09E+09	1.94E+09	1.78E+00	
A8MXY0	Syntaxin 4A (Placental), isoform CRA_c OS=Homo sapiens GN=STX4 PE=2 SV=1 - [A8MXY0_HUMAN]	7.73E+06	0.00E+00	-1.00E+01	
B4DQJ8	6-phosphogluconate dehydrogenase, decarboxylating OS=Homo sapiens GN=PGD PE=2 SV=1 - [B4DQJ8_HUMAN]	5.98E+07	1.45E+08	2.43E+00	
B7Z817	Delta(24)-sterol reductase OS=Homo sapiens GN=DHCR24 PE=2 SV=1 - [B7Z817_HUMAN]	1.49E+07	0.00E+00	-1.00E+01	
C9JFR7	Cytochrome c (Fragment) OS=Homo sapiens GN=CYCS PE=3 SV=1 - [C9JFR7_HUMAN]	2.17E+07	8.54E+07	3.94E+00	
C9JIR6	Protein phosphatase 1B (Fragment) OS=Homo sapiens GN=PPM1B PE=3 SV=1 - [C9JIR6_HUMAN]	8.83E+07	1.24E+08	1.41E+00	
E7EPN3	NADPH--cytochrome P450 reductase OS=Homo sapiens GN=POR PE=4 SV=1 - [E7EPN3_HUMAN]	1.19E+07	0.00E+00	-1.00E+01	
E9PCT3	Caveolin OS=Homo sapiens GN=CAV2 PE=3 SV=1 - [E9PCT3_HUMAN]	7.51E+06	5.33E+07	7.10E+00	
E9PMR4	CD151 antigen OS=Homo sapiens GN=CD151 PE=4 SV=1 - [E9PMR4_HUMAN]	1.17E+08	1.03E+09	8.80E+00	

E9PNW4	CD59 glycoprotein OS=Homo sapiens GN=CD59 PE=4 SV=1 - [E9PNW4_HUMAN]	4.45E+07	1.61E+08	3.62E+00	
F5GY99	Polypeptide N-acetylgalactosaminyltransferase 1 soluble form OS=Homo sapiens GN=GALNT1 PE=3 SV=1 - [F5GY99_HUMAN]	2.37E+07	4.07E+07	1.72E+00	
F5H4W0	Malic enzyme OS=Homo sapiens GN=ME1 PE=3 SV=1 - [F5H4W0_HUMAN]	1.15E+06	7.71E+06	6.68E+00	
F8W785	Golgi integral membrane protein 4 OS=Homo sapiens GN=GOLIM4 PE=4 SV=1 - [F8W785_HUMAN]	2.31E+07	5.24E+07	2.27E+00	
G8JLG1	Structural maintenance of chromosomes protein 1A OS=Homo sapiens GN=SMC1A PE=4 SV=1 - [G8JLG1_HUMAN]	1.07E+07	4.49E+06	-2.38E+00	
H3BM67	Nucleolar protein 3 (Fragment) OS=Homo sapiens GN=NOL3 PE=4 SV=1 - [H3BM67_HUMAN]	2.69E+08	0.00E+00	-1.00E+01	
J3KMX5	40S ribosomal protein S13 OS=Homo sapiens GN=RPS13 PE=4 SV=1 - [J3KMX5_HUMAN]	2.78E+07	4.85E+07	1.74E+00	
J3KR24	Isoleucine--tRNA ligase, cytoplasmic OS=Homo sapiens GN=IARS PE=4 SV=1 - [J3KR24_HUMAN]	4.28E+07	6.76E+07	1.58E+00	
K7EQL6	Ubiquitin carboxyl-terminal hydrolase 32 OS=Homo sapiens GN=USP32 PE=4 SV=1 - [K7EQL6_HUMAN]	1.93E+07	0.00E+00	-1.00E+01	
O15121	Sphingolipid delta(4)-desaturase DES1 OS=Homo sapiens GN=DEGS1 PE=1 SV=1 - [DEGS1_HUMAN]	1.98E+08	1.04E+08	-1.90E+00	YES
O15355	Protein phosphatase 1G OS=Homo sapiens GN=PPM1G PE=1 SV=1 - [PPM1G_HUMAN]	1.12E+09	1.73E+09	1.55E+00	

O15427	Monocarboxylate transporter 4 OS=Homo sapiens GN=SLC16A3 PE=1 SV=1 - [MOT4_HUMAN]	0.00E+00	4.78E+08	1.00E+01	
O60291	E3 ubiquitin-protein ligase MGRN1 OS=Homo sapiens GN=MGRN1 PE=1 SV=2 - [MGRN1_HUMAN]	2.26E+07	0.00E+00	-1.00E+01	YES
O75695	Protein XRP2 OS=Homo sapiens GN=RP2 PE=1 SV=4 - [XRP2_HUMAN]	2.97E+07	0.00E+00	-1.00E+01	YES
O75844	CAAX prenyl protease 1 homolog OS=Homo sapiens GN=ZMPSTE24 PE=1 SV=2 - [FACE1_HUMAN]	0.00E+00	1.03E+07	1.00E+01	
O95466	Formin-like protein 1 OS=Homo sapiens GN=FMNL1 PE=1 SV=3 - [FMNL_HUMAN]	3.58E+07	0.00E+00	-1.00E+01	YES
O96008	Mitochondrial import receptor subunit TOM40 homolog OS=Homo sapiens GN=TOMM40 PE=1 SV=1 - [TOM40_HUMAN]	4.18E+07	0.00E+00	-1.00E+01	
P00387-2	Isoform 2 of NADH-cytochrome b5 reductase 3 OS=Homo sapiens GN=CYB5R3 - [NB5R3_HUMAN]	1.53E+09	0.00E+00	-1.00E+01	YES
P00519	Tyrosine-protein kinase ABL1 OS=Homo sapiens GN=ABL1 PE=1 SV=4 - [ABL1_HUMAN]	2.82E+07	0.00E+00	-1.00E+01	YES
P04899	Guanine nucleotide-binding protein G(i) subunit alpha-2 OS=Homo sapiens GN=GNAI2 PE=1 SV=3 - [GNAI2_HUMAN]	1.82E+09	5.26E+08	-3.46E+00	YES
P07947	Tyrosine-protein kinase Yes OS=Homo sapiens GN=YES1 PE=1 SV=3 - [YES_HUMAN]	1.12E+08	0.00E+00	-1.00E+01	YES
P07948	Tyrosine-protein kinase Lyn OS=Homo sapiens GN=LYN PE=1 SV=3 - [LYN_HUMAN]	8.23E+07	0.00E+00	-1.00E+01	YES
P08708	40S ribosomal protein S17 OS=Homo sapiens GN=RPS17 PE=1 SV=2 - [RS17_HUMAN]	0.00E+00	7.80E+07	1.00E+01	

P08754	Guanine nucleotide-binding protein G(k) subunit alpha OS=Homo sapiens GN=GNAI3 PE=1 SV=3 - [GNAI3_HUMAN]	1.89E+09	5.26E+08	-3.59E+00	YES
P09471-2	Isoform Alpha-2 of Guanine nucleotide-binding protein G(o) subunit alpha OS=Homo sapiens GN=GNAO1 - [GNAO_HUMAN]	1.70E+09	4.61E+08	-3.70E+00	YES
P12931	Proto-oncogene tyrosine-protein kinase Src OS=Homo sapiens GN=SRC PE=1 SV=3 - [SRC_HUMAN]	4.08E+07	0.00E+00	-1.00E+01	YES
P17568	NADH dehydrogenase [ubiquinone] 1 beta subcomplex subunit 7 OS=Homo sapiens GN=NDUFB7 PE=1 SV=4 - [NDUB7_HUMAN]	7.11E+07	4.43E+06	-1.00E+01	YES
P18085	ADP-ribosylation factor 4 OS=Homo sapiens GN=ARF4 PE=1 SV=3 - [ARF4_HUMAN]	6.11E+09	6.90E+09	1.13E+00	YES
P22694-4	Isoform 4 of cAMP-dependent protein kinase catalytic subunit beta OS=Homo sapiens GN=PRKACB - [KAPCB_HUMAN]	7.57E+08	0.00E+00	-1.00E+01	YES
P24534	Elongation factor 1-beta OS=Homo sapiens GN=EEF1B2 PE=1 SV=3 - [EF1B_HUMAN]	1.42E+08	1.34E+08	-1.06E+00	
P26006	Integrin alpha-3 OS=Homo sapiens GN=ITGA3 PE=1 SV=5 - [ITA3_HUMAN]	0.00E+00	1.89E+07	1.00E+01	
P26583	High mobility group protein B2 OS=Homo sapiens GN=HMGB2 PE=1 SV=2 - [HMGB2_HUMAN]	3.98E+07	7.20E+07	1.81E+00	
P27701	CD82 antigen OS=Homo sapiens GN=CD82 PE=1 SV=1 - [CD82_HUMAN]	5.43E+07	1.05E+08	1.92E+00	
P29966	Myristoylated alanine-rich C-kinase substrate OS=Homo sapiens GN=MARCKS PE=1 SV=4 - [MARCS_HUMAN]	1.28E+09	2.59E+06	-1.00E+01	YES

P35813	Protein phosphatase 1A OS=Homo sapiens GN=PPM1A PE=1 SV=1 - [PPM1A_HUMAN]	1.72E+08	1.64E+08	-1.05E+00	YES
P37235	Hippocalcin-like protein 1 OS=Homo sapiens GN=HPCAL1 PE=1 SV=3 - [HPCL1_HUMAN]	5.93E+08	5.17E+08	-1.15E+00	YES
P39656	Dolichyl-diphosphooligosaccharide--protein glycosyltransferase 48 kDa subunit OS=Homo sapiens GN=DDOST PE=1 SV=4 - [OST48_HUMAN]	2.35E+07	3.58E+07	1.52E+00	
P43121	Cell surface glycoprotein MUC18 OS=Homo sapiens GN=MCAM PE=1 SV=2 - [MUC18_HUMAN]	2.52E+07	1.93E+07	-1.31E+00	
P46777	60S ribosomal protein L5 OS=Homo sapiens GN=RPL5 PE=1 SV=3 - [RL5_HUMAN]	5.67E+07	8.40E+07	1.48E+00	
P51659	Peroxisomal multifunctional enzyme type 2 OS=Homo sapiens GN=HSD17B4 PE=1 SV=3 - [DHB4_HUMAN]	1.45E+07	2.28E+07	1.57E+00	
P53701	Cytochrome c-type heme lyase OS=Homo sapiens GN=HCCS PE=1 SV=1 - [CCHL_HUMAN]	2.91E+08	6.89E+06	-1.00E+01	
P54577	Tyrosine--tRNA ligase, cytoplasmic OS=Homo sapiens GN=YARS PE=1 SV=4 - [SYYC_HUMAN]	2.62E+07	4.64E+07	1.77E+00	
P61204	ADP-ribosylation factor 3 OS=Homo sapiens GN=ARF3 PE=1 SV=2 - [ARF3_HUMAN]	6.22E+09	9.25E+09	1.49E+00	YES
P61313	60S ribosomal protein L15 OS=Homo sapiens GN=RPL15 PE=1 SV=2 - [RL15_HUMAN]	1.17E+08	1.79E+07	-6.55E+00	
P61353	60S ribosomal protein L27 OS=Homo sapiens GN=RPL27 PE=1 SV=2 - [RL27_HUMAN]	0.00E+00	6.55E+07	1.00E+01	

P62166	Neuronal calcium sensor 1 OS=Homo sapiens GN=NCS1 PE=1 SV=2 - [NCS1_HUMAN]	9.10E+07	0.00E+00	-1.00E+01	YES
P62191	26S protease regulatory subunit 4 OS=Homo sapiens GN=PSMC1 PE=1 SV=1 - [PRS4_HUMAN]	1.57E+09	5.71E+07	-1.00E+01	YES
P62241	40S ribosomal protein S8 OS=Homo sapiens GN=RPS8 PE=1 SV=2 - [RS8_HUMAN]	3.44E+08	6.57E+08	1.91E+00	
P62266	40S ribosomal protein S23 OS=Homo sapiens GN=RPS23 PE=1 SV=3 - [RS23_HUMAN]	1.10E+08	1.61E+08	1.47E+00	
P62330	ADP-ribosylation factor 6 OS=Homo sapiens GN=ARF6 PE=1 SV=2 - [ARF6_HUMAN]	5.85E+08	7.04E+08	1.20E+00	YES
P62917	60S ribosomal protein L8 OS=Homo sapiens GN=RPL8 PE=1 SV=2 - [RL8_HUMAN]	9.06E+07	1.95E+08	2.15E+00	
P63096	Guanine nucleotide-binding protein G(i) subunit alpha-1 OS=Homo sapiens GN=GNAI1 PE=1 SV=2 - [GNAI1_HUMAN]	1.82E+09	5.26E+08	-3.46E+00	YES
P68104	Elongation factor 1-alpha 1 OS=Homo sapiens GN=EEF1A1 PE=1 SV=1 - [EF1A1_HUMAN]	1.43E+09	3.07E+09	2.15E+00	
P80723	Brain acid soluble protein 1 OS=Homo sapiens GN=BASP1 PE=1 SV=2 - [BASP1_HUMAN]	6.74E+09	8.90E+07	-1.00E+01	YES
P84085	ADP-ribosylation factor 5 OS=Homo sapiens GN=ARF5 PE=1 SV=2 - [ARF5_HUMAN]	4.63E+09	6.90E+09	1.49E+00	YES
Q02952-3	Isoform 3 of A-kinase anchor protein 12 OS=Homo sapiens GN=AKAP12 - [AKA12_HUMAN]	1.87E+08	0.00E+00	-1.00E+01	YES
Q08211	ATP-dependent RNA helicase A OS=Homo sapiens GN=DHX9 PE=1 SV=4 - [DHX9_HUMAN]	6.89E+07	1.81E+08	2.63E+00	

Q08J23	tRNA (cytosine(34)-C(5))-methyltransferase OS=Homo sapiens GN=NSUN2 PE=1 SV=2 - [NSUN2_HUMAN]	5.10E+07	9.43E+07	1.85E+00	
Q14108	Lysosome membrane protein 2 OS=Homo sapiens GN=SCARB2 PE=1 SV=2 - [SCRB2_HUMAN]	9.28E+07	1.78E+08	1.92E+00	
Q14254	Flotillin-2 OS=Homo sapiens GN=FLOT2 PE=1 SV=2 - [FLOT2_HUMAN]	2.28E+08	4.33E+08	1.90E+00	
Q14699	Raftlin OS=Homo sapiens GN=RFTN1 PE=1 SV=4 - [RFTN1_HUMAN]	4.60E+07	0.00E+00	-1.00E+01	YES
Q5T7C4	High mobility group protein B1 OS=Homo sapiens GN=HMGB1 PE=2 SV=1 - [Q5T7C4_HUMAN]	1.87E+08	3.82E+08	2.05E+00	
Q5TC84	Opioid growth factor receptor-like protein 1 OS=Homo sapiens GN=OGFRL1 PE=2 SV=1 - [OGRL1_HUMAN]	7.31E+06	0.00E+00	-1.00E+01	
Q6IAA8	Ragulator complex protein LAMTOR1 OS=Homo sapiens GN=LAMTOR1 PE=1 SV=2 - [LTOR1_HUMAN]	4.81E+08	6.57E+07	-7.32E+00	YES
Q6UB35	Monofunctional C1-tetrahydrofolate synthase, mitochondrial OS=Homo sapiens GN=MTHFD1L PE=1 SV=1 - [C1TM_HUMAN]	2.39E+07	5.46E+07	2.28E+00	
Q7RTS9-2	Isoform 2 of Dymeclin OS=Homo sapiens GN=DYM - [DYM_HUMAN]	2.74E+07	0.00E+00	-1.00E+01	YES
Q8N9N7	Leucine-rich repeat-containing protein 57 OS=Homo sapiens GN=LRRC57 PE=1 SV=1 - [LRC57_HUMAN]	1.14E+08	0.00E+00	-1.00E+01	
Q8NHG8	E3 ubiquitin-protein ligase ZNRF2 OS=Homo sapiens GN=ZNRF2 PE=1 SV=1 - [ZNRF2_HUMAN]	9.88E+07	0.00E+00	-1.00E+01	YES

Q8WWI5	Choline transporter-like protein 1 OS=Homo sapiens GN=SLC44A1 PE=1 SV=1 - [CTL1_HUMAN]	2.45E+07	2.39E+07	-1.03E+00	YES
Q96BS2	Calcineurin B homologous protein 3 OS=Homo sapiens GN=TESC PE=1 SV=3 - [CHP3_HUMAN]	2.57E+08	0.00E+00	-1.00E+01	YES
Q96FZ7	Charged multivesicular body protein 6 OS=Homo sapiens GN=CHMP6 PE=1 SV=3 - [CHMP6_HUMAN]	6.45E+07	0.00E+00	-1.00E+01	YES
Q96PY5	Formin-like protein 2 OS=Homo sapiens GN=FMNL2 PE=1 SV=3 - [FMNL2_HUMAN]	8.62E+06	0.00E+00	-1.00E+01	YES
Q96QC4	MHC class I polypeptide-related sequence A OS=Homo sapiens GN=MICA PE=2 SV=1 - [Q96QC4_HUMAN]	0.00E+00	2.12E+08	1.00E+01	
Q99487	Platelet-activating factor acetylhydrolase 2, cytoplasmic OS=Homo sapiens GN=PAFAH2 PE=1 SV=1 - [PAFA2_HUMAN]	1.57E+07	0.00E+00	-1.00E+01	
Q99570	Phosphoinositide 3-kinase regulatory subunit 4 OS=Homo sapiens GN=PIK3R4 PE=1 SV=3 - [PI3R4_HUMAN]	7.16E+07	6.34E+07	-1.13E+00	YES
Q99618	Cell division cycle-associated protein 3 OS=Homo sapiens GN=CDCA3 PE=1 SV=1 - [CDCA3_HUMAN]	7.14E+07	0.00E+00	-1.00E+01	
Q99653	Calcineurin B homologous protein 1 OS=Homo sapiens GN=CHP1 PE=1 SV=3 - [CHP1_HUMAN]	3.18E+08	0.00E+00	-1.00E+01	YES
Q9BPX3	Condensin complex subunit 3 OS=Homo sapiens GN=NCAPG PE=1 SV=1 - [CND3_HUMAN]	0.00E+00	6.56E+06	1.00E+01	
Q9BRQ6	Coiled-coil-helix-coiled-coil-helix domain-containing protein 6, mitochondrial OS=Homo sapiens GN=CHCHD6 PE=1 SV=1 - [CHCH6_HUMAN]	5.97E+06	0.00E+00	-1.00E+01	YES

Q9BRQ8	Apoptosis-inducing factor 2 OS=Homo sapiens GN=AIFM2 PE=1 SV=1 - [AIFM2_HUMAN]	1.47E+08	0.00E+00	-1.00E+01	YES
Q9C0E8-2	Isoform 2 of Protein lunapark OS=Homo sapiens GN=LNP - [LNP_HUMAN]	8.71E+07	0.00E+00	-1.00E+01	YES
Q9H4G4	Golgi-associated plant pathogenesis-related protein 1 OS=Homo sapiens GN=GLIPR2 PE=1 SV=3 - [GAPR1_HUMAN]	1.09E+08	0.00E+00	-1.00E+01	YES
Q9H8Y8-2	Isoform 2 of Golgi reassembly-stacking protein 2 OS=Homo sapiens GN=GORASP2 - [GORS2_HUMAN]	2.66E+08	0.00E+00	-1.00E+01	YES
Q9HBL7	Plasminogen receptor (KT) OS=Homo sapiens GN=PLGRKT PE=1 SV=1 - [PLRKT_HUMAN]	6.68E+07	0.00E+00	-1.00E+01	
Q9NRX5	Serine incorporator 1 OS=Homo sapiens GN=SERINC1 PE=1 SV=1 - [SERC1_HUMAN]	4.25E+08	3.41E+08	-1.25E+00	YES
Q9NUM4	Transmembrane protein 106B OS=Homo sapiens GN=TMEM106B PE=1 SV=2 - [T106B_HUMAN]	9.58E+07	0.00E+00	-1.00E+01	
Q9NUQ9	Protein FAM49B OS=Homo sapiens GN=FAM49B PE=1 SV=1 - [FA49B_HUMAN]	6.89E+08	1.28E+09	1.85E+00	
Q9NX63	Coiled-coil-helix-coiled-coil-helix domain-containing protein 3, mitochondrial OS=Homo sapiens GN=CHCHD3 PE=1 SV=1 - [CHCH3_HUMAN]	6.51E+08	2.85E+08	-2.28E+00	YES
Q9P032	NADH dehydrogenase [ubiquinone] 1 alpha subcomplex assembly factor 4 OS=Homo sapiens GN=NDUFAF4 PE=1 SV=1 - [NDUF4_HUMAN]	6.97E+07	0.00E+00	-1.00E+01	
Q9P2B2	Prostaglandin F2 receptor negative regulator OS=Homo sapiens GN=PTGFRN PE=1 SV=2 - [FPRP_HUMAN]	1.72E+07	4.72E+07	2.75E+00	

Q9Y266	Nuclear migration protein nudC OS=Homo sapiens GN=NUDC PE=1 SV=1 - [NUDC_HUMAN]	3.01E+07	1.06E+08	3.51E+00	
Q9Y478	5'-AMP-activated protein kinase subunit beta-1 OS=Homo sapiens GN=PRKAB1 PE=1 SV=4 - [AAKB1_HUMAN]	3.89E+07	0.00E+00	-1.00E+01	YES
Q9Y6M5	Zinc transporter 1 OS=Homo sapiens GN=SLC30A1 PE=1 SV=3 - [ZNT1_HUMAN]	3.92E+07	1.52E+08	3.88E+00	

Proteins without N-terminal glycine

Accession	Description	Control	IpaJ-treated	ratio
A6NJZ9	Nucleolar complex protein 3 homolog OS=Homo sapiens GN=NOC3L PE=4 SV=1 - [A6NJZ9_HUMAN]	3.30E+06	7.68E+07	1.00E+01
A6PVH9	Copine I OS=Homo sapiens GN=CPNE1 PE=4 SV=1 - [A6PVH9_HUMAN]	1.20E+07	2.23E+07	1.86E+00
A6PVN6	Protein phosphatase 2A activator, regulatory subunit 4 (Fragment) OS=Homo sapiens GN=PPP2R4 PE=4 SV=1 - [A6PVN6_HUMAN]	6.94E+06	0.00E+00	-1.00E+01
A8K3Z3	26S protease regulatory subunit 8 OS=Homo sapiens GN=PSMC5 PE=2 SV=1 - [A8K3Z3_HUMAN]	5.65E+08	3.08E+07	-1.00E+01
A8K8G0	Hepatoma-derived growth factor OS=Homo sapiens GN=HDGF PE=2 SV=1 - [A8K8G0_HUMAN]	4.84E+07	0.00E+00	-1.00E+01
A8MUD9	60S ribosomal protein L7 OS=Homo sapiens GN=RPL7 PE=3 SV=1 - [A8MUD9_HUMAN]	3.74E+07	1.40E+08	3.73E+00
B1AHB1	DNA replication licensing factor MCM5 OS=Homo sapiens GN=MCM5 PE=3 SV=1 - [B1AHB1_HUMAN]	1.34E+07	4.35E+07	3.25E+00

B1AK87	Capping protein (Actin filament) muscle Z-line, beta OS=Homo sapiens GN=CAPZB PE=4 SV=1 - [B1AK87_HUMAN]	2.76E+07	3.57E+07	1.30E+00
B1ALW1	Thioredoxin OS=Homo sapiens GN=TXN PE=4 SV=1 - [B1ALW1_HUMAN]	3.44E+08	1.26E+08	-2.73E+00
B1ANR0	Poly(A) binding protein, cytoplasmic 4 (Inducible form) OS=Homo sapiens GN=PABPC4 PE=4 SV=1 - [B1ANR0_HUMAN]	5.10E+07	9.90E+07	1.94E+00
B3KQC5	Endoplasmic reticulum mannosyl-oligosaccharide 1,2-alpha-mannosidase OS=Homo sapiens GN=MAN1B1 PE=2 SV=1 - [B3KQC5_HUMAN]	1.94E+06	4.24E+06	2.19E+00
B3KV55	Glutamate dehydrogenase OS=Homo sapiens GN=GLUD1 PE=2 SV=1 - [B3KV55_HUMAN]	6.06E+06	2.67E+07	4.41E+00
B3KXI2	Protein transport protein Sec23A OS=Homo sapiens GN=SEC23A PE=2 SV=1 - [B3KXI2_HUMAN]	8.92E+06	2.83E+07	3.17E+00
B4DFN6	2',3'-cyclic-nucleotide 3'-phosphodiesterase OS=Homo sapiens GN=CNP PE=2 SV=1 - [B4DFN6_HUMAN]	0.00E+00	2.09E+07	1.00E+01
B4DHG0	Dihydrolipoyl dehydrogenase, mitochondrial OS=Homo sapiens GN=DLD PE=2 SV=1 - [B4DHG0_HUMAN]	2.97E+07	5.96E+07	2.01E+00
B4DJ10	Leucine--tRNA ligase, cytoplasmic OS=Homo sapiens GN=LARS PE=2 SV=1 - [B4DJ10_HUMAN]	1.31E+07	4.85E+07	3.71E+00
B4DJP7	Small nuclear ribonucleoprotein Sm D3 OS=Homo sapiens GN=SNRPD3 PE=2 SV=1 - [B4DJP7_HUMAN]	0.00E+00	2.77E+07	1.00E+01
B4DJV2	Citrate synthase OS=Homo sapiens GN=CS PE=2 SV=1 - [B4DJV2_HUMAN]	2.98E+07	1.01E+08	3.39E+00

B4DK69	Aldo-keto reductase family 1 member C2 OS=Homo sapiens GN=AKR1C2 PE=2 SV=1 - [B4DK69_HUMAN]	1.78E+08	3.16E+08	1.77E+00
B4DKB2	Endothelin-converting enzyme 1 OS=Homo sapiens GN=ECE1 PE=2 SV=1 - [B4DKB2_HUMAN]	1.82E+07	4.61E+07	2.53E+00
B4DL14	ATP synthase gamma chain OS=Homo sapiens GN=ATP5C1 PE=2 SV=1 - [B4DL14_HUMAN]	2.18E+07	1.27E+08	5.83E+00
B4DLR8	NAD(P)H dehydrogenase [quinone] 1 OS=Homo sapiens GN=NQO1 PE=2 SV=1 - [B4DLR8_HUMAN]	9.14E+07	1.84E+08	2.01E+00
B4DLW8	Probable ATP-dependent RNA helicase DDX5 OS=Homo sapiens GN=DDX5 PE=2 SV=1 - [B4DLW8_HUMAN]	1.35E+08	2.48E+08	1.84E+00
B4DM74	60S ribosomal protein L18a OS=Homo sapiens GN=RPL18A PE=2 SV=1 - [B4DM74_HUMAN]	7.38E+07	1.92E+08	2.61E+00
B4DN45	S-adenosylmethionine synthase OS=Homo sapiens GN=MAT2A PE=2 SV=1 - [B4DN45_HUMAN]	9.50E+07	8.01E+07	-1.19E+00
B4DPJ8	T-complex protein 1 subunit zeta OS=Homo sapiens GN=CCT6A PE=2 SV=1 - [B4DPJ8_HUMAN]	5.13E+07	8.85E+07	1.73E+00
B4DRF4	Very-long-chain (3R)-3-hydroxyacyl-[acyl-carrier protein] dehydratase 3 OS=Homo sapiens GN=PTPLAD1 PE=2 SV=1 - [B4DRF4_HUMAN]	1.94E+07	7.06E+07	3.65E+00
B4DS13	Eukaryotic translation initiation factor 4B OS=Homo sapiens GN=EIF4B PE=2 SV=1 - [B4DS13_HUMAN]	0.00E+00	3.25E+07	1.00E+01

B4DT72	26S proteasome non-ATPase regulatory subunit 3 OS=Homo sapiens GN=PSMD3 PE=2 SV=1 - [B4DT72_HUMAN]	1.97E+07	3.95E+07	2.00E+00
B4DU58	Macrophage-capping protein OS=Homo sapiens GN=CAPG PE=2 SV=1 - [B4DU58_HUMAN]	0.00E+00	3.30E+07	1.00E+01
B4DUE9	Serine incorporator 3 OS=Homo sapiens GN=SERINC3 PE=2 SV=1 - [B4DUE9_HUMAN]	4.59E+07	9.42E+07	2.05E+00
B4DUR8	T-complex protein 1 subunit gamma OS=Homo sapiens GN=CCT3 PE=2 SV=1 - [B4DUR8_HUMAN]	1.57E+08	2.96E+08	1.89E+00
B4DVY1	Eukaryotic translation initiation factor 3 subunit D OS=Homo sapiens GN=EIF3D PE=2 SV=1 - [B4DVY1_HUMAN]	1.94E+07	2.02E+08	1.00E+01
B4DWJ2	Glutamine--tRNA ligase OS=Homo sapiens GN=QARS PE=2 SV=1 - [B4DWJ2_HUMAN]	1.94E+07	2.86E+07	1.48E+00
B4DWW1	ADP-ribosylation factor-like protein 1 OS=Homo sapiens GN=ARL1 PE=2 SV=1 - [B4DWW1_HUMAN]	3.44E+08	2.30E+08	-1.50E+00
B4DX42	Splicing factor 1 OS=Homo sapiens GN=SF1 PE=2 SV=1 - [B4DX42_HUMAN]	0.00E+00	2.47E+07	1.00E+01
B4DX52	DnaJ homolog subfamily B member 1 OS=Homo sapiens GN=DNAJB1 PE=2 SV=1 - [B4DX52_HUMAN]	4.17E+06	0.00E+00	-1.00E+01
B4DXI8	26S proteasome non-ATPase regulatory subunit 7 OS=Homo sapiens GN=PSMD7 PE=2 SV=1 - [B4DXI8_HUMAN]	0.00E+00	1.34E+07	1.00E+01
B4DY13	Nucleolar GTP-binding protein 1 OS=Homo sapiens GN=GTPBP4 PE=2 SV=1 - [B4DY13_HUMAN]	0.00E+00	1.50E+07	1.00E+01

B4DY66	SUMO-activating enzyme subunit 1 OS=Homo sapiens GN=SAE1 PE=2 SV=1 - [B4DY66_HUMAN]	0.00E+00	1.13E+07	1.00E+01
B4DZI8	Coatomer protein complex, subunit beta 2 (Beta prime), isoform CRA_b OS=Homo sapiens GN=COPB2 PE=2 SV=1 - [B4DZI8_HUMAN]	1.33E+07	2.42E+07	1.82E+00
B4E2V5	Erythrocyte band 7 integral membrane protein OS=Homo sapiens GN=STOM PE=2 SV=1 - [B4E2V5_HUMAN]	4.08E+08	7.36E+08	1.80E+00
B4E2W0	3-ketoacyl-CoA thiolase OS=Homo sapiens GN=HADHB PE=2 SV=1 - [B4E2W0_HUMAN]	2.79E+08	4.60E+08	1.65E+00
B7Z1R5	V-type proton ATPase catalytic subunit A OS=Homo sapiens GN=ATP6V1A PE=2 SV=1 - [B7Z1R5_HUMAN]	1.03E+07	2.80E+07	2.71E+00
B7Z254	Protein disulfide-isomerase A6 OS=Homo sapiens GN=PDIA6 PE=2 SV=1 - [B7Z254_HUMAN]	5.61E+07	8.73E+07	1.56E+00
B7Z2S5	Thioredoxin reductase 1, cytoplasmic OS=Homo sapiens GN=TXNRD1 PE=2 SV=1 - [B7Z2S5_HUMAN]	5.17E+07	1.63E+08	3.15E+00
B7Z5C0	DnaJ homolog subfamily A member 1 OS=Homo sapiens GN=DNAJA1 PE=2 SV=1 - [B7Z5C0_HUMAN]	4.67E+07	5.64E+07	1.21E+00
B7Z6M1	Plastin-3 OS=Homo sapiens GN=PLS3 PE=2 SV=1 - [B7Z6M1_HUMAN]	6.77E+07	1.12E+08	1.65E+00
B7Z9L0	T-complex protein 1 subunit delta OS=Homo sapiens GN=CCT4 PE=2 SV=1 - [B7Z9L0_HUMAN]	6.20E+07	1.80E+08	2.91E+00
C9IZ01	Elongation factor G, mitochondrial OS=Homo sapiens GN=GFM1 PE=4 SV=1 - [C9IZ01_HUMAN]	1.49E+07	1.85E+07	1.24E+00

C9IZZ0	Ras-related protein Rab-7a (Fragment) OS=Homo sapiens GN=RAB7A PE=4 SV=1 - [C9IZZ0_HUMAN]	4.21E+07	8.05E+07	1.91E+00
C9J406	Mitochondrial inner membrane protein OS=Homo sapiens GN=IMMT PE=4 SV=1 - [C9J406_HUMAN]	1.81E+07	2.15E+07	1.19E+00
C9J8H9	ATP synthase subunit f, mitochondrial OS=Homo sapiens GN=ATP5J2 PE=4 SV=1 - [C9J8H9_HUMAN]	2.58E+07	9.44E+07	3.66E+00
C9J9K3	40S ribosomal protein SA (Fragment) OS=Homo sapiens GN=RPSA PE=3 SV=1 - [C9J9K3_HUMAN]	8.93E+07	7.90E+07	-1.13E+00
C9J9W2	LIM and SH3 domain protein 1 (Fragment) OS=Homo sapiens GN=LASP1 PE=4 SV=1 - [C9J9W2_HUMAN]	3.72E+06	6.22E+06	1.67E+00
C9JD32	60S ribosomal protein L23 (Fragment) OS=Homo sapiens GN=RPL23 PE=3 SV=1 - [C9JD32_HUMAN]	4.76E+07	8.76E+07	1.84E+00
C9JFE4	COP9 signalosome complex subunit 1 OS=Homo sapiens GN=GPS1 PE=4 SV=2 - [C9JFE4_HUMAN]	0.00E+00	2.04E+07	1.00E+01
C9JQD4	Peptidyl-prolyl cis-trans isomerase (Fragment) OS=Homo sapiens GN=PPIH PE=3 SV=1 - [C9JQD4_HUMAN]	1.53E+07	0.00E+00	-1.00E+01
C9JTK4	AP-2 complex subunit mu (Fragment) OS=Homo sapiens GN=AP2M1 PE=4 SV=1 - [C9JTK4_HUMAN]	7.05E+06	0.00E+00	-1.00E+01
C9JXB8	60S ribosomal protein L24 OS=Homo sapiens GN=RPL24 PE=4 SV=1 - [C9JXB8_HUMAN]	3.12E+07	7.14E+07	2.29E+00

D3YTB1	60S ribosomal protein L32 (Fragment) OS=Homo sapiens GN=RPL32 PE=4 SV=1 - [D3YTB1_HUMAN]	2.29E+07	3.37E+07	1.47E+00
D6R9P3	Heterogeneous nuclear ribonucleoprotein A/B OS=Homo sapiens GN=HNRNPAB PE=4 SV=1 - [D6R9P3_HUMAN]	4.90E+07	6.84E+07	1.40E+00
D6RA82	Annexin OS=Homo sapiens GN=ANXA3 PE=3 SV=1 - [D6RA82_HUMAN]	4.11E+07	5.76E+07	1.40E+00
D6RDU5	Septin-11 (Fragment) OS=Homo sapiens GN=SEPT11 PE=3 SV=1 - [D6RDU5_HUMAN]	2.10E+07	3.78E+07	1.80E+00
D6REN6	Histidine--tRNA ligase, cytoplasmic OS=Homo sapiens GN=HARS PE=4 SV=1 - [D6REN6_HUMAN]	2.99E+07	5.34E+07	1.79E+00
D6RFH4	Cytochrome b5 type B OS=Homo sapiens GN=CYB5B PE=3 SV=1 - [D6RFH4_HUMAN]	0.00E+00	7.03E+07	1.00E+01
D6RG13	40S ribosomal protein S3a (Fragment) OS=Homo sapiens GN=RPS3A PE=3 SV=1 - [D6RG13_HUMAN]	6.03E+07	1.32E+08	2.19E+00
E5RG31	DNA replication licensing factor MCM4 (Fragment) OS=Homo sapiens GN=MCM4 PE=3 SV=1 - [E5RG31_HUMAN]	8.73E+06	1.11E+07	1.28E+00
E5RHG8	Transcription elongation factor B polypeptide 1 (Fragment) OS=Homo sapiens GN=TCEB1 PE=4 SV=1 - [E5RHG8_HUMAN]	2.85E+07	5.50E+07	1.93E+00
E5RHS5	Eukaryotic translation initiation factor 3 subunit E (Fragment) OS=Homo sapiens GN=EIF3E PE=4 SV=1 - [E5RHS5_HUMAN]	0.00E+00	2.16E+07	1.00E+01

E5RI99	60S ribosomal protein L30 (Fragment) OS=Homo sapiens GN=RPL30 PE=3 SV=1 - [E5RI99_HUMAN]	1.11E+08	1.48E+08	1.33E+00
E5RIW3	Tubulin-specific chaperone A OS=Homo sapiens GN=TBCA PE=4 SV=1 - [E5RIW3_HUMAN]	2.26E+07	6.86E+07	3.04E+00
E5RJA0	Acyl-protein thioesterase 1 OS=Homo sapiens GN=LYPLA1 PE=4 SV=1 - [E5RJA0_HUMAN]	7.67E+07	1.03E+08	1.34E+00
E7EMV0	Protein diaphanous homolog 1 OS=Homo sapiens GN=DIAPH1 PE=4 SV=1 - [E7EMV0_HUMAN]	1.04E+07	1.79E+07	1.73E+00
E7ENZ3	T-complex protein 1 subunit epsilon OS=Homo sapiens GN=CCT5 PE=4 SV=1 - [E7ENZ3_HUMAN]	2.89E+07	1.23E+08	4.24E+00
E7EP00	Protein transport protein Sec24C OS=Homo sapiens GN=SEC24C PE=4 SV=2 - [E7EP00_HUMAN]	0.00E+00	1.50E+07	1.00E+01
E7EP32	Guanine nucleotide-binding protein G(I)/G(S)/G(T) subunit beta-2 OS=Homo sapiens GN=GNB2 PE=4 SV=1 - [E7EP32_HUMAN]	9.80E+06	7.14E+07	7.29E+00
E7EPB3	60S ribosomal protein L14 OS=Homo sapiens GN=RPL14 PE=4 SV=1 - [E7EPB3_HUMAN]	4.39E+07	0.00E+00	-1.00E+01
E7EPK1	Septin-7 OS=Homo sapiens GN=SEPT7 PE=3 SV=1 - [E7EPK1_HUMAN]	1.26E+07	1.95E+07	1.55E+00
E7EQ12	Calpastatin OS=Homo sapiens GN=CAST PE=4 SV=1 - [E7EQ12_HUMAN]	7.14E+06	0.00E+00	-1.00E+01
E7EQR4	Ezrin OS=Homo sapiens GN=EZR PE=4 SV=2 - [E7EQR4_HUMAN]	1.21E+08	3.57E+08	2.94E+00
E7ESG6	Zinc transporter SLC39A7 OS=Homo sapiens GN=SLC39A7 PE=4 SV=1 - [E7ESG6_HUMAN]	1.40E+07	1.52E+07	1.09E+00

E7ESU4	N-acetyltransferase 10 OS=Homo sapiens GN=NAT10 PE=4 SV=1 - [E7ESU4_HUMAN]	0.00E+00	9.78E+06	1.00E+01
E7ET49	Sn1-specific diacylglycerol lipase beta OS=Homo sapiens GN=DAGLB PE=4 SV=1 - [E7ET49_HUMAN]	4.26E+07	5.97E+07	1.40E+00
E7ETY7	Glutathione peroxidase OS=Homo sapiens GN=GPX8 PE=3 SV=1 - [E7ETY7_HUMAN]	0.00E+00	6.60E+07	1.00E+01
E7ETZ4	Basic leucine zipper and W2 domain-containing protein 2 (Fragment) OS=Homo sapiens GN=BZW2 PE=4 SV=1 - [E7ETZ4_HUMAN]	2.28E+07	4.72E+07	2.08E+00
E7EU85	Fragile X mental retardation syndrome-related protein 1 OS=Homo sapiens GN=FXR1 PE=4 SV=1 - [E7EU85_HUMAN]	1.98E+07	1.57E+07	-1.26E+00
E7EUT4	Glyceraldehyde-3-phosphate dehydrogenase OS=Homo sapiens GN=GAPDH PE=3 SV=1 - [E7EUT4_HUMAN]	1.24E+09	2.77E+09	2.24E+00
E7EUT8	Splicing factor 3A subunit 3 OS=Homo sapiens GN=SF3A3 PE=4 SV=1 - [E7EUT8_HUMAN]	1.29E+07	0.00E+00	-1.00E+01
E7EUY0	DNA-dependent protein kinase catalytic subunit OS=Homo sapiens GN=PRKDC PE=4 SV=1 - [E7EUY0_HUMAN]	2.68E+07	4.44E+07	1.66E+00
E9PAM4	Phosphatidylinositol 4-kinase type 2-alpha OS=Homo sapiens GN=PI4K2A PE=4 SV=1 - [E9PAM4_HUMAN]	0.00E+00	1.59E+07	1.00E+01
E9PB51	RNA-binding protein 4 (Fragment) OS=Homo sapiens GN=RBM4 PE=4 SV=1 - [E9PB51_HUMAN]	1.99E+07	0.00E+00	-1.00E+01

E9PBU3	Phosphoribosylaminoimidazolecarboxamide formyltransferase OS=Homo sapiens GN=ATIC PE=4 SV=1 - [E9PBU3_HUMAN]	3.48E+07	7.33E+07	2.11E+00
E9PCI9	Farnesyl pyrophosphate synthase OS=Homo sapiens GN=FDPS PE=3 SV=1 - [E9PCI9_HUMAN]	0.00E+00	3.08E+07	1.00E+01
E9PCY7	Heterogeneous nuclear ribonucleoprotein H OS=Homo sapiens GN=HNRNPH1 PE=4 SV=1 - [E9PCY7_HUMAN]	1.16E+08	2.59E+08	2.23E+00
E9PD53	Structural maintenance of chromosomes protein OS=Homo sapiens GN=SMC4 PE=3 SV=1 - [E9PD53_HUMAN]	6.83E+06	1.62E+07	2.37E+00
E9PDD9	RNA-binding protein 28 OS=Homo sapiens GN=RBM28 PE=4 SV=1 - [E9PDD9_HUMAN]	0.00E+00	6.08E+06	1.00E+01
E9PF10	Nuclear pore complex protein Nup155 OS=Homo sapiens GN=NUP155 PE=4 SV=1 - [E9PF10_HUMAN]	1.31E+06	3.45E+07	1.00E+01
E9PFG7	2-oxoglutarate dehydrogenase, mitochondrial OS=Homo sapiens GN=OGDH PE=4 SV=1 - [E9PFG7_HUMAN]	1.06E+07	1.91E+07	1.81E+00
E9PFH4	Transportin-3 OS=Homo sapiens GN=TNPO3 PE=4 SV=1 - [E9PFH4_HUMAN]	8.53E+06	1.35E+07	1.59E+00
E9PFH8	Lupus La protein OS=Homo sapiens GN=SSB PE=4 SV=1 - [E9PFH8_HUMAN]	2.59E+06	2.47E+07	9.53E+00
E9PGK1	Annexin OS=Homo sapiens GN=ANXA6 PE=3 SV=1 - [E9PGK1_HUMAN]	3.69E+07	8.40E+07	2.28E+00
E9PHS0	LanC-like protein 1 (Fragment) OS=Homo sapiens GN=LANCL1 PE=4 SV=1 - [E9PHS0_HUMAN]	8.94E+07	0.00E+00	-1.00E+01

E9PJD9	60S ribosomal protein L27a OS=Homo sapiens GN=RPL27A PE=3 SV=1 - [E9PJD9_HUMAN]	1.41E+08	2.57E+08	1.82E+00
E9PJK1	CD81 antigen OS=Homo sapiens GN=CD81 PE=4 SV=1 - [E9PJK1_HUMAN]	1.56E+08	2.31E+08	1.48E+00
E9PKG1	Protein arginine N-methyltransferase 1 OS=Homo sapiens GN=PRMT1 PE=4 SV=1 - [E9PKG1_HUMAN]	3.15E+07	6.78E+07	2.15E+00
E9PL22	Hypoxia up-regulated protein 1 OS=Homo sapiens GN=HYOU1 PE=3 SV=1 - [E9PL22_HUMAN]	5.52E+07	7.02E+07	1.27E+00
E9PLK3	Puromycin-sensitive aminopeptidase OS=Homo sapiens GN=NPEPPS PE=4 SV=1 - [E9PLK3_HUMAN]	1.60E+07	2.91E+07	1.82E+00
E9PLT0	Cold shock domain-containing protein E1 OS=Homo sapiens GN=CSDE1 PE=4 SV=1 - [E9PLT0_HUMAN]	0.00E+00	2.40E+07	1.00E+01
E9PP31	Caprin-1 OS=Homo sapiens GN=CAPRIN1 PE=4 SV=1 - [E9PP31_HUMAN]	2.04E+06	8.29E+07	1.00E+01
E9PPJ0	Splicing factor 3B subunit 2 OS=Homo sapiens GN=SF3B2 PE=4 SV=1 - [E9PPJ0_HUMAN]	0.00E+00	3.86E+07	1.00E+01
E9PPQ5	Cysteine and histidine-rich domain-containing protein 1 OS=Homo sapiens GN=CHORDC1 PE=4 SV=1 - [E9PPQ5_HUMAN]	8.82E+06	4.24E+07	4.81E+00
E9PPR1	Elongation factor 1-delta (Fragment) OS=Homo sapiens GN=EEF1D PE=4 SV=1 - [E9PPR1_HUMAN]	5.25E+07	9.39E+07	1.79E+00
E9PQ56	Poly(U)-binding-splicing factor PUF60 (Fragment) OS=Homo sapiens GN=PUF60 PE=4 SV=1 - [E9PQ56_HUMAN]	2.06E+07	4.13E+07	2.01E+00

E9PR16	Nuclear pore complex protein Nup160 OS=Homo sapiens GN=NUP160 PE=4 SV=1 - [E9PR16_HUMAN]	2.15E+07	1.17E+08	5.42E+00
F2Z3F8	Pyridoxal kinase OS=Homo sapiens GN=PDXK PE=4 SV=1 - [F2Z3F8_HUMAN]	1.58E+07	2.38E+07	1.51E+00
F5GWX5	Chromodomain-helicase-DNA-binding protein 4 OS=Homo sapiens GN=CHD4 PE=4 SV=1 - [F5GWX5_HUMAN]	4.38E+05	1.27E+07	1.00E+01
F5GX33	Calcium-binding mitochondrial carrier protein Aralar2 OS=Homo sapiens GN=SLC25A13 PE=3 SV=1 - [F5GX33_HUMAN]	1.62E+07	3.40E+07	2.09E+00
F5GXX5	Dolichyl-diphosphooligosaccharide--protein glycosyltransferase subunit DAD1 OS=Homo sapiens GN=DAD1 PE=4 SV=1 - [F5GXX5_HUMAN]	7.00E+07	1.04E+08	1.48E+00
F5GY55	DNA damage-binding protein 1 OS=Homo sapiens GN=DDB1 PE=4 SV=1 - [F5GY55_HUMAN]	1.58E+07	5.09E+07	3.21E+00
F5GZ27	Lon protease homolog OS=Homo sapiens GN=LONP1 PE=3 SV=1 - [F5GZ27_HUMAN]	1.15E+07	4.25E+07	3.69E+00
F5H265	Polyubiquitin-C (Fragment) OS=Homo sapiens GN=UBC PE=4 SV=1 - [F5H265_HUMAN]	2.37E+08	1.23E+09	5.21E+00
F5H335	Eukaryotic translation initiation factor 3 subunit A OS=Homo sapiens GN=EIF3A PE=4 SV=1 - [F5H335_HUMAN]	7.30E+06	2.15E+07	2.95E+00
F5H3A1	Sodium/potassium-transporting ATPase subunit alpha-1 OS=Homo sapiens GN=ATP1A1 PE=3 SV=1 - [F5H3A1_HUMAN]	4.61E+07	9.01E+07	1.95E+00

F5H3W1	Podocalyxin OS=Homo sapiens GN=PODXL PE=4 SV=1 - [F5H3W1_HUMAN]	0.00E+00	1.58E+08	1.00E+01
F5H5A9	Suppressor of G2 allele of SKP1 homolog OS=Homo sapiens GN=SUGT1 PE=4 SV=1 - [F5H5A9_HUMAN]	2.93E+06	2.04E+07	6.98E+00
F5H667	Aspartyl/asparaginyl beta-hydroxylase OS=Homo sapiens GN=ASPH PE=4 SV=1 - [F5H667_HUMAN]	1.83E+07	2.33E+07	1.28E+00
F5H6N3	Clathrin light chain A OS=Homo sapiens GN=CLTA PE=4 SV=1 - [F5H6N3_HUMAN]	5.10E+07	7.26E+07	1.42E+00
F5H6T1	Actin-related protein 2 OS=Homo sapiens GN=ACTR2 PE=3 SV=1 - [F5H6T1_HUMAN]	0.00E+00	5.72E+07	1.00E+01
F5H6V2	Phosphoglucomutase-2 OS=Homo sapiens GN=PGM2 PE=4 SV=1 - [F5H6V2_HUMAN]	0.00E+00	1.69E+07	1.00E+01
F5H897	Heat shock protein 75 kDa, mitochondrial OS=Homo sapiens GN=TRAP1 PE=3 SV=1 - [F5H897_HUMAN]	5.44E+08	1.36E+08	-4.00E+00
F5H8E5	Ubiquitin carboxyl-terminal hydrolase OS=Homo sapiens GN=USP7 PE=3 SV=1 - [F5H8E5_HUMAN]	1.50E+07	0.00E+00	-1.00E+01
F6SBX2	Isoleucine--tRNA ligase, mitochondrial OS=Homo sapiens GN=IARS2 PE=3 SV=1 - [F6SBX2_HUMAN]	2.12E+07	2.09E+07	-1.02E+00
F6U1T9	Calcineurin subunit B type 1 OS=Homo sapiens GN=PPP3R1 PE=4 SV=1 - [F6U1T9_HUMAN]	2.59E+08	3.26E+08	1.26E+00
F6U784	Ras-related protein Rap-2a OS=Homo sapiens GN=RAP2A PE=4 SV=1 - [F6U784_HUMAN]	2.41E+07	0.00E+00	-1.00E+01

F8VNT9	CD63 antigen (Fragment) OS=Homo sapiens GN=CD63 PE=4 SV=1 - [F8VNT9_HUMAN]	7.87E+08	1.84E+09	2.34E+00
F8VPA0	HLA class I histocompatibility antigen, A-68 alpha chain OS=Homo sapiens GN=HLA-A PE=4 SV=1 - [F8VPA0_HUMAN]	4.46E+07	6.74E+07	1.51E+00
F8VSI6	Flotillin-1 OS=Homo sapiens GN=FLOT1 PE=4 SV=1 - [F8VSI6_HUMAN]	2.11E+07	4.09E+07	1.94E+00
F8VVM2	Phosphate carrier protein, mitochondrial OS=Homo sapiens GN=SLC25A3 PE=3 SV=1 - [F8VVM2_HUMAN]	7.30E+07	2.01E+08	2.76E+00
F8VW92	Tubulin beta chain OS=Homo sapiens GN=TUBB PE=3 SV=1 - [F8VW92_HUMAN]	8.42E+08	1.56E+09	1.85E+00
F8VWC5	60S ribosomal protein L18 OS=Homo sapiens GN=RPL18 PE=3 SV=1 - [F8VWC5_HUMAN]	1.34E+08	2.02E+08	1.50E+00
F8VYE8	Serine/threonine-protein phosphatase OS=Homo sapiens GN=PPP1CC PE=3 SV=1 - [F8VYE8_HUMAN]	1.82E+07	5.46E+07	3.00E+00
F8VZW7	Protein LOC100996747 OS=Homo sapiens GN=LOC100996747 PE=4 SV=1 - [F8VZW7_HUMAN]	2.40E+08	2.49E+08	1.04E+00
F8W118	Nucleosome assembly protein 1-like 1 (Fragment) OS=Homo sapiens GN=NAP1L1 PE=3 SV=1 - [F8W118_HUMAN]	5.33E+07	1.46E+08	2.74E+00
F8W181	60S ribosomal protein L6 (Fragment) OS=Homo sapiens GN=RPL6 PE=3 SV=1 - [F8W181_HUMAN]	2.05E+08	3.95E+08	1.93E+00
F8W1R7	Myosin light polypeptide 6 OS=Homo sapiens GN=MYL6 PE=4 SV=1 - [F8W1R7_HUMAN]	9.58E+07	1.72E+08	1.80E+00

F8W7Q4	Protein FAM162A OS=Homo sapiens GN=FAM162A PE=4 SV=1 - [F8W7Q4_HUMAN]	2.81E+07	6.93E+07	2.46E+00
F8W914	Reticulon-4 OS=Homo sapiens GN=RTN4 PE=4 SV=1 - [F8W914_HUMAN]	0.00E+00	1.21E+08	1.00E+01
F8WAK8	Cohesin subunit SA-2 OS=Homo sapiens GN=STAG2 PE=4 SV=1 - [F8WAK8_HUMAN]	1.73E+06	2.78E+06	1.61E+00
F8WAS3	NADH dehydrogenase [ubiquinone] 1 alpha subcomplex subunit 5 OS=Homo sapiens GN=NDUFA5 PE=4 SV=1 - [F8WAS3_HUMAN]	5.96E+06	9.78E+06	1.64E+00
G3V1A4	Cofilin 1 (Non-muscle), isoform CRA_a OS=Homo sapiens GN=CFL1 PE=4 SV=1 - [G3V1A4_HUMAN]	8.92E+07	4.03E+08	4.51E+00
G3V1B3	60S ribosomal protein L21 OS=Homo sapiens GN=RPL21 PE=4 SV=1 - [G3V1B3_HUMAN]	1.08E+08	1.65E+08	1.53E+00
G3V1P3	Loss of heterozygosity 12 chromosomal region 1 protein OS=Homo sapiens GN=LOH12CR1 PE=4 SV=1 - [G3V1P3_HUMAN]	2.00E+07	0.00E+00	-1.00E+01
G3V1U4	Signal recognition particle 68 kDa protein OS=Homo sapiens GN=SRP68 PE=4 SV=1 - [G3V1U4_HUMAN]	1.08E+07	1.01E+07	-1.07E+00
G3V2B8	C-1-tetrahydrofolate synthase, cytoplasmic OS=Homo sapiens GN=MTHFD1 PE=3 SV=1 - [G3V2B8_HUMAN]	5.02E+07	1.12E+08	2.23E+00
G3V3M6	DNA-(apurinic or apyrimidinic site) lyase (Fragment) OS=Homo sapiens GN=APEX1 PE=4 SV=1 - [G3V3M6_HUMAN]	4.92E+07	8.39E+07	1.70E+00
G3V3U4	Proteasome subunit alpha type OS=Homo sapiens GN=PSMA6 PE=3 SV=1 - [G3V3U4_HUMAN]	2.57E+07	5.24E+07	2.04E+00

G3V4W0	Heterogeneous nuclear ribonucleoproteins C1/C2 (Fragment) OS=Homo sapiens GN=HNRNPC PE=4 SV=1 - [G3V4W0_HUMAN]	1.56E+08	4.30E+08	2.75E+00
G3V5L5	Protein arginine N-methyltransferase 5 (Fragment) OS=Homo sapiens GN=PRMT5 PE=4 SV=1 - [G3V5L5_HUMAN]	2.48E+07	6.51E+07	2.63E+00
G5E9B2	Chaperonin containing TCP1, subunit 8 (Theta), isoform CRA_a OS=Homo sapiens GN=CCT8 PE=3 SV=1 - [G5E9B2_HUMAN]	1.35E+08	2.22E+08	1.65E+00
G5E9H4	Dynactin 1 (P150, glued homolog, Drosophila), isoform CRA_a OS=Homo sapiens GN=DCTN1 PE=4 SV=1 - [G5E9H4_HUMAN]	8.61E+06	3.29E+07	3.82E+00
G5E9R3	60S ribosomal protein L37a OS=Homo sapiens GN=RPL37A PE=4 SV=1 - [G5E9R3_HUMAN]	1.13E+07	1.72E+07	1.53E+00
G5E9Z2	Cisplatin resistance related protein CRR9p, isoform CRA_c OS=Homo sapiens GN=CLPTM1L PE=4 SV=1 - [G5E9Z2_HUMAN]	2.01E+06	1.30E+07	6.44E+00
G5E9Z8	Signal recognition particle 72 kDa protein OS=Homo sapiens GN=SRP72 PE=4 SV=1 - [G5E9Z8_HUMAN]	0.00E+00	3.82E+07	1.00E+01
G5EA52	Protein disulfide isomerase family A, member 3, isoform CRA_b OS=Homo sapiens GN=PDIA3 PE=3 SV=1 - [G5EA52_HUMAN]	1.07E+08	3.39E+08	3.17E+00
H0Y4A6	Valine--tRNA ligase (Fragment) OS=Homo sapiens GN=VARS PE=3 SV=1 - [H0Y4A6_HUMAN]	2.33E+07	2.95E+07	1.26E+00
H0Y4R1	Inosine-5'-monophosphate dehydrogenase 2 (Fragment) OS=Homo sapiens GN=IMPDH2 PE=3 SV=1 -	6.68E+07	1.36E+08	2.03E+00

	[H0Y4R1_HUMAN]			
H0Y4X3	RNA-binding protein 39 (Fragment) OS=Homo sapiens GN=RBM39 PE=4 SV=1 - [H0Y4X3_HUMAN]	2.00E+07	4.10E+07	2.06E+00
H0Y8A7	NEDD4 family-interacting protein 2 (Fragment) OS=Homo sapiens GN=NDFIP2 PE=4 SV=1 - [H0Y8A7_HUMAN]	2.02E+07	6.11E+07	3.02E+00
H0Y8E6	DNA replication licensing factor MCM2 (Fragment) OS=Homo sapiens GN=MCM2 PE=3 SV=1 - [H0Y8E6_HUMAN]	2.11E+07	4.10E+07	1.94E+00
H0YD13	CD44 antigen (Fragment) OS=Homo sapiens GN=CD44 PE=4 SV=1 - [H0YD13_HUMAN]	1.34E+08	7.01E+08	5.23E+00
H0YDD4	Dihydrolipoyllysine-residue acetyltransferase component of pyruvate dehydrogenase complex, mitochondrial (Fragment) OS=Homo sapiens GN=DLAT PE=3 SV=1 - [H0YDD4_HUMAN]	2.51E+07	4.96E+07	1.98E+00
H0YGW7	ATP-binding cassette sub-family F member 1 (Fragment) OS=Homo sapiens GN=ABCF1 PE=3 SV=1 - [H0YGW7_HUMAN]	0.00E+00	3.44E+07	1.00E+01
H0YJG7	Activator of 90 kDa heat shock protein ATPase homolog 1 (Fragment) OS=Homo sapiens GN=AHSA1 PE=4 SV=1 - [H0YJG7_HUMAN]	6.54E+06	6.91E+07	1.00E+01
H0YLC2	Proteasome subunit alpha type OS=Homo sapiens GN=PSMA4 PE=3 SV=1 - [H0YLC2_HUMAN]	3.43E+07	3.28E+07	-1.05E+00

H0YLI6	Isocitrate dehydrogenase (Ashida et al.) subunit alpha, mitochondrial (Fragment) OS=Homo sapiens GN=IDH3A PE=3 SV=1 - [H0YLI6_HUMAN]	1.25E+07	0.00E+00	-1.00E+01
H0YLU7	Electron transfer flavoprotein subunit alpha, mitochondrial (Fragment) OS=Homo sapiens GN=ETFA PE=4 SV=1 - [H0YLU7_HUMAN]	1.56E+07	2.85E+06	-5.49E+00
H3BLW6	Transmembrane protein 63B (Fragment) OS=Homo sapiens GN=TMEM63B PE=4 SV=1 - [H3BLW6_HUMAN]	1.94E+07	9.23E+06	-2.10E+00
H3BPJ9	NADH dehydrogenase [ubiquinone] 1 beta subcomplex subunit 10 OS=Homo sapiens GN=NDUFB10 PE=4 SV=1 - [H3BPJ9_HUMAN]	1.77E+07	2.97E+07	1.68E+00
H3BQZ7	HCG2044799 OS=Homo sapiens GN=hCG_2044799 PE=4 SV=1 - [H3BQZ7_HUMAN]	1.67E+07	1.92E+07	1.15E+00
H3BRG4	Cytochrome b-c1 complex subunit 2, mitochondrial OS=Homo sapiens GN=UQCRC2 PE=3 SV=1 - [H3BRG4_HUMAN]	1.31E+07	4.00E+07	3.07E+00
H3BRU6	Poly(rC)-binding protein 2 (Fragment) OS=Homo sapiens GN=PCBP2 PE=4 SV=1 - [H3BRU6_HUMAN]	6.11E+07	2.33E+08	3.82E+00
H3BRV0	Eukaryotic translation initiation factor 3 subunit C OS=Homo sapiens GN=EIF3C PE=4 SV=1 - [H3BRV0_HUMAN]	2.74E+07	5.33E+07	1.95E+00
H3BS70	Enoyl-CoA delta isomerase 1, mitochondrial (Fragment) OS=Homo sapiens GN=ECI1 PE=3 SV=1 - [H3BS70_HUMAN]	1.77E+07	1.30E+08	7.37E+00

H3BV11	Nuclear pore complex protein Nup93 (Fragment) OS=Homo sapiens GN=NUP93 PE=4 SV=1 - [H3BV11_HUMAN]	4.68E+06	1.57E+07	3.36E+00
H7BXG7	Protein transport protein Sec31A OS=Homo sapiens GN=SEC31A PE=4 SV=1 - [H7BXG7_HUMAN]	1.34E+07	3.15E+07	2.35E+00
H7BXI1	Extended synaptotagmin-2 (Fragment) OS=Homo sapiens GN=ESYT2 PE=4 SV=1 - [H7BXI1_HUMAN]	1.06E+06	0.00E+00	-1.00E+01
H7BXK9	ATP-binding cassette sub-family B member 6, mitochondrial (Fragment) OS=Homo sapiens GN=ABCB6 PE=3 SV=1 - [H7BXK9_HUMAN]	4.39E+06	5.04E+05	-8.71E+00
H7BZ20	Thymidylate kinase (Fragment) OS=Homo sapiens GN=DTYMK PE=4 SV=1 - [H7BZ20_HUMAN]	1.36E+07	3.23E+07	2.38E+00
H7BZT7	S-formylglutathione hydrolase (Fragment) OS=Homo sapiens GN=ESD PE=4 SV=1 - [H7BZT7_HUMAN]	1.87E+07	2.97E+07	1.59E+00
H7C268	Transmembrane protein 168 (Fragment) OS=Homo sapiens GN=TMEM168 PE=4 SV=1 - [H7C268_HUMAN]	0.00E+00	1.76E+07	1.00E+01
H7C3P9	COP9 signalosome complex subunit 3 OS=Homo sapiens GN=COPS3 PE=4 SV=2 - [H7C3P9_HUMAN]	0.00E+00	1.69E+07	1.00E+01
H7C4F6	Importin subunit alpha-4 (Fragment) OS=Homo sapiens GN=KPNA4 PE=4 SV=1 - [H7C4F6_HUMAN]	8.96E+06	0.00E+00	-1.00E+01
H7C5I5	Phospholipid scramblase 1 (Fragment) OS=Homo sapiens GN=PLSCR1 PE=4 SV=1 - [H7C5I5_HUMAN]	6.90E+07	6.61E+07	-1.04E+00

I3L0U2	Testisin (Fragment) OS=Homo sapiens GN=PRSS21 PE=3 SV=1 - [I3L0U2_HUMAN]	1.94E+07	3.03E+07	1.56E+00
I3L1L3	Myb-binding protein 1A (Fragment) OS=Homo sapiens GN=MYBBP1A PE=4 SV=1 - [I3L1L3_HUMAN]	1.58E+07	1.59E+07	1.01E+00
I3L397	Eukaryotic translation initiation factor 5A-1 (Fragment) OS=Homo sapiens GN=EIF5A PE=4 SV=1 - [I3L397_HUMAN]	3.49E+07	2.01E+08	5.74E+00
I3L3U9	Ribosomal L1 domain-containing protein 1 (Fragment) OS=Homo sapiens GN=RSL1D1 PE=4 SV=1 - [I3L3U9_HUMAN]	2.92E+07	3.51E+07	1.20E+00
IPI12345678	Streptavidin (S.avidinii) - [CON_Strepavidin]	2.73E+10	4.68E+10	1.71E+00
J3KNJ2	Eukaryotic translation initiation factor 3 subunit M (Fragment) OS=Homo sapiens GN=EIF3M PE=4 SV=1 - [J3KNJ2_HUMAN]	1.31E+07	0.00E+00	-1.00E+01
J3KNT0	Fascin OS=Homo sapiens GN=FSCN1 PE=3 SV=1 - [J3KNT0_HUMAN]	8.39E+07	2.13E+08	2.54E+00
J3KP29	Nuclear pore complex protein Nup98-Nup96 OS=Homo sapiens GN=NUP98 PE=4 SV=1 - [J3KP29_HUMAN]	5.14E+06	0.00E+00	-1.00E+01
J3KRZ2	Cytoplasmic dynein 1 light intermediate chain 2 (Fragment) OS=Homo sapiens GN=DYNC1LI2 PE=4 SV=1 - [J3KRZ2_HUMAN]	0.00E+00	5.20E+06	1.00E+01
J3KT73	60S ribosomal protein L38 OS=Homo sapiens GN=RPL38 PE=3 SV=1 - [J3KT73_HUMAN]	3.51E+07	2.41E+08	6.89E+00
J3KTF8	Rho GDP-dissociation inhibitor 1 (Fragment) OS=Homo sapiens GN=ARHGDIA PE=4 SV=1 - [J3KTF8_HUMAN]	1.95E+08	3.72E+08	1.91E+00

J3QKR3	Proteasome subunit beta type-3 (Fragment) OS=Homo sapiens GN=PSMB3 PE=3 SV=1 - [J3QKR3_HUMAN]	4.95E+07	6.49E+07	1.31E+00
J3QQT2	60S ribosomal protein L17 (Fragment) OS=Homo sapiens GN=RPL17 PE=3 SV=1 - [J3QQT2_HUMAN]	2.63E+08	1.95E+08	-1.35E+00
J3QR09	Ribosomal protein L19 OS=Homo sapiens GN=RPL19 PE=3 SV=1 - [J3QR09_HUMAN]	9.59E+07	1.24E+08	1.29E+00
J3QRD1	Fatty aldehyde dehydrogenase OS=Homo sapiens GN=ALDH3A2 PE=3 SV=1 - [J3QRD1_HUMAN]	2.79E+07	5.55E+07	1.99E+00
J3QSX4	Mitotic checkpoint protein BUB3 OS=Homo sapiens GN=BUB3 PE=4 SV=1 - [J3QSX4_HUMAN]	2.52E+07	7.10E+07	2.82E+00
K7EJM5	TAR DNA-binding protein 43 (Fragment) OS=Homo sapiens GN=TARDBP PE=4 SV=1 - [K7EJM5_HUMAN]	3.23E+06	1.97E+07	6.10E+00
K7EJT5	60S ribosomal protein L22 (Fragment) OS=Homo sapiens GN=RPL22 PE=4 SV=1 - [K7EJT5_HUMAN]	1.56E+08	3.72E+08	2.38E+00
K7EM73	Calpain small subunit 1 (Fragment) OS=Homo sapiens GN=CAPNS1 PE=4 SV=1 - [K7EM73_HUMAN]	1.19E+07	2.95E+07	2.48E+00
K7EPP9	Syntaxin-10 (Fragment) OS=Homo sapiens GN=STX10 PE=4 SV=1 - [K7EPP9_HUMAN]	0.00E+00	1.39E+07	1.00E+01
K7EQ91	Zinc transporter ZIP6 (Fragment) OS=Homo sapiens GN=SLC39A6 PE=4 SV=1 - [K7EQ91_HUMAN]	0.00E+00	1.34E+07	1.00E+01
K7EQA9	Hsp90 co-chaperone Cdc37 (Fragment) OS=Homo sapiens GN=CDC37 PE=4 SV=1 - [K7EQA9_HUMAN]	2.59E+07	6.61E+07	2.55E+00

K7EQQ1	Cleft lip and palate transmembrane protein 1 (Fragment) OS=Homo sapiens GN=CLPTM1 PE=4 SV=1 - [K7EQQ1_HUMAN]	2.78E+04	9.95E+06	1.00E+01
K7ER90	Eukaryotic translation initiation factor 3 subunit G (Fragment) OS=Homo sapiens GN=EIF3G PE=4 SV=1 - [K7ER90_HUMAN]	2.60E+07	1.92E+07	-1.36E+00
K7ERZ3	Perilipin-3 (Fragment) OS=Homo sapiens GN=PLIN3 PE=4 SV=1 - [K7ERZ3_HUMAN]	1.07E+07	3.24E+07	3.04E+00
O00116	Alkyldihydroxyacetonephosphate synthase, peroxisomal OS=Homo sapiens GN=AGPS PE=1 SV=1 - [ADAS_HUMAN]	2.43E+07	4.00E+07	1.64E+00
O00148	ATP-dependent RNA helicase DDX39A OS=Homo sapiens GN=DDX39A PE=1 SV=2 - [DX39A_HUMAN]	1.13E+08	1.96E+08	1.74E+00
O00161-2	Isoform SNAP-23b of Synaptosomal-associated protein 23 OS=Homo sapiens GN=SNAP23 - [SNP23_HUMAN]	1.65E+07	3.19E+07	1.94E+00
O00231	26S proteasome non-ATPase regulatory subunit 11 OS=Homo sapiens GN=PSMD11 PE=1 SV=3 - [PSD11_HUMAN]	1.50E+07	3.62E+07	2.41E+00
O00232	26S proteasome non-ATPase regulatory subunit 12 OS=Homo sapiens GN=PSMD12 PE=1 SV=3 - [PSD12_HUMAN]	1.84E+07	3.12E+07	1.70E+00
O00299	Chloride intracellular channel protein 1 OS=Homo sapiens GN=CLIC1 PE=1 SV=4 - [CLIC1_HUMAN]	8.07E+07	1.03E+08	1.28E+00
O00303	Eukaryotic translation initiation factor 3 subunit F OS=Homo sapiens GN=EIF3F PE=1 SV=1 - [EIF3F_HUMAN]	3.21E+07	3.31E+07	1.03E+00

O00410	Importin-5 OS=Homo sapiens GN=IPO5 PE=1 SV=4 - [IPO5_HUMAN]	4.78E+07	1.57E+08	3.28E+00
O00429-4	Isoform 3 of Dynamin-1-like protein OS=Homo sapiens GN=DNM1L - [DNM1L_HUMAN]	5.02E+06	8.26E+06	1.64E+00
O00505	Importin subunit alpha-3 OS=Homo sapiens GN=KPNA3 PE=1 SV=2 - [IMA3_HUMAN]	1.20E+07	1.72E+07	1.43E+00
O00567	Nucleolar protein 56 OS=Homo sapiens GN=NOP56 PE=1 SV=4 - [NOP56_HUMAN]	8.51E+06	1.82E+07	2.14E+00
O00571-2	Isoform 2 of ATP-dependent RNA helicase DDX3X OS=Homo sapiens GN=DDX3X - [DDX3X_HUMAN]	8.17E+07	1.27E+08	1.56E+00
O14818	Proteasome subunit alpha type-7 OS=Homo sapiens GN=PSMA7 PE=1 SV=1 - [PSA7_HUMAN]	5.83E+07	1.48E+08	2.54E+00
O14828-2	Isoform 2 of Secretory carrier-associated membrane protein 3 OS=Homo sapiens GN=SCAMP3 - [SCAM3_HUMAN]	1.01E+08	1.96E+08	1.95E+00
O14929-2	Isoform B of Histone acetyltransferase type B catalytic subunit OS=Homo sapiens GN=HAT1 - [HAT1_HUMAN]	2.64E+07	2.35E+07	-1.13E+00
O14974-5	Isoform 5 of Protein phosphatase 1 regulatory subunit 12A OS=Homo sapiens GN=PPP1R12A - [MYPT1_HUMAN]	3.97E+06	2.51E+06	-1.58E+00
O14979-3	Isoform 3 of Heterogeneous nuclear ribonucleoprotein D-like OS=Homo sapiens GN=HNRPDL - [HNRDL_HUMAN]	6.61E+07	1.46E+08	2.21E+00
O14980	Exportin-1 OS=Homo sapiens GN=XPO1 PE=1 SV=1 - [XPO1_HUMAN]	1.48E+07	5.47E+07	3.69E+00

O15067	Phosphoribosylformylglycinamidine synthase OS=Homo sapiens GN=PFAS PE=1 SV=4 - [PUR4_HUMAN]	1.99E+07	3.42E+07	1.72E+00
O15118	Niemann-Pick C1 protein OS=Homo sapiens GN=NPC1 PE=1 SV=2 - [NPC1_HUMAN]	4.61E+07	1.37E+08	2.98E+00
O15144	Actin-related protein 2/3 complex subunit 2 OS=Homo sapiens GN=ARPC2 PE=1 SV=1 - [ARPC2_HUMAN]	1.69E+07	1.85E+07	1.09E+00
O15155	BET1 homolog OS=Homo sapiens GN=BET1 PE=1 SV=1 - [BET1_HUMAN]	2.38E+07	4.58E+07	1.93E+00
O15173	Membrane-associated progesterone receptor component 2 OS=Homo sapiens GN=PGRMC2 PE=1 SV=1 - [PGRC2_HUMAN]	2.21E+07	0.00E+00	-1.00E+01
O15260-2	Isoform 2 of Surfeit locus protein 4 OS=Homo sapiens GN=SURF4 - [SURF4_HUMAN]	2.97E+07	8.00E+07	2.69E+00
O43143	Putative pre-mRNA-splicing factor ATP-dependent RNA helicase DHX15 OS=Homo sapiens GN=DHX15 PE=1 SV=2 - [DHX15_HUMAN]	3.35E+07	7.54E+07	2.25E+00
O43175	D-3-phosphoglycerate dehydrogenase OS=Homo sapiens GN=PHGDH PE=1 SV=4 - [SERA_HUMAN]	7.70E+07	1.65E+08	2.15E+00
O43390	Heterogeneous nuclear ribonucleoprotein R OS=Homo sapiens GN=HNRNPR PE=1 SV=1 - [HNRPR_HUMAN]	1.32E+08	1.07E+08	-1.23E+00
O43399-2	Isoform 2 of Tumor protein D54 OS=Homo sapiens GN=TPD52L2 - [TPD54_HUMAN]	1.65E+07	1.84E+06	-8.99E+00

O43592	Exportin-T OS=Homo sapiens GN=XPOT PE=1 SV=2 - [XPOT_HUMAN]	4.99E+06	0.00E+00	-1.00E+01
O43657	Tetraspanin-6 OS=Homo sapiens GN=TSPAN6 PE=1 SV=1 - [TSN6_HUMAN]	3.61E+07	1.06E+08	2.94E+00
O43707	Alpha-actinin-4 OS=Homo sapiens GN=ACTN4 PE=1 SV=2 - [ACTN4_HUMAN]	3.42E+08	7.49E+08	2.19E+00
O43776	Asparagine--tRNA ligase, cytoplasmic OS=Homo sapiens GN=NARS PE=1 SV=1 - [SYNC_HUMAN]	2.07E+07	2.89E+07	1.40E+00
O43852	Calumenin OS=Homo sapiens GN=CALU PE=1 SV=2 - [CALU_HUMAN]	8.00E+06	5.39E+06	-1.49E+00
O60343-2	Isoform 2 of TBC1 domain family member 4 OS=Homo sapiens GN=TBC1D4 - [TBCD4_HUMAN]	3.85E+06	3.35E+06	-1.15E+00
O60506-3	Isoform 3 of Heterogeneous nuclear ribonucleoprotein Q OS=Homo sapiens GN=SYNCRIP - [HNRPQ_HUMAN]	1.44E+08	1.66E+08	1.15E+00
O60637-3	Isoform 3 of Tetraspanin-3 OS=Homo sapiens GN=TSPAN3 - [TSN3_HUMAN]	8.00E+07	4.33E+08	5.41E+00
O60701	UDP-glucose 6-dehydrogenase OS=Homo sapiens GN=UGDH PE=1 SV=1 - [UGDH_HUMAN]	2.67E+07	3.85E+07	1.44E+00
O60814	Histone H2B type 1-K OS=Homo sapiens GN=HIST1H2BK PE=1 SV=3 - [H2B1K_HUMAN]	7.31E+07	4.08E+08	5.58E+00
O60831	PRA1 family protein 2 OS=Homo sapiens GN=PRAF2 PE=1 SV=1 - [PRAF2_HUMAN]	5.96E+07	4.03E+07	-1.48E+00
O60832	H/ACA ribonucleoprotein complex subunit 4 OS=Homo sapiens GN=DKC1 PE=1 SV=3 - [DKC1_HUMAN]	0.00E+00	2.07E+07	1.00E+01

O75083	WD repeat-containing protein 1 OS=Homo sapiens GN=WDR1 PE=1 SV=4 - [WDR1_HUMAN]	3.28E+06	9.12E+07	1.00E+01
O75110	Probable phospholipid-transporting ATPase IIA OS=Homo sapiens GN=ATP9A PE=1 SV=3 - [ATP9A_HUMAN]	2.54E+07	2.09E+07	-1.21E+00
O75317	Ubiquitin carboxyl-terminal hydrolase 12 OS=Homo sapiens GN=USP12 PE=1 SV=2 - [UBP12_HUMAN]	7.85E+06	0.00E+00	-1.00E+01
O75340-2	Isoform 2 of Programmed cell death protein 6 OS=Homo sapiens GN=PDCD6 - [PDCD6_HUMAN]	2.53E+07	6.08E+07	2.41E+00
O75367-2	Isoform 1 of Core histone macro-H2A.1 OS=Homo sapiens GN=H2AFY - [H2AY_HUMAN]	3.11E+07	8.10E+07	2.60E+00
O75369-6	Isoform 6 of Filamin-B OS=Homo sapiens GN=FLNB - [FLNB_HUMAN]	6.14E+07	1.24E+08	2.02E+00
O75396	Vesicle-trafficking protein SEC22b OS=Homo sapiens GN=SEC22B PE=1 SV=4 - [SC22B_HUMAN]	4.07E+07	6.48E+07	1.59E+00
O75410-7	Isoform 7 of Transforming acidic coiled-coil-containing protein 1 OS=Homo sapiens GN=TACC1 - [TACC1_HUMAN]	2.00E+07	0.00E+00	-1.00E+01
O75439	Mitochondrial-processing peptidase subunit beta OS=Homo sapiens GN=PMPCB PE=1 SV=2 - [MPPB_HUMAN]	0.00E+00	2.13E+07	1.00E+01
O75477	Erlin-1 OS=Homo sapiens GN=ERLIN1 PE=1 SV=1 - [ERLN1_HUMAN]	2.25E+07	3.14E+07	1.40E+00
O75494-5	Isoform 5 of Serine/arginine-rich splicing factor 10 OS=Homo sapiens GN=SRSF10 - [SRS10_HUMAN]	1.75E+07	4.17E+07	2.39E+00

O75533	Splicing factor 3B subunit 1 OS=Homo sapiens GN=SF3B1 PE=1 SV=3 - [SF3B1_HUMAN]	2.39E+07	5.56E+07	2.32E+00
O75643	U5 small nuclear ribonucleoprotein 200 kDa helicase OS=Homo sapiens GN=SNRNP200 PE=1 SV=2 - [U520_HUMAN]	8.40E+06	2.00E+07	2.38E+00
O75874	Isocitrate dehydrogenase [NADP] cytoplasmic OS=Homo sapiens GN=IDH1 PE=1 SV=2 - [IDHC_HUMAN]	2.28E+07	4.09E+07	1.80E+00
O75947	ATP synthase subunit d, mitochondrial OS=Homo sapiens GN=ATP5H PE=1 SV=3 - [ATP5H_HUMAN]	5.30E+07	9.19E+07	1.74E+00
O76003	Glutaredoxin-3 OS=Homo sapiens GN=GLRX3 PE=1 SV=2 - [GLRX3_HUMAN]	4.45E+07	3.38E+07	-1.32E+00
O94826	Mitochondrial import receptor subunit TOM70 OS=Homo sapiens GN=TOMM70A PE=1 SV=1 - [TOM70_HUMAN]	1.22E+07	4.53E+06	-2.69E+00
O94925-3	Isoform 3 of Glutaminase kidney isoform, mitochondrial OS=Homo sapiens GN=GLS - [GLSK_HUMAN]	0.00E+00	3.77E+07	1.00E+01
O95197-3	Isoform 3 of Reticulon-3 OS=Homo sapiens GN=RTN3 - [RTN3_HUMAN]	6.80E+07	9.05E+07	1.33E+00
O95202	LETM1 and EF-hand domain-containing protein 1, mitochondrial OS=Homo sapiens GN=LETM1 PE=1 SV=1 - [LETM1_HUMAN]	0.00E+00	2.72E+07	1.00E+01
O95373	Importin-7 OS=Homo sapiens GN=IPO7 PE=1 SV=1 - [IPO7_HUMAN]	9.19E+07	1.40E+08	1.52E+00
O95573	Long-chain-fatty-acid--CoA ligase 3 OS=Homo sapiens GN=ACSL3 PE=1 SV=3 - [ACSL3_HUMAN]	1.72E+07	7.37E+07	4.29E+00

O95757	Heat shock 70 kDa protein 4L OS=Homo sapiens GN=HSPA4L PE=1 SV=3 - [HS74L_HUMAN]	1.37E+07	0.00E+00	-1.00E+01
O95782-2	Isoform B of AP-2 complex subunit alpha-1 OS=Homo sapiens GN=AP2A1 - [AP2A1_HUMAN]	1.02E+07	5.53E+06	-1.84E+00
O95831-3	Isoform 3 of Apoptosis-inducing factor 1, mitochondrial OS=Homo sapiens GN=AIFM1 - [AIFM1_HUMAN]	2.19E+07	3.18E+07	1.45E+00
O96019-2	Isoform 2 of Actin-like protein 6A OS=Homo sapiens GN=ACTL6A - [ACL6A_HUMAN]	0.00E+00	3.00E+07	1.00E+01
P00338	L-lactate dehydrogenase A chain OS=Homo sapiens GN=LDHA PE=1 SV=2 - [LDHA_HUMAN]	1.25E+09	2.67E+09	2.14E+00
P00390-2	Isoform Cytoplasmic of Glutathione reductase, mitochondrial OS=Homo sapiens GN=GSR - [GSHR_HUMAN]	4.89E+07	1.09E+08	2.23E+00
P00492	Hypoxanthine-guanine phosphoribosyltransferase OS=Homo sapiens GN=HPRT1 PE=1 SV=2 - [HPRT_HUMAN]	2.43E+07	3.44E+07	1.42E+00
P00505	Aspartate aminotransferase, mitochondrial OS=Homo sapiens GN=GOT2 PE=1 SV=3 - [AATM_HUMAN]	1.83E+08	3.02E+08	1.65E+00
P00558	Phosphoglycerate kinase 1 OS=Homo sapiens GN=PGK1 PE=1 SV=3 - [PGK1_HUMAN]	3.43E+08	5.50E+08	1.60E+00
P00568	Adenylate kinase isoenzyme 1 OS=Homo sapiens GN=AK1 PE=1 SV=3 - [KAD1_HUMAN]	4.36E+06	2.76E+07	6.32E+00
P00918	Carbonic anhydrase 2 OS=Homo sapiens GN=CA2 PE=1 SV=2 - [CAH2_HUMAN]	2.47E+06	2.55E+07	1.00E+01

P02545	Prelamin-A/C OS=Homo sapiens GN=LMNA PE=1 SV=1 - [LMNA_HUMAN]	1.37E+08	4.10E+08	2.99E+00
P02786	Transferrin receptor protein 1 OS=Homo sapiens GN=TFRC PE=1 SV=2 - [TFR1_HUMAN]	4.78E+08	2.07E+09	4.33E+00
P04075	Fructose-bisphosphate aldolase A OS=Homo sapiens GN=ALDOA PE=1 SV=2 - [ALDOA_HUMAN]	7.72E+08	1.50E+09	1.95E+00
P04083	Annexin A1 OS=Homo sapiens GN=ANXA1 PE=1 SV=2 - [ANXA1_HUMAN]	5.67E+07	1.47E+08	2.59E+00
P04150-7	Isoform GR-A beta of Glucocorticoid receptor OS=Homo sapiens GN=NR3C1 - [GCR_HUMAN]	2.04E+07	0.00E+00	-1.00E+01
P04792	Heat shock protein beta-1 OS=Homo sapiens GN=HSPB1 PE=1 SV=2 - [HSPB1_HUMAN]	4.37E+08	5.59E+08	1.28E+00
P04843	Dolichyl-diphosphooligosaccharide--protein glycosyltransferase subunit 1 OS=Homo sapiens GN=RPN1 PE=1 SV=1 - [RPN1_HUMAN]	1.81E+07	4.33E+07	2.39E+00
P04844-2	Isoform 2 of Dolichyl-diphosphooligosaccharide--protein glycosyltransferase subunit 2 OS=Homo sapiens GN=RPN2 - [RPN2_HUMAN]	1.05E+07	1.65E+07	1.57E+00
P05141	ADP/ATP translocase 2 OS=Homo sapiens GN=SLC25A5 PE=1 SV=7 - [ADT2_HUMAN]	2.27E+08	3.90E+08	1.72E+00
P05165-2	Isoform 2 of Propionyl-CoA carboxylase alpha chain, mitochondrial OS=Homo sapiens GN=PCCA - [PCCA_HUMAN]	3.69E+08	8.49E+08	2.30E+00

P05186-3	Isoform 3 of Alkaline phosphatase, tissue-nonspecific isozyme OS=Homo sapiens GN=ALPL - [PPBT_HUMAN]	3.37E+06	3.42E+07	1.00E+01
P05198	Eukaryotic translation initiation factor 2 subunit 1 OS=Homo sapiens GN=EIF2S1 PE=1 SV=3 - [IF2A_HUMAN]	2.60E+07	7.94E+07	3.05E+00
P05556	Integrin beta-1 OS=Homo sapiens GN=ITGB1 PE=1 SV=2 - [ITB1_HUMAN]	9.84E+06	2.41E+07	2.45E+00
P05787	Keratin, type II cytoskeletal 8 OS=Homo sapiens GN=KRT8 PE=1 SV=7 - [K2C8_HUMAN]	1.23E+08	5.35E+08	4.34E+00
P06493	Cyclin-dependent kinase 1 OS=Homo sapiens GN=CDK1 PE=1 SV=3 - [CDK1_HUMAN]	6.77E+07	8.44E+07	1.25E+00
P06576	ATP synthase subunit beta, mitochondrial OS=Homo sapiens GN=ATP5B PE=1 SV=3 - [ATPB_HUMAN]	5.51E+07	7.58E+07	1.38E+00
P06703	Protein S100-A6 OS=Homo sapiens GN=S100A6 PE=1 SV=1 - [S10A6_HUMAN]	3.74E+08	1.13E+09	3.03E+00
P06733	Alpha-enolase OS=Homo sapiens GN=ENO1 PE=1 SV=2 - [ENOA_HUMAN]	1.08E+09	2.72E+09	2.51E+00
P06744	Glucose-6-phosphate isomerase OS=Homo sapiens GN=GPI PE=1 SV=4 - [G6PI_HUMAN]	2.09E+08	5.03E+08	2.40E+00
P06748-2	Isoform 2 of Nucleophosmin OS=Homo sapiens GN=NPM1 - [NPM_HUMAN]	1.12E+09	2.20E+09	1.96E+00
P07195	L-lactate dehydrogenase B chain OS=Homo sapiens GN=LDHB PE=1 SV=2 - [LDHB_HUMAN]	1.19E+09	2.35E+09	1.98E+00
P07237	Protein disulfide-isomerase OS=Homo sapiens GN=P4HB PE=1 SV=3 - [PDIA1_HUMAN]	7.77E+07	2.08E+08	2.68E+00

P07355	Annexin A2 OS=Homo sapiens GN=ANXA2 PE=1 SV=2 - [ANXA2_HUMAN]	2.88E+08	6.43E+08	2.23E+00
P07737	Profilin-1 OS=Homo sapiens GN=PFN1 PE=1 SV=2 - [PROF1_HUMAN]	6.05E+08	1.18E+09	1.96E+00
P07814	Bifunctional glutamate/proline--tRNA ligase OS=Homo sapiens GN=EPRS PE=1 SV=5 - [SYEP_HUMAN]	3.10E+07	5.34E+07	1.72E+00
P07900	Heat shock protein HSP 90-alpha OS=Homo sapiens GN=HSP90AA1 PE=1 SV=5 - [HS90A_HUMAN]	8.61E+08	1.85E+09	2.15E+00
P07954-2	Isoform Cytoplasmic of Fumarate hydratase, mitochondrial OS=Homo sapiens GN=FH - [FUMH_HUMAN]	3.66E+07	6.49E+07	1.78E+00
P08107	Heat shock 70 kDa protein 1A/1B OS=Homo sapiens GN=HSPA1A PE=1 SV=5 - [HSP71_HUMAN]	6.26E+08	1.73E+09	2.77E+00
P08195-2	Isoform 2 of 4F2 cell-surface antigen heavy chain OS=Homo sapiens GN=SLC3A2 - [4F2_HUMAN]	3.54E+08	8.99E+08	2.54E+00
P08238	Heat shock protein HSP 90-beta OS=Homo sapiens GN=HSP90AB1 PE=1 SV=4 - [HS90B_HUMAN]	9.33E+08	1.85E+09	1.98E+00
P08559-3	Isoform 3 of Pyruvate dehydrogenase E1 component subunit alpha, somatic form, mitochondrial OS=Homo sapiens GN=PDHA1 - [ODPA_HUMAN]	1.17E+07	2.00E+07	1.71E+00
P08574	Cytochrome c1, heme protein, mitochondrial OS=Homo sapiens GN=CYC1 PE=1 SV=3 - [CY1_HUMAN]	4.93E+07	1.23E+08	2.49E+00
P08621-2	Isoform 2 of U1 small nuclear ribonucleoprotein 70 kDa OS=Homo sapiens GN=SNRNP70 - [RU17_HUMAN]	9.63E+06	0.00E+00	-1.00E+01

P08670	Vimentin OS=Homo sapiens GN=VIM PE=1 SV=4 - [VIME_HUMAN]	9.13E+07	1.58E+08	1.73E+00
P08729	Keratin, type II cytoskeletal 7 OS=Homo sapiens GN=KRT7 PE=1 SV=5 - [K2C7_HUMAN]	7.48E+07	2.21E+08	2.95E+00
P08758	Annexin A5 OS=Homo sapiens GN=ANXA5 PE=1 SV=2 - [ANXA5_HUMAN]	9.41E+07	1.97E+08	2.09E+00
P09211	Glutathione S-transferase P OS=Homo sapiens GN=GSTP1 PE=1 SV=2 - [GSTP1_HUMAN]	1.42E+08	3.20E+08	2.26E+00
P09382	Galectin-1 OS=Homo sapiens GN=LGALS1 PE=1 SV=2 - [LEG1_HUMAN]	4.37E+07	8.53E+07	1.95E+00
P09651-3	Isoform 2 of Heterogeneous nuclear ribonucleoprotein A1 OS=Homo sapiens GN=HNRNPA1 - [ROA1_HUMAN]	2.73E+08	4.30E+08	1.57E+00
P09874	Poly [ADP-ribose] polymerase 1 OS=Homo sapiens GN=PARP1 PE=1 SV=4 - [PARP1_HUMAN]	5.30E+07	7.93E+07	1.50E+00
P09960-3	Isoform 3 of Leukotriene A-4 hydrolase OS=Homo sapiens GN=LTA4H - [LKHA4_HUMAN]	0.00E+00	4.68E+07	1.00E+01
P10620	Microsomal glutathione S-transferase 1 OS=Homo sapiens GN=MGST1 PE=1 SV=1 - [MGST1_HUMAN]	5.54E+07	0.00E+00	-1.00E+01
P10809	60 kDa heat shock protein, mitochondrial OS=Homo sapiens GN=HSPD1 PE=1 SV=2 - [CH60_HUMAN]	6.51E+08	1.65E+09	2.53E+00
P11021	78 kDa glucose-regulated protein OS=Homo sapiens GN=HSPA5 PE=1 SV=2 - [GRP78_HUMAN]	6.36E+08	2.25E+09	3.54E+00
P11142	Heat shock cognate 71 kDa protein OS=Homo sapiens GN=HSPA8 PE=1 SV=1 - [HSP7C_HUMAN]	1.13E+09	2.46E+09	2.18E+00

P11166	Solute carrier family 2, facilitated glucose transporter member 1 OS=Homo sapiens GN=SLC2A1 PE=1 SV=2 - [GTR1_HUMAN]	1.76E+07	4.23E+07	2.40E+00
P11177-2	Isoform 2 of Pyruvate dehydrogenase E1 component subunit beta, mitochondrial OS=Homo sapiens GN=PDHB - [ODPB_HUMAN]	2.86E+07	4.02E+07	1.41E+00
P11387	DNA topoisomerase 1 OS=Homo sapiens GN=TOP1 PE=1 SV=2 - [TOP1_HUMAN]	2.25E+07	2.77E+07	1.23E+00
P11388	DNA topoisomerase 2-alpha OS=Homo sapiens GN=TOP2A PE=1 SV=3 - [TOP2A_HUMAN]	1.25E+07	1.65E+07	1.32E+00
P11413	Glucose-6-phosphate 1-dehydrogenase OS=Homo sapiens GN=G6PD PE=1 SV=4 - [G6PD_HUMAN]	4.13E+07	7.26E+07	1.76E+00
P11498	Pyruvate carboxylase, mitochondrial OS=Homo sapiens GN=PC PE=1 SV=2 - [PYC_HUMAN]	1.29E+09	3.41E+09	2.65E+00
P11940-2	Isoform 2 of Polyadenylate-binding protein 1 OS=Homo sapiens GN=PABPC1 - [PABP1_HUMAN]	7.57E+07	1.33E+08	1.76E+00
P12004	Proliferating cell nuclear antigen OS=Homo sapiens GN=PCNA PE=1 SV=1 - [PCNA_HUMAN]	2.43E+07	0.00E+00	-1.00E+01
P12236	ADP/ATP translocase 3 OS=Homo sapiens GN=SLC25A6 PE=1 SV=4 - [ADT3_HUMAN]	1.47E+08	3.79E+08	2.58E+00
P12270	Nucleoprotein TPR OS=Homo sapiens GN=TPR PE=1 SV=3 - [TPR_HUMAN]	2.15E+06	2.33E+06	1.09E+00
P12277	Creatine kinase B-type OS=Homo sapiens GN=CKB PE=1 SV=1 - [KCRB_HUMAN]	7.74E+07	1.17E+08	1.51E+00

P12814-2	Isoform 2 of Alpha-actinin-1 OS=Homo sapiens GN=ACTN1 - [ACTN1_HUMAN]	2.71E+08	6.32E+08	2.33E+00
P12956	X-ray repair cross-complementing protein 6 OS=Homo sapiens GN=XRCC6 PE=1 SV=2 - [XRCC6_HUMAN]	2.29E+08	3.97E+08	1.73E+00
P13010	X-ray repair cross-complementing protein 5 OS=Homo sapiens GN=XRCC5 PE=1 SV=3 - [XRCC5_HUMAN]	9.19E+07	1.49E+08	1.62E+00
P13639	Elongation factor 2 OS=Homo sapiens GN=EEF2 PE=1 SV=4 - [EF2_HUMAN]	4.00E+08	5.81E+08	1.45E+00
P13645	Keratin, type I cytoskeletal 10 OS=Homo sapiens GN=KRT10 PE=1 SV=6 - [K1C10_HUMAN]	3.44E+08	1.48E+09	4.30E+00
P13647	Keratin, type II cytoskeletal 5 OS=Homo sapiens GN=KRT5 PE=1 SV=3 - [K2C5_HUMAN]	1.41E+08	5.64E+08	4.01E+00
P13667	Protein disulfide-isomerase A4 OS=Homo sapiens GN=PDIA4 PE=1 SV=2 - [PDIA4_HUMAN]	8.01E+06	2.85E+07	3.56E+00
P14174	Macrophage migration inhibitory factor OS=Homo sapiens GN=MIF PE=1 SV=4 - [MIF_HUMAN]	4.49E+08	9.61E+08	2.14E+00
P14314-2	Isoform 2 of Glucosidase 2 subunit beta OS=Homo sapiens GN=PRKCSH - [GLU2B_HUMAN]	1.05E+07	2.67E+07	2.54E+00
P14618	Pyruvate kinase isozymes M1/M2 OS=Homo sapiens GN=PKM PE=1 SV=4 - [KPYM_HUMAN]	5.58E+08	1.10E+09	1.97E+00
P14625	Endoplasmin OS=Homo sapiens GN=HSP90B1 PE=1 SV=1 - [ENPL_HUMAN]	1.51E+08	6.95E+08	4.60E+00
P14866	Heterogeneous nuclear ribonucleoprotein L OS=Homo sapiens GN=HNRNPL PE=1 SV=2 - [HNRPL_HUMAN]	7.76E+07	2.51E+08	3.23E+00

P14923	Junction plakoglobin OS=Homo sapiens GN=JUP PE=1 SV=3 - [PLAK_HUMAN]	2.57E+07	1.88E+07	-1.36E+00
P15151-3	Isoform Gamma of Poliovirus receptor OS=Homo sapiens GN=PVR - [PVR_HUMAN]	3.93E+06	1.55E+07	3.95E+00
P15291-2	Isoform Short of Beta-1,4-galactosyltransferase 1 OS=Homo sapiens GN=B4GALT1 - [B4GT1_HUMAN]	1.28E+08	3.05E+08	2.39E+00
P15529-15	Isoform K of Membrane cofactor protein OS=Homo sapiens GN=CD46 - [MCP_HUMAN]	2.68E+06	9.47E+06	3.53E+00
P15880	40S ribosomal protein S2 OS=Homo sapiens GN=RPS2 PE=1 SV=2 - [RS2_HUMAN]	1.91E+08	3.78E+08	1.98E+00
P16152	Carbonyl reductase [NADPH] 1 OS=Homo sapiens GN=CBR1 PE=1 SV=3 - [CBR1_HUMAN]	6.13E+07	1.20E+08	1.96E+00
P16615-2	Isoform 2 of Sarcoplasmic/endoplasmic reticulum calcium ATPase 2 OS=Homo sapiens GN=ATP2A2 - [AT2A2_HUMAN]	5.69E+07	9.61E+07	1.69E+00
P17612-2	Isoform 2 of cAMP-dependent protein kinase catalytic subunit alpha OS=Homo sapiens GN=PRKACA - [KAPCA_HUMAN]	9.05E+08	0.00E+00	-1.00E+01
P17655	Calpain-2 catalytic subunit OS=Homo sapiens GN=CAPN2 PE=1 SV=6 - [CAN2_HUMAN]	1.56E+07	2.66E+07	1.70E+00
P17812	CTP synthase 1 OS=Homo sapiens GN=CTPS1 PE=1 SV=2 - [PYRG1_HUMAN]	2.63E+07	3.33E+07	1.26E+00
P17980	26S protease regulatory subunit 6A OS=Homo sapiens GN=PSMC3 PE=1 SV=3 - [PRS6A_HUMAN]	4.18E+07	5.37E+07	1.29E+00
P17987	T-complex protein 1 subunit alpha OS=Homo sapiens GN=TCP1 PE=1 SV=1 -	3.39E+07	6.38E+08	1.00E+01

	[TCPA_HUMAN]			
P18077	60S ribosomal protein L35a OS=Homo sapiens GN=RPL35A PE=1 SV=2 - [RL35A_HUMAN]	1.73E+08	3.12E+08	1.80E+00
P18206-2	Isoform 1 of Vinculin OS=Homo sapiens GN=VCL - [VINC_HUMAN]	4.55E+07	1.44E+08	3.16E+00
P18669	Phosphoglycerate mutase 1 OS=Homo sapiens GN=PGAM1 PE=1 SV=2 - [PGAM1_HUMAN]	5.89E+07	9.65E+07	1.64E+00
P19105	Myosin regulatory light chain 12A OS=Homo sapiens GN=MYL12A PE=1 SV=2 - [ML12A_HUMAN]	0.00E+00	1.91E+07	1.00E+01
P19338	Nucleolin OS=Homo sapiens GN=NCL PE=1 SV=3 - [NUCL_HUMAN]	2.31E+08	4.88E+08	2.12E+00
P20042	Eukaryotic translation initiation factor 2 subunit 2 OS=Homo sapiens GN=EIF2S2 PE=1 SV=2 - [IF2B_HUMAN]	1.73E+07	2.67E+07	1.55E+00
P20700	Lamin-B1 OS=Homo sapiens GN=LMNB1 PE=1 SV=2 - [LMNB1_HUMAN]	1.15E+08	1.36E+08	1.19E+00
P21266	Glutathione S-transferase Mu 3 OS=Homo sapiens GN=GSTM3 PE=1 SV=3 - [GSTM3_HUMAN]	2.52E+07	5.02E+07	1.99E+00
P21291	Cysteine and glycine-rich protein 1 OS=Homo sapiens GN=CSRP1 PE=1 SV=3 - [CSRP1_HUMAN]	7.82E+07	1.22E+08	1.55E+00
P21333-2	Isoform 2 of Filamin-A OS=Homo sapiens GN=FLNA - [FLNA_HUMAN]	2.44E+08	4.99E+08	2.05E+00
P21796	Voltage-dependent anion-selective channel protein 1 OS=Homo sapiens GN=VDAC1 PE=1 SV=2 - [VDAC1_HUMAN]	4.48E+07	9.54E+07	2.13E+00

P22087	rRNA 2'-O-methyltransferase fibrillarin OS=Homo sapiens GN=FBL PE=1 SV=2 - [FBRL_HUMAN]	1.93E+07	3.37E+07	1.74E+00
P22102	Trifunctional purine biosynthetic protein adenosine-3 OS=Homo sapiens GN=GART PE=1 SV=1 - [PUR2_HUMAN]	2.19E+07	2.63E+07	1.20E+00
P22234	Multifunctional protein ADE2 OS=Homo sapiens GN=PAICS PE=1 SV=3 - [PUR6_HUMAN]	6.03E+07	1.17E+08	1.94E+00
P22314	Ubiquitin-like modifier-activating enzyme 1 OS=Homo sapiens GN=UBA1 PE=1 SV=3 - [UBA1_HUMAN]	8.87E+07	2.15E+08	2.43E+00
P22626	Heterogeneous nuclear ribonucleoproteins A2/B1 OS=Homo sapiens GN=HNRNPA2B1 PE=1 SV=2 - [ROA2_HUMAN]	7.34E+08	1.25E+09	1.71E+00
P23246	Splicing factor, proline- and glutamine-rich OS=Homo sapiens GN=SFPQ PE=1 SV=2 - [SFPQ_HUMAN]	7.07E+07	3.11E+08	4.40E+00
P23284	Peptidyl-prolyl cis-trans isomerase B OS=Homo sapiens GN=PPIB PE=1 SV=2 - [PPIB_HUMAN]	6.21E+07	1.70E+08	2.74E+00
P23396	40S ribosomal protein S3 OS=Homo sapiens GN=RPS3 PE=1 SV=2 - [RS3_HUMAN]	1.27E+08	5.27E+08	4.14E+00
P23526	Adenosylhomocysteinase OS=Homo sapiens GN=AHCY PE=1 SV=4 - [SAHH_HUMAN]	1.25E+08	3.46E+08	2.78E+00
P23921	Ribonucleoside-diphosphate reductase large subunit OS=Homo sapiens GN=RRM1 PE=1 SV=1 - [RIR1_HUMAN]	4.65E+07	1.01E+08	2.16E+00

P24539	ATP synthase subunit b, mitochondrial OS=Homo sapiens GN=ATP5F1 PE=1 SV=2 - [AT5F1_HUMAN]	3.55E+07	4.32E+07	1.22E+00
P24752	Acetyl-CoA acetyltransferase, mitochondrial OS=Homo sapiens GN=ACAT1 PE=1 SV=1 - [THIL_HUMAN]	2.86E+07	5.54E+07	1.94E+00
P25205	DNA replication licensing factor MCM3 OS=Homo sapiens GN=MCM3 PE=1 SV=3 - [MCM3_HUMAN]	1.85E+07	3.62E+07	1.96E+00
P25398	40S ribosomal protein S12 OS=Homo sapiens GN=RPS12 PE=1 SV=3 - [RS12_HUMAN]	5.37E+07	1.09E+08	2.04E+00
P25705	ATP synthase subunit alpha, mitochondrial OS=Homo sapiens GN=ATP5A1 PE=1 SV=1 - [ATPA_HUMAN]	1.57E+08	2.60E+08	1.66E+00
P25786	Proteasome subunit alpha type-1 OS=Homo sapiens GN=PSMA1 PE=1 SV=1 - [PSA1_HUMAN]	0.00E+00	3.59E+07	1.00E+01
P25788-2	Isoform 2 of Proteasome subunit alpha type-3 OS=Homo sapiens GN=PSMA3 - [PSA3_HUMAN]	1.28E+07	4.61E+07	3.62E+00
P26038	Moesin OS=Homo sapiens GN=MSN PE=1 SV=3 - [MOES_HUMAN]	1.21E+08	3.57E+08	2.95E+00
P26358	DNA (cytosine-5)-methyltransferase 1 OS=Homo sapiens GN=DNMT1 PE=1 SV=2 - [DNMT1_HUMAN]	0.00E+00	1.29E+07	1.00E+01
P26373	60S ribosomal protein L13 OS=Homo sapiens GN=RPL13 PE=1 SV=4 - [RL13_HUMAN]	1.70E+08	4.24E+08	2.49E+00
P26447	Protein S100-A4 OS=Homo sapiens GN=S100A4 PE=1 SV=1 - [S10A4_HUMAN]	2.08E+07	2.77E+07	1.33E+00

P26599	Polypyrimidine tract-binding protein 1 OS=Homo sapiens GN=PTBP1 PE=1 SV=1 - [PTBP1_HUMAN]	9.73E+07	2.23E+08	2.29E+00
P26639	Threonine--tRNA ligase, cytoplasmic OS=Homo sapiens GN=TARS PE=1 SV=3 - [SYTC_HUMAN]	7.78E+07	1.51E+08	1.94E+00
P26641	Elongation factor 1-gamma OS=Homo sapiens GN=EEF1G PE=1 SV=3 - [EF1G_HUMAN]	1.84E+08	4.71E+08	2.56E+00
P27348	14-3-3 protein theta OS=Homo sapiens GN=YWHAQ PE=1 SV=1 - [1433T_HUMAN]	1.67E+08	8.43E+08	5.05E+00
P27797	Calreticulin OS=Homo sapiens GN=CALR PE=1 SV=1 - [CALR_HUMAN]	8.99E+07	2.46E+08	2.74E+00
P27816-6	Isoform 6 of Microtubule-associated protein 4 OS=Homo sapiens GN=MAP4 - [MAP4_HUMAN]	7.52E+06	3.90E+07	5.19E+00
P27824	Calnexin OS=Homo sapiens GN=CANX PE=1 SV=2 - [CALX_HUMAN]	1.28E+09	1.90E+09	1.49E+00
P28066	Proteasome subunit alpha type-5 OS=Homo sapiens GN=PSMA5 PE=1 SV=3 - [PSA5_HUMAN]	2.21E+07	8.82E+07	3.98E+00
P28070	Proteasome subunit beta type-4 OS=Homo sapiens GN=PSMB4 PE=1 SV=4 - [PSB4_HUMAN]	5.34E+07	1.78E+08	3.34E+00
P28074	Proteasome subunit beta type-5 OS=Homo sapiens GN=PSMB5 PE=1 SV=3 - [PSB5_HUMAN]	5.51E+07	6.86E+07	1.25E+00
P28838-2	Isoform 2 of Cytosol aminopeptidase OS=Homo sapiens GN=LAP3 - [AMPL_HUMAN]	1.26E+07	0.00E+00	-1.00E+01
P29401	Transketolase OS=Homo sapiens GN=TKT PE=1 SV=3 - [TKT_HUMAN]	6.86E+08	1.31E+09	1.91E+00

P29992	Guanine nucleotide-binding protein subunit alpha-11 OS=Homo sapiens GN=GNA11 PE=1 SV=2 - [GNA11_HUMAN]	0.00E+00	5.78E+06	1.00E+01
P30040	Endoplasmic reticulum resident protein 29 OS=Homo sapiens GN=ERP29 PE=1 SV=4 - [ERP29_HUMAN]	2.29E+07	0.00E+00	-1.00E+01
P30041	Peroxiredoxin-6 OS=Homo sapiens GN=PRDX6 PE=1 SV=3 - [PRDX6_HUMAN]	4.01E+07	7.36E+07	1.84E+00
P30044-2	Isoform Cytoplasmic+peroxisomal of Peroxiredoxin-5, mitochondrial OS=Homo sapiens GN=PRDX5 - [PRDX5_HUMAN]	4.58E+07	6.97E+07	1.52E+00
P30050-2	Isoform 2 of 60S ribosomal protein L12 OS=Homo sapiens GN=RPL12 - [RL12_HUMAN]	9.96E+07	2.30E+08	2.31E+00
P30084	Enoyl-CoA hydratase, mitochondrial OS=Homo sapiens GN=ECHS1 PE=1 SV=4 - [ECHM_HUMAN]	1.16E+07	2.34E+07	2.02E+00
P30086	Phosphatidylethanolamine-binding protein 1 OS=Homo sapiens GN=PEBP1 PE=1 SV=3 - [PEBP1_HUMAN]	0.00E+00	4.58E+07	1.00E+01
P30153	Serine/threonine-protein phosphatase 2A 65 kDa regulatory subunit A alpha isoform OS=Homo sapiens GN=PPP2R1A PE=1 SV=4 - [2AAA_HUMAN]	4.41E+07	9.74E+07	2.21E+00
P30520	Adenylosuccinate synthetase isozyme 2 OS=Homo sapiens GN=ADSS PE=1 SV=3 - [PURA2_HUMAN]	2.50E+07	2.46E+07	-1.02E+00
P30837	Aldehyde dehydrogenase X, mitochondrial OS=Homo sapiens GN=ALDH1B1 PE=1 SV=3 - [AL1B1_HUMAN]	1.50E+07	2.28E+07	1.52E+00

P31040	Succinate dehydrogenase [ubiquinone] flavoprotein subunit, mitochondrial OS=Homo sapiens GN=SDHA PE=1 SV=2 - [DHSA_HUMAN]	3.59E+07	1.13E+08	3.14E+00
P31327	Carbamoyl-phosphate synthase [ammonia], mitochondrial OS=Homo sapiens GN=CPS1 PE=1 SV=2 - [CPSM_HUMAN]	1.77E+08	4.13E+08	2.33E+00
P31930	Cytochrome b-c1 complex subunit 1, mitochondrial OS=Homo sapiens GN=UQCRC1 PE=1 SV=3 - [QCR1_HUMAN]	4.87E+07	5.86E+07	1.21E+00
P31942-3	Isoform 3 of Heterogeneous nuclear ribonucleoprotein H3 OS=Homo sapiens GN=HNRNPH3 - [HNRH3_HUMAN]	8.59E+06	7.44E+07	8.66E+00
P31946-2	Isoform Short of 14-3-3 protein beta/alpha OS=Homo sapiens GN=YWHAB - [1433B_HUMAN]	1.48E+08	8.43E+08	5.68E+00
P31948	Stress-induced-phosphoprotein 1 OS=Homo sapiens GN=STIP1 PE=1 SV=1 - [STIP1_HUMAN]	1.36E+08	3.01E+08	2.21E+00
P31949	Protein S100-A11 OS=Homo sapiens GN=S100A11 PE=1 SV=2 - [S10AB_HUMAN]	0.00E+00	2.87E+07	1.00E+01
P32119	Peroxiredoxin-2 OS=Homo sapiens GN=PRDX2 PE=1 SV=5 - [PRDX2_HUMAN]	2.31E+07	2.93E+08	1.00E+01
P32969	60S ribosomal protein L9 OS=Homo sapiens GN=RPL9 PE=1 SV=1 - [RL9_HUMAN]	1.01E+08	1.05E+08	1.04E+00
P33176	Kinesin-1 heavy chain OS=Homo sapiens GN=KIF5B PE=1 SV=1 - [KINH_HUMAN]	5.01E+06	8.89E+06	1.78E+00
P33316-2	Isoform 2 of Deoxyuridine 5'-triphosphate nucleotidohydrolase, mitochondrial OS=Homo sapiens GN=DUT - [DUT_HUMAN]	4.31E+07	3.35E+07	-1.29E+00

P33993	DNA replication licensing factor MCM7 OS=Homo sapiens GN=MCM7 PE=1 SV=4 - [MCM7_HUMAN]	1.85E+07	4.79E+07	2.59E+00
P34897-3	Isoform 3 of Serine hydroxymethyltransferase, mitochondrial OS=Homo sapiens GN=SHMT2 - [GLYM_HUMAN]	5.32E+07	1.11E+08	2.08E+00
P34932	Heat shock 70 kDa protein 4 OS=Homo sapiens GN=HSPA4 PE=1 SV=4 - [HSP74_HUMAN]	1.15E+08	1.95E+08	1.70E+00
P35221	Catenin alpha-1 OS=Homo sapiens GN=CTNNA1 PE=1 SV=1 - [CTNA1_HUMAN]	1.93E+07	9.46E+07	4.90E+00
P35232	Prohibitin OS=Homo sapiens GN=PHB PE=1 SV=1 - [PHB_HUMAN]	8.66E+07	1.77E+08	2.04E+00
P35237	Serpin B6 OS=Homo sapiens GN=SERPINB6 PE=1 SV=3 - [SPB6_HUMAN]	4.71E+07	0.00E+00	-1.00E+01
P35241	Radixin OS=Homo sapiens GN=RDX PE=1 SV=1 - [RADI_HUMAN]	1.21E+08	3.57E+08	2.94E+00
P35520	Cystathionine beta-synthase OS=Homo sapiens GN=CBS PE=1 SV=2 - [CBS_HUMAN]	0.00E+00	1.51E+07	1.00E+01
P35579	Myosin-9 OS=Homo sapiens GN=MYH9 PE=1 SV=4 - [MYH9_HUMAN]	6.53E+07	1.53E+08	2.34E+00
P35637-2	Isoform Short of RNA-binding protein FUS OS=Homo sapiens GN=FUS - [FUS_HUMAN]	4.44E+07	0.00E+00	-1.00E+01
P35659	Protein DEK OS=Homo sapiens GN=DEK PE=1 SV=1 - [DEK_HUMAN]	1.99E+07	2.01E+07	1.01E+00
P35908	Keratin, type II cytoskeletal 2 epidermal OS=Homo sapiens GN=KRT2 PE=1 SV=2 - [K22E_HUMAN]	5.02E+08	2.19E+09	4.35E+00

P35998	26S protease regulatory subunit 7 OS=Homo sapiens GN=PSMC2 PE=1 SV=3 - [PRS7_HUMAN]	8.16E+07	4.81E+07	-1.70E+00
P36578	60S ribosomal protein L4 OS=Homo sapiens GN=RPL4 PE=1 SV=5 - [RL4_HUMAN]	1.21E+08	3.86E+08	3.19E+00
P36952	Serpin B5 OS=Homo sapiens GN=SERPINB5 PE=1 SV=2 - [SPB5_HUMAN]	2.64E+07	3.36E+07	1.27E+00
P36957	Dihydrolipoyllysine-residue succinyltransferase component of 2-oxoglutarate dehydrogenase complex, mitochondrial OS=Homo sapiens GN=DLST PE=1 SV=4 - [ODO2_HUMAN]	4.30E+07	8.55E+07	1.99E+00
P37802	Transgelin-2 OS=Homo sapiens GN=TAGLN2 PE=1 SV=3 - [TAGL2_HUMAN]	2.59E+08	6.32E+08	2.44E+00
P37837	Transaldolase OS=Homo sapiens GN=TALDO1 PE=1 SV=2 - [TALDO_HUMAN]	3.67E+07	8.11E+07	2.21E+00
P38646	Stress-70 protein, mitochondrial OS=Homo sapiens GN=HSPA9 PE=1 SV=2 - [GRP75_HUMAN]	3.47E+08	6.20E+08	1.79E+00
P38919	Eukaryotic initiation factor 4A-III OS=Homo sapiens GN=EIF4A3 PE=1 SV=4 - [IF4A3_HUMAN]	6.60E+07	1.38E+08	2.09E+00
P39023	60S ribosomal protein L3 OS=Homo sapiens GN=RPL3 PE=1 SV=2 - [RL3_HUMAN]	1.41E+08	3.21E+08	2.28E+00
P40429	60S ribosomal protein L13a OS=Homo sapiens GN=RPL13A PE=1 SV=2 - [RL13A_HUMAN]	1.54E+07	1.86E+08	1.00E+01
P40925	Malate dehydrogenase, cytoplasmic OS=Homo sapiens GN=MDH1 PE=1 SV=4 - [MDHC_HUMAN]	7.98E+07	1.36E+08	1.71E+00

P40926	Malate dehydrogenase, mitochondrial OS=Homo sapiens GN=MDH2 PE=1 SV=3 - [MDHM_HUMAN]	1.43E+07	1.46E+08	1.00E+01
P40939	Trifunctional enzyme subunit alpha, mitochondrial OS=Homo sapiens GN=HADHA PE=1 SV=2 - [ECHA_HUMAN]	4.97E+07	8.55E+07	1.72E+00
P41091	Eukaryotic translation initiation factor 2 subunit 3 OS=Homo sapiens GN=EIF2S3 PE=1 SV=3 - [IF2G_HUMAN]	5.39E+07	9.23E+07	1.71E+00
P41250	Glycine--tRNA ligase OS=Homo sapiens GN=GARS PE=1 SV=3 - [SYG_HUMAN]	1.42E+07	5.28E+07	3.71E+00
P42167	Lamina-associated polypeptide 2, isoforms beta/gamma OS=Homo sapiens GN=TMPO PE=1 SV=2 - [LAP2B_HUMAN]	5.26E+07	8.38E+07	1.59E+00
P42330	Aldo-keto reductase family 1 member C3 OS=Homo sapiens GN=AKR1C3 PE=1 SV=4 - [AK1C3_HUMAN]	2.11E+08	3.59E+08	1.70E+00
P42704	Leucine-rich PPR motif-containing protein, mitochondrial OS=Homo sapiens GN=LRPPRC PE=1 SV=3 - [LPPRC_HUMAN]	5.28E+07	1.18E+08	2.23E+00
P42765	3-ketoacyl-CoA thiolase, mitochondrial OS=Homo sapiens GN=ACAA2 PE=1 SV=2 - [THIM_HUMAN]	4.23E+07	1.25E+08	2.95E+00
P43007	Neutral amino acid transporter A OS=Homo sapiens GN=SLC1A4 PE=1 SV=1 - [SATT_HUMAN]	1.81E+07	1.87E+07	1.03E+00
P43243	Matrin-3 OS=Homo sapiens GN=MATR3 PE=1 SV=2 - [MATR3_HUMAN]	1.04E+08	2.13E+08	2.05E+00

P43304-2	Isoform 2 of Glycerol-3-phosphate dehydrogenase, mitochondrial OS=Homo sapiens GN=GPD2 - [GPDM_HUMAN]	0.00E+00	1.58E+07	1.00E+01
P45880-2	Isoform 2 of Voltage-dependent anion-selective channel protein 2 OS=Homo sapiens GN=VDAC2 - [VDAC2_HUMAN]	1.64E+08	2.98E+08	1.82E+00
P45974-2	Isoform Short of Ubiquitin carboxyl-terminal hydrolase 5 OS=Homo sapiens GN=USP5 - [UBP5_HUMAN]	1.62E+07	3.24E+07	2.00E+00
P46013	Antigen KI-67 OS=Homo sapiens GN=MKI67 PE=1 SV=2 - [KI67_HUMAN]	2.94E+06	4.72E+06	1.60E+00
P46060	Ran GTPase-activating protein 1 OS=Homo sapiens GN=RANGAP1 PE=1 SV=1 - [RAGP1_HUMAN]	2.75E+07	0.00E+00	-1.00E+01
P46779	60S ribosomal protein L28 OS=Homo sapiens GN=RPL28 PE=1 SV=3 - [RL28_HUMAN]	6.18E+07	7.71E+07	1.25E+00
P46781	40S ribosomal protein S9 OS=Homo sapiens GN=RPS9 PE=1 SV=3 - [RS9_HUMAN]	2.45E+08	3.39E+08	1.38E+00
P46782	40S ribosomal protein S5 OS=Homo sapiens GN=RPS5 PE=1 SV=4 - [RS5_HUMAN]	1.53E+07	1.04E+08	6.83E+00
P46940	Ras GTPase-activating-like protein IQGAP1 OS=Homo sapiens GN=IQGAP1 PE=1 SV=1 - [IQGA1_HUMAN]	5.96E+07	1.17E+08	1.97E+00
P46977	Dolichyl-diphosphooligosaccharide--protein glycosyltransferase subunit STT3A OS=Homo sapiens GN=STT3A PE=1 SV=2 - [STT3A_HUMAN]	2.74E+07	3.31E+07	1.21E+00
P47712	Cytosolic phospholipase A2 OS=Homo sapiens GN=PLA2G4A PE=1 SV=2 - [PA24A_HUMAN]	2.36E+07	7.13E+07	3.02E+00

P47914	60S ribosomal protein L29 OS=Homo sapiens GN=RPL29 PE=1 SV=2 - [RL29_HUMAN]	1.95E+08	1.09E+09	5.56E+00
P48047	ATP synthase subunit O, mitochondrial OS=Homo sapiens GN=ATP5O PE=1 SV=1 - [ATPO_HUMAN]	3.33E+07	7.88E+07	2.37E+00
P48444	Coatomer subunit delta OS=Homo sapiens GN=ARCN1 PE=1 SV=1 - [COPD_HUMAN]	7.63E+06	0.00E+00	-1.00E+01
P48960-2	Isoform 2 of CD97 antigen OS=Homo sapiens GN=CD97 - [CD97_HUMAN]	3.53E+07	4.51E+07	1.28E+00
P49327	Fatty acid synthase OS=Homo sapiens GN=FASN PE=1 SV=3 - [FAS_HUMAN]	6.13E+07	2.92E+08	4.77E+00
P49411	Elongation factor Tu, mitochondrial OS=Homo sapiens GN=TUFM PE=1 SV=2 - [EFTU_HUMAN]	8.58E+07	2.40E+08	2.79E+00
P49588	Alanine--tRNA ligase, cytoplasmic OS=Homo sapiens GN=AARS PE=1 SV=2 - [SYAC_HUMAN]	1.78E+07	2.77E+07	1.56E+00
P49721	Proteasome subunit beta type-2 OS=Homo sapiens GN=PSMB2 PE=1 SV=1 - [PSB2_HUMAN]	0.00E+00	3.78E+07	1.00E+01
P49748	Very long-chain specific acyl-CoA dehydrogenase, mitochondrial OS=Homo sapiens GN=ACADVL PE=1 SV=1 - [ACADV_HUMAN]	2.87E+07	7.56E+07	2.63E+00
P49755	Transmembrane emp24 domain-containing protein 10 OS=Homo sapiens GN=TMED10 PE=1 SV=2 - [TMEDA_HUMAN]	6.31E+07	1.18E+08	1.87E+00
P49756	RNA-binding protein 25 OS=Homo sapiens GN=RBM25 PE=1 SV=3 - [RBM25_HUMAN]	2.23E+07	3.20E+07	1.43E+00

P49915	GMP synthase [glutamine-hydrolyzing] OS=Homo sapiens GN=GMPS PE=1 SV=1 - [GUAA_HUMAN]	1.70E+07	2.19E+07	1.29E+00
P50395	Rab GDP dissociation inhibitor beta OS=Homo sapiens GN=GDI2 PE=1 SV=2 - [GDIB_HUMAN]	5.85E+07	1.22E+08	2.09E+00
P50416	Carnitine O-palmitoyltransferase 1, liver isoform OS=Homo sapiens GN=CPT1A PE=1 SV=2 - [CPT1A_HUMAN]	5.65E+06	1.41E+07	2.50E+00
P50454	Serpin H1 OS=Homo sapiens GN=SERPINH1 PE=1 SV=2 - [SERPH_HUMAN]	5.75E+07	8.78E+07	1.53E+00
P50502	Hsc70-interacting protein OS=Homo sapiens GN=ST13 PE=1 SV=2 - [F10A1_HUMAN]	8.52E+07	2.56E+08	3.00E+00
P51148	Ras-related protein Rab-5C OS=Homo sapiens GN=RAB5C PE=1 SV=2 - [RAB5C_HUMAN]	2.27E+07	0.00E+00	-1.00E+01
P51571	Translocon-associated protein subunit delta OS=Homo sapiens GN=SSR4 PE=1 SV=1 - [SSRD_HUMAN]	1.67E+06	2.15E+07	1.00E+01
P51572	B-cell receptor-associated protein 31 OS=Homo sapiens GN=BCAP31 PE=1 SV=3 - [BAP31_HUMAN]	1.47E+07	4.54E+07	3.09E+00
P51991	Heterogeneous nuclear ribonucleoprotein A3 OS=Homo sapiens GN=HNRNPA3 PE=1 SV=2 - [ROA3_HUMAN]	1.68E+08	1.14E+08	-1.48E+00
P52272-2	Isoform 2 of Heterogeneous nuclear ribonucleoprotein M OS=Homo sapiens GN=HNRNPM - [HNRPM_HUMAN]	7.93E+07	1.23E+08	1.55E+00
P52292	Importin subunit alpha-2 OS=Homo sapiens GN=KPNA2 PE=1 SV=1 - [IMA2_HUMAN]	1.92E+07	6.12E+07	3.19E+00

P52597	Heterogeneous nuclear ribonucleoprotein F OS=Homo sapiens GN=HNRNPF PE=1 SV=3 - [HNRPF_HUMAN]	9.48E+07	2.11E+08	2.22E+00
P52907	F-actin-capping protein subunit alpha-1 OS=Homo sapiens GN=CAPZA1 PE=1 SV=3 - [CAZA1_HUMAN]	3.64E+07	2.50E+08	6.88E+00
P53396-2	Isoform 2 of ATP-citrate synthase OS=Homo sapiens GN=ACLY - [ACLY_HUMAN]	1.13E+08	1.66E+08	1.47E+00
P53597	Succinyl-CoA ligase [ADP/GDP-forming] subunit alpha, mitochondrial OS=Homo sapiens GN=SUCLG1 PE=1 SV=4 - [SUCA_HUMAN]	6.23E+06	2.55E+06	-2.45E+00
P53618	Coatomer subunit beta OS=Homo sapiens GN=COPB1 PE=1 SV=3 - [COPB_HUMAN]	5.30E+06	9.06E+06	1.71E+00
P53621	Coatomer subunit alpha OS=Homo sapiens GN=COPA PE=1 SV=2 - [COPA_HUMAN]	2.49E+07	2.89E+07	1.16E+00
P53985	Monocarboxylate transporter 1 OS=Homo sapiens GN=SLC16A1 PE=1 SV=3 - [MOT1_HUMAN]	3.73E+07	6.53E+07	1.75E+00
P54136-2	Isoform Monomeric of Arginine--tRNA ligase, cytoplasmic OS=Homo sapiens GN=RARS - [SYRC_HUMAN]	2.06E+07	4.77E+07	2.31E+00
P54886-2	Isoform Short of Delta-1-pyrroline-5-carboxylate synthase OS=Homo sapiens GN=ALDH18A1 - [P5CS_HUMAN]	2.92E+07	7.17E+07	2.45E+00
P55060-3	Isoform 3 of Exportin-2 OS=Homo sapiens GN=CSE1L - [XPO2_HUMAN]	5.67E+07	1.43E+08	2.52E+00
P55072	Transitional endoplasmic reticulum ATPase OS=Homo sapiens GN=VCP PE=1 SV=4 - [TERA_HUMAN]	9.22E+07	2.73E+08	2.95E+00

P55809	Succinyl-CoA:3-ketoacid coenzyme A transferase 1, mitochondrial OS=Homo sapiens GN=OXCT1 PE=1 SV=1 - [SCOT1_HUMAN]	7.72E+07	1.61E+08	2.08E+00
P55884	Eukaryotic translation initiation factor 3 subunit B OS=Homo sapiens GN=EIF3B PE=1 SV=3 - [EIF3B_HUMAN]	2.25E+07	3.70E+07	1.65E+00
P56192	Methionine--tRNA ligase, cytoplasmic OS=Homo sapiens GN=MARS PE=1 SV=2 - [SYMC_HUMAN]	1.57E+07	6.18E+06	-2.54E+00
P58546	Myotrophin OS=Homo sapiens GN=MTPN PE=1 SV=2 - [MTPN_HUMAN]	1.13E+08	7.63E+07	-1.48E+00
P60174-1	Isoform 2 of Triosephosphate isomerase OS=Homo sapiens GN=TPI1 - [TPIS_HUMAN]	2.17E+08	6.27E+08	2.89E+00
P60468	Protein transport protein Sec61 subunit beta OS=Homo sapiens GN=SEC61B PE=1 SV=2 - [SC61B_HUMAN]	2.28E+07	7.79E+07	3.42E+00
P60842	Eukaryotic initiation factor 4A-I OS=Homo sapiens GN=EIF4A1 PE=1 SV=1 - [IF4A1_HUMAN]	1.51E+08	2.88E+08	1.91E+00
P60866	40S ribosomal protein S20 OS=Homo sapiens GN=RPS20 PE=1 SV=1 - [RS20_HUMAN]	3.39E+07	1.67E+08	4.92E+00
P60953	Cell division control protein 42 homolog OS=Homo sapiens GN=CDC42 PE=1 SV=2 - [CDC42_HUMAN]	2.51E+07	7.74E+07	3.09E+00
P60981-2	Isoform 2 of Destrin OS=Homo sapiens GN=DSTN - [DEST_HUMAN]	3.03E+07	4.63E+07	1.53E+00
P61006	Ras-related protein Rab-8A OS=Homo sapiens GN=RAB8A PE=1 SV=1 - [RAB8A_HUMAN]	8.85E+07	2.10E+08	2.37E+00

P61019	Ras-related protein Rab-2A OS=Homo sapiens GN=RAB2A PE=1 SV=1 - [RAB2A_HUMAN]	1.42E+07	5.03E+07	3.54E+00
P61026	Ras-related protein Rab-10 OS=Homo sapiens GN=RAB10 PE=1 SV=1 - [RAB10_HUMAN]	1.46E+08	2.22E+08	1.52E+00
P61073	C-X-C chemokine receptor type 4 OS=Homo sapiens GN=CXCR4 PE=1 SV=1 - [CXCR4_HUMAN]	1.96E+07	1.71E+07	-1.15E+00
P61081	NEDD8-conjugating enzyme Ubc12 OS=Homo sapiens GN=UBE2M PE=1 SV=1 - [UBC12_HUMAN]	3.52E+07	2.84E+07	-1.24E+00
P61158	Actin-related protein 3 OS=Homo sapiens GN=ACTR3 PE=1 SV=3 - [ARP3_HUMAN]	2.33E+07	2.96E+07	1.27E+00
P61221	ATP-binding cassette sub-family E member 1 OS=Homo sapiens GN=ABCE1 PE=1 SV=1 - [ABCE1_HUMAN]	2.67E+07	5.75E+07	2.15E+00
P61254	60S ribosomal protein L26 OS=Homo sapiens GN=RPL26 PE=1 SV=1 - [RL26_HUMAN]	9.56E+06	0.00E+00	-1.00E+01
P61289	Proteasome activator complex subunit 3 OS=Homo sapiens GN=PSME3 PE=1 SV=1 - [PSME3_HUMAN]	1.65E+07	5.53E+07	3.35E+00
P61586	Transforming protein RhoA OS=Homo sapiens GN=RHOA PE=1 SV=1 - [RHOA_HUMAN]	1.65E+07	3.72E+07	2.26E+00
P61604	10 kDa heat shock protein, mitochondrial OS=Homo sapiens GN=HSPE1 PE=1 SV=2 - [CH10_HUMAN]	2.55E+07	1.08E+08	4.22E+00
P61619-3	Isoform 3 of Protein transport protein Sec61 subunit alpha isoform 1 OS=Homo sapiens GN=SEC61A1 - [S61A1_HUMAN]	1.93E+07	0.00E+00	-1.00E+01

P61956-2	Isoform 2 of Small ubiquitin-related modifier 2 OS=Homo sapiens GN=SUMO2 - [SUMO2_HUMAN]	5.99E+07	1.48E+08	2.46E+00
P61978	Heterogeneous nuclear ribonucleoprotein K OS=Homo sapiens GN=HNRNPK PE=1 SV=1 - [HNRPK_HUMAN]	1.41E+08	5.40E+08	3.82E+00
P61981	14-3-3 protein gamma OS=Homo sapiens GN=YWHAG PE=1 SV=2 - [1433G_HUMAN]	1.44E+08	8.43E+08	5.84E+00
P62249	40S ribosomal protein S16 OS=Homo sapiens GN=RPS16 PE=1 SV=2 - [RS16_HUMAN]	7.82E+07	0.00E+00	-1.00E+01
P62258	14-3-3 protein epsilon OS=Homo sapiens GN=YWHAE PE=1 SV=1 - [1433E_HUMAN]	3.06E+08	9.08E+08	2.97E+00
P62263	40S ribosomal protein S14 OS=Homo sapiens GN=RPS14 PE=1 SV=3 - [RS14_HUMAN]	1.23E+08	5.21E+08	4.23E+00
P62280	40S ribosomal protein S11 OS=Homo sapiens GN=RPS11 PE=1 SV=3 - [RS11_HUMAN]	1.18E+08	8.24E+07	-1.43E+00
P62333	26S protease regulatory subunit 10B OS=Homo sapiens GN=PSMC6 PE=1 SV=1 - [PRS10_HUMAN]	4.11E+07	4.46E+07	1.09E+00
P62424	60S ribosomal protein L7a OS=Homo sapiens GN=RPL7A PE=1 SV=2 - [RL7A_HUMAN]	2.58E+08	5.42E+08	2.10E+00
P62701	40S ribosomal protein S4, X isoform OS=Homo sapiens GN=RPS4X PE=1 SV=2 - [RS4X_HUMAN]	1.02E+08	2.17E+08	2.12E+00
P62745	Rho-related GTP-binding protein RhoB OS=Homo sapiens GN=RHOB PE=1 SV=1 - [RHOB_HUMAN]	1.39E+07	1.25E+07	-1.11E+00
P62753	40S ribosomal protein S6 OS=Homo sapiens GN=RPS6 PE=1 SV=1 - [RS6_HUMAN]	8.80E+07	9.01E+07	1.02E+00

P62805	Histone H4 OS=Homo sapiens GN=HIST1H4A PE=1 SV=2 - [H4_HUMAN]	2.34E+08	2.46E+08	1.05E+00
P62826	GTP-binding nuclear protein Ran OS=Homo sapiens GN=RAN PE=1 SV=3 - [RAN_HUMAN]	4.99E+08	8.14E+08	1.63E+00
P62851	40S ribosomal protein S25 OS=Homo sapiens GN=RPS25 PE=1 SV=1 - [RS25_HUMAN]	8.93E+07	1.61E+08	1.80E+00
P62906	60S ribosomal protein L10a OS=Homo sapiens GN=RPL10A PE=1 SV=2 - [RL10A_HUMAN]	2.69E+08	4.53E+08	1.68E+00
P62913-2	Isoform 2 of 60S ribosomal protein L11 OS=Homo sapiens GN=RPL11 - [RL11_HUMAN]	1.32E+08	2.11E+08	1.60E+00
P62937	Peptidyl-prolyl cis-trans isomerase A OS=Homo sapiens GN=PPIA PE=1 SV=2 - [PPIA_HUMAN]	5.53E+08	6.80E+08	1.23E+00
P63104	14-3-3 protein zeta/delta OS=Homo sapiens GN=YWHAZ PE=1 SV=1 - [1433Z_HUMAN]	4.96E+08	1.03E+09	2.08E+00
P63151	Serine/threonine-protein phosphatase 2A 55 kDa regulatory subunit B alpha isoform OS=Homo sapiens GN=PPP2R2A PE=1 SV=1 - [2ABA_HUMAN]	1.25E+07	7.90E+06	-1.58E+00
P63167	Dynein light chain 1, cytoplasmic OS=Homo sapiens GN=DYNLL1 PE=1 SV=1 - [DYL1_HUMAN]	6.50E+07	8.68E+07	1.34E+00
P63244	Guanine nucleotide-binding protein subunit beta-2-like 1 OS=Homo sapiens GN=GNB2L1 PE=1 SV=3 - [GBLP_HUMAN]	1.09E+08	1.90E+08	1.74E+00
P63261	Actin, cytoplasmic 2 OS=Homo sapiens GN=ACTG1 PE=1 SV=1 - [ACTG_HUMAN]	8.31E+09	1.21E+10	1.45E+00

P67775-2	Isoform 2 of Serine/threonine-protein phosphatase 2A catalytic subunit alpha isoform OS=Homo sapiens GN=PPP2CA - [PP2AA_HUMAN]	2.11E+07	0.00E+00	-1.00E+01
P67809	Nuclease-sensitive element-binding protein 1 OS=Homo sapiens GN=YBX1 PE=1 SV=3 - [YBOX1_HUMAN]	1.53E+07	3.04E+07	2.00E+00
P67936	Tropomyosin alpha-4 chain OS=Homo sapiens GN=TPM4 PE=1 SV=3 - [TPM4_HUMAN]	3.94E+07	7.46E+07	1.89E+00
P68371	Tubulin beta-4B chain OS=Homo sapiens GN=TUBB4B PE=1 SV=1 - [TBB4B_HUMAN]	6.52E+08	1.50E+09	2.31E+00
P78310-2	Isoform 2 of Coxsackievirus and adenovirus receptor OS=Homo sapiens GN=CXADR - [CXAR_HUMAN]	1.24E+07	3.16E+07	2.55E+00
P78347-2	Isoform 2 of General transcription factor II-I OS=Homo sapiens GN=GTF2I - [GTF2I_HUMAN]	1.30E+07	3.33E+07	2.56E+00
P78371	T-complex protein 1 subunit beta OS=Homo sapiens GN=CCT2 PE=1 SV=4 - [TCPB_HUMAN]	7.85E+07	1.59E+08	2.03E+00
P82909	28S ribosomal protein S36, mitochondrial OS=Homo sapiens GN=MRPS36 PE=1 SV=2 - [RT36_HUMAN]	1.09E+08	0.00E+00	-1.00E+01
P83881	60S ribosomal protein L36a OS=Homo sapiens GN=RPL36A PE=1 SV=2 - [RL36A_HUMAN]	3.26E+07	0.00E+00	-1.00E+01
P84090	Enhancer of rudimentary homolog OS=Homo sapiens GN=ERH PE=1 SV=1 - [ERH_HUMAN]	4.50E+07	9.03E+07	2.01E+00
P98082-2	Isoform 2 of Disabled homolog 2 OS=Homo sapiens GN=DAB2 - [DAB2_HUMAN]	1.85E+07	2.77E+07	1.50E+00

Q00341	Vigilin OS=Homo sapiens GN=HDLBP PE=1 SV=2 - [VIGLN_HUMAN]	2.97E+07	2.69E+07	-1.10E+00
Q00610-2	Isoform 2 of Clathrin heavy chain 1 OS=Homo sapiens GN=CLTC - [CLH1_HUMAN]	1.21E+08	3.37E+08	2.79E+00
Q00688	Peptidyl-prolyl cis-trans isomerase FKBP3 OS=Homo sapiens GN=FKBP3 PE=1 SV=1 - [FKBP3_HUMAN]	0.00E+00	3.97E+07	1.00E+01
Q00765	Receptor expression-enhancing protein 5 OS=Homo sapiens GN=REEP5 PE=1 SV=3 - [REEP5_HUMAN]	3.39E+07	4.34E+07	1.28E+00
Q00839	Heterogeneous nuclear ribonucleoprotein U OS=Homo sapiens GN=HNRNPU PE=1 SV=6 - [HNRPU_HUMAN]	3.48E+08	4.93E+08	1.42E+00
Q01081	Splicing factor U2AF 35 kDa subunit OS=Homo sapiens GN=U2AF1 PE=1 SV=3 - [U2AF1_HUMAN]	2.23E+06	3.98E+07	1.00E+01
Q01082	Spectrin beta chain, non-erythrocytic 1 OS=Homo sapiens GN=SPTBN1 PE=1 SV=2 - [SPTB2_HUMAN]	1.19E+07	3.26E+07	2.75E+00
Q01105-2	Isoform 2 of Protein SET OS=Homo sapiens GN=SET - [SET_HUMAN]	1.20E+07	7.82E+07	6.53E+00
Q01518	Adenylyl cyclase-associated protein 1 OS=Homo sapiens GN=CAP1 PE=1 SV=5 - [CAP1_HUMAN]	7.49E+07	1.46E+08	1.95E+00
Q01628	Interferon-induced transmembrane protein 3 OS=Homo sapiens GN=IFITM3 PE=1 SV=2 - [IFM3_HUMAN]	8.91E+07	1.00E+09	1.00E+01
Q01650	Large neutral amino acids transporter small subunit 1 OS=Homo sapiens GN=SLC7A5 PE=1 SV=2 - [LAT1_HUMAN]	3.36E+08	6.12E+08	1.82E+00

Q01813	6-phosphofructokinase type C OS=Homo sapiens GN=PFKP PE=1 SV=2 - [K6PP_HUMAN]	7.94E+07	1.10E+08	1.39E+00
Q01995	Transgelin OS=Homo sapiens GN=TAGLN PE=1 SV=4 - [TAGL_HUMAN]	6.67E+07	1.55E+08	2.32E+00
Q02790	Peptidyl-prolyl cis-trans isomerase FKBP4 OS=Homo sapiens GN=FKBP4 PE=1 SV=3 - [FKBP4_HUMAN]	4.71E+07	1.77E+08	3.76E+00
Q03135	Caveolin-1 OS=Homo sapiens GN=CAV1 PE=1 SV=4 - [CAV1_HUMAN]	5.96E+07	6.38E+07	1.07E+00
Q04446	1,4-alpha-glucan-branching enzyme OS=Homo sapiens GN=GBE1 PE=1 SV=3 - [GLGB_HUMAN]	5.15E+06	2.44E+07	4.73E+00
Q04637-6	Isoform E of Eukaryotic translation initiation factor 4 gamma 1 OS=Homo sapiens GN=EIF4G1 - [IF4G1_HUMAN]	3.68E+07	5.90E+07	1.60E+00
Q04695	Keratin, type I cytoskeletal 17 OS=Homo sapiens GN=KRT17 PE=1 SV=2 - [K1C17_HUMAN]	3.18E+08	8.17E+08	2.57E+00
Q05682-5	Isoform 5 of Caldesmon OS=Homo sapiens GN=CALD1 - [CALD1_HUMAN]	2.08E+07	9.42E+07	4.53E+00
Q06830	Peroxiredoxin-1 OS=Homo sapiens GN=PRDX1 PE=1 SV=1 - [PRDX1_HUMAN]	3.15E+08	6.10E+08	1.94E+00
Q07021	Complement component 1 Q subcomponent-binding protein, mitochondrial OS=Homo sapiens GN=C1QBP PE=1 SV=1 - [C1QBP_HUMAN]	5.33E+07	1.22E+08	2.29E+00
Q07065	Cytoskeleton-associated protein 4 OS=Homo sapiens GN=CKAP4 PE=1 SV=2 - [CKAP4_HUMAN]	1.70E+08	2.59E+08	1.52E+00

Q07617	Sperm-associated antigen 1 OS=Homo sapiens GN=SPAG1 PE=1 SV=3 - [SPAG1_HUMAN]	3.44E+07	0.00E+00	-1.00E+01
Q07666-3	Isoform 3 of KH domain-containing, RNA-binding, signal transduction-associated protein 1 OS=Homo sapiens GN=KHDRBS1 - [KHDR1_HUMAN]	3.68E+07	4.29E+07	1.17E+00
Q07955	Serine/arginine-rich splicing factor 1 OS=Homo sapiens GN=SRSF1 PE=1 SV=2 - [SRSF1_HUMAN]	1.73E+07	3.75E+07	2.17E+00
Q09028-3	Isoform 3 of Histone-binding protein RBBP4 OS=Homo sapiens GN=RBBP4 - [RBBP4_HUMAN]	3.87E+07	1.10E+08	2.83E+00
Q09161	Nuclear cap-binding protein subunit 1 OS=Homo sapiens GN=NCBP1 PE=1 SV=1 - [NCBP1_HUMAN]	1.85E+07	0.00E+00	-1.00E+01
Q09666	Neuroblast differentiation-associated protein AHNAK OS=Homo sapiens GN=AHNAK PE=1 SV=2 - [AHNK_HUMAN]	0.00E+00	5.80E+07	1.00E+01
Q10471	Polypeptide N-acetylgalactosaminyltransferase 2 OS=Homo sapiens GN=GALNT2 PE=1 SV=1 - [GALT2_HUMAN]	1.11E+08	2.56E+08	2.31E+00
Q10589	Bone marrow stromal antigen 2 OS=Homo sapiens GN=BST2 PE=1 SV=1 - [BST2_HUMAN]	4.39E+08	2.11E+09	4.81E+00
Q12905	Interleukin enhancer-binding factor 2 OS=Homo sapiens GN=ILF2 PE=1 SV=2 - [ILF2_HUMAN]	3.86E+07	4.77E+07	1.24E+00
Q12906-5	Isoform 5 of Interleukin enhancer-binding factor 3 OS=Homo sapiens GN=ILF3 - [ILF3_HUMAN]	8.55E+07	1.26E+08	1.47E+00

Q13085	Acetyl-CoA carboxylase 1 OS=Homo sapiens GN=ACACA PE=1 SV=2 - [ACACA_HUMAN]	4.63E+08	8.36E+08	1.81E+00
Q13126-4	Isoform 4 of S-methyl-5'-thioadenosine phosphorylase OS=Homo sapiens GN=MTAP - [MTAP_HUMAN]	1.56E+07	3.45E+07	2.22E+00
Q13131	5'-AMP-activated protein kinase catalytic subunit alpha-1 OS=Homo sapiens GN=PRKAA1 PE=1 SV=4 - [AAPK1_HUMAN]	3.54E+07	0.00E+00	-1.00E+01
Q13151	Heterogeneous nuclear ribonucleoprotein A0 OS=Homo sapiens GN=HNRNPA0 PE=1 SV=1 - [ROA0_HUMAN]	2.01E+08	9.66E+07	-2.09E+00
Q13155	Aminoacyl tRNA synthase complex-interacting multifunctional protein 2 OS=Homo sapiens GN=AIMP2 PE=1 SV=2 - [AIMP2_HUMAN]	2.80E+07	2.85E+07	1.02E+00
Q13162	Peroxiredoxin-4 OS=Homo sapiens GN=PRDX4 PE=1 SV=1 - [PRDX4_HUMAN]	2.03E+07	5.47E+07	2.70E+00
Q13185	Chromobox protein homolog 3 OS=Homo sapiens GN=CBX3 PE=1 SV=4 - [CBX3_HUMAN]	3.81E+07	6.54E+07	1.72E+00
Q13200	26S proteasome non-ATPase regulatory subunit 2 OS=Homo sapiens GN=PSMD2 PE=1 SV=3 - [PSMD2_HUMAN]	4.01E+07	4.73E+07	1.18E+00
Q13247-3	Isoform SRP55-3 of Serine/arginine-rich splicing factor 6 OS=Homo sapiens GN=SRSF6 - [SRSF6_HUMAN]	3.09E+07	4.56E+07	1.48E+00
Q13263	Transcription intermediary factor 1-beta OS=Homo sapiens GN=TRIM28 PE=1 SV=5 - [TIF1B_HUMAN]	5.99E+07	1.03E+08	1.71E+00

Q13283	Ras GTPase-activating protein-binding protein 1 OS=Homo sapiens GN=G3BP1 PE=1 SV=1 - [G3BP1_HUMAN]	3.40E+07	1.08E+08	3.19E+00
Q13347	Eukaryotic translation initiation factor 3 subunit I OS=Homo sapiens GN=EIF3I PE=1 SV=1 - [EIF3I_HUMAN]	0.00E+00	4.71E+07	1.00E+01
Q13409-6	Isoform 2F of Cytoplasmic dynein 1 intermediate chain 2 OS=Homo sapiens GN=DYNC1I2 - [DC1I2_HUMAN]	1.07E+07	2.22E+07	2.08E+00
Q13423	NAD(P) transhydrogenase, mitochondrial OS=Homo sapiens GN=NNT PE=1 SV=3 - [NNTM_HUMAN]	2.21E+07	5.80E+07	2.62E+00
Q13428-2	Isoform 2 of Treacle protein OS=Homo sapiens GN=TCOF1 - [TCOF_HUMAN]	1.09E+07	1.96E+07	1.81E+00
Q13501-2	Isoform 2 of Sequestosome-1 OS=Homo sapiens GN=SQSTM1 - [SQSTM_HUMAN]	1.77E+07	1.78E+08	1.00E+01
Q13619	Cullin-4A OS=Homo sapiens GN=CUL4A PE=1 SV=3 - [CUL4A_HUMAN]	2.00E+07	2.51E+07	1.25E+00
Q13813-3	Isoform 3 of Spectrin alpha chain, non-erythrocytic 1 OS=Homo sapiens GN=SPTAN1 - [SPTN1_HUMAN]	2.34E+07	6.63E+07	2.84E+00
Q13838	Spliceosome RNA helicase DDX39B OS=Homo sapiens GN=DDX39B PE=1 SV=1 - [DX39B_HUMAN]	1.13E+08	1.96E+08	1.74E+00
Q14008-2	Isoform 2 of Cytoskeleton-associated protein 5 OS=Homo sapiens GN=CKAP5 - [CKAP5_HUMAN]	3.45E+06	8.08E+06	2.35E+00

Q14103-3	Isoform 3 of Heterogeneous nuclear ribonucleoprotein D0 OS=Homo sapiens GN=HNRNPD - [HNRPD_HUMAN]	1.51E+08	2.76E+08	1.83E+00
Q14126	Desmoglein-2 OS=Homo sapiens GN=DSG2 PE=1 SV=2 - [DSG2_HUMAN]	1.38E+08	5.32E+07	-2.60E+00
Q14151	Scaffold attachment factor B2 OS=Homo sapiens GN=SAFB2 PE=1 SV=1 - [SAFB2_HUMAN]	0.00E+00	5.23E+06	1.00E+01
Q14204	Cytoplasmic dynein 1 heavy chain 1 OS=Homo sapiens GN=DYNC1H1 PE=1 SV=5 - [DYHC1_HUMAN]	4.28E+06	1.04E+07	2.42E+00
Q14244-5	Isoform 5 of Ensconsin OS=Homo sapiens GN=MAP7 - [MAP7_HUMAN]	0.00E+00	4.45E+06	1.00E+01
Q14247-3	Isoform 3 of Src substrate cortactin OS=Homo sapiens GN=CTTN - [SRC8_HUMAN]	4.31E+07	1.04E+08	2.42E+00
Q14258	E3 ubiquitin/ISG15 ligase TRIM25 OS=Homo sapiens GN=TRIM25 PE=1 SV=2 - [TRI25_HUMAN]	0.00E+00	1.07E+07	1.00E+01
Q14566	DNA replication licensing factor MCM6 OS=Homo sapiens GN=MCM6 PE=1 SV=1 - [MCM6_HUMAN]	2.83E+07	7.11E+07	2.51E+00
Q14974	Importin subunit beta-1 OS=Homo sapiens GN=KPNB1 PE=1 SV=2 - [IMB1_HUMAN]	5.99E+07	2.68E+08	4.47E+00
Q14978	Nucleolar and coiled-body phosphoprotein 1 OS=Homo sapiens GN=NOLC1 PE=1 SV=2 - [NOLC1_HUMAN]	2.18E+06	2.36E+06	1.09E+00
Q14980-4	Isoform Numa-s of Nuclear mitotic apparatus protein 1 OS=Homo sapiens GN=NUMA1 - [NUMA1_HUMAN]	0.00E+00	6.46E+06	1.00E+01
Q15005	Signal peptidase complex subunit 2 OS=Homo sapiens GN=SPCS2 PE=1 SV=3 -	1.64E+07	3.40E+07	2.08E+00

	[SPCS2_HUMAN]			
Q15029-2	Isoform 2 of 116 kDa U5 small nuclear ribonucleoprotein component OS=Homo sapiens GN=EFTUD2 - [U5S1_HUMAN]	1.65E+07	5.61E+07	3.41E+00
Q15043-2	Isoform 2 of Zinc transporter ZIP14 OS=Homo sapiens GN=SLC39A14 - [S39AE_HUMAN]	8.11E+07	4.13E+07	-1.97E+00
Q15050	Ribosome biogenesis regulatory protein homolog OS=Homo sapiens GN=RRS1 PE=1 SV=2 - [RRS1_HUMAN]	5.65E+06	2.10E+07	3.72E+00
Q15056-2	Isoform Short of Eukaryotic translation initiation factor 4H OS=Homo sapiens GN=EIF4H - [IF4H_HUMAN]	5.00E+07	1.17E+08	2.35E+00
Q15233	Non-POU domain-containing octamer-binding protein OS=Homo sapiens GN=NONO PE=1 SV=4 - [NONO_HUMAN]	6.63E+07	2.35E+08	3.55E+00
Q15365	Poly(rC)-binding protein 1 OS=Homo sapiens GN=PCBP1 PE=1 SV=2 - [PCBP1_HUMAN]	7.68E+07	1.92E+08	2.50E+00
Q15393	Splicing factor 3B subunit 3 OS=Homo sapiens GN=SF3B3 PE=1 SV=4 - [SF3B3_HUMAN]	1.33E+07	9.43E+07	7.10E+00
Q15459	Splicing factor 3A subunit 1 OS=Homo sapiens GN=SF3A1 PE=1 SV=1 - [SF3A1_HUMAN]	1.16E+07	1.52E+07	1.31E+00
Q15645	Pachytene checkpoint protein 2 homolog OS=Homo sapiens GN=TRIP13 PE=1 SV=2 - [PCH2_HUMAN]	2.23E+07	3.42E+07	1.53E+00
Q15758	Neutral amino acid transporter B(0) OS=Homo sapiens GN=SLC1A5 PE=1 SV=2 - [AAAT_HUMAN]	8.36E+07	6.45E+08	7.72E+00

Q15836	Vesicle-associated membrane protein 3 OS=Homo sapiens GN=VAMP3 PE=1 SV=3 - [VAMP3_HUMAN]	4.25E+07	2.50E+08	5.89E+00
Q15942	Zyxin OS=Homo sapiens GN=ZYX PE=1 SV=1 - [ZYX_HUMAN]	2.22E+06	6.60E+05	-3.37E+00
Q16401	26S proteasome non-ATPase regulatory subunit 5 OS=Homo sapiens GN=PSMD5 PE=1 SV=3 - [PSMD5_HUMAN]	9.08E+06	1.57E+07	1.73E+00
Q16629-3	Isoform 3 of Serine/arginine-rich splicing factor 7 OS=Homo sapiens GN=SRSF7 - [SRSF7_HUMAN]	0.00E+00	6.66E+07	1.00E+01
Q16719	Kynureninase OS=Homo sapiens GN=KYNU PE=1 SV=1 - [KYNU_HUMAN]	3.53E+07	7.31E+07	2.07E+00
Q16836	Hydroxyacyl-coenzyme A dehydrogenase, mitochondrial OS=Homo sapiens GN=HADH PE=1 SV=3 - [HCDH_HUMAN]	4.91E+07	2.74E+07	-1.79E+00
Q16850-2	Isoform 2 of Lanosterol 14-alpha demethylase OS=Homo sapiens GN=CYP51A1 - [CP51A_HUMAN]	4.03E+06	1.60E+07	3.97E+00
Q16851-2	Isoform 2 of UTP--glucose-1-phosphate uridylyltransferase OS=Homo sapiens GN=UGP2 - [UGPA_HUMAN]	8.07E+06	1.35E+07	1.68E+00
Q32P28	Prolyl 3-hydroxylase 1 OS=Homo sapiens GN=LEPRE1 PE=1 SV=2 - [P3H1_HUMAN]	0.00E+00	7.65E+06	1.00E+01
Q3B7A4	60S acidic ribosomal protein P0 OS=Homo sapiens GN=RPLP0 PE=2 SV=1 - [Q3B7A4_HUMAN]	3.21E+08	5.83E+08	1.81E+00
Q3ZCQ8	Mitochondrial import inner membrane translocase subunit TIM50 OS=Homo sapiens GN=TIMM50 PE=1 SV=2 - [TIM50_HUMAN]	1.19E+07	8.56E+06	-1.39E+00

Q5H907	Melanoma antigen family D, 2 OS=Homo sapiens GN=MAGED2 PE=2 SV=1 - [Q5H907_HUMAN]	0.00E+00	1.98E+07	1.00E+01
Q5HY57	Emerin OS=Homo sapiens GN=EMD PE=2 SV=1 - [Q5HY57_HUMAN]	8.63E+06	1.12E+07	1.30E+00
Q5JTH9-2	Isoform 2 of RRP12-like protein OS=Homo sapiens GN=RRP12 - [RRP12_HUMAN]	1.01E+07	8.78E+06	-1.14E+00
Q5M775-4	Isoform 4 of Cytospin-B OS=Homo sapiens GN=SPECC1 - [CYTSB_HUMAN]	1.10E+08	0.00E+00	-1.00E+01
Q5QPM0	RNA binding protein, autoantigenic (HnRNP-associated with lethal yellow homolog (Mouse)) (Fragment) OS=Homo sapiens GN=RALY PE=2 SV=1 - [Q5QPM0_HUMAN]	0.00E+00	1.44E+07	1.00E+01
Q5QPQ0	Acyl-protein thioesterase 2 OS=Homo sapiens GN=LYPLA2 PE=2 SV=1 - [Q5QPQ0_HUMAN]	2.23E+07	4.73E+07	2.12E+00
Q5T6Z8	Transmembrane protein 59 OS=Homo sapiens GN=TMEM59 PE=2 SV=1 - [Q5T6Z8_HUMAN]	8.09E+07	1.61E+08	1.99E+00
Q5TA02	Glutathione S-transferase omega 1 (Fragment) OS=Homo sapiens GN=GSTO1 PE=2 SV=1 - [Q5TA02_HUMAN]	1.46E+07	0.00E+00	-1.00E+01
Q5TCU6	Talin 1 OS=Homo sapiens GN=TLN1 PE=2 SV=1 - [Q5TCU6_HUMAN]	3.83E+07	7.38E+07	1.93E+00
Q5TEE2	Histone deacetylase 1 (Fragment) OS=Homo sapiens GN=HDAC1 PE=2 SV=1 - [Q5TEE2_HUMAN]	3.30E+07	6.81E+07	2.07E+00
Q5VT66-3	Isoform 3 of MOSC domain-containing protein 1, mitochondrial OS=Homo sapiens GN=MARC1 - [MOSC1_HUMAN]	2.08E+07	0.00E+00	-1.00E+01

Q68CR9	Aspartate--tRNA ligase, cytoplasmic OS=Homo sapiens GN=DKFZp781B11202 PE=2 SV=1 - [Q68CR9_HUMAN]	3.18E+07	5.85E+07	1.84E+00
Q68DB1	Metastasis-associated protein MTA2 OS=Homo sapiens GN=DKFZp686F2281 PE=2 SV=1 - [Q68DB1_HUMAN]	2.40E+07	3.73E+07	1.55E+00
Q6NTF9	Rhomboid domain-containing protein 2 OS=Homo sapiens GN=RHBDD2 PE=2 SV=2 - [RHBD2_HUMAN]	1.07E+07	4.17E+07	3.91E+00
Q6P2Q9	Pre-mRNA-processing-splicing factor 8 OS=Homo sapiens GN=PRPF8 PE=1 SV=2 - [PRP8_HUMAN]	7.42E+06	1.46E+07	1.97E+00
Q6PKG0	La-related protein 1 OS=Homo sapiens GN=LARP1 PE=1 SV=2 - [LARP1_HUMAN]	9.59E+06	1.58E+07	1.65E+00
Q6YN16-2	Isoform 2 of Hydroxysteroid dehydrogenase-like protein 2 OS=Homo sapiens GN=HSDL2 - [HSDL2_HUMAN]	1.55E+07	2.63E+07	1.70E+00
Q7KZF4	Staphylococcal nuclease domain-containing protein 1 OS=Homo sapiens GN=SND1 PE=1 SV=1 - [SND1_HUMAN]	3.95E+07	9.75E+07	2.47E+00
Q7L1Q6	Basic leucine zipper and W2 domain-containing protein 1 OS=Homo sapiens GN=BZW1 PE=1 SV=1 - [BZW1_HUMAN]	4.44E+07	9.49E+07	2.14E+00
Q7L2E3-3	Isoform 3 of Putative ATP-dependent RNA helicase DHX30 OS=Homo sapiens GN=DHX30 - [DHX30_HUMAN]	1.10E+07	2.84E+07	2.57E+00
Q7Z451	AP-2 complex subunit beta OS=Homo sapiens GN=AP2B1 PE=2 SV=1 - [Q7Z451_HUMAN]	1.03E+07	4.58E+07	4.46E+00

Q86UE4	Protein LYRIC OS=Homo sapiens GN=MTDH PE=1 SV=2 - [LYRIC_HUMAN]	4.16E+07	6.27E+07	1.51E+00
Q86VP6	Cullin-associated NEDD8-dissociated protein 1 OS=Homo sapiens GN=CAND1 PE=1 SV=2 - [CAND1_HUMAN]	2.52E+07	8.53E+07	3.39E+00
Q86XP3-2	Isoform 2 of ATP-dependent RNA helicase DDX42 OS=Homo sapiens GN=DDX42 - [DDX42_HUMAN]	1.41E+07	2.35E+07	1.67E+00
Q86YZ3	Hornerin OS=Homo sapiens GN=HRNR PE=1 SV=2 - [HORN_HUMAN]	3.26E+06	4.01E+07	1.00E+01
Q8IVT2	Uncharacterized protein C19orf21 OS=Homo sapiens GN=C19orf21 PE=1 SV=1 - [CS021_HUMAN]	5.66E+06	9.38E+06	1.66E+00
Q8IWA5-3	Isoform 3 of Choline transporter-like protein 2 OS=Homo sapiens GN=SLC44A2 - [CTL2_HUMAN]	1.02E+07	1.98E+07	1.95E+00
Q8N726-2	Isoform 6 of Cyclin-dependent kinase inhibitor 2A, isoform 4 OS=Homo sapiens GN=CDKN2A - [CD2A2_HUMAN]	2.80E+07	3.37E+07	1.20E+00
Q8NC51-4	Isoform 4 of Plasminogen activator inhibitor 1 RNA-binding protein OS=Homo sapiens GN=SERBP1 - [PAIRB_HUMAN]	1.19E+07	6.52E+07	5.46E+00
Q8NCW5-2	Isoform 2 of NAD(P)H-hydrate epimerase OS=Homo sapiens GN=APOA1BP - [NNRE_HUMAN]	2.03E+07	5.15E+07	2.54E+00
Q8NF37	Lysophosphatidylcholine acyltransferase 1 OS=Homo sapiens GN=LPCAT1 PE=1 SV=2 - [PCAT1_HUMAN]	9.10E+06	2.51E+07	2.76E+00
Q8NFJ5	Retinoic acid-induced protein 3 OS=Homo sapiens GN=GPRC5A PE=1 SV=2 - [RAI3_HUMAN]	6.07E+07	2.25E+08	3.70E+00

Q8NI36	WD repeat-containing protein 36 OS=Homo sapiens GN=WDR36 PE=1 SV=1 - [WDR36_HUMAN]	5.24E+06	6.80E+06	1.30E+00
Q8TCJ2	Dolichyl-diphosphooligosaccharide--protein glycosyltransferase subunit STT3B OS=Homo sapiens GN=STT3B PE=1 SV=1 - [STT3B_HUMAN]	1.73E+07	1.85E+07	1.07E+00
Q8TCT9-5	Isoform 5 of Minor histocompatibility antigen H13 OS=Homo sapiens GN=HM13 - [HM13_HUMAN]	2.80E+07	0.00E+00	-1.00E+01
Q8TDN6	Ribosome biogenesis protein BRX1 homolog OS=Homo sapiens GN=BRIX1 PE=1 SV=2 - [BRX1_HUMAN]	1.84E+07	2.40E+07	1.31E+00
Q8WTV0-4	Isoform 4 of Scavenger receptor class B member 1 OS=Homo sapiens GN=SCARB1 - [SCRB1_HUMAN]	4.59E+07	0.00E+00	-1.00E+01
Q8WU90	Zinc finger CCCH domain-containing protein 15 OS=Homo sapiens GN=ZC3H15 PE=1 SV=1 - [ZC3HF_HUMAN]	2.85E+06	0.00E+00	-1.00E+01
Q8WUM4	Programmed cell death 6-interacting protein OS=Homo sapiens GN=PDCD6IP PE=1 SV=1 - [PDC6I_HUMAN]	2.39E+07	3.84E+07	1.60E+00
Q8WWM7-6	Isoform 6 of Ataxin-2-like protein OS=Homo sapiens GN=ATXN2L - [ATX2L_HUMAN]	4.11E+06	1.44E+07	3.50E+00
Q92499	ATP-dependent RNA helicase DDX1 OS=Homo sapiens GN=DDX1 PE=1 SV=2 - [DDX1_HUMAN]	2.52E+06	2.06E+07	8.16E+00
Q92598-2	Isoform Beta of Heat shock protein 105 kDa OS=Homo sapiens GN=HSPH1 - [HS105_HUMAN]	2.04E+07	3.88E+07	1.90E+00

Q92616	Translational activator GCN1 OS=Homo sapiens GN=GCN1L1 PE=1 SV=6 - [GCN1L_HUMAN]	2.54E+06	1.19E+07	4.70E+00
Q92621	Nuclear pore complex protein Nup205 OS=Homo sapiens GN=NUP205 PE=1 SV=3 - [NU205_HUMAN]	0.00E+00	1.73E+07	1.00E+01
Q92688-2	Isoform 2 of Acidic leucine-rich nuclear phosphoprotein 32 family member B OS=Homo sapiens GN=ANP32B - [AN32B_HUMAN]	2.69E+07	0.00E+00	-1.00E+01
Q92841-1	Isoform 2 of Probable ATP-dependent RNA helicase DDX17 OS=Homo sapiens GN=DDX17 - [DDX17_HUMAN]	1.24E+08	2.30E+08	1.86E+00
Q92922	SWI/SNF complex subunit SMARCC1 OS=Homo sapiens GN=SMARCC1 PE=1 SV=3 - [SMRC1_HUMAN]	5.06E+06	4.88E+06	-1.04E+00
Q92945	Far upstream element-binding protein 2 OS=Homo sapiens GN=KHSRP PE=1 SV=4 - [FUBP2_HUMAN]	4.12E+07	9.53E+07	2.31E+00
Q92973-2	Isoform 2 of Transportin-1 OS=Homo sapiens GN=TNPO1 - [TNPO1_HUMAN]	9.19E+07	1.33E+08	1.45E+00
Q93086-2	Isoform 3 of P2X purinoceptor 5 OS=Homo sapiens GN=P2RX5 - [P2RX5_HUMAN]	2.16E+07	0.00E+00	-1.00E+01
Q96A33	Coiled-coil domain-containing protein 47 OS=Homo sapiens GN=CCDC47 PE=1 SV=1 - [CCD47_HUMAN]	1.35E+07	1.02E+07	-1.32E+00
Q96AC1-2	Isoform 2 of Fermitin family homolog 2 OS=Homo sapiens GN=FERMT2 - [FERM2_HUMAN]	9.54E+06	3.97E+07	4.16E+00
Q96AE4	Far upstream element-binding protein 1 OS=Homo sapiens GN=FUBP1 PE=1 SV=3 - [FUBP1_HUMAN]	9.99E+07	1.41E+08	1.41E+00

Q96AG4	Leucine-rich repeat-containing protein 59 OS=Homo sapiens GN=LRRC59 PE=1 SV=1 - [LRC59_HUMAN]	4.43E+07	6.36E+07	1.44E+00
Q96C36	Pyrroline-5-carboxylate reductase 2 OS=Homo sapiens GN=PYCR2 PE=1 SV=1 - [P5CR2_HUMAN]	0.00E+00	2.77E+07	1.00E+01
Q96CX2	BTB/POZ domain-containing protein KCTD12 OS=Homo sapiens GN=KCTD12 PE=1 SV=1 - [KCD12_HUMAN]	3.84E+07	1.07E+08	2.79E+00
Q96DX4	RING finger and SPRY domain-containing protein 1 OS=Homo sapiens GN=RSPRY1 PE=2 SV=1 - [RSPRY_HUMAN]	1.18E+07	0.00E+00	-1.00E+01
Q96I24	Far upstream element-binding protein 3 OS=Homo sapiens GN=FUBP3 PE=1 SV=2 - [FUBP3_HUMAN]	2.73E+07	1.89E+07	-1.44E+00
Q96KK5	Histone H2A type 1-H OS=Homo sapiens GN=HIST1H2AH PE=1 SV=3 - [H2A1H_HUMAN]	1.56E+08	4.73E+08	3.03E+00
Q96P70	Importin-9 OS=Homo sapiens GN=IPO9 PE=1 SV=3 - [IPO9_HUMAN]	2.79E+07	1.89E+07	-1.48E+00
Q96QD8	Sodium-coupled neutral amino acid transporter 2 OS=Homo sapiens GN=SLC38A2 PE=1 SV=2 - [S38A2_HUMAN]	9.52E+07	1.94E+08	2.04E+00
Q96QK1	Vacuolar protein sorting-associated protein 35 OS=Homo sapiens GN=VPS35 PE=1 SV=2 - [VPS35_HUMAN]	1.46E+07	4.64E+07	3.17E+00
Q96RQ3	Methylcrotonoyl-CoA carboxylase subunit alpha, mitochondrial OS=Homo sapiens GN=MCCC1 PE=1 SV=3 - [MCCA_HUMAN]	2.05E+08	5.75E+08	2.81E+00

Q96S97	Myeloid-associated differentiation marker OS=Homo sapiens GN=MYADM PE=1 SV=2 - [MYADM_HUMAN]	8.54E+07	8.05E+07	-1.06E+00
Q96TA1-2	Isoform 2 of Niban-like protein 1 OS=Homo sapiens GN=FAM129B - [NIBL1_HUMAN]	8.83E+08	1.98E+09	2.25E+00
Q99436	Proteasome subunit beta type-7 OS=Homo sapiens GN=PSMB7 PE=1 SV=1 - [PSB7_HUMAN]	1.47E+07	2.61E+07	1.78E+00
Q99460-2	Isoform 2 of 26S proteasome non-ATPase regulatory subunit 1 OS=Homo sapiens GN=PSMD1 - [PSMD1_HUMAN]	0.00E+00	4.23E+07	1.00E+01
Q99471-2	Isoform 2 of Prefoldin subunit 5 OS=Homo sapiens GN=PFDN5 - [PFD5_HUMAN]	6.56E+06	1.13E+07	1.72E+00
Q99497	Protein DJ-1 OS=Homo sapiens GN=PARK7 PE=1 SV=2 - [PARK7_HUMAN]	4.43E+07	1.67E+08	3.77E+00
Q99615-2	Isoform 2 of DnaJ homolog subfamily C member 7 OS=Homo sapiens GN=DNAJC7 - [DNJC7_HUMAN]	3.16E+06	8.40E+06	2.66E+00
Q99714	3-hydroxyacyl-CoA dehydrogenase type-2 OS=Homo sapiens GN=HSD17B10 PE=1 SV=3 - [HCD2_HUMAN]	4.56E+07	1.21E+08	2.66E+00
Q99733	Nucleosome assembly protein 1-like 4 OS=Homo sapiens GN=NAP1L4 PE=1 SV=1 - [NP1L4_HUMAN]	9.97E+07	1.37E+08	1.37E+00
Q99798	Aconitate hydratase, mitochondrial OS=Homo sapiens GN=ACO2 PE=1 SV=2 - [ACON_HUMAN]	2.82E+07	4.01E+07	1.42E+00
Q99805	Transmembrane 9 superfamily member 2 OS=Homo sapiens GN=TM9SF2 PE=1 SV=1 - [TM9S2_HUMAN]	1.59E+07	3.96E+07	2.50E+00

Q99832	T-complex protein 1 subunit eta OS=Homo sapiens GN=CCT7 PE=1 SV=2 - [TCPH_HUMAN]	9.90E+07	1.80E+08	1.82E+00
Q9BQ67	Glutamate-rich WD repeat-containing protein 1 OS=Homo sapiens GN=GRWD1 PE=1 SV=1 - [GRWD1_HUMAN]	0.00E+00	3.79E+07	1.00E+01
Q9BSJ8	Extended synaptotagmin-1 OS=Homo sapiens GN=ESYT1 PE=1 SV=1 - [ESYT1_HUMAN]	1.63E+07	3.66E+07	2.25E+00
Q9BT67	NEDD4 family-interacting protein 1 OS=Homo sapiens GN=NDFIP1 PE=1 SV=1 - [NFIP1_HUMAN]	1.58E+07	2.97E+07	1.89E+00
Q9BUF5	Tubulin beta-6 chain OS=Homo sapiens GN=TUBB6 PE=1 SV=1 - [TBB6_HUMAN]	5.00E+08	8.41E+08	1.68E+00
Q9BUJ2-3	Isoform 3 of Heterogeneous nuclear ribonucleoprotein U-like protein 1 OS=Homo sapiens GN=HNRNPUL1 - [HNRL1_HUMAN]	1.49E+07	1.20E+07	-1.25E+00
Q9BVP2-2	Isoform 2 of Guanine nucleotide-binding protein-like 3 OS=Homo sapiens GN=GNL3 - [GNL3_HUMAN]	1.56E+07	0.00E+00	-1.00E+01
Q9BWH2	FUN14 domain-containing protein 2 OS=Homo sapiens GN=FUNDC2 PE=1 SV=2 - [FUND2_HUMAN]	1.43E+07	2.46E+06	-5.80E+00
Q9BXJ9	N-alpha-acetyltransferase 15, NatA auxiliary subunit OS=Homo sapiens GN=NAA15 PE=1 SV=1 - [NAA15_HUMAN]	0.00E+00	4.40E+07	1.00E+01
Q9BXP5-5	Isoform 5 of Serrate RNA effector molecule homolog OS=Homo sapiens GN=SRRT - [SRRT_HUMAN]	0.00E+00	3.29E+07	1.00E+01
Q9BZZ5-3	Isoform 3 of Apoptosis inhibitor 5 OS=Homo sapiens GN=API5 - [API5_HUMAN]	1.63E+07	1.23E+07	-1.33E+00

Q9C0H2-3	Isoform 3 of Protein tweety homolog 3 OS=Homo sapiens GN=TTYH3 - [TTYH3_HUMAN]	0.00E+00	1.75E+07	1.00E+01
Q9GZL7	Ribosome biogenesis protein WDR12 OS=Homo sapiens GN=WDR12 PE=1 SV=2 - [WDR12_HUMAN]	7.23E+06	1.34E+07	1.86E+00
Q9H2H9	Sodium-coupled neutral amino acid transporter 1 OS=Homo sapiens GN=SLC38A1 PE=1 SV=1 - [S38A1_HUMAN]	6.99E+07	1.13E+08	1.61E+00
Q9H3N1	Thioredoxin-related transmembrane protein 1 OS=Homo sapiens GN=TMX1 PE=1 SV=1 - [TMX1_HUMAN]	1.63E+07	9.93E+07	6.09E+00
Q9H3Z4	DnaJ homolog subfamily C member 5 OS=Homo sapiens GN=DNAJC5 PE=1 SV=1 - [DNJC5_HUMAN]	1.16E+08	2.42E+08	2.09E+00
Q9H773	dCTP pyrophosphatase 1 OS=Homo sapiens GN=DCTPP1 PE=1 SV=1 - [DCTP1_HUMAN]	1.41E+07	3.50E+07	2.48E+00
Q9H9B4	Sideroflexin-1 OS=Homo sapiens GN=SFXN1 PE=1 SV=4 - [SFXN1_HUMAN]	3.35E+07	2.07E+07	-1.62E+00
Q9HB71	Calcyclin-binding protein OS=Homo sapiens GN=CACYBP PE=1 SV=2 - [CYBP_HUMAN]	2.86E+07	6.54E+07	2.28E+00
Q9HDC9	Adipocyte plasma membrane-associated protein OS=Homo sapiens GN=APMAP PE=1 SV=2 - [APMAP_HUMAN]	1.91E+07	3.59E+07	1.88E+00
Q9NR12	PDZ and LIM domain protein 7 OS=Homo sapiens GN=PDLIM7 PE=1 SV=1 - [PDLI7_HUMAN]	1.50E+07	1.74E+07	1.16E+00
Q9NR30	Nucleolar RNA helicase 2 OS=Homo sapiens GN=DDX21 PE=1 SV=5 - [DDX21_HUMAN]	4.17E+07	1.48E+08	3.55E+00

Q9NRF9	DNA polymerase epsilon subunit 3 OS=Homo sapiens GN=POLE3 PE=1 SV=1 - [DPOE3_HUMAN]	3.15E+07	1.70E+07	-1.85E+00
Q9NVI7-2	Isoform 2 of ATPase family AAA domain-containing protein 3A OS=Homo sapiens GN=ATAD3A - [ATD3A_HUMAN]	2.21E+07	5.36E+07	2.42E+00
Q9NXH9-2	Isoform 2 of tRNA (guanine(26)-N(2))-dimethyltransferase OS=Homo sapiens GN=TRMT1 - [TRM1_HUMAN]	0.00E+00	5.30E+06	1.00E+01
Q9NY33-4	Isoform 4 of Dipeptidyl peptidase 3 OS=Homo sapiens GN=DPP3 - [DPP3_HUMAN]	1.20E+07	0.00E+00	-1.00E+01
Q9NZ01	Very-long-chain enoyl-CoA reductase OS=Homo sapiens GN=TECR PE=1 SV=1 - [TECR_HUMAN]	8.13E+07	1.64E+08	2.02E+00
Q9NZM1-2	Isoform 2 of Myoferlin OS=Homo sapiens GN=MYOF - [MYOF_HUMAN]	2.62E+07	5.62E+07	2.14E+00
Q9P0L0	Vesicle-associated membrane protein-associated protein A OS=Homo sapiens GN=VAPA PE=1 SV=3 - [VAPA_HUMAN]	0.00E+00	2.94E+07	1.00E+01
Q9P258	Protein RCC2 OS=Homo sapiens GN=RCC2 PE=1 SV=2 - [RCC2_HUMAN]	2.15E+07	4.22E+07	1.97E+00
Q9UBB4	Ataxin-10 OS=Homo sapiens GN=ATXN10 PE=1 SV=1 - [ATX10_HUMAN]	1.93E+07	5.81E+06	-3.32E+00
Q9UBX3	Mitochondrial dicarboxylate carrier OS=Homo sapiens GN=SLC25A10 PE=1 SV=2 - [DIC_HUMAN]	8.13E+06	1.45E+07	1.78E+00
Q9UI26	Importin-11 OS=Homo sapiens GN=IPO11 PE=1 SV=1 - [IPO11_HUMAN]	5.40E+06	1.01E+07	1.86E+00

Q9UIA9	Exportin-7 OS=Homo sapiens GN=XPO7 PE=1 SV=3 - [XPO7_HUMAN]	8.92E+06	1.28E+07	1.43E+00
Q9UIQ6-3	Isoform 3 of Leucyl-cystinyl aminopeptidase OS=Homo sapiens GN=LNPEP - [LCAP_HUMAN]	8.34E+06	7.97E+06	-1.05E+00
Q9UL15	BAG family molecular chaperone regulator 5 OS=Homo sapiens GN=BAG5 PE=1 SV=1 - [BAG5_HUMAN]	4.08E+07	1.22E+07	-3.34E+00
Q9UL46	Proteasome activator complex subunit 2 OS=Homo sapiens GN=PSME2 PE=1 SV=4 - [PSME2_HUMAN]	1.05E+07	3.54E+07	3.36E+00
Q9ULV4	Coronin-1C OS=Homo sapiens GN=CORO1C PE=1 SV=1 - [COR1C_HUMAN]	0.00E+00	1.28E+07	1.00E+01
Q9UMS4	Pre-mRNA-processing factor 19 OS=Homo sapiens GN=PRPF19 PE=1 SV=1 - [PRP19_HUMAN]	1.36E+07	4.31E+07	3.17E+00
Q9UN86-2	Isoform B of Ras GTPase-activating protein-binding protein 2 OS=Homo sapiens GN=G3BP2 - [G3BP2_HUMAN]	2.57E+07	7.06E+07	2.75E+00
Q9UPT8	Zinc finger CCCH domain-containing protein 4 OS=Homo sapiens GN=ZC3H4 PE=1 SV=3 - [ZC3H4_HUMAN]	0.00E+00	4.52E+06	1.00E+01
Q9UQ80	Proliferation-associated protein 2G4 OS=Homo sapiens GN=PA2G4 PE=1 SV=3 - [PA2G4_HUMAN]	9.86E+07	1.41E+08	1.43E+00
Q9Y230	RuvB-like 2 OS=Homo sapiens GN=RUVBL2 PE=1 SV=3 - [RUVB2_HUMAN]	3.69E+07	1.10E+08	2.97E+00
Q9Y262	Eukaryotic translation initiation factor 3 subunit L OS=Homo sapiens GN=EIF3L PE=1 SV=1 - [EIF3L_HUMAN]	1.96E+07	3.03E+07	1.55E+00

Q9Y265-2	Isoform 2 of RuvB-like 1 OS=Homo sapiens GN=RUVBL1 - [RUVB1_HUMAN]	2.83E+07	3.42E+07	1.21E+00
Q9Y277	Voltage-dependent anion-selective channel protein 3 OS=Homo sapiens GN=VDAC3 PE=1 SV=1 - [VDAC3_HUMAN]	6.79E+07	8.53E+07	1.26E+00
Q9Y282-2	Isoform 2 of Endoplasmic reticulum-Golgi intermediate compartment protein 3 OS=Homo sapiens GN=ERGIC3 - [ERGI3_HUMAN]	1.56E+07	3.73E+07	2.39E+00
Q9Y287	Integral membrane protein 2B OS=Homo sapiens GN=ITM2B PE=1 SV=1 - [ITM2B_HUMAN]	5.04E+07	9.14E+07	1.81E+00
Q9Y295	Developmentally-regulated GTP-binding protein 1 OS=Homo sapiens GN=DRG1 PE=1 SV=1 - [DRG1_HUMAN]	1.27E+07	3.18E+07	2.50E+00
Q9Y2W1	Thyroid hormone receptor-associated protein 3 OS=Homo sapiens GN=THRAP3 PE=1 SV=2 - [TR150_HUMAN]	1.09E+06	2.82E+06	2.59E+00
Q9Y2X3	Nucleolar protein 58 OS=Homo sapiens GN=NOP58 PE=1 SV=1 - [NOP58_HUMAN]	2.40E+07	3.44E+07	1.43E+00
Q9Y305-3	Isoform 3 of Acyl-coenzyme A thioesterase 9, mitochondrial OS=Homo sapiens GN=ACOT9 - [ACOT9_HUMAN]	0.00E+00	1.92E+07	1.00E+01
Q9Y383-3	Isoform 3 of Putative RNA-binding protein Luc7-like 2 OS=Homo sapiens GN=LUC7L2 - [LC7L2_HUMAN]	1.52E+07	1.50E+07	-1.02E+00
Q9Y3F4	Serine-threonine kinase receptor-associated protein OS=Homo sapiens GN=STRAP PE=1 SV=1 - [STRAP_HUMAN]	4.77E+07	5.50E+07	1.15E+00

Q9Y3I0	tRNA-splicing ligase RtcB homolog OS=Homo sapiens GN=C22orf28 PE=1 SV=1 - [RTCB_HUMAN]	0.00E+00	3.66E+07	1.00E+01
Q9Y3U8	60S ribosomal protein L36 OS=Homo sapiens GN=RPL36 PE=1 SV=3 - [RL36_HUMAN]	7.91E+07	7.90E+07	-1.00E+00
Q9Y4W6	AFG3-like protein 2 OS=Homo sapiens GN=AFG3L2 PE=1 SV=2 - [AFG32_HUMAN]	4.51E+06	1.17E+07	2.60E+00
Q9Y5B9	FACT complex subunit SPT16 OS=Homo sapiens GN=SUPT16H PE=1 SV=1 - [SP16H_HUMAN]	1.70E+07	2.87E+07	1.69E+00
Q9Y5J1	U3 small nucleolar RNA-associated protein 18 homolog OS=Homo sapiens GN=UTP18 PE=1 SV=3 - [UTP18_HUMAN]	8.69E+06	2.30E+07	2.65E+00
Q9Y617-2	Isoform 2 of Phosphoserine aminotransferase OS=Homo sapiens GN=PSAT1 - [SERC_HUMAN]	2.35E+07	4.67E+07	1.99E+00
Q9Y678	Coatomer subunit gamma-1 OS=Homo sapiens GN=COPG1 PE=1 SV=1 - [COPG1_HUMAN]	1.40E+07	3.09E+07	2.21E+00
Q9Y697-2	Isoform Cytoplasmic of Cysteine desulfurase, mitochondrial OS=Homo sapiens GN=NFS1 - [NFS1_HUMAN]	2.15E+06	3.25E+06	1.51E+00
Q9Y6C9	Mitochondrial carrier homolog 2 OS=Homo sapiens GN=MTCH2 PE=1 SV=1 - [MTCH2_HUMAN]	2.86E+07	4.22E+07	1.47E+00

APPENDIX B
Protein abundance upon *Shigella* infection (experiment 1)

*Ratios higher than +10 or lower than -10 are equaled to +10 or -10 respectively for visualization purposes.

Proteins with N-terminal glycine

Accession	Description	Wild type Shigella	ΔipaJ Shigella	non infected	wild type /ΔipaJ ratio*
B4DQJ8	6-phosphogluconate dehydrogenase, decarboxylating OS=Homo sapiens GN=PGD PE=2 SV=1	2.45E+07	2.62E+07	2.75E+07	-1.07E+00
B4DWW1	ADP-ribosylation factor-like protein 1 OS=Homo sapiens GN=ARL1 PE=2 SV=1	7.05E+07	3.15E+08	3.66E+08	-4.47E+00
C9JHG2	Raftlin (Fragment) OS=Homo sapiens GN=RFTN1 PE=4 SV=1	1.66E+07	1.71E+07	2.21E+07	-1.03E+00
E7EQV9	Ribosomal protein L15 (Fragment) OS=Homo sapiens GN=RPL15 PE=3 SV=1	6.95E+07	7.93E+07	7.29E+07	-1.14E+00
E7EWT1	Dolichyl-diphosphooligosaccharide--protein glycosyltransferase 48 kDa subunit OS=Homo sapiens GN=DDOST PE=4 SV=1	1.03E+07	1.35E+07	4.56E+06	-1.31E+00
E9PKZ0	60S ribosomal protein L8 OS=Homo sapiens GN=RPL8 PE=4 SV=1	4.62E+07	4.97E+07	4.85E+07	-1.08E+00
E9PNW4	CD59 glycoprotein OS=Homo sapiens GN=CD59 PE=4 SV=1	1.19E+08	1.10E+08	1.17E+08	1.08E+00
F5GY99	Polypeptide N-acetylgalactosaminyltransferase 1 soluble form OS=Homo sapiens GN=GALNT1 PE=3 SV=1	0.00E+00	1.05E+07	0.00E+00	-1.00E+01
F8VVN7	Transmembrane protein 106C OS=Homo sapiens GN=TMEM106C PE=4 SV=1	0.00E+00	3.59E+07	5.01E+07	-1.00E+01
F8W785	Golgi integral membrane protein 4 OS=Homo sapiens GN=GOLIM4 PE=4 SV=1	3.50E+06	3.98E+06	3.70E+06	-1.14E+00
H0YKJ9	Tetraspanin-3 OS=Homo sapiens GN=TSPAN3 PE=4 SV=1	1.99E+08	2.14E+08	1.71E+08	-1.08E+00
H3BM67	Nucleolar protein 3 (Fragment) OS=Homo sapiens GN=NOL3 PE=4 SV=1	1.08E+08	1.22E+08	1.73E+08	-1.13E+00

O15121	Sphingolipid delta(4)-desaturase DES1 OS=Homo sapiens GN=DEGS1 PE=1 SV=1	1.12E+08	6.80E+08	9.46E+07	-6.09E+00
O15260-2	Isoform 2 of Surfeit locus protein 4 OS=Homo sapiens GN=SURF4	1.69E+07	2.33E+07	1.69E+07	-1.38E+00
O15355	Protein phosphatase 1G OS=Homo sapiens GN=PPM1G PE=1 SV=1	3.68E+08	3.12E+08	4.89E+08	1.18E+00
O15427	Monocarboxylate transporter 4 OS=Homo sapiens GN=SLC16A3 PE=1 SV=1	1.28E+08	1.19E+08	1.19E+08	1.08E+00
O75688	Protein phosphatase 1B OS=Homo sapiens GN=PPM1B PE=1 SV=1	2.22E+07	3.25E+07	3.24E+07	-1.47E+00
O75695	Protein XRP2 OS=Homo sapiens GN=RP2 PE=1 SV=4	1.58E+07	1.63E+07	2.56E+07	-1.03E+00
O75844	CAAX prenyl protease 1 homolog OS=Homo sapiens GN=ZMPSTE24 PE=1 SV=2	1.59E+07	2.07E+07	1.98E+07	-1.30E+00
O95210	Starch-binding domain-containing protein 1 OS=Homo sapiens GN=STBD1 PE=1 SV=1	7.59E+06	7.75E+06	2.18E+07	-1.02E+00
O96008	Mitochondrial import receptor subunit TOM40 homolog OS=Homo sapiens GN=TOMM40 PE=1 SV=1	1.06E+07	9.42E+06	8.95E+06	1.13E+00
P00387-2	Isoform 2 of NADH-cytochrome b5 reductase 3 OS=Homo sapiens GN=CYB5R3	8.91E+08	7.98E+08	6.39E+08	1.12E+00
P04406	Glyceraldehyde-3-phosphate dehydrogenase OS=Homo sapiens GN=GAPDH PE=1 SV=3	9.76E+08	9.64E+08	1.47E+09	1.01E+00
P04899	Guanine nucleotide-binding protein G(i) subunit alpha-2 OS=Homo sapiens GN=GNAI2 PE=1 SV=3	6.72E+08	6.56E+08	4.95E+08	1.02E+00
P05023-3	Isoform 3 of Sodium/potassium-transporting ATPase subunit alpha-1 OS=Homo sapiens GN=ATP1A1	2.04E+07	2.63E+07	2.24E+07	-1.29E+00
P07947	Tyrosine-protein kinase Yes OS=Homo sapiens GN=YES1 PE=1 SV=3	3.08E+07	2.60E+07	6.35E+07	1.18E+00
P07948-2	Isoform 2 of Tyrosine-protein kinase Lyn OS=Homo sapiens GN=LYN	1.49E+07	1.44E+07	3.25E+07	1.03E+00
P08708	40S ribosomal protein S17 OS=Homo sapiens GN=RPS17 PE=1 SV=2	1.86E+07	2.29E+07	2.56E+07	-1.24E+00
P08754	Guanine nucleotide-binding protein G(k) subunit alpha OS=Homo sapiens GN=GNAI3 PE=1 SV=3	7.17E+08	7.03E+08	5.62E+08	1.02E+00
P11717	Cation-independent mannose-6-phosphate receptor OS=Homo sapiens GN=IGF2R	0.00E+00	3.84E+06	1.12E+07	-1.00E+01

	PE=1 SV=3				
P17568	NADH dehydrogena	4.38E+07	5.09E+07	3.63E+07	-1.16E+00
P17612	cAMP-dependent protein kinase catalytic subunit alpha OS=Homo sapiens GN=PRKACA PE=1 SV=2	3.69E+08	3.62E+08	4.73E+08	1.02E+00
P18085	ADP-ribosylation factor 4 OS=Homo sapiens GN=ARF4 PE=1 SV=3	1.69E+09	3.73E+09	4.45E+09	-2.21E+00
P22694	cAMP-dependent protein kinase catalytic subunit beta OS=Homo sapiens GN=PRKACB PE=1 SV=2	1.92E+08	1.39E+08	2.80E+08	1.38E+00
P24534	Elongation factor 1-beta OS=Homo sapiens GN=EEF1B2 PE=1 SV=3	3.49E+07	3.91E+07	5.04E+07	-1.12E+00
P26006	Integrin alpha-3 OS=Homo sapiens GN=ITGA3 PE=1 SV=5	7.55E+06	6.31E+06	0.00E+00	1.20E+00
P27635	60S ribosomal protein L10 OS=Homo sapiens GN=RPL10 PE=1 SV=4	3.08E+07	3.07E+07	3.93E+07	1.00E+00
P29966	Myristoylated alanine-rich C-kinase substrate OS=Homo sapiens GN=MARCKS PE=1 SV=4	4.74E+08	6.73E+08	1.21E+09	-1.42E+00
P30044-2	Isoform Cytoplasmic+peroxisomal of Peroxiredoxin-5, mitochondrial OS=Homo sapiens GN=PRDX5	2.42E+07	2.69E+07	2.87E+07	-1.11E+00
P35813	Protein phosphatase 1A OS=Homo sapiens GN=PPM1A PE=1 SV=1	5.20E+07	4.03E+07	6.88E+07	1.29E+00
P37235	Hippocalcin-like protein 1 OS=Homo sapiens GN=HPCAL1 PE=1 SV=3	1.73E+08	1.66E+08	2.35E+08	1.04E+00
P43121	Cell surface glycoprotein MUC18 OS=Homo sapiens GN=MCAM PE=1 SV=2	2.83E+07	3.27E+07	2.67E+07	-1.16E+00
P46777	60S ribosomal protein L5 OS=Homo sapiens GN=RPL5 PE=1 SV=3	1.56E+07	1.85E+07	2.51E+07	-1.19E+00
P48960-2	Isoform 2 of CD97 antigen OS=Homo sapiens GN=CD97	2.55E+07	2.22E+07	0.00E+00	1.15E+00
P49006	MARCKS-related protein OS=Homo sapiens GN=MARCKSL1 PE=1 SV=2	1.93E+08	2.06E+08	2.99E+08	-1.07E+00
P53701	Cytochrome c-type heme lyase OS=Homo sapiens GN=HCCS PE=1 SV=1	1.75E+08	1.75E+08	2.00E+08	-1.00E+00
P54577	Tyrosine--tRNA ligase, cytoplasmic OS=Homo sapiens GN=YARS PE=1 SV=4	0.00E+00	6.66E+06	7.56E+06	-1.00E+01
P61204	ADP-ribosylation factor 3 OS=Homo sapiens GN=ARF3 PE=1 SV=2	1.73E+09	3.73E+09	4.76E+09	-2.16E+00

P61353	60S ribosomal protein L27 OS=Homo sapiens GN=RPL27 PE=1 SV=2	1.34E+07	1.38E+07	1.36E+07	-1.03E+00
P62166	Neuronal calcium sensor 1 OS=Homo sapiens GN=NCS1 PE=1 SV=2	1.30E+07	9.01E+06	0.00E+00	1.44E+00
P62191	26S protease regulatory subunit 4 OS=Homo sapiens GN=PSMC1 PE=1 SV=1	5.76E+08	8.01E+08	8.03E+08	-1.39E+00
P62241	40S ribosomal protein S8 OS=Homo sapiens GN=RPS8 PE=1 SV=2	1.14E+08	1.62E+08	1.08E+08	-1.43E+00
P62266	40S ribosomal protein S23 OS=Homo sapiens GN=RPS23 PE=1 SV=3	4.78E+07	5.06E+07	4.87E+07	-1.06E+00
P62330	ADP-ribosylation factor 6 OS=Homo sapiens GN=ARF6 PE=1 SV=2	2.59E+08	2.08E+08	1.16E+09	1.25E+00
P63096	Guanine nucleotide-binding protein G(i) subunit alpha-1 OS=Homo sapiens GN=GNAI1 PE=1 SV=2	6.47E+08	6.52E+08	4.33E+08	-1.01E+00
P68104	Elongation factor 1-alpha 1 OS=Homo sapiens GN=EEF1A1 PE=1 SV=1	7.75E+08	4.80E+08	9.03E+08	1.61E+00
P80723	Brain acid soluble protein 1 OS=Homo sapiens GN=BASP1 PE=1 SV=2	1.00E+10	1.15E+10	1.50E+10	-1.15E+00
P84085	ADP-ribosylation factor 5 OS=Homo sapiens GN=ARF5 PE=1 SV=2	1.69E+09	3.73E+09	4.45E+09	-2.21E+00
Q02952-3	Isoform 3 of A-kinase anchor protein 12 OS=Homo sapiens GN=AKAP12	2.53E+07	1.68E+07	6.30E+07	1.51E+00
Q04917	14-3-3 protein eta OS=Homo sapiens GN=YWHAH PE=1 SV=4	9.87E+07	9.41E+07	1.11E+08	1.05E+00
Q05639	Elongation factor 1-alpha 2 OS=Homo sapiens GN=EEF1A2 PE=1 SV=1	3.45E+08	4.59E+08	3.85E+08	-1.33E+00
Q08211	ATP-dependent RNA helicase A OS=Homo sapiens GN=DHX9 PE=1 SV=4	5.22E+07	6.26E+07	4.73E+07	-1.20E+00
Q13286-2	Isoform 2 of Battenin OS=Homo sapiens GN=CLN3	1.95E+07	1.94E+07	1.43E+07	1.01E+00
Q13530	Serine incorporator 3 OS=Homo sapiens GN=SERINC3 PE=2 SV=2	3.70E+07	3.52E+07	1.72E+07	1.05E+00
Q14108	Lysosome membrane protein 2 OS=Homo sapiens GN=SCARB2 PE=1 SV=2	8.65E+07	1.06E+08	1.62E+08	-1.22E+00
Q14254	Flotillin-2 OS=Homo sapiens GN=FLOT2 PE=1 SV=2	1.26E+08	1.27E+08	1.18E+08	-1.01E+00
Q5BJF2	Transmembrane protein 97 OS=Homo sapiens GN=TMEM97 PE=1 SV=1	1.21E+07	0.00E+00	1.47E+07	1.00E+01
Q5T7C4	High mobility group protein B1 OS=Homo sapiens GN=HMGB1 PE=2	4.32E+07	8.58E+07	7.53E+07	-1.99E+00

	SV=1				
Q6IAA8	Ragulator complex protein LAMTOR1 OS=Homo sapiens GN=LAMTOR1 PE=1 SV=2	1.58E+08	1.54E+08	3.76E+08	1.03E+00
Q6NUT3-2	Isoform 2 of Major facilitator superfamily domain-containing protein 12 OS=Homo sapiens GN=MFSD12	1.92E+07	1.70E+07	1.24E+07	1.13E+00
Q6UB35	Monofunctional C1-tetrahydrofolate synthase, mitochondrial OS=Homo sapiens GN=MTHFD1L PE=1 SV=1	7.93E+06	9.13E+06	1.04E+07	-1.15E+00
Q7RTS9	Dymeclin OS=Homo sapiens GN=DYM PE=1 SV=1	2.55E+07	2.48E+07	3.15E+07	1.03E+00
Q8IWA5-3	Isoform 3 of Choline transporter-like protein 2 OS=Homo sapiens GN=SLC44A2	1.62E+07	1.16E+07	1.42E+07	1.39E+00
Q8N9N7	Leucine-rich repeat-containing protein 57 OS=Homo sapiens GN=LRRC57 PE=1 SV=1	2.75E+07	2.52E+07	4.17E+07	1.09E+00
Q8NHG8	E3 ubiquitin-protein ligase ZNRF2 OS=Homo sapiens GN=ZNRF2 PE=1 SV=1	0.00E+00	1.74E+07	5.18E+07	-1.00E+01
Q8WTV0-4	Isoform 4 of Scavenger receptor class B member 1 OS=Homo sapiens GN=SCARB1	4.47E+07	3.23E+07	4.82E+07	1.38E+00
Q8WWI5	Choline transporter-like protein 1 OS=Homo sapiens GN=SLC44A1 PE=1 SV=1	4.47E+07	4.69E+07	3.97E+07	-1.05E+00
Q969Z3	MOSC domain-containing protein 2, mitochondrial OS=Homo sapiens GN=MARC2 PE=1 SV=1	2.66E+07	3.75E+07	3.38E+07	-1.41E+00
Q96BS2-3	Isoform 3 of Calcineurin B homologous protein 3 OS=Homo sapiens GN=TESC	0.00E+00	1.12E+07	1.62E+07	-1.00E+01
Q96GE9-2	Isoform 2 of Transmembrane protein C9orf123 OS=Homo sapiens GN=C9orf123	1.95E+08	1.68E+08	2.42E+08	1.16E+00
Q96TA1-2	Isoform 2 of Niban-like protein 1 OS=Homo sapiens GN=FAM129B	5.76E+08	4.40E+08	6.89E+08	1.31E+00
Q99487	Platelet-activating factor acetylhydrolase 2, cytoplasmic OS=Homo sapiens GN=PAFAH2 PE=1 SV=1	8.55E+06	0.00E+00	9.85E+06	1.00E+01
Q99570	Phosphoinositide 3-kinase regulatory subunit 4 OS=Homo sapiens GN=PIK3R4 PE=1 SV=3	3.66E+07	2.64E+07	3.60E+07	1.39E+00

Q99653	Calcineurin B homologous protein 1 OS=Homo sapiens GN=CHP1 PE=1 SV=3	9.65E+07	1.21E+08	9.04E+07	-1.26E+00
Q9BPX3	Condensin complex subunit 3 OS=Homo sapiens GN=NCAPG PE=1 SV=1	2.46E+06	0.00E+00	2.12E+07	1.00E+01
Q9BQQ3-3	Isoform 3 of Golgi reassembly-stacking protein 1 OS=Homo sapiens GN=GORASP1	2.31E+07	1.89E+07	2.77E+07	1.22E+00
Q9BRQ8	Apoptosis-inducing factor 2 OS=Homo sapiens GN=AIFM2 PE=1 SV=1	5.67E+07	6.92E+07	1.01E+08	-1.22E+00
Q9BXP5-4	Isoform 4 of Serrate RNA effector molecule homolog OS=Homo sapiens GN=SRRT	6.57E+06	7.21E+06	1.03E+07	-1.10E+00
Q9C0E8-2	Isoform 2 of Protein lunapark OS=Homo sapiens GN=LNP	3.02E+07	2.19E+07	3.61E+07	1.38E+00
Q9H8Y8	Golgi reassembly-stacking protein 2 OS=Homo sapiens GN=GORASP2 PE=1 SV=3	1.23E+08	1.24E+08	1.70E+08	-1.00E+00
Q9HBL7	Plasminogen receptor (KT) OS=Homo sapiens GN=PLGRKT PE=1 SV=1	1.57E+07	1.81E+07	2.31E+07	-1.15E+00
Q9NRX5	Serine incorporator 1 OS=Homo sapiens GN=SERINC1 PE=1 SV=1	1.08E+08	1.41E+08	8.55E+07	-1.31E+00
Q9NUM4	Transmembrane protein 106B OS=Homo sapiens GN=TMEM106B PE=1 SV=2	3.52E+07	3.73E+07	4.19E+07	-1.06E+00
Q9NUQ9	Protein FAM49B OS=Homo sapiens GN=FAM49B PE=1 SV=1	2.16E+08	1.90E+08	3.33E+08	1.13E+00
Q9NX63	Coiled-coil-helix-coiled-coil-helix domain-containing protein 3, mitochondrial OS=Homo sapiens GN=CHCHD3 PE=1 SV=1	3.43E+08	4.61E+08	2.81E+08	-1.34E+00
Q9NYU2-2	Isoform 2 of UDP-glucose:glycoprotein glucosyltransferase 1 OS=Homo sapiens GN=UGGT1	5.10E+06	7.72E+06	4.94E+06	-1.51E+00
Q9P032	NADH dehydrogena	6.71E+07	7.40E+07	4.88E+07	-1.10E+00
Q9P2B2	Prostaglandin F2 receptor negative regulator OS=Homo sapiens GN=PTGFRN PE=1 SV=2	1.44E+07	1.79E+07	2.07E+07	-1.24E+00
Q9Y266	Nuclear migration protein nudC OS=Homo sapiens GN=NUDC PE=1 SV=1	9.02E+06	8.68E+06	1.26E+07	1.04E+00
Q9Y478	5'-AMP-activated protein kinase subunit beta-1 OS=Homo sapiens GN=PRKAB1 PE=1 SV=4	1.07E+07	9.04E+06	2.13E+07	1.18E+00
Q9Y6M0-3	Isoform 3 of Testisin OS=Homo sapiens GN=PRSS21	1.13E+07	9.19E+06	1.50E+07	1.23E+00

Q9Y6M5	Zinc transporter 1 OS=Homo sapiens GN=SLC30A1 PE=1 SV=3	2.63E+07	2.11E+07	3.02E+07	1.25E+00

Proteins without N-terminal glycine

Accession	Description	Wild type Shigella	ΔipaJ Shigella	non infected	wild type /ΔipaJ ratio
A6NDN0	Trafficking protein particle complex 3, isoform CRA_a OS=Homo sapiens GN=TRAPPC3 PE=4 SV=1	5.04E+06	4.32E+06	7.03E+06	1.17E+00
A6NNI4	CD9 antigen OS=Homo sapiens GN=CD9 PE=4 SV=1	1.63E+08	1.76E+08	1.75E+08	-1.08E+00
A8K3Z3	26S protease regulatory subunit 8 OS=Homo sapiens GN=PSMC5 PE=2 SV=1	8.86E+07	1.45E+07	2.34E+08	6.09E+00
A8MUD9	60S ribosomal protein L7 OS=Homo sapiens GN=RPL7 PE=3 SV=1	2.76E+07	1.99E+07	3.42E+07	1.39E+00
B0V109	Flotillin 1 (Fragment) OS=Homo sapiens GN=FLOT1 PE=4 SV=1	1.72E+07	1.84E+07	1.92E+07	-1.07E+00
B1ANR0	Poly(A) binding protein, cytoplasmic 4 (Inducible form) OS=Homo sapiens GN=PABPC4 PE=4 SV=1	4.69E+07	5.02E+07	6.89E+07	-1.07E+00
B3KQ25	Proteasome activator complex subunit 3 OS=Homo sapiens GN=PSME3 PE=2 SV=1	9.79E+06	1.05E+07	1.27E+07	-1.07E+00
B3KQC5	Endoplasmic reticulum mannosyl-oligosaccharide 1,2-alpha-mannosidase OS=Homo sapiens GN=MAN1B1 PE=2 SV=1	0.00E+00	7.84E+06	5.20E+06	-1.00E+01
B4DDS0	Putative uncharacterized protein FLJ13576 OS=Homo sapiens GN=TMEM168 PE=2 SV=1	1.55E+07	1.57E+07	1.28E+07	-1.01E+00
B4DET3	Niemann-Pick C1 protein OS=Homo sapiens GN=NPC1 PE=2 SV=1	2.82E+07	4.41E+07	3.10E+07	-1.56E+00
B4DJV2	Citrate synthase OS=Homo sapiens GN=CS PE=2 SV=1	4.18E+07	3.26E+07	3.79E+07	1.28E+00
B4DKB2	Endothelin-converting enzyme 1 OS=Homo sapiens GN=ECE1 PE=2 SV=1	1.24E+07	1.38E+07	2.35E+07	-1.11E+00
B4DL14	ATP synthase gamma chain OS=Homo sapiens GN=ATP5C1 PE=2 SV=1	2.32E+07	5.03E+07	3.62E+07	-2.17E+00
B4DM74	60S ribosomal protein L18a OS=Homo sapiens GN=RPL18A PE=2 SV=1	4.11E+07	4.18E+07	4.42E+07	-1.02E+00
B4DP11	Prostaglandin E synthase 3 OS=Homo sapiens GN=PTGES3 PE=2 SV=1	1.80E+07	1.50E+07	1.95E+07	1.20E+00

B4DTE8	Phospholipid scramblase 1 OS=Homo sapiens GN=PLSCR1 PE=2 SV=1	1.19E+07	1.42E+07	1.07E+07	-1.19E+00
B4DVY1	Eukaryotic translation initiation factor 3 subunit D OS=Homo sapiens GN=EIF3D PE=2 SV=1	1.76E+07	3.22E+07	2.10E+07	-1.83E+00
B4E2V5	Erythrocyte band 7 integral membrane protein OS=Homo sapiens GN=STOM PE=2 SV=1	2.33E+08	2.80E+08	2.44E+08	-1.20E+00
B4E2W0	3-ketoacyl-CoA thiolase OS=Homo sapiens GN=HADHB PE=2 SV=1	8.70E+07	1.30E+08	8.27E+07	-1.50E+00
B7Z972	Protein-L-isoaspartate O-methyltransferase OS=Homo sapiens GN=PCMT1 PE=2 SV=1	9.46E+06	9.48E+06	1.66E+07	-1.00E+00
B7Z9L0	T-complex protein 1 subunit delta OS=Homo sapiens GN=CCT4 PE=2 SV=1	3.33E+07	5.22E+07	3.86E+07	-1.57E+00
C9IZZ0	Ras-related protein Rab-7a (Fragment) OS=Homo sapiens GN=RAB7A PE=4 SV=1	1.09E+07	1.69E+07	1.38E+07	-1.55E+00
C9J8H9	ATP synthase subunit f, mitochondrial OS=Homo sapiens GN=ATP5J2 PE=4 SV=1	4.00E+07	5.19E+07	3.27E+07	-1.30E+00
C9J9K3	40S ribosomal protein SA (Fragment) OS=Homo sapiens GN=RPSA PE=3 SV=1	3.87E+07	3.51E+07	3.73E+07	1.10E+00
C9JB50	60S ribosomal protein L28 OS=Homo sapiens GN=RPL28 PE=4 SV=1	3.97E+07	4.37E+07	8.43E+07	-1.10E+00
C9JD32	60S ribosomal protein L23 (Fragment) OS=Homo sapiens GN=RPL23 PE=3 SV=1	2.86E+07	2.83E+07	2.84E+07	1.01E+00
C9JL85	Myotrophin OS=Homo sapiens GN=MTPN PE=4 SV=1	1.83E+07	1.75E+07	2.28E+07	1.04E+00
C9JSZ2	Proton-coupled folate transporter OS=Homo sapiens GN=SLC46A1 PE=4 SV=1	8.39E+06	9.40E+06	6.89E+06	-1.12E+00
C9JXB8	60S ribosomal protein L24 OS=Homo sapiens GN=RPL24 PE=4 SV=1	1.69E+07	1.94E+07	2.78E+07	-1.15E+00
D3YTB1	60S ribosomal protein L32 (Fragment) OS=Homo sapiens GN=RPL32 PE=4 SV=1	7.85E+06	8.26E+06	9.37E+06	-1.05E+00
D6R904	Tropomyosin alpha-3 chain OS=Homo sapiens GN=TPM3 PE=4 SV=1	1.37E+07	1.41E+07	1.47E+07	-1.03E+00
D6RG13	40S ribosomal protein S3a (Fragment) OS=Homo sapiens GN=RPS3A PE=3 SV=1	5.31E+07	5.30E+07	3.61E+07	1.00E+00

D6RGI3	Septin 11, isoform CRA_b OS=Homo sapiens GN=SEPT11 PE=3 SV=1	1.08E+07	1.58E+07	7.08E+06	-1.47E+00
D6RIU4	Vesicular integral-membrane protein VIP36 (Fragment) OS=Homo sapiens GN=LMAN2 PE=4 SV=1	0.00E+00	4.87E+06	1.07E+07	-1.00E+01
E5RHG8	Transcription elongation factor B polypeptide 1 (Fragment) OS=Homo sapiens GN=TCEB1 PE=4 SV=1	0.00E+00	5.76E+06	8.45E+06	-1.00E+01
E5RIW3	Tubulin-specific chaperone A OS=Homo sapiens GN=TBCA PE=4 SV=1	6.80E+06	0.00E+00	8.16E+06	1.00E+01
E7ESG6	Zinc transporter SLC39A7 OS=Homo sapiens GN=SLC39A7 PE=4 SV=1	9.66E+06	1.35E+07	5.04E+06	-1.40E+00
E9PIR7	Thioredoxin reductase 1, cytoplasmic OS=Homo sapiens GN=TXNRD1 PE=3 SV=1	5.15E+07	5.27E+07	5.81E+07	-1.02E+00
E9PJC7	CD82 antigen (Fragment) OS=Homo sapiens GN=CD82 PE=4 SV=1	3.56E+07	3.72E+07	5.59E+07	-1.05E+00
E9PJD9	60S ribosomal protein L27a OS=Homo sapiens GN=RPL27A PE=3 SV=1	4.08E+07	4.25E+07	5.38E+07	-1.04E+00
E9PJK1	CD81 antigen OS=Homo sapiens GN=CD81 PE=4 SV=1	3.09E+07	3.22E+07	2.87E+07	-1.04E+00
E9PL82	CD151 antigen OS=Homo sapiens GN=CD151 PE=4 SV=1	1.63E+08	2.08E+08	1.78E+08	-1.28E+00
E9PLK3	Puromycin-sensitive aminopeptidase OS=Homo sapiens GN=NPEPPS PE=4 SV=1	8.54E+06	8.43E+06	1.17E+07	1.01E+00
E9PM69	26S protease regulatory subunit 6A OS=Homo sapiens GN=PSMC3 PE=3 SV=1	1.67E+07	1.60E+07	1.80E+07	1.05E+00
E9PN41	Tetraspanin-4 (Fragment) OS=Homo sapiens GN=TSPAN4 PE=4 SV=1	6.25E+07	6.61E+07	6.17E+07	-1.06E+00
E9PS44	Interferon-induced transmembrane protein 3 OS=Homo sapiens GN=IFITM3 PE=4 SV=1	2.39E+08	2.97E+08	3.56E+08	-1.24E+00
F5GX33	Calcium-binding mitochondrial carrier protein Aralar2 OS=Homo sapiens GN=SLC25A13 PE=3 SV=1	7.26E+06	7.12E+06	4.91E+06	1.02E+00
F5GXX5	Dolichyl-diphosphooligosaccharide--protein glycosyltransferase subunit DAD1 OS=Homo sapiens GN=DAD1 PE=4 SV=1	1.39E+07	1.72E+07	1.56E+07	-1.23E+00
F5GZ27	Lon protease homolog OS=Homo sapiens GN=LONP1 PE=3 SV=1	1.11E+07	1.49E+07	1.20E+07	-1.34E+00
F5GZE5	Septin-7 OS=Homo sapiens GN=SEPT7 PE=4 SV=1	2.08E+07	2.79E+07	1.70E+07	-1.34E+00

F5H265	Polyubiquitin-C (Fragment) OS=Homo sapiens GN=UBC PE=4 SV=1	2.56E+08	2.95E+08	3.67E+08	-1.15E+00
F5H335	Eukaryotic translation initiation factor 3 subunit A OS=Homo sapiens GN=EIF3A PE=4 SV=1	1.31E+07	1.82E+07	1.57E+07	-1.39E+00
F5H3W1	Podocalyxin OS=Homo sapiens GN=PODXL PE=4 SV=1	0.00E+00	5.60E+07	4.64E+07	-1.00E+01
F5H608	ATP synthase subunit d, mitochondrial OS=Homo sapiens GN=ATP5H PE=4 SV=2	3.58E+07	3.36E+07	2.86E+07	1.07E+00
F6RFD5	Destrin OS=Homo sapiens GN=DSTN PE=4 SV=1	0.00E+00	6.68E+06	3.40E+07	-1.00E+01
F6U1T9	Calcineurin subunit B type 1 OS=Homo sapiens GN=PPP3R1 PE=4 SV=1	7.60E+07	8.70E+07	1.01E+08	-1.15E+00
F8VV40	Leukotriene A-4 hydrolase OS=Homo sapiens GN=LTA4H PE=4 SV=1	9.31E+06	0.00E+00	5.81E+06	1.00E+01
F8VV56	CD63 antigen OS=Homo sapiens GN=CD63 PE=4 SV=1	2.96E+08	3.60E+08	3.57E+08	-1.22E+00
F8VW92	Tubulin beta chain OS=Homo sapiens GN=TUBB PE=3 SV=1	5.24E+08	5.54E+08	6.12E+08	-1.06E+00
F8VWC5	60S ribosomal protein L18 OS=Homo sapiens GN=RPL18 PE=3 SV=1	1.38E+07	2.50E+07	4.49E+07	-1.81E+00
F8VWU4	Ras-related protein Rab-5C (Fragment) OS=Homo sapiens GN=RAB5C PE=4 SV=1	8.52E+06	1.15E+07	0.00E+00	-1.35E+00
F8VY04	Adenylate kinase 2, mitochondrial OS=Homo sapiens GN=AK2 PE=3 SV=1	1.62E+07	2.11E+07	2.13E+07	-1.30E+00
F8W181	60S ribosomal protein L6 (Fragment) OS=Homo sapiens GN=RPL6 PE=3 SV=1	7.26E+07	7.10E+07	1.06E+08	1.02E+00
F8W914	Reticulon-4 OS=Homo sapiens GN=RTN4 PE=4 SV=1	2.72E+07	4.67E+07	2.19E+07	-1.72E+00
F8WBS5	60S ribosomal protein L35a OS=Homo sapiens GN=RPL35A PE=4 SV=1	5.03E+07	0.00E+00	6.63E+07	1.00E+01
G3V1B3	60S ribosomal protein L21 OS=Homo sapiens GN=RPL21 PE=4 SV=1	4.65E+07	5.43E+07	5.91E+07	-1.17E+00
G3V279	Enhancer of rudimentary homolog OS=Homo sapiens GN=ERH PE=4 SV=1	0.00E+00	1.55E+07	8.84E+06	-1.00E+01
G3V3U4	Proteasome subunit alpha type OS=Homo sapiens GN=PSMA6 PE=3 SV=1	1.05E+07	8.84E+06	6.26E+06	1.19E+00
G3XAF4	L1 cell adhesion molecule, isoform CRA_a OS=Homo sapiens GN=L1CAM PE=4 SV=1	9.48E+06	9.37E+06	1.64E+07	1.01E+00
G8JLH4	Eukaryotic translation initiation factor 3 subunit L OS=Homo sapiens GN=EIF3L	1.27E+07	1.14E+07	9.81E+06	1.12E+00

	PE=4 SV=1				
H0YCQ8	Eukaryotic translation initiation factor 3 subunit M (Fragment) OS=Homo sapiens GN=EIF3M PE=4 SV=1	1.51E+07	1.64E+07	1.53E+07	-1.09E+00
H0YCU9	Transgelin (Fragment) OS=Homo sapiens GN=TAGLN PE=4 SV=1	8.49E+06	9.99E+06	2.10E+07	-1.18E+00
H0YD13	CD44 antigen (Fragment) OS=Homo sapiens GN=CD44 PE=4 SV=1	3.14E+08	3.43E+08	2.86E+08	-1.09E+00
H0YDD4	Dihydrolipoyllysine-residue acetyltransferase component of pyruvate dehydrogenase complex, mitochondrial (Fragment) OS=Homo sapiens GN=DLAT PE=3 SV=1	1.29E+07	1.46E+07	9.36E+06	-1.13E+00
H0YJG7	Activator of 90 kDa heat shock protein ATPase homolog 1 (Fragment) OS=Homo sapiens GN=AHSA1 PE=4 SV=1	0.00E+00	1.91E+07	2.37E+07	-1.00E+01
H0YM70	Proteasome activator complex subunit 2 OS=Homo sapiens GN=PSME2 PE=4 SV=1	1.56E+07	1.57E+07	1.33E+07	-1.01E+00
H0YMA1	Proteasome subunit alpha type (Fragment) OS=Homo sapiens GN=PSMA4 PE=3 SV=1	1.59E+07	1.46E+07	1.07E+07	1.09E+00
H3BQZ7	HCG2044799 OS=Homo sapiens GN=hCG_2044799 PE=4 SV=1	2.23E+07	1.87E+07	1.73E+07	1.20E+00
H3BRV0	Eukaryotic translation initiation factor 3 subunit C OS=Homo sapiens GN=EIF3C PE=4 SV=1	7.55E+06	4.68E+06	0.00E+00	1.62E+00
H3BUX2	Cytochrome b5 type B OS=Homo sapiens GN=CYB5B PE=3 SV=1	7.24E+06	3.48E+07	6.80E+06	-4.81E+00
H7C463	Mitochondrial inner membrane protein (Fragment) OS=Homo sapiens GN=IMMT PE=4 SV=1	0.00E+00	1.03E+07	0.00E+00	-1.00E+01
I3L4G8	Charged multivesicular body protein 6 (Fragment) OS=Homo sapiens GN=CHMP6 PE=4 SV=1	1.42E+07	2.30E+07	2.17E+07	-1.62E+00
IPI12345678	Streptavidin (S.avidinii)	1.35E+10	1.41E+10	1.13E+10	-1.04E+00
J3KNT0	Fascin OS=Homo sapiens GN=FSCN1 PE=3 SV=1	6.34E+07	5.92E+07	7.46E+07	1.07E+00
J3KT73	60S ribosomal protein L38 OS=Homo sapiens GN=RPL38 PE=3 SV=1	5.92E+07	7.26E+07	9.55E+07	-1.23E+00
J3QKR3	Proteasome subunit beta type-3 (Fragment) OS=Homo sapiens GN=PSMB3 PE=3 SV=1	2.04E+07	3.21E+07	1.75E+07	-1.57E+00

J3QQT2	60S ribosomal protein L17 (Fragment) OS=Homo sapiens GN=RPL17 PE=3 SV=1	3.56E+07	2.94E+07	3.22E+07	1.21E+00
J3QR09	Ribosomal protein L19 OS=Homo sapiens GN=RPL19 PE=3 SV=1	3.34E+07	4.15E+07	4.22E+07	-1.24E+00
J3QSV6	Ribosomal L1 domain-containing protein 1 (Fragment) OS=Homo sapiens GN=RSL1D1 PE=4 SV=1	2.54E+07	2.18E+07	2.33E+07	1.17E+00
K7EIV0	Calpain small subunit 1 OS=Homo sapiens GN=CAPNS1 PE=4 SV=1	0.00E+00	6.31E+06	6.34E+06	-1.00E+01
K7ESA3	Synaptic vesicle membrane protein VAT-1 homolog (Fragment) OS=Homo sapiens GN=VAT1 PE=4 SV=1	5.74E+06	6.23E+06	6.61E+06	-1.08E+00
O00161	Synaptosomal-associated protein 23 OS=Homo sapiens GN=SNAP23 PE=1 SV=1	2.64E+07	2.68E+07	4.40E+07	-1.02E+00
O00220	Tumor necrosis factor receptor superfamily member 10A OS=Homo sapiens GN=TNFRSF10A PE=1 SV=3	1.80E+07	0.00E+00	1.81E+07	1.00E+01
O00231	26S proteasome non-ATPase regulatory subunit 11 OS=Homo sapiens GN=PSMD11 PE=1 SV=3	9.41E+06	6.43E+06	6.95E+06	1.46E+00
O00303	Eukaryotic translation initiation factor 3 subunit F OS=Homo sapiens GN=EIF3F PE=1 SV=1	6.50E+06	8.11E+06	7.67E+06	-1.25E+00
O00411	DNA-directed RNA polymerase, mitochondrial OS=Homo sapiens GN=POLRMT PE=1 SV=2	5.68E+06	0.00E+00	9.53E+06	1.00E+01
O14818	Proteasome subunit alpha type-7 OS=Homo sapiens GN=PSMA7 PE=1 SV=1	2.23E+07	3.04E+07	2.51E+07	-1.37E+00
O14828	Secretory carrier-associated membrane protein 3 OS=Homo sapiens GN=SCAMP3 PE=1 SV=3	6.61E+07	6.08E+07	1.04E+08	1.09E+00
O14880	Microsomal glutathione S-transferase 3 OS=Homo sapiens GN=MGST3 PE=1 SV=1	2.48E+07	3.11E+07	1.89E+07	-1.26E+00
O14979-3	Isoform 3 of Heterogeneous nuclear ribonucleoprotein D-like OS=Homo sapiens GN=HNRPDL	1.42E+07	1.35E+07	1.48E+07	1.05E+00
O15031	Plexin-B2 OS=Homo sapiens GN=PLXNB2 PE=1 SV=3	4.05E+06	2.79E+06	7.58E+06	1.45E+00
O15127	Secretory carrier-associated membrane protein 2 OS=Homo sapiens GN=SCAMP2 PE=1 SV=2	1.69E+07	0.00E+00	4.93E+06	1.00E+01

O15372	Eukaryotic translation initiation factor 3 subunit H OS=Homo sapiens GN=EIF3H PE=1 SV=1	6.92E+06	7.95E+06	8.46E+06	-1.15E+00
O15439-2	Isoform 2 of Multidrug resistance-associated protein 4 OS=Homo sapiens GN=ABCC4	9.43E+06	9.90E+06	7.28E+06	-1.05E+00
O43242	26S proteasome non-ATPase regulatory subunit 3 OS=Homo sapiens GN=PSMD3 PE=1 SV=2	6.31E+06	6.94E+06	5.84E+06	-1.10E+00
O43657	Tetraspanin-6 OS=Homo sapiens GN=TSPAN6 PE=1 SV=1	4.44E+07	4.75E+07	3.58E+07	-1.07E+00
O43813	LanC-like protein 1 OS=Homo sapiens GN=LANCL1 PE=1 SV=1	1.75E+07	2.02E+07	2.83E+07	-1.16E+00
O60814	Histone H2B type 1-K OS=Homo sapiens GN=HIST1H2BK PE=1 SV=3	1.72E+08	1.90E+08	1.16E+08	-1.11E+00
O60831	PRA1 family protein 2 OS=Homo sapiens GN=PRAF2 PE=1 SV=1	1.53E+07	2.71E+07	1.38E+07	-1.77E+00
O75110	Probable phospholipid-transporting ATPase IIA OS=Homo sapiens GN=ATP9A PE=1 SV=3	1.27E+07	1.31E+07	1.55E+07	-1.03E+00
O75340-2	Isoform 2 of Programmed cell death protein 6 OS=Homo sapiens GN=PDCD6	2.23E+07	2.74E+07	1.87E+07	-1.23E+00
O75494-5	Isoform 5 of Serine/arginine-rich splicing factor 10 OS=Homo sapiens GN=SRSF10	1.44E+07	1.41E+07	1.22E+07	1.02E+00
O75533	Splicing factor 3B subunit 1 OS=Homo sapiens GN=SF3B1 PE=1 SV=3	1.25E+07	1.37E+07	1.31E+07	-1.10E+00
O95197-3	Isoform 3 of Reticulon-3 OS=Homo sapiens GN=RTN3	0.00E+00	1.44E+07	1.55E+07	-1.00E+01
O95372	Acyl-protein thioesterase 2 OS=Homo sapiens GN=LYPLA2 PE=1 SV=1	1.99E+07	2.18E+07	2.50E+07	-1.10E+00
O95807	Transmembrane protein 50A OS=Homo sapiens GN=TMEM50A PE=1 SV=1	1.05E+07	4.74E+06	4.01E+06	2.22E+00
P00338	L-lactate dehydrogenase A chain OS=Homo sapiens GN=LDHA PE=1 SV=2	4.05E+08	5.50E+08	5.66E+08	-1.36E+00
P00367	Glutamate dehydrogenase 1, mitochondrial OS=Homo sapiens GN=GLUD1 PE=1 SV=2	1.08E+07	5.92E+06	1.03E+07	1.83E+00
P00390-2	Isoform Cytoplasmic of Glutathione reductase, mitochondrial OS=Homo sapiens GN=GSR	2.62E+07	2.37E+07	1.68E+07	1.10E+00
P00403	Cytochrome c oxidase subunit 2 OS=Homo sapiens GN=MT-CO2 PE=1 SV=1	2.73E+07	3.66E+07	1.98E+07	-1.34E+00

P00491	Purine nucleoside phosphorylase OS=Homo sapiens GN=PNP PE=1 SV=2	4.68E+06	5.78E+06	6.83E+06	-1.23E+00
P00492	Hypoxanthine-guanine phosphoribosyltransferase OS=Homo sapiens GN=HPRT1 PE=1 SV=2	1.04E+07	9.93E+06	8.92E+06	1.05E+00
P00519	Tyrosine-protein kinase ABL1 OS=Homo sapiens GN=ABL1 PE=1 SV=4	5.08E+06	0.00E+00	9.54E+06	1.00E+01
P00568	Adenylate kinase isoenzyme 1 OS=Homo sapiens GN=AK1 PE=1 SV=3	0.00E+00	5.99E+06	9.91E+06	-1.00E+01
P01891	HLA class I histocompatibility antigen, A-68 alpha chain OS=Homo sapiens GN=HLA-A PE=1 SV=4	8.48E+07	1.14E+08	5.61E+07	-1.35E+00
P02786	Transferrin receptor protein 1 OS=Homo sapiens GN=TFRC PE=1 SV=2	4.11E+08	4.54E+08	4.11E+08	-1.11E+00
P04843	Dolichyl-diphosphooligosaccharide--protein glycosyltransferase subunit 1 OS=Homo sapiens GN=RPN1 PE=1 SV=1	1.99E+07	3.09E+07	1.11E+07	-1.55E+00
P05141	ADP/ATP translocase 2 OS=Homo sapiens GN=SLC25A5 PE=1 SV=7	1.17E+08	1.46E+08	1.07E+08	-1.25E+00
P05186-2	Isoform 2 of Alkaline phosphatase, tissue-nonspecific isozyme OS=Homo sapiens GN=ALPL	1.75E+07	3.73E+07	1.67E+07	-2.13E+00
P05198	Eukaryotic translation initiation factor 2 subunit 1 OS=Homo sapiens GN=EIF2S1 PE=1 SV=3	1.34E+07	9.92E+06	8.89E+06	1.36E+00
P06493	Cyclin-dependent kinase 1 OS=Homo sapiens GN=CDK1 PE=1 SV=3	1.14E+07	1.05E+07	1.99E+07	1.09E+00
P06576	ATP synthase subunit beta, mitochondrial OS=Homo sapiens GN=ATP5B PE=1 SV=3	2.27E+07	3.61E+07	2.06E+07	-1.59E+00
P06748-2	Isoform 2 of Nucleophosmin OS=Homo sapiens GN=NPM1	4.10E+08	4.49E+08	4.76E+08	-1.09E+00
P06899	Histone H2B type 1-J OS=Homo sapiens GN=HIST1H2BJ PE=1 SV=3	1.73E+08	2.61E+08	1.52E+08	-1.51E+00
P07195	L-lactate dehydrogenase B chain OS=Homo sapiens GN=LDHB PE=1 SV=2	3.94E+08	4.23E+08	4.31E+08	-1.07E+00
P08107	Heat shock 70 kDa protein 1A/1B OS=Homo sapiens GN=HSPA1A PE=1 SV=5	2.95E+08	3.71E+08	4.05E+08	-1.26E+00
P08559-3	Isoform 3 of Pyruvate dehydrogenase E1 component subunit alpha, somatic form, mitochondrial OS=Homo sapiens GN=PDHA1	0.00E+00	8.27E+06	4.32E+06	-1.00E+01

P08574	Cytochrome c1, heme protein, mitochondrial OS=Homo sapiens GN=CYC1 PE=1 SV=3	2.32E+07	2.12E+07	2.18E+07	1.09E+00
P08670	Vimentin OS=Homo sapiens GN=VIM PE=1 SV=4	1.10E+08	6.03E+07	8.07E+07	1.82E+00
P09382	Galectin-1 OS=Homo sapiens GN=LGALS1 PE=1 SV=2	1.58E+07	1.84E+07	1.89E+07	-1.16E+00
P09543-2	Isoform CNPI of 2',3'-cyclic-nucleotide 3'-phosphodiesterase OS=Homo sapiens GN=CNP	6.09E+06	6.89E+06	4.49E+06	-1.13E+00
P10620	Microsomal glutathione S-transferase 1 OS=Homo sapiens GN=MGST1 PE=1 SV=1	1.18E+07	1.12E+07	4.93E+06	1.06E+00
P11177-2	Isoform 2 of Pyruvate dehydrogenase E1 component subunit beta, mitochondrial OS=Homo sapiens GN=PDHB	2.98E+07	0.00E+00	7.80E+06	1.00E+01
P11940-2	Isoform 2 of Polyadenylate-binding protein 1 OS=Homo sapiens GN=PABPC1	4.69E+07	5.02E+07	7.00E+07	-1.07E+00
P12236	ADP/ATP translocase 3 OS=Homo sapiens GN=SLC25A6 PE=1 SV=4	1.13E+08	1.46E+08	1.07E+08	-1.29E+00
P13010	X-ray repair cross-complementing protein 5 OS=Homo sapiens GN=XRCC5 PE=1 SV=3	9.10E+07	9.04E+07	9.36E+07	1.01E+00
P14174	Macrophage migration inhibitory factor OS=Homo sapiens GN=MIF PE=1 SV=4	1.95E+08	1.86E+08	2.92E+08	1.05E+00
P14923	Junction plakoglobin OS=Homo sapiens GN=JUP PE=1 SV=3	1.65E+07	3.48E+06	5.41E+06	4.74E+00
P15151-3	Isoform Gamma of Poliovirus receptor OS=Homo sapiens GN=PVR	2.38E+07	1.53E+07	2.51E+07	1.56E+00
P15291	Beta-1,4-galactosyltransferase 1 OS=Homo sapiens GN=B4GALT1 PE=1 SV=5	3.96E+07	4.59E+07	4.10E+07	-1.16E+00
P15559-2	Isoform 2 of NAD(P)H dehydrogena	4.02E+07	4.24E+07	5.61E+07	-1.05E+00
P15880	40S ribosomal protein S2 OS=Homo sapiens GN=RPS2 PE=1 SV=2	8.63E+07	2.21E+07	8.33E+07	3.90E+00
P16152	Carbonyl reducta	1.99E+07	1.98E+07	2.97E+07	1.01E+00
P17987	T-complex protein 1 subunit alpha OS=Homo sapiens GN=TCP1 PE=1 SV=1	3.01E+07	3.42E+07	2.66E+07	-1.14E+00
P20645	Cation-dependent mannose-6-phosphate receptor OS=Homo sapiens GN=M6PR PE=1 SV=1	3.41E+07	3.93E+07	3.27E+07	-1.15E+00

P22392-2	Isoform 3 of Nucleoside diphosphate kinase B OS=Homo sapiens GN=NME2	4.79E+07	1.25E+08	5.78E+07	-2.61E+00
P23284	Peptidyl-prolyl cis-trans isomerase B OS=Homo sapiens GN=PPIB PE=1 SV=2	4.24E+07	6.02E+07	4.24E+07	-1.42E+00
P23396	40S ribosomal protein S3 OS=Homo sapiens GN=RPS3 PE=1 SV=2	1.35E+08	1.52E+08	1.30E+08	-1.13E+00
P23526	Adenosylhomocysteinase OS=Homo sapiens GN=AHCY PE=1 SV=4	3.83E+07	4.17E+07	4.76E+07	-1.09E+00
P24390	ER lumen protein retaining receptor 1 OS=Homo sapiens GN=KDELR1 PE=1 SV=1	1.32E+07	1.14E+07	1.04E+07	1.16E+00
P24539	ATP synthase subunit b, mitochondrial OS=Homo sapiens GN=ATP5F1 PE=1 SV=2	1.05E+07	1.13E+07	8.70E+06	-1.07E+00
P25398	40S ribosomal protein S12 OS=Homo sapiens GN=RPS12 PE=1 SV=3	4.03E+07	4.04E+07	1.75E+07	-1.00E+00
P25705	ATP synthase subunit alpha, mitochondrial OS=Homo sapiens GN=ATP5A1 PE=1 SV=1	4.95E+07	6.40E+07	3.67E+07	-1.29E+00
P25786	Proteasome subunit alpha type-1 OS=Homo sapiens GN=PSMA1 PE=1 SV=1	1.71E+07	1.55E+07	2.15E+07	1.10E+00
P25788-2	Isoform 2 of Proteasome subunit alpha type-3 OS=Homo sapiens GN=PSMA3	7.34E+06	1.08E+07	1.39E+07	-1.47E+00
P26196	Probable ATP-dependent RNA helicase DDX6 OS=Homo sapiens GN=DDX6 PE=1 SV=2	4.16E+06	0.00E+00	1.28E+07	1.00E+01
P26373	60S ribosomal protein L13 OS=Homo sapiens GN=RPL13 PE=1 SV=4	5.79E+07	6.08E+07	7.43E+07	-1.05E+00
P27348	14-3-3 protein theta OS=Homo sapiens GN=YWHAQ PE=1 SV=1	1.05E+08	1.08E+08	1.28E+08	-1.02E+00
P27824	Calnexin OS=Homo sapiens GN=CANX PE=1 SV=2	7.33E+08	9.37E+08	7.21E+08	-1.28E+00
P28070	Proteasome subunit beta type-4 OS=Homo sapiens GN=PSMB4 PE=1 SV=4	2.37E+07	2.66E+07	2.26E+07	-1.12E+00
P30040	Endoplasmic reticulum resident protein 29 OS=Homo sapiens GN=ERP29 PE=1 SV=4	1.39E+07	1.40E+07	1.26E+07	-1.01E+00
P30050	60S ribosomal protein L12 OS=Homo sapiens GN=RPL12 PE=1 SV=1	8.16E+07	7.73E+07	7.48E+07	1.06E+00
P30419	Glycylpeptide N-tetradecanoyltransferase 1 OS=Homo sapiens GN=NMT1 PE=1 SV=2	6.58E+06	1.19E+07	7.05E+06	-1.80E+00

P31689	DnaJ homolog subfamily A member 1 OS=Homo sapiens GN=DNAJA1 PE=1 SV=2	3.09E+07	3.93E+07	3.14E+07	-1.27E+00
P31930	Cytochrome b-c1 complex subunit 1, mitochondrial OS=Homo sapiens GN=UQCRC1 PE=1 SV=3	2.97E+07	2.74E+07	3.46E+07	1.08E+00
P31942-3	Isoform 3 of Heterogeneous nuclear ribonucleoprotein H3 OS=Homo sapiens GN=HNRNPH3	1.21E+07	9.15E+06	1.27E+07	1.32E+00
P31943	Heterogeneous nuclear ribonucleoprotein H OS=Homo sapiens GN=HNRNPH1 PE=1 SV=4	6.22E+07	6.38E+07	7.45E+07	-1.03E+00
P31946-2	Isoform Short of 14-3-3 protein beta/alpha OS=Homo sapiens GN=YWHAB	1.01E+08	1.08E+08	1.28E+08	-1.06E+00
P33316-2	Isoform 2 of Deoxyuridine 5'-triphosphate nucleotidohydrolase, mitochondrial OS=Homo sapiens GN=DUT	1.35E+07	8.92E+06	1.27E+07	1.51E+00
P33947	ER lumen protein retaining receptor 2 OS=Homo sapiens GN=KDELR2 PE=1 SV=1	2.21E+07	1.93E+07	1.87E+07	1.15E+00
P35232	Prohibitin OS=Homo sapiens GN=PHB PE=1 SV=1	2.89E+07	3.46E+07	2.47E+07	-1.20E+00
P35237	Serpin B6 OS=Homo sapiens GN=SERPINB6 PE=1 SV=3	1.73E+07	2.40E+07	3.39E+07	-1.39E+00
P35268	60S ribosomal protein L22 OS=Homo sapiens GN=RPL22 PE=1 SV=2	6.74E+07	7.63E+07	7.15E+07	-1.13E+00
P35659-2	Isoform 2 of Protein DEK OS=Homo sapiens GN=DEK	7.92E+06	1.64E+07	8.59E+06	-2.07E+00
P35998	26S protease regulatory subunit 7 OS=Homo sapiens GN=PSMC2 PE=1 SV=3	0.00E+00	1.11E+07	8.46E+06	-1.00E+01
P36578	60S ribosomal protein L4 OS=Homo sapiens GN=RPL4 PE=1 SV=5	7.37E+07	7.08E+07	6.80E+07	1.04E+00
P37802	Transgelin-2 OS=Homo sapiens GN=TAGLN2 PE=1 SV=3	1.09E+08	9.33E+07	1.52E+08	1.16E+00
P38919	Eukaryotic initiation factor 4A-III OS=Homo sapiens GN=EIF4A3 PE=1 SV=4	6.35E+07	6.16E+07	6.95E+07	1.03E+00
P39023	60S ribosomal protein L3 OS=Homo sapiens GN=RPL3 PE=1 SV=2	7.30E+07	8.55E+07	1.49E+08	-1.17E+00
P40429	60S ribosomal protein L13a OS=Homo sapiens GN=RPL13A PE=1 SV=2	0.00E+00	4.19E+07	2.43E+07	-1.00E+01
P41091	Eukaryotic translation initiation factor 2 subunit 3 OS=Homo sapiens GN=EIF2S3	1.70E+07	2.13E+07	1.85E+07	-1.25E+00

	PE=1 SV=3				
P41250	Glycine--tRNA ligase OS=Homo sapiens GN=GARS PE=1 SV=3	2.07E+07	2.20E+07	2.36E+07	-1.06E+00
P42126-2	Isoform 2 of Enoyl-CoA delta isomerase 1, mitochondrial OS=Homo sapiens GN=ECI1	0.00E+00	1.08E+07	0.00E+00	-1.00E+01
P42765	3-ketoacyl-CoA thiolase, mitochondrial OS=Homo sapiens GN=ACAA2 PE=1 SV=2	1.56E+07	1.81E+07	1.45E+07	-1.16E+00
P43007	Neutral amino acid transporter A OS=Homo sapiens GN=SLC1A4 PE=1 SV=1	1.03E+07	1.22E+07	1.89E+07	-1.18E+00
P45880-2	Isoform 2 of Voltage-dependent anion-selective channel protein 2 OS=Homo sapiens GN=VDAC2	7.45E+07	9.70E+07	3.51E+07	-1.30E+00
P45974-2	Isoform Short of Ubiquitin carboxyl-terminal hydrolase 5 OS=Homo sapiens GN=USP5	1.28E+07	1.62E+07	2.05E+07	-1.26E+00
P46781	40S ribosomal protein S9 OS=Homo sapiens GN=RPS9 PE=1 SV=3	5.40E+07	5.48E+07	6.03E+07	-1.02E+00
P46782	40S ribosomal protein S5 OS=Homo sapiens GN=RPS5 PE=1 SV=4	4.14E+07	4.60E+07	3.99E+07	-1.11E+00
P46940	Ras GTPase-activating-like protein IQGAP1 OS=Homo sapiens GN=IQGAP1 PE=1 SV=1	3.73E+07	4.38E+07	3.85E+07	-1.18E+00
P46977	Dolichyl-diphosphooligosaccharide--protein glycosyltransferase subunit STT3A OS=Homo sapiens GN=STT3A PE=1 SV=2	1.22E+07	1.16E+07	7.36E+06	1.05E+00
P47914	60S ribosomal protein L29 OS=Homo sapiens GN=RPL29 PE=1 SV=2	9.91E+07	0.00E+00	1.18E+08	1.00E+01
P48047	ATP synthase subunit O, mitochondrial OS=Homo sapiens GN=ATP5O PE=1 SV=1	2.10E+07	1.48E+07	9.18E+06	1.42E+00
P48643	T-complex protein 1 subunit epsilon OS=Homo sapiens GN=CCT5 PE=1 SV=1	3.89E+07	4.87E+07	4.53E+07	-1.25E+00
P49368	T-complex protein 1 subunit gamma OS=Homo sapiens GN=CCT3 PE=1 SV=4	7.62E+07	9.00E+07	7.82E+07	-1.18E+00
P49411	Elongation factor Tu, mitochondrial OS=Homo sapiens GN=TUFM PE=1 SV=2	2.46E+07	2.46E+07	3.24E+07	1.00E+00

P49419-2	Isoform 2 of Alpha-aminoadipic semialdehyde dehydrogenase OS=Homo sapiens GN=ALDH7A1	8.72E+06	1.07E+07	7.74E+06	-1.23E+00
P49721	Proteasome subunit beta type-2 OS=Homo sapiens GN=PSMB2 PE=1 SV=1	1.13E+07	1.30E+07	0.00E+00	-1.15E+00
P49755	Transmembrane emp24 domain-containing protein 10 OS=Homo sapiens GN=TMED10 PE=1 SV=2	3.44E+07	3.57E+07	1.75E+07	-1.04E+00
P50416-2	Isoform 2 of Carnitine O-palmitoyltransferase 1, liver isoform OS=Homo sapiens GN=CPT1A	5.09E+06	1.11E+07	0.00E+00	-2.17E+00
P50443	Sulfate transporter OS=Homo sapiens GN=SLC26A2 PE=1 SV=2	6.21E+06	7.55E+06	4.83E+06	-1.22E+00
P50990	T-complex protein 1 subunit theta OS=Homo sapiens GN=CCT8 PE=1 SV=4	5.00E+07	5.86E+07	4.32E+07	-1.17E+00
P51572	B-cell receptor-associated protein 31 OS=Homo sapiens GN=BCAP31 PE=1 SV=3	0.00E+00	1.08E+07	4.50E+06	-1.00E+01
P53618	Coatomer subunit beta OS=Homo sapiens GN=COPB1 PE=1 SV=3	8.34E+06	7.53E+06	8.67E+06	1.11E+00
P53621	Coatomer subunit alpha OS=Homo sapiens GN=COPA PE=1 SV=2	1.68E+07	1.40E+07	1.41E+07	1.20E+00
P54289-4	Isoform 4 of Voltage-dependent calcium channel subunit alpha-2/delta-1 OS=Homo sapiens GN=CACNA2D1	3.41E+07	4.21E+07	2.47E+07	-1.23E+00
P54886-2	Isoform Short of Delta-1-pyrroline-5-carboxylate synthase OS=Homo sapiens GN=ALDH18A1	1.03E+07	1.33E+07	1.01E+07	-1.29E+00
P55809	Succinyl-CoA:3-ketoacid coenzyme A transferase 1, mitochondrial OS=Homo sapiens GN=OXCT1 PE=1 SV=1	2.82E+07	3.44E+07	2.52E+07	-1.22E+00
P56192	Methionine--tRNA ligase, cytoplasmic OS=Homo sapiens GN=MARS PE=1 SV=2	0.00E+00	7.64E+06	7.47E+06	-1.00E+01
P60468	Protein transport protein Sec61 subunit beta OS=Homo sapiens GN=SEC61B PE=1 SV=2	5.49E+06	5.90E+06	2.47E+06	-1.08E+00
P60842	Eukaryotic initiation factor 4A-I OS=Homo sapiens GN=EIF4A1 PE=1 SV=1	1.34E+08	1.09E+08	1.35E+08	1.23E+00
P60953	Cell division control protein 42 homolog OS=Homo sapiens GN=CDC42 PE=1 SV=2	1.52E+07	1.69E+07	9.63E+06	-1.11E+00

P61019-2	Isoform 2 of Ras-related protein Rab-2A OS=Homo sapiens GN=RAB2A	1.02E+07	8.43E+06	1.16E+07	1.21E+00
P61026	Ras-related protein Rab-10 OS=Homo sapiens GN=RAB10 PE=1 SV=1	2.23E+07	5.23E+07	2.87E+07	-2.35E+00
P61158	Actin-related protein 3 OS=Homo sapiens GN=ACTR3 PE=1 SV=3	2.36E+07	2.21E+07	2.52E+07	1.07E+00
P61160	Actin-related protein 2 OS=Homo sapiens GN=ACTR2 PE=1 SV=1	1.14E+07	1.04E+07	1.46E+07	1.10E+00
P61224-3	Isoform 3 of Ras-related protein Rap-1b OS=Homo sapiens GN=RAP1B	4.14E+07	5.81E+07	1.03E+07	-1.41E+00
P61586	Transforming protein RhoA OS=Homo sapiens GN=RHOA PE=1 SV=1	3.49E+07	4.22E+07	1.25E+07	-1.21E+00
P61604	10 kDa heat shock protein, mitochondrial OS=Homo sapiens GN=HSPE1 PE=1 SV=2	2.06E+07	1.87E+07	1.44E+07	1.10E+00
P61619	Protein transport protein Sec61 subunit alpha isoform 1 OS=Homo sapiens GN=SEC61A1 PE=1 SV=2	1.34E+07	1.42E+07	9.21E+06	-1.06E+00
P61981	14-3-3 protein gamma OS=Homo sapiens GN=YWHAG PE=1 SV=2	1.06E+08	1.01E+08	1.22E+08	1.05E+00
P62249	40S ribosomal protein S16 OS=Homo sapiens GN=RPS16 PE=1 SV=2	1.96E+07	2.74E+07	1.85E+07	-1.40E+00
P62258	14-3-3 protein epsilon OS=Homo sapiens GN=YWHAE PE=1 SV=1	1.33E+08	1.25E+08	1.42E+08	1.06E+00
P62280	40S ribosomal protein S11 OS=Homo sapiens GN=RPS11 PE=1 SV=3	5.06E+07	4.76E+07	5.39E+07	1.06E+00
P62333	26S protease regulatory subunit 10B OS=Homo sapiens GN=PSMC6 PE=1 SV=1	1.11E+07	1.89E+07	1.23E+07	-1.70E+00
P62701	40S ribosomal protein S4, X isoform OS=Homo sapiens GN=RPS4X PE=1 SV=2	5.63E+07	4.58E+07	3.68E+07	1.23E+00
P62714	Serine/threonine-protein phosphatase 2A catalytic subunit beta isoform OS=Homo sapiens GN=PPP2CB PE=1 SV=1	1.26E+07	8.74E+06	1.35E+07	1.44E+00
P62745	Rho-related GTP-binding protein RhoB OS=Homo sapiens GN=RHOB PE=1 SV=1	1.88E+07	1.67E+07	1.14E+07	1.13E+00
P62753	40S ribosomal protein S6 OS=Homo sapiens GN=RPS6 PE=1 SV=1	6.70E+07	7.33E+07	7.15E+07	-1.10E+00
P62851	40S ribosomal protein S25 OS=Homo sapiens GN=RPS25 PE=1 SV=1	3.64E+07	6.35E+07	2.05E+07	-1.74E+00
P62873	Guanine nucleotide-binding protein G(I)/G(S)/G(T) subunit beta-1 OS=Homo sapiens GN=GNB1 PE=1 SV=3	3.10E+07	1.86E+07	1.06E+07	1.66E+00

P62879	Guanine nucleotide-binding protein G(I)/G(S)/G(T) subunit beta-2 OS=Homo sapiens GN=GNB2 PE=1 SV=3	1.55E+07	1.96E+07	1.04E+07	-1.26E+00
P62913-2	Isoform 2 of 60S ribosomal protein L11 OS=Homo sapiens GN=RPL11	2.76E+07	5.27E+07	4.03E+07	-1.91E+00
P63000	Ras-related C3 botulinum toxin substrate 1 OS=Homo sapiens GN=RAC1 PE=1 SV=1	1.91E+07	1.73E+07	5.53E+06	1.10E+00
P63241	Eukaryotic translation initiation factor 5A-1 OS=Homo sapiens GN=EIF5A PE=1 SV=2	8.65E+07	8.88E+07	1.20E+08	-1.03E+00
P63244	Guanine nucleotide-binding protein subunit beta-2-like 1 OS=Homo sapiens GN=GNB2L1 PE=1 SV=3	4.61E+07	4.63E+07	5.22E+07	-1.00E+00
P78310-2	Isoform 2 of Coxsackievirus and adenovirus receptor OS=Homo sapiens GN=CXADR	1.47E+07	1.61E+07	2.20E+07	-1.10E+00
P78371	T-complex protein 1 subunit beta OS=Homo sapiens GN=CCT2 PE=1 SV=4	2.24E+07	3.56E+07	2.52E+07	-1.59E+00
P78527	DNA-dependent protein kinase catalytic subunit OS=Homo sapiens GN=PRKDC PE=1 SV=3	1.86E+07	2.46E+07	1.57E+07	-1.32E+00
P82909	28S ribosomal protein S36, mitochondrial OS=Homo sapiens GN=MRPS36 PE=1 SV=2	2.85E+07	4.02E+07	2.85E+07	-1.41E+00
P83881	60S ribosomal protein L36a OS=Homo sapiens GN=RPL36A PE=1 SV=2	0.00E+00	3.87E+07	0.00E+00	-1.00E+01
Q00325-2	Isoform B of Phosphate carrier protein, mitochondrial OS=Homo sapiens GN=SLC25A3	4.07E+07	5.86E+07	3.09E+07	-1.44E+00
Q02790	Peptidyl-prolyl cis-trans isomerase FKBP4 OS=Homo sapiens GN=FKBP4 PE=1 SV=3	3.42E+07	3.05E+07	3.47E+07	1.12E+00
Q03135	Caveolin-1 OS=Homo sapiens GN=CAV1 PE=1 SV=4	8.02E+07	5.53E+07	5.32E+07	1.45E+00
Q04637-6	Isoform E of Eukaryotic translation initiation factor 4 gamma 1 OS=Homo sapiens GN=EIF4G1	8.45E+06	7.42E+06	1.11E+07	1.14E+00
Q04695	Keratin, type I cytoskeletal 17 OS=Homo sapiens GN=KRT17 PE=1 SV=2	4.99E+08	1.86E+08	2.00E+08	2.68E+00
Q06830	Peroxiredoxin-1 OS=Homo sapiens GN=PRDX1 PE=1 SV=1	2.65E+08	3.02E+08	2.27E+08	-1.14E+00

Q07021	Complement component 1 Q subcomponent-binding protein, mitochondrial OS=Homo sapiens GN=C1QBP PE=1 SV=1	4.38E+07	4.59E+07	3.06E+07	-1.05E+00
Q07065	Cytoskeleton-associated protein 4 OS=Homo sapiens GN=CKAP4 PE=1 SV=2	3.91E+07	4.04E+07	3.77E+07	-1.03E+00
Q07617	Sperm-associated antigen 1 OS=Homo sapiens GN=SPAG1 PE=1 SV=3	4.65E+06	6.95E+06	9.09E+06	-1.50E+00
Q09028-3	Isoform 3 of Histone-binding protein RBBP4 OS=Homo sapiens GN=RBBP4	1.90E+07	1.90E+07	2.30E+07	1.00E+00
Q10589	Bone marrow stromal antigen 2 OS=Homo sapiens GN=BST2 PE=1 SV=1	4.78E+08	5.38E+08	2.58E+08	-1.13E+00
Q13126-4	Isoform 4 of S-methyl-5'-thioadenosine phosphorylase OS=Homo sapiens GN=MTAP	0.00E+00	1.43E+07	1.19E+07	-1.00E+01
Q13200	26S proteasome non-ATPase regulatory subunit 2 OS=Homo sapiens GN=PSMD2 PE=1 SV=3	1.78E+07	1.73E+07	1.83E+07	1.03E+00
Q13247-3	Isoform SRP55-3 of Serine/arginine-rich splicing factor 6 OS=Homo sapiens GN=SRSF6	0.00E+00	1.32E+07	1.62E+07	-1.00E+01
Q13283	Ras GTPase-activating protein-binding protein 1 OS=Homo sapiens GN=G3BP1 PE=1 SV=1	1.39E+07	1.19E+07	2.18E+07	1.17E+00
Q13347	Eukaryotic translation initiation factor 3 subunit I OS=Homo sapiens GN=EIF3I PE=1 SV=1	4.70E+06	9.79E+06	7.48E+06	-2.08E+00
Q13423	NAD(P) transhydrogenase, mitochondrial OS=Homo sapiens GN=NNT PE=1 SV=3	1.28E+07	3.53E+07	1.48E+07	-2.75E+00
Q14103-3	Isoform 3 of Heterogeneous nuclear ribonucleoprotein D0 OS=Homo sapiens GN=HNRNPD	4.98E+07	5.76E+07	5.61E+07	-1.16E+00
Q14126	Desmoglein-2 OS=Homo sapiens GN=DSG2 PE=1 SV=2	2.36E+07	1.24E+07	2.75E+07	1.90E+00
Q14165	Malectin OS=Homo sapiens GN=MLEC PE=1 SV=1	1.78E+07	2.41E+07	1.81E+07	-1.35E+00
Q14247-3	Isoform 3 of Src substrate cortactin OS=Homo sapiens GN=CTTN	1.21E+07	1.29E+07	2.21E+07	-1.06E+00
Q15005	Signal peptidase complex subunit 2 OS=Homo sapiens GN=SPCS2 PE=1 SV=3	1.18E+06	8.93E+06	0.00E+00	-7.57E+00
Q15056-2	Isoform Short of Eukaryotic translation initiation factor 4H OS=Homo sapiens	1.96E+07	1.71E+07	2.60E+07	1.15E+00

	GN=EIF4H				
Q15393	Splicing factor 3B subunit 3 OS=Homo sapiens GN=SF3B3 PE=1 SV=4	1.14E+07	1.60E+07	1.23E+07	-1.41E+00
Q15427	Splicing factor 3B subunit 4 OS=Homo sapiens GN=SF3B4 PE=1 SV=1	7.20E+06	1.60E+07	1.60E+07	-2.22E+00
Q15758	Neutral amino acid transporter B(0) OS=Homo sapiens GN=SLC1A5 PE=1 SV=2	1.64E+08	1.80E+08	2.09E+08	-1.10E+00
Q15836	Vesicle-associated membrane protein 3 OS=Homo sapiens GN=VAMP3 PE=1 SV=3	2.39E+07	2.66E+07	3.68E+07	-1.11E+00
Q16629-3	Isoform 3 of Serine/arginine-rich splicing factor 7 OS=Homo sapiens GN=SRSF7	6.84E+06	9.23E+06	0.00E+00	-1.35E+00
Q16719	Kynureninase OS=Homo sapiens GN=KYNU PE=1 SV=1	7.18E+06	7.37E+06	8.48E+06	-1.03E+00
Q16836	Hydroxyacyl-coenzyme A dehydrogenase, mitochondrial OS=Homo sapiens GN=HADH PE=1 SV=3	1.56E+07	2.01E+07	1.58E+07	-1.29E+00
Q3B7A4	60S acidic ribosomal protein P0 OS=Homo sapiens GN=RPLP0 PE=2 SV=1	9.56E+07	1.18E+08	9.19E+07	-1.23E+00
Q5M775-4	Isoform 4 of Cytospin-B OS=Homo sapiens GN=SPECC1	3.68E+07	2.80E+07	7.00E+07	1.32E+00
Q5QPM0	RNA binding protein, autoantigenic (HnRNP-associated with lethal yellow homolog (Mouse)) (Fragment) OS=Homo sapiens GN=RALY PE=2 SV=1	1.15E+07	1.12E+07	7.53E+06	1.03E+00
Q5T092	Protein RER1 (Fragment) OS=Homo sapiens GN=RER1 PE=2 SV=1	1.37E+07	1.99E+07	9.01E+06	-1.45E+00
Q5T3F8-2	Isoform 2 of Transmembrane protein 63B OS=Homo sapiens GN=TMEM63B	6.97E+06	7.16E+06	6.11E+06	-1.03E+00
Q5T4L4	40S ribosomal protein S27 OS=Homo sapiens GN=RPS27 PE=4 SV=1	4.05E+07	5.03E+07	4.91E+07	-1.24E+00
Q5T8R5	Monocarboxylate transporter 1 (Fragment) OS=Homo sapiens GN=SLC16A1 PE=2 SV=1	5.02E+07	0.00E+00	2.12E+07	1.00E+01
Q5T9A4	ATPase family AAA domain-containing protein 3B OS=Homo sapiens GN=ATAD3B PE=1 SV=1	1.73E+07	1.70E+07	1.89E+07	1.02E+00
Q68CR9	Aspartate--tRNA ligase, cytoplasmic OS=Homo sapiens GN=DKFZp781B11202 PE=2 SV=1	1.44E+07	1.28E+07	1.14E+07	1.12E+00
Q6N075	Major facilitator superfamily domain-containing protein 5 OS=Homo sapiens	6.68E+06	6.15E+06	8.58E+06	1.09E+00

	GN=MFSD5 PE=2 SV=2				
Q6YN16-2	Isoform 2 of Hydroxysteroid dehydrogenase-like protein 2 OS=Homo sapiens GN=HSDL2	0.00E+00	1.15E+07	0.00E+00	-1.00E+01
Q7L1Q6-2	Isoform 2 of Basic leucine zipper and W2 domain-containing protein 1 OS=Homo sapiens GN=BZW1	1.23E+07	1.39E+07	1.62E+07	-1.13E+00
Q7L2E3-3	Isoform 3 of Putative ATP-dependent RNA helicase DHX30 OS=Homo sapiens GN=DHX30	0.00E+00	5.49E+06	0.00E+00	-1.00E+01
Q86T03	Transmembrane protein 55B OS=Homo sapiens GN=TMEM55B PE=1 SV=1	2.55E+07	1.29E+07	0.00E+00	1.98E+00
Q8IYS2	Uncharacterized protein KIAA2013 OS=Homo sapiens GN=KIAA2013 PE=2 SV=1	0.00E+00	5.00E+06	7.56E+06	-1.00E+01
Q8N726	Cyclin-dependent kinase inhibitor 2A, isoform 4 OS=Homo sapiens GN=CDKN2A PE=1 SV=2	9.55E+06	9.24E+06	9.84E+06	1.03E+00
Q8NBN3-3	Isoform 3 of Transmembrane protein 87A OS=Homo sapiens GN=TMEM87A	1.41E+07	1.90E+07	1.56E+07	-1.35E+00
Q8NCG7	Sn1-specific diacylglycerol lipase beta OS=Homo sapiens GN=DAGLB PE=1 SV=2	2.39E+07	2.73E+07	2.77E+07	-1.14E+00
Q8NFJ5	Retinoic acid-induced protein 3 OS=Homo sapiens GN=GPRC5A PE=1 SV=2	8.93E+07	8.64E+07	8.28E+07	1.03E+00
Q8TB61-3	Isoform 3 of Adenosine 3'-phospho 5'-phosphosulfate transporter 1 OS=Homo sapiens GN=SLC35B2	2.91E+07	4.18E+07	4.04E+07	-1.43E+00
Q8TCJ2	Dolichyl-diphosphooligosaccharide--protein glycosyltransferase subunit STT3B OS=Homo sapiens GN=STT3B PE=1 SV=1	1.50E+07	1.17E+07	1.64E+07	1.28E+00
Q8TCT9-5	Isoform 5 of Minor histocompatibility antigen H13 OS=Homo sapiens GN=HM13	2.02E+07	2.56E+07	2.88E+07	-1.27E+00
Q969X5-2	Isoform 2 of Endoplasmic reticulum-Golgi intermediate compartment protein 1 OS=Homo sapiens GN=ERGIC1	6.34E+06	0.00E+00	0.00E+00	1.00E+01
Q96AG4	Leucine-rich repeat-containing protein 59 OS=Homo sapiens GN=LRRC59 PE=1 SV=1	1.38E+07	2.12E+07	1.76E+07	-1.54E+00
Q96CX2	BTB/POZ domain-containing protein KCTD12 OS=Homo sapiens	1.04E+07	0.00E+00	8.72E+06	1.00E+01

	GN=KCTD12 PE=1 SV=1				
Q96FX8	p53 apoptosis effector related to PMP-22 OS=Homo sapiens GN=PERP PE=2 SV=1	2.01E+08	2.25E+08	8.64E+07	-1.12E+00
Q96JJ7	Protein disulfide-isomerase TMX3 OS=Homo sapiens GN=TMX3 PE=1 SV=2	1.19E+07	6.95E+06	0.00E+00	1.71E+00
Q96P70	Importin-9 OS=Homo sapiens GN=IPO9 PE=1 SV=3	5.54E+06	0.00E+00	1.31E+07	1.00E+01
Q96QD8	Sodium-coupled neutral amino acid transporter 2 OS=Homo sapiens GN=SLC38A2 PE=1 SV=2	6.08E+07	6.75E+07	7.14E+07	-1.11E+00
Q96S97	Myeloid-associated differentiation marker OS=Homo sapiens GN=MYADM PE=1 SV=2	5.54E+07	6.64E+07	6.34E+07	-1.20E+00
Q99497	Protein DJ-1 OS=Homo sapiens GN=PARK7 PE=1 SV=2	3.48E+07	0.00E+00	3.75E+07	1.00E+01
Q99714	3-hydroxyacyl-CoA dehydrogenase type-2 OS=Homo sapiens GN=HSD17B10 PE=1 SV=3	2.21E+07	2.75E+07	1.55E+07	-1.24E+00
Q99805	Transmembrane 9 superfamily member 2 OS=Homo sapiens GN=TM9SF2 PE=1 SV=1	1.14E+07	1.20E+07	0.00E+00	-1.06E+00
Q99832-3	Isoform 3 of T-complex protein 1 subunit eta OS=Homo sapiens GN=CCT7	4.38E+07	4.89E+07	1.12E+09	-1.12E+00
Q9BTU6	Phosphatidylinositol 4-kinase type 2-alpha OS=Homo sapiens GN=PI4K2A PE=1 SV=1	1.04E+07	1.31E+07	9.32E+06	-1.26E+00
Q9BUF5	Tubulin beta-6 chain OS=Homo sapiens GN=TUBB6 PE=1 SV=1	2.89E+08	2.33E+08	3.33E+08	1.24E+00
Q9H0U4	Ras-related protein Rab-1B OS=Homo sapiens GN=RAB1B PE=1 SV=1	3.01E+07	4.98E+07	3.53E+07	-1.66E+00
Q9H2D1	Mitochondrial folate transporter/carrier OS=Homo sapiens GN=SLC25A32 PE=1 SV=2	0.00E+00	1.21E+07	0.00E+00	-1.00E+01
Q9H3N1	Thioredoxin-related transmembrane protein 1 OS=Homo sapiens GN=TMX1 PE=1 SV=1	3.02E+07	4.29E+07	4.76E+07	-1.42E+00
Q9H3Z4	DnaJ homolog subfamily C member 5 OS=Homo sapiens GN=DNAJC5 PE=1 SV=1	7.52E+07	7.35E+07	1.16E+08	1.02E+00
Q9H6X2	Anthrax toxin receptor 1 OS=Homo sapiens GN=ANTXR1 PE=1 SV=2	5.21E+06	1.37E+07	1.13E+07	-2.63E+00

Q9HB71	Calcyclin-binding protein OS=Homo sapiens GN=CACYBP PE=1 SV=2	1.25E+07	1.22E+07	1.91E+07	1.03E+00
Q9NP58-4	Isoform 2 of ATP-binding cassette sub-family B member 6, mitochondrial OS=Homo sapiens GN=ABCB6	1.63E+07	1.74E+07	1.68E+07	-1.07E+00
Q9NVA4	Transmembrane protein 184C OS=Homo sapiens GN=TMEM184C PE=2 SV=2	8.08E+06	9.37E+06	2.02E+07	-1.16E+00
Q9NZ01	Very-long-chain enoyl-CoA reductase OS=Homo sapiens GN=TECR PE=1 SV=1	1.20E+07	1.31E+07	1.94E+07	-1.10E+00
Q9UBM7	7-dehydrocholesterol reductase OS=Homo sapiens GN=DHCR7 PE=1 SV=1	8.01E+06	7.81E+06	0.00E+00	1.03E+00
Q9UHX1-4	Isoform 4 of Poly(U)-binding-splicing factor PUF60 OS=Homo sapiens GN=PUF60	1.11E+07	1.22E+07	2.08E+07	-1.10E+00
Q9UIQ6-3	Isoform 3 of Leucyl-cystinyl aminopeptidase OS=Homo sapiens GN=LNPEP	4.94E+06	1.02E+07	1.23E+07	-2.06E+00
Q9UL15	BAG family molecular chaperone regulator 5 OS=Homo sapiens GN=BAG5 PE=1 SV=1	2.12E+07	2.06E+07	2.66E+07	1.03E+00
Q9UNM6	26S proteasome non-ATPase regulatory subunit 13 OS=Homo sapiens GN=PSMD13 PE=1 SV=2	8.31E+06	1.01E+07	7.70E+06	-1.21E+00
Q9UNN8	Endothelial protein C receptor OS=Homo sapiens GN=PROCR PE=1 SV=1	1.66E+07	1.36E+07	1.56E+07	1.22E+00
Q9Y277	Voltage-dependent anion-selective channel protein 3 OS=Homo sapiens GN=VDAC3 PE=1 SV=1	3.33E+07	7.16E+07	1.95E+07	-2.15E+00
Q9Y282-2	Isoform 2 of Endoplasmic reticulum-Golgi intermediate compartment protein 3 OS=Homo sapiens GN=ERGIC3	1.48E+07	1.20E+07	2.13E+07	1.23E+00
Q9Y287	Integral membrane protein 2B OS=Homo sapiens GN=ITM2B PE=1 SV=1	2.93E+07	3.00E+07	3.39E+07	-1.03E+00
Q9Y289	Sodium-dependent multivitamin transporter OS=Homo sapiens GN=SLC5A6 PE=2 SV=2	5.75E+06	0.00E+00	7.40E+06	1.00E+01
Q9Y2X3	Nucleolar protein 58 OS=Homo sapiens GN=NOP58 PE=1 SV=1	5.32E+06	7.71E+06	6.14E+06	-1.45E+00
Q9Y3U8	60S ribosomal protein L36 OS=Homo sapiens GN=RPL36 PE=1 SV=3	3.55E+07	2.86E+07	4.78E+07	1.24E+00
Q9Y678	Coatomer subunit gamma-1 OS=Homo sapiens GN=COPG1 PE=1 SV=1	1.16E+07	1.16E+07	1.42E+07	1.00E+00

Q9Y6C9	Mitochondrial carrier homolog 2 OS=Homo sapiens GN=MTCH2 PE=1 SV=1	2.55E+07	4.41E+07	1.20E+07	-1.73E+00

APPENDIX C
Protein abundance upon Shigella infection (experiment 2)

*Ratios higher than +10 or lower than -10 are equaled to +10 or -10 respectively for visualization purposes.

Proteins with N-terminal glycine

Accession	Description	Wild type Shigella	ΔipaJ Shigella	non infected	wild type /ΔipaJ ratio*
Q03405-2	Isoform 2 of Urokinase plasminogen activator surface receptor OS=Homo sapiens GN=PLAUR	0.00E+00	3.00E+07	0.00E+00	-1.00E+01
B4DMZ1	Solute carrier family 26 member 6 OS=Homo sapiens GN=SLC26A6 PE=2 SV=1	0.00E+00	3.23E+07	3.41E+07	-1.00E+01
P51659	Peroxisomal multifunctional enzyme type 2 OS=Homo sapiens GN=HSD17B4 PE=1 SV=3	0.00E+00	3.25E+07	0.00E+00	-1.00E+01
Q5BJF2	Transmembrane protein 97 OS=Homo sapiens GN=TMEM97 PE=1 SV=1	6.10E+07	0.00E+00	0.00E+00	10
E9PLX2	RING finger protein 141 (Fragment) OS=Homo sapiens GN=RNF141 PE=4 SV=1	2.96E+07	3.30E+07	4.40E+07	-1.12E+00
Q5H9U9	Probable ATP-dependent RNA helicase DDX60-like OS=Homo sapiens GN=DDX60L PE=2 SV=2	7.03E+07	0.00E+00	3.27E+07	10
Q5VT66	MOSC domain-containing protein 1, mitochondrial OS=Homo sapiens GN=MARC1 PE=1 SV=1	8.11E+07	0.00E+00	0.00E+00	10
H0Y8C3	Mitochondrial carrier homolog 1 (Fragment) OS=Homo sapiens GN=MTCH1 PE=3 SV=1	3.08E+07	5.11E+07	8.18E+07	-1.66E+00
P61970	Nuclear transport factor 2 OS=Homo sapiens GN=NUTF2 PE=1 SV=1	6.01E+07	2.74E+07	9.01E+07	2.20E+00
I3L0U2	Testisin (Fragment) OS=Homo sapiens GN=PRSS21 PE=3 SV=1	5.77E+07	4.11E+07	2.99E+07	1.40E+00

Q9P2G1	Ankyrin repeat and IBR domain-containing protein 1 OS=Homo sapiens GN=ANKIB1 PE=1 SV=3	5.08E+07	4.88E+07	5.73E+07	1.04E+00
K7EPJ5	E3 ubiquitin-protein ligase MGRN1 (Fragment) OS=Homo sapiens GN=MGRN1 PE=4 SV=1	8.35E+06	9.39E+07	1.31E+07	-1.00E+01
O96008	Mitochondrial import receptor subunit TOM40 homolog OS=Homo sapiens GN=TOMM40 PE=1 SV=1	5.31E+07	5.21E+07	4.43E+07	1.02E+00
Q8IWA5	Choline transporter-like protein 2 OS=Homo sapiens GN=SLC44A2 PE=1 SV=3	5.26E+07	5.52E+07	3.71E+07	-1.05E+00
P26006	Integrin alpha-3 OS=Homo sapiens GN=ITGA3 PE=1 SV=5	5.89E+07	6.09E+07	6.19E+07	-1.04E+00
Q96PY5-3	Isoform 2 of Formin-like protein 2 OS=Homo sapiens GN=FMNL2	5.58E+07	7.14E+07	1.01E+08	-1.28E+00
Q99487	Platelet-activating factor acetylhydrolase 2, cytoplasmic OS=Homo sapiens GN=PAFAH2 PE=1 SV=1	6.39E+07	6.90E+07	6.13E+07	-1.08E+00
E9PAY3	Neuronal calcium sensor 1 OS=Homo sapiens GN=NCS1 PE=4 SV=1	8.14E+07	6.22E+07	9.33E+07	1.31E+00
P12931	Proto-oncogene tyrosine-protein kinase Src OS=Homo sapiens GN=SRC PE=1 SV=3	9.74E+07	6.03E+07	9.79E+07	1.61E+00
Q9BQQ3	Golgi reassembly-stacking protein 1 OS=Homo sapiens GN=GORASP1 PE=1 SV=3	9.18E+07	7.11E+07	8.56E+07	1.29E+00
O75844	CAAX prenyl protease 1 homolog OS=Homo sapiens GN=ZMPSTE24 PE=1 SV=2	4.50E+07	1.25E+08	4.59E+08	-2.78E+00
Q9HBL7	Plasminogen receptor (KT) OS=Homo sapiens GN=PLGRKT PE=1 SV=1	7.71E+07	9.40E+07	1.08E+08	-1.22E+00
Q969Z3	MOSC domain-containing protein 2, mitochondrial OS=Homo sapiens GN=MARC2 PE=1 SV=1	1.04E+08	7.20E+07	9.41E+07	1.44E+00

F8W785	Golgi integral membrane protein 4 OS=Homo sapiens GN=GOLIM4 PE=4 SV=1	6.03E+07	1.17E+08	9.98E+07	-1.95E+00
P07948	Tyrosine-protein kinase Lyn OS=Homo sapiens GN=LYN PE=1 SV=3	8.32E+07	1.01E+08	1.43E+08	-1.21E+00
Q08J23	tRNA (cytosine(34)-C(5))-methyltransferase OS=Homo sapiens GN=NSUN2 PE=1 SV=2	9.63E+07	9.01E+07	1.09E+08	1.07E+00
Q6NUT3-2	Isoform 2 of Major facilitator superfamily domain-containing protein 12 OS=Homo sapiens GN=MFSD12	5.00E+07	1.53E+08	0.00E+00	-3.05E+00
Q8N9N7	Leucine-rich repeat-containing protein 57 OS=Homo sapiens GN=LRRC57 PE=1 SV=1	1.02E+08	1.00E+08	1.29E+08	1.02E+00
E7EUZ9	Serine incorporator 2 OS=Homo sapiens GN=SERINC2 PE=4 SV=1	6.50E+07	1.39E+08	0.00E+00	-2.14E+00
C9JFR7	Cytochrome c (Fragment) OS=Homo sapiens GN=CYCS PE=3 SV=1	1.16E+08	8.97E+07	3.81E+08	1.29E+00
P30044	Peroxiredoxin-5, mitochondrial OS=Homo sapiens GN=PRDX5 PE=1 SV=4	1.01E+08	1.05E+08	1.09E+08	-1.03E+00
O75695	Protein XRP2 OS=Homo sapiens GN=RP2 PE=1 SV=4	1.06E+08	1.01E+08	1.31E+08	1.05E+00
O95466-2	Isoform 2 of Formin-like protein 1 OS=Homo sapiens GN=FMNL1	7.32E+07	1.39E+08	1.13E+08	-1.89E+00
P62266	40S ribosomal protein S23 OS=Homo sapiens GN=RPS23 PE=1 SV=3	2.18E+08	0.00E+00	2.07E+08	10
F8W8W4	Prenylcysteine oxidase 1 OS=Homo sapiens GN=PCYOX1 PE=4 SV=1	0.00E+00	2.22E+08	0.00E+00	-1.00E+01
P48960-2	Isoform 2 of CD97 antigen OS=Homo sapiens GN=CD97	1.24E+08	9.98E+07	1.14E+08	1.24E+00
J3QRU1	Tyrosine-protein kinase Yes OS=Homo sapiens GN=YES1 PE=4 SV=1	1.16E+08	1.17E+08	1.65E+08	-1.01E+00
Q14699	Raftlin OS=Homo sapiens GN=RFTN1 PE=1 SV=4	6.59E+07	1.70E+08	6.55E+07	-2.57E+00

P62917	60S ribosomal protein L8 OS=Homo sapiens GN=RPL8 PE=1 SV=2	9.82E+07	1.38E+08	1.35E+08	-1.41E+00
Q9BVX2	Transmembrane protein 106C OS=Homo sapiens GN=TMEM106C PE=2 SV=1	1.10E+08	1.29E+08	1.21E+08	-1.17E+00
P17568	NADH dehydrogena	1.10E+08	1.44E+08	1.02E+08	-1.31E+00
O15260-2	Isoform 2 of Surfeit locus protein 4 OS=Homo sapiens GN=SURF4	1.17E+08	1.38E+08	1.07E+08	-1.18E+00
Q96BS2	Calcineurin B homologous protein 3 OS=Homo sapiens GN=TESC PE=1 SV=3	1.09E+08	1.49E+08	1.58E+08	-1.37E+00
F5H3A1	Sodium/potassium-transporting ATPase subunit alpha-1 OS=Homo sapiens GN=ATP1A1 PE=3 SV=1	8.80E+07	1.92E+08	9.60E+07	-2.18E+00
Q9BPX3	Condensin complex subunit 3 OS=Homo sapiens GN=NCAPG PE=1 SV=1	6.07E+07	2.23E+08	7.22E+07	-3.68E+00
P08708	40S ribosomal protein S17 OS=Homo sapiens GN=RPS17 PE=1 SV=2	1.32E+08	1.61E+08	1.30E+08	-1.22E+00
P26583	High mobility group protein B2 OS=Homo sapiens GN=HMGB2 PE=1 SV=2	1.29E+08	1.81E+08	7.70E+07	-1.40E+00
O75688	Protein phosphatase 1B OS=Homo sapiens GN=PPM1B PE=1 SV=1	1.23E+08	1.93E+08	1.68E+08	-1.57E+00
F5H1N7	Uncharacterized protein KIAA1211 OS=Homo sapiens GN=KIAA1211 PE=4 SV=1	0.00E+00	3.26E+08	0.00E+00	-1.00E+01
P43121	Cell surface glycoprotein MUC18 OS=Homo sapiens GN=MCAM PE=1 SV=2	1.54E+08	1.90E+08	1.39E+08	-1.24E+00
Q9C0E8	Protein lunapark OS=Homo sapiens GN=LNP PE=1 SV=2	2.13E+08	1.32E+08	2.55E+08	1.62E+00
Q7RTS9	Dymeclin OS=Homo sapiens GN=DYM PE=1 SV=1	2.15E+08	1.37E+08	1.95E+08	1.57E+00
O95210	Starch-binding domain-containing protein 1 OS=Homo sapiens GN=STBD1 PE=1 SV=1	2.54E+07	3.32E+08	1.24E+08	-1.00E+01

Q99570	Phosphoinositide 3-kinase regulatory subunit 4 OS=Homo sapiens GN=PIK3R4 PE=1 SV=3	1.96E+08	1.70E+08	1.95E+08	1.15E+00
Q9Y478	5'-AMP-activated protein kinase subunit beta-1 OS=Homo sapiens GN=PRKAB1 PE=1 SV=4	2.53E+08	1.18E+08	2.14E+08	2.14E+00
K7ELC7	60S ribosomal protein L27 (Fragment) OS=Homo sapiens GN=RPL27 PE=4 SV=1	3.15E+08	6.75E+07	8.40E+07	4.68E+00
P46777	60S ribosomal protein L5 OS=Homo sapiens GN=RPL5 PE=1 SV=3	1.78E+08	2.17E+08	1.21E+08	-1.22E+00
P35813	Protein phosphatase 1A OS=Homo sapiens GN=PPM1A PE=1 SV=1	2.02E+08	2.02E+08	2.58E+08	1.00E+00
P11717	Cation-independent mannose-6-phosphate receptor OS=Homo sapiens GN=IGF2R PE=1 SV=3	1.77E+08	2.27E+08	1.54E+08	-1.28E+00
Q13530	Serine incorporator 3 OS=Homo sapiens GN=SERINC3 PE=2 SV=2	1.92E+08	2.15E+08	1.88E+08	-1.12E+00
Q13286-2	Isoform 2 of Battenin OS=Homo sapiens GN=CLN3	2.32E+08	1.75E+08	1.53E+08	1.32E+00
Q9NUM4	Transmembrane protein 106B OS=Homo sapiens GN=TMEM106B PE=1 SV=2	2.40E+08	1.75E+08	2.15E+08	1.37E+00
Q6P9B6	TLD domain-containing protein KIAA1609 OS=Homo sapiens GN=KIAA1609 PE=1 SV=2	3.72E+08	4.87E+07	6.21E+07	7.64E+00
Q8WTV0-4	Isoform 4 of Scavenger receptor class B member 1 OS=Homo sapiens GN=SCARB1	2.18E+08	2.08E+08	4.44E+08	1.05E+00
Q9Y487	V-type proton ATPase 116 kDa subunit a isoform 2 OS=Homo sapiens GN=ATP6V0A2 PE=1 SV=2	2.15E+08	2.16E+08	4.35E+08	-1.01E+00
Q9Y6M5	Zinc transporter 1 OS=Homo sapiens GN=SLC30A1 PE=1 SV=3	2.04E+08	2.28E+08	2.40E+08	-1.12E+00

P30825	High affinity cationic amino acid transporter 1 OS=Homo sapiens GN=SLC7A1 PE=1 SV=1	1.40E+08	2.93E+08	1.61E+08	-2.09E+00
Q9BXP5-4	Isoform 4 of Serrate RNA effector molecule homolog OS=Homo sapiens GN=SRRT	2.46E+08	1.90E+08	2.65E+08	1.29E+00
P24534	Elongation factor 1-beta OS=Homo sapiens GN=EEF1B2 PE=1 SV=3	2.25E+08	2.51E+08	2.12E+08	-1.12E+00
P27635	60S ribosomal protein L10 OS=Homo sapiens GN=RPL10 PE=1 SV=4	2.71E+08	2.13E+08	2.35E+08	1.27E+00
O43149	Zinc finger ZZ-type and EF-hand domain-containing protein 1 OS=Homo sapiens GN=ZZEF1 PE=1 SV=6	2.66E+08	2.27E+08	2.40E+08	1.17E+00
Q5T7C4	High mobility group protein B1 OS=Homo sapiens GN=HMGB1 PE=2 SV=1	2.40E+08	2.62E+08	2.81E+08	-1.09E+00
Q8WWI5	Choline transporter-like protein 1 OS=Homo sapiens GN=SLC44A1 PE=1 SV=1	2.44E+08	2.75E+08	2.25E+08	-1.13E+00
Q8NFA0	Ubiquitin carboxyl-terminal hydrolase 32 OS=Homo sapiens GN=USP32 PE=1 SV=1	1.19E+08	4.06E+08	2.01E+08	-3.42E+00
Q9BRQ8	Apoptosis-inducing factor 2 OS=Homo sapiens GN=AIFM2 PE=1 SV=1	2.37E+08	3.14E+08	4.46E+08	-1.32E+00
P39656	Dolichyl-diphosphooligosaccharide--protein glycosyltransferase 48 kDa subunit OS=Homo sapiens GN=DDOST PE=1 SV=4	2.68E+08	3.02E+08	2.64E+08	-1.13E+00
P51572	B-cell receptor-associated protein 31 OS=Homo sapiens GN=BCAP31 PE=1 SV=3	2.67E+08	3.31E+08	2.54E+08	-1.24E+00
P27701	CD82 antigen OS=Homo sapiens GN=CD82 PE=1 SV=1	2.81E+08	3.33E+08	2.73E+08	-1.18E+00
Q9P032	NADH dehydrogena	2.95E+08	3.24E+08	2.11E+08	-1.10E+00
E9PR17	CD59 glycoprotein OS=Homo sapiens GN=CD59 PE=4 SV=1	2.97E+08	3.30E+08	3.42E+08	-1.11E+00

P61313	60S ribosomal protein L15 OS=Homo sapiens GN=RPL15 PE=1 SV=2	3.00E+08	3.28E+08	2.64E+08	-1.09E+00
Q99653	Calcineurin B homologous protein 1 OS=Homo sapiens GN=CHP1 PE=1 SV=3	3.51E+08	2.88E+08	2.23E+08	1.22E+00
Q6UB35	Monofunctional C1-tetrahydrofolate synthase, mitochondrial OS=Homo sapiens GN=MTHFD1L PE=1 SV=1	4.31E+08	2.16E+08	1.61E+08	2.00E+00
P16435	NADPH--cytochrome P450 reductase OS=Homo sapiens GN=POR PE=1 SV=2	5.99E+08	5.20E+07	6.30E+07	1.00E+01
H0YDL9	CD81 antigen (Fragment) OS=Homo sapiens GN=CD81 PE=4 SV=1	3.19E+08	3.47E+08	3.19E+08	-1.09E+00
Q02952-3	Isoform 3 of A-kinase anchor protein 12 OS=Homo sapiens GN=AKAP12	2.96E+08	4.17E+08	5.53E+08	-1.41E+00
Q08211	ATP-dependent RNA helicase A OS=Homo sapiens GN=DHX9 PE=1 SV=4	3.52E+08	3.92E+08	3.38E+08	-1.11E+00
F6U1T9	Calcineurin subunit B type 1 OS=Homo sapiens GN=PPP3R1 PE=4 SV=1	4.15E+08	3.98E+08	4.44E+08	1.04E+00
J3QQ67	60S ribosomal protein L18 (Fragment) OS=Homo sapiens GN=RPL18 PE=3 SV=1	4.16E+08	4.20E+08	4.45E+08	-1.01E+00
Q8NHG8	E3 ubiquitin-protein ligase ZNRF2 OS=Homo sapiens GN=ZNRF2 PE=1 SV=1	0.00E+00	8.64E+08	1.01E+08	-1.00E+01
H3BUP2	Nucleolar protein 3 (Fragment) OS=Homo sapiens GN=NOL3 PE=4 SV=1	4.15E+08	4.50E+08	6.04E+08	-1.09E+00
Q14254	Flotillin-2 OS=Homo sapiens GN=FLOT2 PE=1 SV=2	4.35E+08	4.55E+08	4.05E+08	-1.04E+00
P62241	40S ribosomal protein S8 OS=Homo sapiens GN=RPS8 PE=1 SV=2	4.24E+08	4.67E+08	8.62E+08	-1.10E+00
O15427	Monocarboxylate transporter 4 OS=Homo sapiens GN=SLC16A3 PE=1 SV=1	4.04E+08	4.92E+08	4.23E+08	-1.22E+00

P53701	Cytochrome c-type heme lyase OS=Homo sapiens GN=HCCS PE=1 SV=1	4.44E+08	4.67E+08	4.86E+08	-1.05E+00
P49006	MARCKS-related protein OS=Homo sapiens GN=MARCKSL1 PE=1 SV=2	4.43E+08	5.41E+08	7.86E+08	-1.22E+00
B4DKT0	Golgi reassembly-stacking protein 2 OS=Homo sapiens GN=GORASP2 PE=2 SV=1	4.51E+08	5.92E+08	6.22E+08	-1.31E+00
H0YKJ9	Tetraspanin-3 OS=Homo sapiens GN=TSPAN3 PE=4 SV=1	5.88E+08	5.36E+08	4.13E+08	1.10E+00
Q9NRX5	Serine incorporator 1 OS=Homo sapiens GN=SERINC1 PE=1 SV=1	5.19E+08	6.13E+08	5.19E+08	-1.18E+00
Q96FZ7	Charged multivesicular body protein 6 OS=Homo sapiens GN=CHMP6 PE=1 SV=3	5.44E+08	5.94E+08	6.26E+08	-1.09E+00
Q14108	Lysosome membrane protein 2 OS=Homo sapiens GN=SCARB2 PE=1 SV=2	3.78E+08	7.68E+08	3.44E+08	-2.03E+00
Q6IAA8	Ragulator complex protein LAMTOR1 OS=Homo sapiens GN=LAMTOR1 PE=1 SV=2	7.52E+08	5.36E+08	9.83E+08	1.40E+00
P22694-7	Isoform 7 of cAMP-dependent protein kinase catalytic subunit beta OS=Homo sapiens GN=PRKACB	7.48E+08	7.32E+08	1.10E+09	1.02E+00
P37235	Hippocalcin-like protein 1 OS=Homo sapiens GN=HPCAL1 PE=1 SV=3	6.73E+08	8.14E+08	9.56E+08	-1.21E+00
B4DWW1	ADP-ribosylation factor-like protein 1 OS=Homo sapiens GN=ARL1 PE=2 SV=1	2.71E+08	1.24E+09	1.35E+09	-4.56E+00
P62330	ADP-ribosylation factor 6 OS=Homo sapiens GN=ARF6 PE=1 SV=2	6.33E+08	9.30E+08	1.23E+09	-1.47E+00
Q96GE9-2	Isoform 2 of Transmembrane protein C9orf123 OS=Homo sapiens GN=C9orf123	4.37E+08	1.18E+09	7.62E+08	-2.70E+00
Q9NUQ9	Protein FAM49B OS=Homo sapiens GN=FAM49B PE=1 SV=1	8.44E+08	8.18E+08	1.16E+09	1.03E+00

E9PMR4	CD151 antigen OS=Homo sapiens GN=CD151 PE=4 SV=1	9.15E+08	8.22E+08	8.62E+08	1.11E+00
Q9Y266	Nuclear migration protein nudC OS=Homo sapiens GN=NUDC PE=1 SV=1	8.77E+08	9.14E+08	5.27E+08	-1.04E+00
Q04917	14-3-3 protein eta OS=Homo sapiens GN=YWHAH PE=1 SV=4	6.32E+08	1.18E+09	1.28E+09	-1.86E+00
Q9NYU2-2	Isoform 2 of UDP-glucose:glycoprotein glucosyltransferase 1 OS=Homo sapiens GN=UGGT1	1.74E+09	9.50E+07	7.40E+07	1.00E+01
B7Z904	Thioredoxin reductase 1 OS=Homo sapiens GN=TXNRD1 PE=2 SV=1	2.84E+08	1.69E+09	2.33E+08	-5.97E+00
O60841	Eukaryotic translation initiation factor 5B OS=Homo sapiens GN=EIF5B PE=1 SV=4	2.39E+08	1.85E+09	1.70E+09	-7.72E+00
P17612-2	Isoform 2 of cAMP-dependent protein kinase catalytic subunit alpha OS=Homo sapiens GN=PRKACA	1.15E+09	1.10E+09	1.48E+09	1.05E+00
C9JRZ6	Coiled-coil-helix-coiled-coil-helix domain-containing protein 3, mitochondrial OS=Homo sapiens GN=CHCHD3 PE=4 SV=1	1.04E+09	1.28E+09	7.90E+08	-1.24E+00
Q9P2B2	Prostaglandin F2 receptor negative regulator OS=Homo sapiens GN=PTGFRN PE=1 SV=2	6.42E+07	2.31E+09	2.57E+09	-1.00E+01
O15355	Protein phosphatase 1G OS=Homo sapiens GN=PPM1G PE=1 SV=1	1.46E+09	1.24E+09	2.03E+09	1.17E+00
O15121	Sphingolipid delta(4)-desaturase DES1 OS=Homo sapiens GN=DEGS1 PE=1 SV=1	1.35E+09	1.49E+09	1.33E+09	-1.11E+00
A6NI00	Guanine nucleotide-binding protein G(s) subunit alpha isoforms short OS=Homo sapiens GN=GNAS PE=4 SV=3	1.26E+09	1.61E+09	1.29E+09	-1.28E+00

P68104	Elongation factor 1-alpha 1 OS=Homo sapiens GN=EEF1A1 PE=1 SV=1	1.67E+09	1.58E+09	2.01E+09	1.06E+00
Q96TA1-2	Isoform 2 of Niban-like protein 1 OS=Homo sapiens GN=FAM129B	1.96E+09	1.65E+09	2.35E+09	1.19E+00
P63096	Guanine nucleotide-binding protein G(i) subunit alpha-1 OS=Homo sapiens GN=GNAI1 PE=1 SV=2	2.42E+09	2.08E+09	2.36E+09	1.16E+00
P08754	Guanine nucleotide-binding protein G(k) subunit alpha OS=Homo sapiens GN=GNAI3 PE=1 SV=3	2.46E+09	2.22E+09	2.50E+09	1.11E+00
P62191	26S protease regulatory subunit 4 OS=Homo sapiens GN=PSMC1 PE=1 SV=1	2.18E+09	3.01E+09	3.52E+09	-1.38E+00
P29966	Myristoylated alanine-rich C-kinase substrate OS=Homo sapiens GN=MARCKS PE=1 SV=4	2.23E+09	2.98E+09	4.45E+09	-1.33E+00
P00387-3	Isoform 3 of NADH-cytochrome b5 reductase 3 OS=Homo sapiens GN=CYB5R3	3.11E+09	3.51E+09	2.15E+09	-1.13E+00
P04899	Guanine nucleotide-binding protein G(i) subunit alpha-2 OS=Homo sapiens GN=GNAI2 PE=1 SV=3	6.75E+09	2.15E+09	2.36E+09	3.14E+00
P04406	Glyceraldehyde-3-phosphate dehydrogenase OS=Homo sapiens GN=GAPDH PE=1 SV=3	5.10E+09	4.17E+09	5.68E+09	1.22E+00
B7ZB63	ADP-ribosylation factor 3 OS=Homo sapiens GN=ARF3 PE=2 SV=1	3.52E+09	6.95E+09	9.40E+09	-1.98E+00
P84085	ADP-ribosylation factor 5 OS=Homo sapiens GN=ARF5 PE=1 SV=2	4.93E+09	1.06E+10	1.33E+10	-2.16E+00
P18085	ADP-ribosylation factor 4 OS=Homo sapiens GN=ARF4 PE=1 SV=3	4.93E+09	1.06E+10	1.33E+10	-2.16E+00
P80723	Brain acid soluble protein 1 OS=Homo sapiens GN=BASP1 PE=1 SV=2	1.60E+10	1.64E+10	1.81E+10	-1.03E+00

Proteins without N-terminal glycine

Accession	Description	Wild type Shigella	ΔipaJ Shigella	non infected	wild type /ΔipaJ ratio
Q96CP7	TLC domain-containing protein 1 OS=Homo sapiens GN=TLCD1 PE=2 SV=1	7.17E+06	0.00E+00	0.00E+00	1.00E+01
Q9Y5J1	U3 small nucleolar RNA-associated protein 18 homolog OS=Homo sapiens GN=UTP18 PE=1 SV=3	0.00E+00	1.29E+07	0.00E+00	-1.00E+01
Q6ZMG9	Ceramide synthase 6 OS=Homo sapiens GN=CERS6 PE=1 SV=1	1.39E+07	0.00E+00	0.00E+00	1.00E+01
J3KNQ4	Alpha-parvin OS=Homo sapiens GN=PARVA PE=4 SV=1	1.55E+07	0.00E+00	1.02E+08	1.00E+01
B4DWJ2	Glutamine--tRNA ligase OS=Homo sapiens GN=QARS PE=2 SV=1	0.00E+00	1.64E+07	5.85E+07	-1.00E+01
P13693	Translationally-controlled tumor protein OS=Homo sapiens GN=TPT1 PE=1 SV=1	1.77E+07	0.00E+00	1.42E+08	1.00E+01
P24530-3	Isoform C of Endothelin B receptor OS=Homo sapiens GN=EDNRB	0.00E+00	1.97E+07	0.00E+00	-1.00E+01
J3KPP4	Cisplatin resistance-associated overexpressed protein, isoform CRA_b OS=Homo sapiens GN=LUC7L3 PE=4 SV=1	0.00E+00	2.26E+07	0.00E+00	-1.00E+01
P13667	Protein disulfide-isomerase A4 OS=Homo sapiens GN=PDIA4 PE=1 SV=2	2.40E+07	0.00E+00	0.00E+00	1.00E+01
Q9Y5M8	Signal recognition particle receptor subunit beta OS=Homo sapiens GN=SRPRB PE=1 SV=3	0.00E+00	2.51E+07	0.00E+00	-1.00E+01
P62306	Small nuclear ribonucleoprotein F OS=Homo sapiens GN=SNRPF PE=1 SV=1	0.00E+00	2.53E+07	3.10E+07	-1.00E+01
F5H6P7	Protein mago nashi homolog 2 OS=Homo sapiens GN=MAGOHB PE=4 SV=1	0.00E+00	2.58E+07	3.77E+07	-1.00E+01
F8VZ44	Aladin OS=Homo sapiens GN=AAAS PE=4 SV=1	0.00E+00	2.65E+07	5.63E+07	-1.00E+01

B2RDB2	GDP-fucose transporter 1 OS=Homo sapiens GN=SLC35C1 PE=2 SV=1	0.00E+00	2.65E+07	0.00E+00	-1.00E+01
D6RBV2	Vesicular integral-membrane protein VIP36 OS=Homo sapiens GN=LMAN2 PE=4 SV=1	0.00E+00	2.67E+07	0.00E+00	-1.00E+01
Q96T76-9	Isoform 6 of MMS19 nucleotide excision repair protein homolog OS=Homo sapiens GN=MMS19	2.71E+07	0.00E+00	2.51E+07	1.00E+01
P68402	Platelet-activating factor acetylhydrolase IB subunit beta OS=Homo sapiens GN=PAFAH1B2 PE=1 SV=1	2.75E+07	0.00E+00	2.64E+07	1.00E+01
Q9UID3	Vacuolar protein sorting-associated protein 51 homolog OS=Homo sapiens GN=VPS51 PE=1 SV=2	0.00E+00	2.79E+07	0.00E+00	-1.00E+01
B5MCX3	Septin-2 OS=Homo sapiens GN=SEPT2 PE=3 SV=1	2.89E+07	0.00E+00	4.81E+07	1.00E+01
O15397	Importin-8 OS=Homo sapiens GN=IPO8 PE=1 SV=2	3.02E+07	0.00E+00	1.82E+07	1.00E+01
P54920	Alpha-soluble NSF attachment protein OS=Homo sapiens GN=NAPA PE=1 SV=3	3.21E+07	0.00E+00	3.87E+07	1.00E+01
G8JLH9	Signal transducer and activator of transcription 3 OS=Homo sapiens GN=STAT3 PE=4 SV=1	0.00E+00	3.30E+07	4.93E+07	-1.00E+01
O15031	Plexin-B2 OS=Homo sapiens GN=PLXNB2 PE=1 SV=3	0.00E+00	3.33E+07	6.08E+07	-1.00E+01
P49773	Histidine triad nucleotide-binding protein 1 OS=Homo sapiens GN=HINT1 PE=1 SV=2	3.42E+07	0.00E+00	7.95E+07	1.00E+01
P42771	Cyclin-dependent kinase inhibitor 2A, isoforms 1/2/3 OS=Homo sapiens GN=CDKN2A PE=1 SV=2	3.49E+07	0.00E+00	3.05E+07	1.00E+01
D6R9S8	Claudin domain-containing protein 1 (Fragment) OS=Homo sapiens GN=CLDND1 PE=4 SV=1	0.00E+00	3.63E+07	3.52E+07	-1.00E+01

H3BSJ9	Cytochrome b-c1 complex subunit 2, mitochondrial OS=Homo sapiens GN=UQCRC2 PE=4 SV=1	0.00E+00	3.69E+07	3.34E+07	-1.00E+01
Q14739	Lamin-B receptor OS=Homo sapiens GN=LBR PE=1 SV=2	0.00E+00	3.76E+07	4.33E+07	-1.00E+01
Q99436	Proteasome subunit beta type-7 OS=Homo sapiens GN=PSMB7 PE=1 SV=1	3.83E+07	0.00E+00	5.18E+07	1.00E+01
Q9P0S9	Transmembrane protein 14C OS=Homo sapiens GN=TMEM14C PE=1 SV=1	0.00E+00	3.97E+07	0.00E+00	-1.00E+01
P13804	Electron transfer flavoprotein subunit alpha, mitochondrial OS=Homo sapiens GN=ETFA PE=1 SV=1	3.97E+07	0.00E+00	0.00E+00	1.00E+01
O15228	Dihydroxyacetone phosphate acyltransferase OS=Homo sapiens GN=GNPAT PE=1 SV=1	0.00E+00	4.05E+07	1.22E+07	-1.00E+01
P29992	Guanine nucleotide-binding protein subunit alpha-11 OS=Homo sapiens GN=GNA11 PE=1 SV=2	4.12E+07	0.00E+00	4.78E+09	1.00E+01
O94925	Glutaminase kidney isoform, mitochondrial OS=Homo sapiens GN=GLS PE=1 SV=1	0.00E+00	4.18E+07	0.00E+00	-1.00E+01
C9JHL4	Negative elongation factor A (Fragment) OS=Homo sapiens GN=WHSC2 PE=4 SV=1	4.23E+07	0.00E+00	0.00E+00	1.00E+01
Q15012	Lysosomal-associated transmembrane protein 4A OS=Homo sapiens GN=LAPTM4A PE=1 SV=1	4.33E+07	0.00E+00	4.31E+07	1.00E+01
F5H6U7	Vesicle transport protein GOT1B OS=Homo sapiens GN=GOLT1B PE=4 SV=1	0.00E+00	4.36E+07	6.61E+06	-1.00E+01
B1AK87	Capping protein (Actin filament) muscle Z-line, beta OS=Homo sapiens GN=CAPZB PE=4 SV=1	4.39E+07	0.00E+00	0.00E+00	1.00E+01
F8W651	Coatomer subunit zeta-1 OS=Homo sapiens GN=COPZ1 PE=4 SV=1	2.12E+07	2.29E+07	3.05E+07	-1.08E+00

P08237-2	Isoform 2 of 6-phosphofructokinase, muscle type OS=Homo sapiens GN=PFKM	4.42E+07	0.00E+00	7.31E+07	1.00E+01
Q9BTV4	Transmembrane protein 43 OS=Homo sapiens GN=TMEM43 PE=1 SV=1	0.00E+00	4.48E+07	0.00E+00	-1.00E+01
Q9H2V7-3	Isoform 3 of Protein spinster homolog 1 OS=Homo sapiens GN=SPNS1	2.09E+07	2.64E+07	0.00E+00	-1.26E+00
F5H7E2	Superkiller viralicidic activity 2-like 2 OS=Homo sapiens GN=SKIV2L2 PE=4 SV=1	4.77E+07	0.00E+00	5.69E+07	1.00E+01
P18031	Tyrosine-protein phosphatase non-receptor type 1 OS=Homo sapiens GN=PTPN1 PE=1 SV=1	4.84E+07	0.00E+00	0.00E+00	1.00E+01
B4DDD2	Dihydrofolate reductase OS=Homo sapiens GN=DHFR PE=2 SV=1	4.88E+07	0.00E+00	4.95E+07	1.00E+01
Q9HAV4	Exportin-5 OS=Homo sapiens GN=XPO5 PE=1 SV=1	4.91E+07	0.00E+00	0.00E+00	1.00E+01
Q9UHV9	Prefoldin subunit 2 OS=Homo sapiens GN=PFDN2 PE=1 SV=1	4.92E+07	0.00E+00	0.00E+00	1.00E+01
P14735	Insulin-degrading enzyme OS=Homo sapiens GN=IDE PE=1 SV=4	5.00E+07	0.00E+00	0.00E+00	1.00E+01
G5E9Z2	Cisplatin resistance related protein CRR9p, isoform CRA_c OS=Homo sapiens GN=CLPTM1L PE=4 SV=1	0.00E+00	5.02E+07	5.62E+07	-1.00E+01
Q99805	Transmembrane 9 superfamily member 2 OS=Homo sapiens GN=TM9SF2 PE=1 SV=1	0.00E+00	5.03E+07	4.80E+07	-1.00E+01
G3XAF4	L1 cell adhesion molecule, isoform CRA_a OS=Homo sapiens GN=L1CAM PE=4 SV=1	5.10E+07	0.00E+00	2.56E+08	1.00E+01
Q96HC4	PDZ and LIM domain protein 5 OS=Homo sapiens GN=PDLIM5 PE=1 SV=5	5.24E+07	0.00E+00	6.72E+07	1.00E+01
P60468	Protein transport protein Sec61 subunit beta OS=Homo sapiens GN=SEC61B PE=1 SV=2	0.00E+00	5.28E+07	0.00E+00	-1.00E+01

P63010	AP-2 complex subunit beta OS=Homo sapiens GN=AP2B1 PE=1 SV=1	0.00E+00	5.37E+07	7.40E+07	-1.00E+01
Q658P3-4	Isoform 4 of Metalloreductase STEAP3 OS=Homo sapiens GN=STEAP3	2.34E+07	3.04E+07	4.07E+07	-1.30E+00
Q96I24-2	Isoform 2 of Far upstream element-binding protein 3 OS=Homo sapiens GN=FUBP3	0.00E+00	5.43E+07	7.59E+07	-1.00E+01
Q12874	Splicing factor 3A subunit 3 OS=Homo sapiens GN=SF3A3 PE=1 SV=1	2.65E+07	2.81E+07	2.90E+07	-1.06E+00
Q9Y265	RuvB-like 1 OS=Homo sapiens GN=RUVBL1 PE=1 SV=1	0.00E+00	5.49E+07	6.40E+07	-1.00E+01
P25787	Proteasome subunit alpha type-2 OS=Homo sapiens GN=PSMA2 PE=1 SV=2	5.50E+07	0.00E+00	6.06E+07	1.00E+01
Q5ZPR3-3	Isoform 3 of CD276 antigen OS=Homo sapiens GN=CD276	0.00E+00	5.51E+07	0.00E+00	-1.00E+01
O00231	26S proteasome non-ATPase regulatory subunit 11 OS=Homo sapiens GN=PSMD11 PE=1 SV=3	0.00E+00	5.51E+07	7.10E+07	-1.00E+01
O15155	BET1 homolog OS=Homo sapiens GN=BET1 PE=1 SV=1	1.48E+07	4.11E+07	4.96E+07	-2.77E+00
O96005	Cleft lip and palate transmembrane protein 1 OS=Homo sapiens GN=CLPTM1 PE=1 SV=1	0.00E+00	5.61E+07	0.00E+00	-1.00E+01
P52294	Importin subunit alpha-1 OS=Homo sapiens GN=KPNA1 PE=1 SV=3	2.66E+07	2.96E+07	2.64E+07	-1.11E+00
P33992	DNA replication licensing factor MCM5 OS=Homo sapiens GN=MCM5 PE=1 SV=5	5.67E+07	0.00E+00	7.00E+07	1.00E+01
O95831-3	Isoform 3 of Apoptosis-inducing factor 1, mitochondrial OS=Homo sapiens GN=AIFM1	5.73E+07	0.00E+00	0.00E+00	1.00E+01
O76003	Glutaredoxin-3 OS=Homo sapiens GN=GLRX3 PE=1 SV=2	5.78E+07	0.00E+00	1.33E+08	1.00E+01
P11413	Glucose-6-phosphate 1-dehydrogenase OS=Homo sapiens GN=G6PD PE=1 SV=4	5.80E+07	0.00E+00	6.51E+07	1.00E+01

P48047	ATP synthase subunit O, mitochondrial OS=Homo sapiens GN=ATP5O PE=1 SV=1	5.81E+07	0.00E+00	8.28E+07	1.00E+01
Q14118	Dystroglycan OS=Homo sapiens GN=DAG1 PE=1 SV=2	5.88E+07	0.00E+00	8.49E+07	1.00E+01
F5H579	Probable cysteine--tRNA ligase, mitochondrial (Fragment) OS=Homo sapiens GN=CARS2 PE=4 SV=1	0.00E+00	5.91E+07	4.81E+07	-1.00E+01
O15127	Secretory carrier-associated membrane protein 2 OS=Homo sapiens GN=SCAMP2 PE=1 SV=2	0.00E+00	5.93E+07	0.00E+00	-1.00E+01
P11766	Alcohol dehydrogenase class-3 OS=Homo sapiens GN=ADH5 PE=1 SV=4	5.96E+07	0.00E+00	3.66E+07	1.00E+01
Q9UBM7	7-dehydrocholesterol reductase OS=Homo sapiens GN=DHCR7 PE=1 SV=1	0.00E+00	5.97E+07	0.00E+00	-1.00E+01
Q16401	26S proteasome non-ATPase regulatory subunit 5 OS=Homo sapiens GN=PSMD5 PE=1 SV=3	4.10E+07	1.91E+07	0.00E+00	2.15E+00
O60664-3	Isoform 3 of Perilipin-3 OS=Homo sapiens GN=PLIN3	6.16E+07	0.00E+00	6.13E+07	1.00E+01
O15173	Membrane-associated progesterone receptor component 2 OS=Homo sapiens GN=PGRMC2 PE=1 SV=1	0.00E+00	6.17E+07	0.00E+00	-1.00E+01
P19623	Spermidine synthase OS=Homo sapiens GN=SRM PE=1 SV=1	2.83E+07	3.34E+07	0.00E+00	-1.18E+00
B4DNL6	Ribose-phosphate pyrophosphokinase OS=Homo sapiens GN=PRPS1 PE=2 SV=1	2.33E+07	3.88E+07	3.39E+07	-1.67E+00
H3BP91	Enoyl-CoA delta isomerase 1, mitochondrial (Fragment) OS=Homo sapiens GN=ECI1 PE=3 SV=1	3.26E+07	3.11E+07	0.00E+00	1.05E+00
P56537	Eukaryotic translation initiation factor 6 OS=Homo sapiens GN=EIF6 PE=1 SV=1	0.00E+00	6.43E+07	4.96E+07	-1.00E+01

H0Y711	Methylosome protein 50 (Fragment) OS=Homo sapiens GN=WDR77 PE=4 SV=1	1.51E+07	4.94E+07	0.00E+00	-3.27E+00
B4DT77	Annexin OS=Homo sapiens GN=ANXA7 PE=2 SV=1	0.00E+00	6.55E+07	0.00E+00	-1.00E+01
Q08945	FACT complex subunit SSRP1 OS=Homo sapiens GN=SSRP1 PE=1 SV=1	0.00E+00	6.56E+07	0.00E+00	-1.00E+01
P05387	60S acidic ribosomal protein P2 OS=Homo sapiens GN=RPLP2 PE=1 SV=1	3.18E+07	3.42E+07	6.51E+07	-1.07E+00
Q8N3C0	Activating signal cointegrator 1 complex subunit 3 OS=Homo sapiens GN=ASCC3 PE=1 SV=3	6.60E+07	0.00E+00	0.00E+00	1.00E+01
I3L4G9	Phosphoribosyl pyrophosphate synthase-associated protein 2 (Fragment) OS=Homo sapiens GN=PRPSAP2 PE=4 SV=1	2.37E+07	4.34E+07	9.33E+06	-1.84E+00
F8WA86	Calponin-3 OS=Homo sapiens GN=CNN3 PE=4 SV=1	0.00E+00	6.74E+07	0.00E+00	-1.00E+01
P14314-2	Isoform 2 of Glucosidase 2 subunit beta OS=Homo sapiens GN=PRKCSH	3.86E+07	2.89E+07	1.95E+08	1.34E+00
Q7L576	Cytoplasmic FMR1-interacting protein 1 OS=Homo sapiens GN=CYFIP1 PE=1 SV=1	0.00E+00	6.78E+07	0.00E+00	-1.00E+01
Q96DX4	RING finger and SPRY domain-containing protein 1 OS=Homo sapiens GN=RSPRY1 PE=2 SV=1	0.00E+00	6.86E+07	8.74E+07	-1.00E+01
Q9Y5K6	CD2-associated protein OS=Homo sapiens GN=CD2AP PE=1 SV=1	6.87E+07	0.00E+00	0.00E+00	1.00E+01
P04632	Calpain small subunit 1 OS=Homo sapiens GN=CAPNS1 PE=1 SV=1	6.87E+07	0.00E+00	6.97E+07	1.00E+01
H0Y9D8	Inorganic pyrophosphatase 2, mitochondrial (Fragment) OS=Homo sapiens GN=PPA2 PE=4 SV=1	6.95E+07	0.00E+00	3.00E+07	1.00E+01
B4DVE7	Annexin OS=Homo sapiens GN=ANXA11 PE=2 SV=1	0.00E+00	7.19E+07	1.26E+08	-1.00E+01

F5H5I6	G-rich sequence factor 1 OS=Homo sapiens GN=GRSF1 PE=4 SV=1	0.00E+00	7.28E+07	0.00E+00	-1.00E+01
Q9HB71	Calcyclin-binding protein OS=Homo sapiens GN=CACYBP PE=1 SV=2	7.30E+07	0.00E+00	1.43E+08	1.00E+01
O95292	Vesicle-associated membrane protein-associated protein B/C OS=Homo sapiens GN=VAPB PE=1 SV=3	0.00E+00	7.32E+07	0.00E+00	-1.00E+01
Q09161	Nuclear cap-binding protein subunit 1 OS=Homo sapiens GN=NCBP1 PE=1 SV=1	3.15E+07	4.25E+07	0.00E+00	-1.35E+00
Q8IYS2	Uncharacterized protein KIAA2013 OS=Homo sapiens GN=KIAA2013 PE=2 SV=1	3.57E+07	3.86E+07	2.84E+07	-1.08E+00
Q9NYL9	Tropomodulin-3 OS=Homo sapiens GN=TMOD3 PE=1 SV=1	0.00E+00	7.61E+07	2.73E+07	-1.00E+01
C9JSZ2	Proton-coupled folate transporter OS=Homo sapiens GN=SLC46A1 PE=4 SV=1	3.85E+07	3.77E+07	0.00E+00	1.02E+00
Q63ZY4	ATXN2L protein OS=Homo sapiens GN=ATXN2L PE=2 SV=1	7.70E+07	0.00E+00	1.15E+08	1.00E+01
P28072	Proteasome subunit beta type-6 OS=Homo sapiens GN=PSMB6 PE=1 SV=4	4.72E+07	3.04E+07	3.56E+07	1.55E+00
P49768-6	Isoform 6 of Presenilin-1 OS=Homo sapiens GN=PSEN1	4.50E+07	3.27E+07	0.00E+00	1.38E+00
P55263	Adenosine kinase OS=Homo sapiens GN=ADK PE=1 SV=2	7.82E+07	0.00E+00	0.00E+00	1.00E+01
Q00765	Receptor expression-enhancing protein 5 OS=Homo sapiens GN=REEP5 PE=1 SV=3	0.00E+00	7.86E+07	2.65E+08	-1.00E+01
P00492	Hypoxanthine-guanine phosphoribosyltransferase OS=Homo sapiens GN=HPRT1 PE=1 SV=2	4.59E+07	3.28E+07	4.49E+07	1.40E+00
P55735	Protein SEC13 homolog OS=Homo sapiens GN=SEC13 PE=1 SV=3	7.92E+07	0.00E+00	8.17E+07	1.00E+01
O95832	Claudin-1 OS=Homo sapiens GN=CLDN1 PE=1 SV=1	0.00E+00	7.95E+07	5.93E+07	-1.00E+01

P09543	2',3'-cyclic-nucleotide 3'-phosphodiesterase OS=Homo sapiens GN=CNP PE=1 SV=2	0.00E+00	8.03E+07	0.00E+00	-1.00E+01
E9PH82	Protein FAM98A OS=Homo sapiens GN=FAM98A PE=4 SV=1	0.00E+00	8.05E+07	1.20E+08	-1.00E+01
Q8WUM0	Nuclear pore complex protein Nup133 OS=Homo sapiens GN=NUP133 PE=1 SV=2	0.00E+00	8.05E+07	0.00E+00	-1.00E+01
P61073-2	Isoform 2 of C-X-C chemokine receptor type 4 OS=Homo sapiens GN=CXCR4	3.85E+07	4.29E+07	4.48E+07	-1.12E+00
B4DPX4	Synaptic vesicle membrane protein VAT-1 homolog OS=Homo sapiens GN=VAT1 PE=2 SV=1	4.27E+07	3.89E+07	3.31E+07	1.10E+00
Q9Y3I0	tRNA-splicing ligase RtcB homolog OS=Homo sapiens GN=C22orf28 PE=1 SV=1	0.00E+00	8.19E+07	0.00E+00	-1.00E+01
P61225	Ras-related protein Rap-2b OS=Homo sapiens GN=RAP2B PE=1 SV=1	4.17E+07	4.03E+07	3.59E+07	1.03E+00
O14929-2	Isoform B of Histone acetyltransferase type B catalytic subunit OS=Homo sapiens GN=HAT1	4.16E+07	4.06E+07	3.53E+07	1.02E+00
O75954	Tetraspanin-9 OS=Homo sapiens GN=TSPAN9 PE=1 SV=1	0.00E+00	8.29E+07	0.00E+00	-1.00E+01
Q9UNS2	COP9 signalosome complex subunit 3 OS=Homo sapiens GN=COPS3 PE=1 SV=3	0.00E+00	8.30E+07	2.42E+07	-1.00E+01
Q15645	Pachytene checkpoint protein 2 homolog OS=Homo sapiens GN=TRIP13 PE=1 SV=2	8.35E+07	0.00E+00	0.00E+00	1.00E+01
P11177	Pyruvate dehydrogenase E1 component subunit beta, mitochondrial OS=Homo sapiens GN=PDHB PE=1 SV=3	3.27E+07	5.16E+07	5.58E+07	-1.58E+00
A7MAP0	Coronin OS=Homo sapiens GN=CORO1C PE=2 SV=1	0.00E+00	8.48E+07	1.16E+08	-1.00E+01
F6SBX2	Isoleucine--tRNA ligase, mitochondrial OS=Homo sapiens GN=IARS2 PE=3 SV=1	8.50E+07	0.00E+00	2.24E+08	1.00E+01

P09234	U1 small nuclear ribonucleoprotein C OS=Homo sapiens GN=SNRPC PE=1 SV=1	8.55E+07	0.00E+00	7.50E+07	1.00E+01
Q9BU23	Lipase maturation factor 2 OS=Homo sapiens GN=LMF2 PE=1 SV=2	3.92E+07	4.74E+07	0.00E+00	-1.21E+00
Q13867	Bleomycin hydrolase OS=Homo sapiens GN=BLMH PE=1 SV=1	4.60E+07	4.10E+07	4.59E+07	1.12E+00
Q8NF37	Lysophosphatidylcholine acyltransferase 1 OS=Homo sapiens GN=LPCAT1 PE=1 SV=2	4.99E+07	3.75E+07	0.00E+00	1.33E+00
P48444	Coatomer subunit delta OS=Homo sapiens GN=ARCN1 PE=1 SV=1	8.79E+07	0.00E+00	0.00E+00	1.00E+01
O43776	Asparagine--tRNA ligase, cytoplasmic OS=Homo sapiens GN=NARS PE=1 SV=1	8.88E+07	0.00E+00	9.07E+07	1.00E+01
O15439	Multidrug resistance-associated protein 4 OS=Homo sapiens GN=ABCC4 PE=1 SV=3	4.88E+07	4.04E+07	0.00E+00	1.21E+00
F8WDV0	Importin-11 OS=Homo sapiens GN=IPO11 PE=4 SV=1	0.00E+00	8.94E+07	3.51E+07	-1.00E+01
B3KS98	Eukaryotic translation initiation factor 3 subunit H OS=Homo sapiens GN=EIF3S3 PE=2 SV=1	4.21E+07	4.74E+07	3.52E+07	-1.13E+00
P10301	Ras-related protein R-Ras OS=Homo sapiens GN=RRAS PE=1 SV=1	3.48E+07	5.48E+07	2.96E+07	-1.58E+00
O43809	Cleavage and polyadenylation specificity factor subunit 5 OS=Homo sapiens GN=NUDT21 PE=1 SV=1	3.44E+07	5.55E+07	2.18E+07	-1.61E+00
P63208	S-phase kinase-associated protein 1 OS=Homo sapiens GN=SKP1 PE=1 SV=2	5.09E+07	3.95E+07	4.86E+07	1.29E+00
O95807	Transmembrane protein 50A OS=Homo sapiens GN=TMEM50A PE=1 SV=1	0.00E+00	9.10E+07	0.00E+00	-1.00E+01
P61081	NEDD8-conjugating enzyme Ubc12 OS=Homo sapiens GN=UBE2M PE=1 SV=1	9.11E+07	0.00E+00	3.79E+07	1.00E+01

O00767	Acyl-CoA desaturase OS=Homo sapiens GN=SCD PE=1 SV=2	4.80E+07	4.43E+07	7.68E+07	1.08E+00
Q92581-2	Isoform 2 of Sodium/hydrogen exchanger 6 OS=Homo sapiens GN=SLC9A6	6.07E+07	3.25E+07	3.54E+07	1.87E+00
Q15392	Delta(24)-sterol reductase OS=Homo sapiens GN=DHCR24 PE=1 SV=2	3.22E+07	6.11E+07	2.04E+07	-1.89E+00
E2QRH7	Elongation of very long chain fatty acids protein 5 OS=Homo sapiens GN=ELOVL5 PE=4 SV=2	0.00E+00	9.44E+07	1.01E+08	-1.00E+01
P25205	DNA replication licensing factor MCM3 OS=Homo sapiens GN=MCM3 PE=1 SV=3	6.28E+07	3.20E+07	4.84E+07	1.96E+00
I3L4X2	Multidrug resistance-associated protein 1 (Fragment) OS=Homo sapiens GN=ABCC1 PE=3 SV=1	0.00E+00	9.55E+07	4.21E+07	-1.00E+01
O75396	Vesicle-trafficking protein SEC22b OS=Homo sapiens GN=SEC22B PE=1 SV=4	3.87E+07	5.75E+07	4.89E+07	-1.49E+00
Q92688-2	Isoform 2 of Acidic leucine-rich nuclear phosphoprotein 32 family member B OS=Homo sapiens GN=ANP32B	5.22E+07	4.40E+07	8.99E+07	1.19E+00
Q86YZ3	Hornerin OS=Homo sapiens GN=HRNR PE=1 SV=2	9.65E+07	0.00E+00	0.00E+00	1.00E+01
Q96CG1	ETF1 protein OS=Homo sapiens GN=ETF1 PE=2 SV=1	7.49E+07	2.20E+07	6.09E+07	3.40E+00
Q9UHD8-5	Isoform 5 of Septin-9 OS=Homo sapiens GN=SEPT9	5.16E+07	4.57E+07	4.03E+07	1.13E+00
P51148	Ras-related protein Rab-5C OS=Homo sapiens GN=RAB5C PE=1 SV=2	3.44E+07	6.31E+07	0.00E+00	-1.83E+00
E7ESG6	Zinc transporter SLC39A7 OS=Homo sapiens GN=SLC39A7 PE=4 SV=1	5.16E+07	4.80E+07	2.04E+07	1.08E+00
B4DNJ6	Serine-threonine kinase receptor-associated protein OS=Homo sapiens GN=STRAP PE=2 SV=1	5.07E+07	4.93E+07	5.71E+07	1.03E+00

O00220	Tumor necrosis factor receptor superfamily member 10A OS=Homo sapiens GN=TNFRSF10A PE=1 SV=3	8.47E+07	1.57E+07	1.12E+08	5.40E+00
Q7Z5G4	Golgin subfamily A member 7 OS=Homo sapiens GN=GOLGA7 PE=1 SV=2	4.19E+07	5.90E+07	2.83E+07	-1.41E+00
Q5H9R7-5	Isoform 5 of Serine/threonine-protein phosphatase 6 regulatory subunit 3 OS=Homo sapiens GN=PPP6R3	1.01E+08	0.00E+00	1.32E+08	1.00E+01
B3KRS5	Histone deacetylase OS=Homo sapiens GN=HDAC2 PE=2 SV=1	4.28E+07	5.88E+07	2.28E+07	-1.37E+00
Q16555	Dihydropyrimidinase-related protein 2 OS=Homo sapiens GN=DPYSL2 PE=1 SV=1	6.57E+07	3.60E+07	0.00E+00	1.82E+00
P20618	Proteasome subunit beta type-1 OS=Homo sapiens GN=PSMB1 PE=1 SV=2	0.00E+00	1.02E+08	2.22E+07	-1.00E+01
B7Z972	Protein-L-isoaspartate O-methyltransferase OS=Homo sapiens GN=PCMT1 PE=2 SV=1	1.02E+08	0.00E+00	1.12E+08	1.00E+01
P48163	NADP-dependent malic enzyme OS=Homo sapiens GN=ME1 PE=1 SV=1	2.64E+07	7.65E+07	8.21E+07	-2.89E+00
Q15427	Splicing factor 3B subunit 4 OS=Homo sapiens GN=SF3B4 PE=1 SV=1	0.00E+00	1.03E+08	6.08E+07	-1.00E+01
P33176	Kinesin-1 heavy chain OS=Homo sapiens GN=KIF5B PE=1 SV=1	1.03E+08	0.00E+00	1.56E+08	1.00E+01
Q969X1	Protein lifeguard 3 OS=Homo sapiens GN=TMBIM1 PE=1 SV=2	0.00E+00	1.04E+08	0.00E+00	-1.00E+01
Q13501	Sequestosome-1 OS=Homo sapiens GN=SQSTM1 PE=1 SV=1	4.44E+07	6.09E+07	7.71E+07	-1.37E+00
P78417	Glutathione S-transferase omega-1 OS=Homo sapiens GN=GSTO1 PE=1 SV=2	1.06E+08	0.00E+00	7.52E+07	1.00E+01

E9PC80	Interferon-induced, double-stranded RNA-activated protein kinase OS=Homo sapiens GN=EIF2AK2 PE=4 SV=1	1.06E+08	0.00E+00	4.43E+07	1.00E+01
P43487	Ran-specific GTPase-activating protein OS=Homo sapiens GN=RANBP1 PE=1 SV=1	1.07E+08	0.00E+00	1.40E+08	1.00E+01
Q02809	Procollagen-lysine,2-oxoglutarate 5-dioxygenase 1 OS=Homo sapiens GN=PLOD1 PE=1 SV=2	5.23E+07	5.51E+07	4.93E+07	-1.05E+00
P30419	Glycylpeptide N-tetradecanoyltransferase 1 OS=Homo sapiens GN=NMT1 PE=1 SV=2	3.31E+07	7.48E+07	1.44E+07	-2.26E+00
Q9UIA9	Exportin-7 OS=Homo sapiens GN=XPO7 PE=1 SV=3	1.09E+08	0.00E+00	7.79E+07	1.00E+01
D6RGI3	Septin 11, isoform CRA_b OS=Homo sapiens GN=SEPT11 PE=3 SV=1	7.16E+07	3.98E+07	3.86E+07	1.80E+00
Q16719	Kynureninase OS=Homo sapiens GN=KYNU PE=1 SV=1	5.91E+07	5.39E+07	8.77E+07	1.10E+00
P54136	Arginine--tRNA ligase, cytoplasmic OS=Homo sapiens GN=RARS PE=1 SV=2	5.62E+07	5.76E+07	6.33E+07	-1.03E+00
G3V295	Proteasome subunit alpha type OS=Homo sapiens GN=PSMA6 PE=3 SV=1	5.46E+07	5.95E+07	1.18E+08	-1.09E+00
P06493	Cyclin-dependent kinase 1 OS=Homo sapiens GN=CDK1 PE=1 SV=3	5.86E+07	5.66E+07	8.66E+07	1.04E+00
H7BYD0	NADH dehydrogena	5.51E+07	6.04E+07	0.00E+00	-1.10E+00
Q9Y678	Coatomer subunit gamma-1 OS=Homo sapiens GN=COPG1 PE=1 SV=1	6.19E+07	5.43E+07	9.97E+07	1.14E+00
Q96AG4	Leucine-rich repeat-containing protein 59 OS=Homo sapiens GN=LRRC59 PE=1 SV=1	0.00E+00	1.17E+08	7.78E+07	-1.00E+01
G3V1N7	Major facilitator superfamily domain containing 5, isoform CRA_a OS=Homo sapiens GN=MFSD5 PE=4 SV=1	5.37E+07	6.32E+07	1.13E+08	-1.18E+00
Q99829	Copine-1 OS=Homo sapiens GN=CPNE1 PE=1 SV=1	7.29E+07	4.43E+07	0.00E+00	1.65E+00

Q04760-2	Isoform 2 of Lactoylglutathione lyase OS=Homo sapiens GN=GLO1	8.00E+07	3.73E+07	3.09E+07	2.14E+00
P05198	Eukaryotic translation initiation factor 2 subunit 1 OS=Homo sapiens GN=EIF2S1 PE=1 SV=3	5.20E+07	6.63E+07	7.31E+07	-1.27E+00
E7ES68	Zinc phosphodiesterase ELAC protein 2 (Fragment) OS=Homo sapiens GN=ELAC2 PE=4 SV=2	0.00E+00	1.19E+08	3.97E+07	-1.00E+01
Q8N726	Cyclin-dependent kinase inhibitor 2A, isoform 4 OS=Homo sapiens GN=CDKN2A PE=1 SV=2	6.22E+07	5.73E+07	4.77E+07	1.09E+00
P15121	Aldose reductase OS=Homo sapiens GN=AKR1B1 PE=1 SV=3	5.77E+07	6.25E+07	8.27E+07	-1.08E+00
P04844-2	Isoform 2 of Dolichyl-diphosphooligosaccharide--protein glycosyltransferase subunit 2 OS=Homo sapiens GN=RPN2	5.85E+07	6.17E+07	5.97E+07	-1.06E+00
Q8NC51-2	Isoform 2 of Plasminogen activator inhibitor 1 RNA-binding protein OS=Homo sapiens GN=SERBP1	6.32E+07	5.72E+07	7.46E+07	1.10E+00
P21281	V-type proton ATPase subunit B, brain isoform OS=Homo sapiens GN=ATP6V1B2 PE=1 SV=3	3.74E+07	8.31E+07	0.00E+00	-2.22E+00
B1AHD1	NHP2 non-histone chromosome protein 2-like 1 (S. cerevisiae) OS=Homo sapiens GN=NHP2L1 PE=4 SV=1	6.98E+07	5.17E+07	7.89E+07	1.35E+00
H0Y8E6	DNA replication licensing factor MCM2 (Fragment) OS=Homo sapiens GN=MCM2 PE=3 SV=1	7.95E+07	4.21E+07	5.98E+07	1.89E+00
C9JNW5	60S ribosomal protein L24 OS=Homo sapiens GN=RPL24 PE=4 SV=1	0.00E+00	1.23E+08	9.94E+07	-1.00E+01
O00487	26S proteasome non-ATPase regulatory subunit 14 OS=Homo sapiens GN=PSMD14 PE=1 SV=1	6.56E+07	5.73E+07	5.91E+07	1.15E+00

O43242	26S proteasome non-ATPase regulatory subunit 3 OS=Homo sapiens GN=PSMD3 PE=1 SV=2	7.75E+07	4.59E+07	7.46E+07	1.69E+00
H0YKC5	Deoxyuridine 5'-triphosphate nucleotidohydrolase, mitochondrial (Fragment) OS=Homo sapiens GN=DUT PE=4 SV=1	3.79E+07	8.77E+07	5.00E+07	-2.32E+00
B4DGU4	Catenin beta-1 OS=Homo sapiens GN=CTNNB1 PE=2 SV=1	1.26E+08	0.00E+00	7.52E+07	1.00E+01
Q8N357	Transmembrane protein C2orf18 OS=Homo sapiens GN=C2orf18 PE=1 SV=1	5.43E+07	7.26E+07	4.91E+07	-1.34E+00
P62333	26S protease regulatory subunit 10B OS=Homo sapiens GN=PSMC6 PE=1 SV=1	8.00E+07	4.68E+07	5.97E+07	1.71E+00
P46977	Dolichyl-diphosphooligosaccharide--protein glycosyltransferase subunit STT3A OS=Homo sapiens GN=STT3A PE=1 SV=2	7.21E+07	5.66E+07	6.44E+07	1.27E+00
P26368-2	Isoform 2 of Splicing factor U2AF 65 kDa subunit OS=Homo sapiens GN=U2AF2	0.00E+00	1.29E+08	8.61E+07	-1.00E+01
Q14444-2	Isoform 2 of Caprin-1 OS=Homo sapiens GN=CAPRIN1	6.96E+07	6.02E+07	1.09E+08	1.16E+00
O43237	Cytoplasmic dynein 1 light intermediate chain 2 OS=Homo sapiens GN=DYNC1LI2 PE=1 SV=1	0.00E+00	1.30E+08	0.00E+00	-1.00E+01
Q07666-3	Isoform 3 of KH domain-containing, RNA-binding, signal transduction-associated protein 1 OS=Homo sapiens GN=KHDRBS1	9.00E+07	4.21E+07	0.00E+00	2.14E+00
P07384	Calpain-1 catalytic subunit OS=Homo sapiens GN=CAPN1 PE=1 SV=1	3.37E+07	1.00E+08	4.47E+07	-2.97E+00
Q9P035	Very-long-chain (3R)-3-hydroxyac	6.93E+07	6.48E+07	4.64E+07	1.07E+00

Q9UL46	Proteasome activator complex subunit 2 OS=Homo sapiens GN=PSME2 PE=1 SV=4	9.95E+07	3.47E+07	8.09E+07	2.87E+00
P45974-2	Isoform Short of Ubiquitin carboxyl-terminal hydrolase 5 OS=Homo sapiens GN=USP5	1.34E+08	0.00E+00	1.24E+08	1.00E+01
Q9ULC5	Long-chain-fatty-acid--CoA ligase 5 OS=Homo sapiens GN=ACSL5 PE=1 SV=1	0.00E+00	1.35E+08	0.00E+00	-1.00E+01
Q8TDN6	Ribosome biogenesis protein BRX1 homolog OS=Homo sapiens GN=BRIX1 PE=1 SV=2	1.09E+08	2.70E+07	2.84E+08	4.04E+00
P52907	F-actin-capping protein subunit alpha-1 OS=Homo sapiens GN=CAPZA1 PE=1 SV=3	0.00E+00	1.36E+08	5.61E+07	-1.00E+01
H0YJ34	Fermitin family homolog 2 (Fragment) OS=Homo sapiens GN=FERMT2 PE=4 SV=1	8.04E+07	5.68E+07	8.92E+07	1.42E+00
Q8WUX1-2	Isoform 2 of Sodium-coupled neutral amino acid transporter 5 OS=Homo sapiens GN=SLC38A5	0.00E+00	1.37E+08	0.00E+00	-1.00E+01
P16402	Histone H1.3 OS=Homo sapiens GN=HIST1H1D PE=1 SV=2	5.66E+07	8.10E+07	3.57E+09	-1.43E+00
Q13347	Eukaryotic translation initiation factor 3 subunit I OS=Homo sapiens GN=EIF3I PE=1 SV=1	7.31E+07	6.46E+07	6.01E+07	1.13E+00
Q14156-2	Isoform 2 of Protein EFR3 homolog A OS=Homo sapiens GN=EFR3A	8.01E+07	5.78E+07	1.18E+08	1.38E+00
P51809	Vesicle-associated membrane protein 7 OS=Homo sapiens GN=VAMP7 PE=1 SV=3	9.85E+07	4.03E+07	4.17E+07	2.44E+00
O00425	Insulin-like growth factor 2 mRNA-binding protein 3 OS=Homo sapiens GN=IGF2BP3 PE=1 SV=2	0.00E+00	1.39E+08	0.00E+00	-1.00E+01
P50443	Sulfate transporter OS=Homo sapiens GN=SLC26A2 PE=1 SV=2	6.90E+07	7.13E+07	4.06E+07	-1.03E+00
P29692	Elongation factor 1-delta OS=Homo sapiens GN=EEF1D PE=1 SV=5	9.78E+07	4.26E+07	1.85E+08	2.30E+00

P28288	ATP-binding cassette sub-family D member 3 OS=Homo sapiens GN=ABCD3 PE=1 SV=1	1.01E+08	3.93E+07	0.00E+00	2.57E+00
P24539	ATP synthase subunit b, mitochondrial OS=Homo sapiens GN=ATP5F1 PE=1 SV=2	4.49E+07	9.58E+07	3.06E+07	-2.13E+00
P38606	V-type proton ATPase catalytic subunit A OS=Homo sapiens GN=ATP6V1A PE=1 SV=2	9.55E+07	4.52E+07	2.56E+08	2.11E+00
P10768	S-formylglutathione hydrolase OS=Homo sapiens GN=ESD PE=1 SV=2	8.53E+07	5.54E+07	7.95E+07	1.54E+00
Q9ULF5	Zinc transporter ZIP10 OS=Homo sapiens GN=SLC39A10 PE=1 SV=2	9.18E+07	4.97E+07	9.70E+07	1.85E+00
P12429	Annexin A3 OS=Homo sapiens GN=ANXA3 PE=1 SV=3	6.81E+07	7.40E+07	1.69E+08	-1.09E+00
O75439	Mitochondrial-processing peptidase subunit beta OS=Homo sapiens GN=PMPCB PE=1 SV=2	6.82E+07	7.42E+07	1.13E+08	-1.09E+00
Q9Y2X3	Nucleolar protein 58 OS=Homo sapiens GN=NOP58 PE=1 SV=1	8.11E+07	6.36E+07	0.00E+00	1.28E+00
P49419-2	Isoform 2 of Alpha-aminoadipic semialdehyde dehydrogenase OS=Homo sapiens GN=ALDH7A1	1.13E+08	3.20E+07	2.76E+07	3.52E+00
P36957	Dihydrolipoyllysine-residue succinyltransferase component of 2-oxoglutarate dehydrogenase complex, mitochondrial OS=Homo sapiens GN=DLST PE=1 SV=4	7.01E+07	7.50E+07	3.98E+08	-1.07E+00
P31949	Protein S100-A11 OS=Homo sapiens GN=S100A11 PE=1 SV=2	6.20E+07	8.30E+07	1.34E+08	-1.34E+00
P61019	Ras-related protein Rab-2A OS=Homo sapiens GN=RAB2A PE=1 SV=1	6.68E+07	7.87E+07	4.75E+07	-1.18E+00
Q6DD88	Atlastin-3 OS=Homo sapiens GN=ATL3 PE=1 SV=1	6.05E+07	8.51E+07	4.17E+07	-1.41E+00

P84098	60S ribosomal protein L19 OS=Homo sapiens GN=RPL19 PE=1 SV=1	7.62E+07	7.03E+07	9.07E+07	1.08E+00
Q9BT67	NEDD4 family-interacting protein 1 OS=Homo sapiens GN=NDFIP1 PE=1 SV=1	6.90E+07	7.86E+07	8.98E+07	-1.14E+00
G3V5W5	Protein arginine N-methyltransferase 5 OS=Homo sapiens GN=PRMT5 PE=4 SV=1	5.47E+07	9.31E+07	8.99E+07	-1.70E+00
P27695	DNA-(apurinic or apyrimidinic site) lyase OS=Homo sapiens GN=APEX1 PE=1 SV=2	7.98E+07	6.81E+07	9.17E+07	1.17E+00
Q13283	Ras GTPase-activating protein-binding protein 1 OS=Homo sapiens GN=G3BP1 PE=1 SV=1	5.92E+07	8.87E+07	1.20E+08	-1.50E+00
Q9Y289	Sodium-dependent multivitamin transporter OS=Homo sapiens GN=SLC5A6 PE=2 SV=2	8.08E+07	6.86E+07	3.15E+07	1.18E+00
P04040	Catalase OS=Homo sapiens GN=CAT PE=1 SV=3	8.10E+07	6.89E+07	0.00E+00	1.18E+00
Q9BTU6	Phosphatidylinositol 4-kinase type 2-alpha OS=Homo sapiens GN=PI4K2A PE=1 SV=1	6.57E+07	8.41E+07	8.72E+07	-1.28E+00
F5GXX5	Dolichyl-diphosphooligosaccharide--protein glycosyltransferase subunit DAD1 OS=Homo sapiens GN=DAD1 PE=4 SV=1	6.06E+07	8.96E+07	8.85E+07	-1.48E+00
Q9UMS4	Pre-mRNA-processing factor 19 OS=Homo sapiens GN=PRPF19 PE=1 SV=1	7.21E+07	7.82E+07	9.71E+07	-1.08E+00
P62714	Serine/threonine-protein phosphatase 2A catalytic subunit beta isoform OS=Homo sapiens GN=PPP2CB PE=1 SV=1	7.65E+07	7.48E+07	6.94E+07	1.02E+00
O15258	Protein RER1 OS=Homo sapiens GN=RER1 PE=1 SV=1	6.75E+07	8.43E+07	1.05E+08	-1.25E+00
Q13126-2	Isoform 2 of S-methyl-5'-thioadenosine phosphorylase OS=Homo sapiens GN=MTAP	6.78E+07	8.43E+07	8.45E+07	-1.24E+00

B3KSH1	Eukaryotic translation initiation factor 3 subunit F OS=Homo sapiens GN=EIF3F PE=2 SV=1	6.65E+07	8.58E+07	4.62E+07	-1.29E+00
P15170	Eukaryotic peptide chain release factor GTP-binding subunit ERF3A OS=Homo sapiens GN=GSPT1 PE=1 SV=1	8.30E+07	6.93E+07	3.51E+07	1.20E+00
Q9BWD1	Acetyl-CoA acetyltransferase, cytosolic OS=Homo sapiens GN=ACAT2 PE=1 SV=2	4.93E+07	1.03E+08	1.45E+08	-2.09E+00
P43304-2	Isoform 2 of Glycerol-3-phosphate dehydrogenase, mitochondrial OS=Homo sapiens GN=GPD2	6.97E+07	8.31E+07	1.43E+08	-1.19E+00
O75531	Barrier-to-autointegration factor OS=Homo sapiens GN=BANF1 PE=1 SV=1	7.16E+07	8.13E+07	0.00E+00	-1.14E+00
Q8TCT9-5	Isoform 5 of Minor histocompatibility antigen H13 OS=Homo sapiens GN=HM13	6.52E+07	8.78E+07	5.51E+07	-1.35E+00
Q9H0V1	Transmembrane protein 168 OS=Homo sapiens GN=TMEM168 PE=1 SV=2	7.13E+07	8.17E+07	8.40E+07	-1.15E+00
P58546	Myotrophin OS=Homo sapiens GN=MTPN PE=1 SV=2	6.32E+07	9.07E+07	8.14E+07	-1.44E+00
Q9NVA4	Transmembrane protein 184C OS=Homo sapiens GN=TMEM184C PE=2 SV=2	6.62E+07	8.77E+07	9.22E+07	-1.32E+00
Q86T03	Transmembrane protein 55B OS=Homo sapiens GN=TMEM55B PE=1 SV=1	9.60E+07	5.84E+07	5.92E+07	1.64E+00
J3KPV4	DNA replication licensing factor MCM4 OS=Homo sapiens GN=MCM4 PE=3 SV=1	9.04E+07	6.40E+07	1.06E+08	1.41E+00
P62913-2	Isoform 2 of 60S ribosomal protein L11 OS=Homo sapiens GN=RPL11	0.00E+00	1.55E+08	0.00E+00	-1.00E+01
P05556-5	Isoform Beta-1D of Integrin beta-1 OS=Homo sapiens GN=ITGB1	8.73E+07	6.75E+07	8.95E+07	1.29E+00
Q9H773	dCTP pyrophosphatase 1 OS=Homo sapiens GN=DCTPP1 PE=1 SV=1	8.23E+07	7.29E+07	1.07E+08	1.13E+00

Q9BWF3	RNA-binding protein 4 OS=Homo sapiens GN=RBM4 PE=1 SV=1	0.00E+00	1.56E+08	0.00E+00	-1.00E+01
Q969Z0-2	Isoform 2 of Protein TBRG4 OS=Homo sapiens GN=TBRG4	1.12E+08	4.34E+07	0.00E+00	2.59E+00
O43592	Exportin-T OS=Homo sapiens GN=XPOT PE=1 SV=2	4.53E+07	1.11E+08	9.29E+07	-2.44E+00
P49721	Proteasome subunit beta type-2 OS=Homo sapiens GN=PSMB2 PE=1 SV=1	7.18E+07	8.46E+07	0.00E+00	-1.18E+00
P25788-2	Isoform 2 of Proteasome subunit alpha type-3 OS=Homo sapiens GN=PSMA3	1.58E+08	0.00E+00	1.42E+08	1.00E+01
O94979-6	Isoform 6 of Protein transport protein Sec31A OS=Homo sapiens GN=SEC31A	9.05E+07	6.91E+07	1.18E+08	1.31E+00
F8W1A4	Adenylate kinase 2, mitochondrial OS=Homo sapiens GN=AK2 PE=3 SV=1	5.60E+07	1.05E+08	0.00E+00	-1.87E+00
Q9UHX1-6	Isoform 6 of Poly(U)-binding-splicing factor PUF60 OS=Homo sapiens GN=PUF60	9.62E+07	6.52E+07	8.85E+07	1.47E+00
O43813	LanC-like protein 1 OS=Homo sapiens GN=LANCL1 PE=1 SV=1	7.13E+07	9.05E+07	1.14E+08	-1.27E+00
P16152	Carbonyl reducta	6.42E+07	9.77E+07	9.42E+07	-1.52E+00
H0Y368	Dolichol-phosphate mannosyltransferase (Fragment) OS=Homo sapiens GN=DPM1 PE=4 SV=1	0.00E+00	1.63E+08	6.11E+07	-1.00E+01
P28066	Proteasome subunit alpha type-5 OS=Homo sapiens GN=PSMA5 PE=1 SV=3	7.09E+07	9.21E+07	6.24E+08	-1.30E+00
Q9BZZ5-1	Isoform 1 of Apoptosis inhibitor 5 OS=Homo sapiens GN=API5	6.87E+07	9.43E+07	8.52E+07	-1.37E+00
P36952	Serpin B5 OS=Homo sapiens GN=SERPINB5 PE=1 SV=2	1.65E+08	0.00E+00	1.99E+08	1.00E+01
P52292	Importin subunit alpha-2 OS=Homo sapiens GN=KPNA2 PE=1 SV=1	8.31E+07	8.35E+07	9.07E+07	-1.01E+00
H0YL69	Proteasome subunit alpha type (Fragment) OS=Homo sapiens GN=PSMA4 PE=3 SV=1	7.30E+07	9.40E+07	5.17E+07	-1.29E+00
P35237	Serpin B6 OS=Homo sapiens GN=SERPINB6 PE=1 SV=3	7.01E+07	9.73E+07	1.33E+08	-1.39E+00

O95372	Acyl-protein thioesterase 2 OS=Homo sapiens GN=LYPLA2 PE=1 SV=1	7.86E+07	8.91E+07	1.93E+08	-1.13E+00
P78310	Coxsackievirus and adenovirus receptor OS=Homo sapiens GN=CXADR PE=1 SV=1	7.75E+07	9.08E+07	7.54E+07	-1.17E+00
Q9BZE4	Nucleolar GTP-binding protein 1 OS=Homo sapiens GN=GTPBP4 PE=1 SV=3	1.68E+08	0.00E+00	6.90E+07	1.00E+01
Q12769	Nuclear pore complex protein Nup160 OS=Homo sapiens GN=NUP160 PE=1 SV=3	5.38E+07	1.16E+08	7.57E+07	-2.15E+00
B4DKB2	Endothelin-converting enzyme 1 OS=Homo sapiens GN=ECE1 PE=2 SV=1	8.70E+07	8.25E+07	1.01E+08	1.05E+00
P53618	Coatomer subunit beta OS=Homo sapiens GN=COPB1 PE=1 SV=3	6.90E+07	1.01E+08	2.39E+08	-1.46E+00
Q96PK6	RNA-binding protein 14 OS=Homo sapiens GN=RBM14 PE=1 SV=2	1.70E+08	0.00E+00	0.00E+00	1.00E+01
H0Y449	Nuclease-sensitive element-binding protein 1 (Fragment) OS=Homo sapiens GN=YBX1 PE=4 SV=1	2.43E+07	1.47E+08	5.76E+07	-6.03E+00
F5H801	2-oxoglutarate dehydrogenase, mitochondrial OS=Homo sapiens GN=OGDH PE=4 SV=1	7.71E+07	9.40E+07	6.53E+07	-1.22E+00
P53985	Monocarboxylate transporter 1 OS=Homo sapiens GN=SLC16A1 PE=1 SV=3	7.59E+07	9.60E+07	2.44E+08	-1.27E+00
P62136	Serine/threonine-protein phosphatase PP1-alpha catalytic subunit OS=Homo sapiens GN=PPP1CA PE=1 SV=1	9.85E+07	7.38E+07	6.92E+07	1.34E+00
P50416-2	Isoform 2 of Carnitine O-palmitoyltransferase 1, liver isoform OS=Homo sapiens GN=CPT1A	8.13E+07	9.17E+07	6.04E+07	-1.13E+00
P09382	Galectin-1 OS=Homo sapiens GN=LGALS1 PE=1 SV=2	9.54E+07	7.76E+07	1.17E+08	1.23E+00

P15151-3	Isoform Gamma of Poliovirus receptor OS=Homo sapiens GN=PVR	7.06E+07	1.03E+08	1.22E+08	-1.46E+00
P06737-2	Isoform 2 of Glycogen phosphorylase, liver form OS=Homo sapiens GN=PYGL	7.77E+07	9.57E+07	1.50E+08	-1.23E+00
Q14247	Src substrate cortactin OS=Homo sapiens GN=CTTN PE=1 SV=2	1.19E+08	5.50E+07	9.93E+07	2.16E+00
F5H365	Protein transport protein Sec23A OS=Homo sapiens GN=SEC23A PE=4 SV=1	6.61E+07	1.08E+08	4.30E+07	-1.64E+00
Q13185	Chromobox protein homolog 3 OS=Homo sapiens GN=CBX3 PE=1 SV=4	7.74E+07	9.72E+07	1.01E+08	-1.26E+00
Q99798	Aconitate hydratase, mitochondrial OS=Homo sapiens GN=ACO2 PE=1 SV=2	1.75E+08	0.00E+00	1.52E+08	1.00E+01
P05386	60S acidic ribosomal protein P1 OS=Homo sapiens GN=RPLP1 PE=1 SV=1	7.65E+07	9.85E+07	8.32E+07	-1.29E+00
Q9HDC9	Adipocyte plasma membrane-associated protein OS=Homo sapiens GN=APMAP PE=1 SV=2	3.20E+07	1.45E+08	3.73E+07	-4.52E+00
I3L3X5	Phospholipid scramblase 3 OS=Homo sapiens GN=PLSCR3 PE=4 SV=1	8.80E+07	8.93E+07	8.25E+07	-1.01E+00
E9PPJ0	Splicing factor 3B subunit 2 OS=Homo sapiens GN=SF3B2 PE=4 SV=1	0.00E+00	1.78E+08	9.50E+07	-1.00E+01
P61221	ATP-binding cassette sub-family E member 1 OS=Homo sapiens GN=ABCE1 PE=1 SV=1	1.01E+08	7.73E+07	8.76E+07	1.30E+00
J3KNE5	Histidine--tRNA ligase, cytoplasmic OS=Homo sapiens GN=HARS PE=4 SV=1	7.50E+07	1.03E+08	1.03E+08	-1.38E+00
P60953	Cell division control protein 42 homolog OS=Homo sapiens GN=CDC42 PE=1 SV=2	7.44E+07	1.04E+08	6.55E+07	-1.40E+00
P31930	Cytochrome b-c1 complex subunit 1, mitochondrial OS=Homo sapiens GN=UQCRC1 PE=1 SV=3	9.51E+07	8.38E+07	5.25E+07	1.13E+00

Q16836-2	Isoform 2 of Hydroxyacyl-coenzyme A dehydrogenase, mitochondrial OS=Homo sapiens GN=HADH	7.54E+07	1.05E+08	1.03E+08	-1.39E+00
Q96G23	Ceramide synthase 2 OS=Homo sapiens GN=CERS2 PE=1 SV=1	9.39E+07	8.65E+07	0.00E+00	1.09E+00
P41250	Glycine--tRNA ligase OS=Homo sapiens GN=GARS PE=1 SV=3	9.13E+07	8.95E+07	2.25E+08	1.02E+00
Q92542-2	Isoform 2 of Nicastrin OS=Homo sapiens GN=NCSTN	9.32E+07	8.79E+07	0.00E+00	1.06E+00
O75475	PC4 and SFRS1-interacting protein OS=Homo sapiens GN=PSIP1 PE=1 SV=1	0.00E+00	1.81E+08	1.94E+08	-1.00E+01
P51149	Ras-related protein Rab-7a OS=Homo sapiens GN=RAB7A PE=1 SV=1	7.56E+07	1.06E+08	8.98E+07	-1.40E+00
P78347-2	Isoform 2 of General transcription factor II-I OS=Homo sapiens GN=GTF2I	0.00E+00	1.82E+08	1.20E+08	-1.00E+01
Q9C0H2-2	Isoform 2 of Protein tweety homolog 3 OS=Homo sapiens GN=TTYH3	7.47E+07	1.07E+08	8.08E+07	-1.44E+00
O60831	PRA1 family protein 2 OS=Homo sapiens GN=PRAF2 PE=1 SV=1	7.90E+07	1.03E+08	7.76E+07	-1.30E+00
B4DR61	Protein transport protein Sec61 subunit alpha isoform 1 OS=Homo sapiens GN=SEC61A1 PE=2 SV=1	8.48E+07	9.72E+07	1.26E+08	-1.15E+00
P84090	Enhancer of rudimentary homolog OS=Homo sapiens GN=ERH PE=1 SV=1	1.05E+08	7.69E+07	8.36E+07	1.37E+00
P49720	Proteasome subunit beta type-3 OS=Homo sapiens GN=PSMB3 PE=1 SV=2	7.82E+07	1.04E+08	6.50E+07	-1.33E+00
P62857	40S ribosomal protein S28 OS=Homo sapiens GN=RPS28 PE=1 SV=1	8.07E+07	1.04E+08	1.06E+08	-1.28E+00
P62304	Small nuclear ribonucleoprotein E OS=Homo sapiens GN=SNRPE PE=1 SV=1	1.21E+08	6.46E+07	9.30E+07	1.87E+00

Q13200	26S proteasome non-ATPase regulatory subunit 2 OS=Homo sapiens GN=PSMD2 PE=1 SV=3	8.20E+07	1.04E+08	8.53E+07	-1.27E+00
D6R9P3	Heterogeneous nuclear ribonucleoprotein A/B OS=Homo sapiens GN=HNRNPAB PE=4 SV=1	1.13E+08	7.27E+07	1.12E+08	1.56E+00
O75131	Copine-3 OS=Homo sapiens GN=CPNE3 PE=1 SV=1	0.00E+00	1.87E+08	0.00E+00	-1.00E+01
Q06210	Glutamine--fructose-6-phosphate aminotransfera	0.00E+00	1.87E+08	0.00E+00	-1.00E+01
Q13162	Peroxiredoxin-4 OS=Homo sapiens GN=PRDX4 PE=1 SV=1	9.87E+07	8.85E+07	2.09E+08	1.11E+00
E9PCT3	Caveolin OS=Homo sapiens GN=CAV2 PE=3 SV=1	8.81E+07	9.93E+07	9.03E+07	-1.13E+00
Q8TCJ2	Dolichyl-diphosphooligosaccharide--protein glycosyltransferase subunit STT3B OS=Homo sapiens GN=STT3B PE=1 SV=1	1.17E+08	7.38E+07	5.83E+07	1.58E+00
O94826	Mitochondrial import receptor subunit TOM70 OS=Homo sapiens GN=TOMM70A PE=1 SV=1	3.26E+07	1.58E+08	3.36E+08	-4.86E+00
Q9H7F0	Probable cation-transporting ATPase 13A3 OS=Homo sapiens GN=ATP13A3 PE=1 SV=4	1.93E+08	0.00E+00	1.77E+08	1.00E+01
O75608-2	Isoform 2 of Acyl-protein thioesterase 1 OS=Homo sapiens GN=LYPLA1	1.10E+08	8.34E+07	9.57E+07	1.31E+00
E9PH29	Thioredoxin-dependent peroxide reductase, mitochondrial OS=Homo sapiens GN=PRDX3 PE=4 SV=1	1.22E+08	7.18E+07	0.00E+00	1.69E+00
Q7L2H7	Eukaryotic translation initiation factor 3 subunit M OS=Homo sapiens GN=EIF3M PE=1 SV=1	9.30E+07	1.01E+08	9.00E+07	-1.08E+00
Q14498-3	Isoform 3 of RNA-binding protein 39 OS=Homo sapiens GN=RBM39	7.73E+07	1.17E+08	4.51E+08	-1.51E+00

Q9BUJ2-2	Isoform 2 of Heterogeneous nuclear ribonucleoprotein U-like protein 1 OS=Homo sapiens GN=HNRNPUL1	9.37E+07	1.02E+08	8.22E+07	-1.09E+00
P07954	Fumarate hydratase, mitochondrial OS=Homo sapiens GN=FH PE=1 SV=3	1.30E+08	6.57E+07	9.97E+07	1.98E+00
Q9H9B4	Sideroflexin-1 OS=Homo sapiens GN=SFXN1 PE=1 SV=4	1.14E+08	8.22E+07	4.72E+07	1.38E+00
P35659	Protein DEK OS=Homo sapiens GN=DEK PE=1 SV=1	1.35E+08	6.11E+07	1.41E+08	2.21E+00
H0Y8A7	NEDD4 family-interacting protein 2 (Fragment) OS=Homo sapiens GN=NDFIP2 PE=4 SV=1	9.49E+07	1.02E+08	9.40E+07	-1.07E+00
P09496-2	Isoform Non-brain of Clathrin light chain A OS=Homo sapiens GN=CLTA	4.48E+07	1.52E+08	4.35E+07	-3.40E+00
P00367	Glutamate dehydrogenase 1, mitochondrial OS=Homo sapiens GN=GLUD1 PE=1 SV=2	5.72E+07	1.40E+08	4.91E+07	-2.45E+00
Q05682-5	Isoform 5 of Caldesmon OS=Homo sapiens GN=CALD1	3.58E+07	1.63E+08	6.49E+07	-4.56E+00
P49915	GMP syntha	1.99E+08	0.00E+00	0.00E+00	1.00E+01
P40925	Malate dehydrogenase, cytoplasmic OS=Homo sapiens GN=MDH1 PE=1 SV=4	1.15E+08	8.56E+07	1.06E+08	1.35E+00
Q15393	Splicing factor 3B subunit 3 OS=Homo sapiens GN=SF3B3 PE=1 SV=4	8.46E+07	1.17E+08	1.39E+08	-1.38E+00
Q9UNM6	26S proteasome non-ATPase regulatory subunit 13 OS=Homo sapiens GN=PSMD13 PE=1 SV=2	7.74E+07	1.25E+08	4.99E+07	-1.61E+00
Q16850	Lanosterol 14-alpha demethylase OS=Homo sapiens GN=CYP51A1 PE=1 SV=3	0.00E+00	2.02E+08	0.00E+00	-1.00E+01
Q8N1F7	Nuclear pore complex protein Nup93 OS=Homo sapiens GN=NUP93 PE=1 SV=2	7.26E+07	1.30E+08	2.67E+08	-1.80E+00

Q15043-2	Isoform 2 of Zinc transporter ZIP14 OS=Homo sapiens GN=SLC39A14	9.43E+07	1.09E+08	7.29E+07	-1.15E+00
Q96JJ7	Protein disulfide-isomerase TMX3 OS=Homo sapiens GN=TMX3 PE=1 SV=2	5.53E+07	1.48E+08	7.97E+07	-2.68E+00
Q5SRE5-2	Isoform 2 of Nucleoporin NUP188 homolog OS=Homo sapiens GN=NUP188	0.00E+00	2.04E+08	2.27E+08	-1.00E+01
P15559-2	Isoform 2 of NAD(P)H dehydrogena	1.28E+08	7.70E+07	1.80E+08	1.66E+00
Q92621	Nuclear pore complex protein Nup205 OS=Homo sapiens GN=NUP205 PE=1 SV=3	1.27E+08	7.81E+07	2.83E+08	1.62E+00
Q9UL15	BAG family molecular chaperone regulator 5 OS=Homo sapiens GN=BAG5 PE=1 SV=1	1.01E+08	1.05E+08	1.50E+08	-1.04E+00
P62249	40S ribosomal protein S16 OS=Homo sapiens GN=RPS16 PE=1 SV=2	9.21E+07	1.15E+08	1.54E+08	-1.25E+00
P51665	26S proteasome non-ATPase regulatory subunit 7 OS=Homo sapiens GN=PSMD7 PE=1 SV=2	9.64E+07	1.11E+08	7.14E+07	-1.15E+00
P14324	Farnesyl pyrophosphate synthase OS=Homo sapiens GN=FDPS PE=1 SV=4	1.37E+08	7.08E+07	8.27E+07	1.93E+00
E9PSH2	Complement decay-accelerating factor OS=Homo sapiens GN=CD55 PE=4 SV=1	5.48E+07	1.53E+08	1.26E+08	-2.79E+00
O75083	WD repeat-containing protein 1 OS=Homo sapiens GN=WDR1 PE=1 SV=4	1.17E+08	9.06E+07	1.32E+08	1.30E+00
Q15836	Vesicle-associated membrane protein 3 OS=Homo sapiens GN=VAMP3 PE=1 SV=3	1.03E+08	1.07E+08	1.80E+08	-1.04E+00
P23229-7	Isoform 7 of Integrin alpha-6 OS=Homo sapiens GN=ITGA6	1.23E+08	8.67E+07	0.00E+00	1.42E+00
P21291	Cysteine and glycine-rich protein 1 OS=Homo sapiens GN=CSRP1 PE=1 SV=3	1.08E+08	1.03E+08	1.42E+08	1.06E+00
Q9Y230	RuvB-like 2 OS=Homo sapiens GN=RUVBL2 PE=1 SV=3	8.06E+07	1.31E+08	7.76E+07	-1.62E+00

Q8IY95-2	Isoform 2 of Transmembrane protein 192 OS=Homo sapiens GN=TMEM192	1.69E+08	4.26E+07	0.00E+00	3.96E+00
O00116	Alkyldihydroxyacetonephosphate synthase, peroxisomal OS=Homo sapiens GN=AGPS PE=1 SV=1	1.04E+08	1.09E+08	9.70E+07	-1.05E+00
D6RAA6	Transmembrane protein 33 (Fragment) OS=Homo sapiens GN=TMEM33 PE=4 SV=1	1.60E+08	5.31E+07	3.79E+07	3.00E+00
P55786	Puromycin-sensitive aminopeptidase OS=Homo sapiens GN=NPEPPS PE=1 SV=2	6.54E+07	1.48E+08	4.66E+07	-2.26E+00
Q9H6X2	Anthrax toxin receptor 1 OS=Homo sapiens GN=ANTXR1 PE=1 SV=2	1.17E+08	9.59E+07	1.27E+08	1.22E+00
O95197-3	Isoform 3 of Reticulon-3 OS=Homo sapiens GN=RTN3	7.77E+07	1.36E+08	3.48E+08	-1.75E+00
B4DTE8	Phospholipid scramblase 1 OS=Homo sapiens GN=PLSCR1 PE=2 SV=1	1.01E+08	1.14E+08	1.42E+08	-1.13E+00
P00390-2	Isoform Cytoplasmic of Glutathione reductase, mitochondrial OS=Homo sapiens GN=GSR	9.50E+07	1.20E+08	7.86E+07	-1.26E+00
O15126	Secretory carrier-associated membrane protein 1 OS=Homo sapiens GN=SCAMP1 PE=1 SV=2	1.28E+08	8.68E+07	1.67E+08	1.47E+00
Q96AE4	Far upstream element-binding protein 1 OS=Homo sapiens GN=FUBP1 PE=1 SV=3	1.12E+08	1.04E+08	1.55E+08	1.07E+00
Q07002	Cyclin-dependent kinase 18 OS=Homo sapiens GN=CDK18 PE=1 SV=3	0.00E+00	2.17E+08	2.37E+08	-1.00E+01
O94886	Transmembrane protein 63A OS=Homo sapiens GN=TMEM63A PE=1 SV=3	1.14E+08	1.04E+08	0.00E+00	1.09E+00
P53621	Coatomer subunit alpha OS=Homo sapiens GN=COPA PE=1 SV=2	1.27E+08	9.16E+07	6.74E+07	1.38E+00
O75494-2	Isoform 2 of Serine/arginine-rich splicing factor 10 OS=Homo sapiens GN=SRSF10	5.76E+07	1.61E+08	0.00E+00	-2.80E+00

Q9UIQ6	Leucyl-cystinyl aminopeptidase OS=Homo sapiens GN=LNPEP PE=1 SV=3	1.45E+08	7.53E+07	0.00E+00	1.92E+00
O14980	Exportin-1 OS=Homo sapiens GN=XPO1 PE=1 SV=1	1.21E+08	1.00E+08	1.13E+08	1.20E+00
P33993	DNA replication licensing factor MCM7 OS=Homo sapiens GN=MCM7 PE=1 SV=4	1.11E+08	1.10E+08	1.68E+08	1.00E+00
P12955	Xaa-Pro dipeptidase OS=Homo sapiens GN=PEPD PE=1 SV=3	1.75E+08	4.65E+07	0.00E+00	3.77E+00
O60716-13	Isoform 2A of Catenin delta-1 OS=Homo sapiens GN=CTNND1	3.65E+07	1.85E+08	5.01E+07	-5.08E+00
Q9NRN7	L-aminoadipate-semialdehyde dehydrogenase-phosphopantetheinyl transferase OS=Homo sapiens GN=AASDHPPT PE=1 SV=2	1.07E+08	1.15E+08	2.18E+08	-1.07E+00
Q8WUM4	Programmed cell death 6-interacting protein OS=Homo sapiens GN=PDCD6IP PE=1 SV=1	1.21E+08	1.02E+08	5.53E+07	1.19E+00
P20645	Cation-dependent mannose-6-phosphate receptor OS=Homo sapiens GN=M6PR PE=1 SV=1	9.12E+07	1.32E+08	1.03E+08	-1.44E+00
P30040	Endoplasmic reticulum resident protein 29 OS=Homo sapiens GN=ERP29 PE=1 SV=4	1.43E+08	8.03E+07	4.73E+07	1.78E+00
P24390	ER lumen protein retaining receptor 1 OS=Homo sapiens GN=KDELR1 PE=1 SV=1	9.93E+07	1.26E+08	9.85E+07	-1.26E+00
F6RFD5	Destrin OS=Homo sapiens GN=DSTN PE=4 SV=1	7.09E+07	1.55E+08	1.66E+08	-2.18E+00
Q9Y5L0-3	Isoform 3 of Transportin-3 OS=Homo sapiens GN=TNPO3	0.00E+00	2.26E+08	0.00E+00	-1.00E+01
Q01081	Splicing factor U2AF 35 kDa subunit OS=Homo sapiens GN=U2AF1 PE=1 SV=3	3.98E+07	1.86E+08	8.12E+07	-4.68E+00
P30041	Peroxiredoxin-6 OS=Homo sapiens GN=PRDX6 PE=1 SV=3	1.33E+08	9.44E+07	1.53E+08	1.41E+00
P55884	Eukaryotic translation initiation factor 3 subunit B OS=Homo sapiens GN=EIF3B PE=1 SV=3	1.04E+08	1.24E+08	9.72E+07	-1.20E+00

Q13619	Cullin-4A OS=Homo sapiens GN=CUL4A PE=1 SV=3	8.61E+07	1.43E+08	6.91E+07	-1.66E+00
Q12905	Interleukin enhancer-binding factor 2 OS=Homo sapiens GN=ILF2 PE=1 SV=2	1.11E+08	1.19E+08	7.96E+07	-1.07E+00
O43175	D-3-phosphoglycerate dehydrogenase OS=Homo sapiens GN=PHGDH PE=1 SV=4	1.22E+08	1.10E+08	1.32E+08	1.11E+00
Q5VU59	Tropomyosin 3 OS=Homo sapiens GN=TPM3 PE=2 SV=1	8.26E+07	1.49E+08	7.59E+07	-1.80E+00
Q9NP58	ATP-binding cassette sub-family B member 6, mitochondrial OS=Homo sapiens GN=ABCB6 PE=1 SV=1	1.03E+08	1.32E+08	1.58E+08	-1.28E+00
P43686	26S protease regulatory subunit 6B OS=Homo sapiens GN=PSMC4 PE=1 SV=2	1.84E+08	5.04E+07	5.90E+07	3.65E+00
P12268	Inosine-5'-monophosphate dehydrogenase 2 OS=Homo sapiens GN=IMPDH2 PE=1 SV=2	9.90E+07	1.35E+08	1.18E+08	-1.37E+00
O75874	Isocitrate dehydrogena	5.98E+07	1.77E+08	0.00E+00	-2.96E+00
H0YLX4	WD repeat-containing protein 72 OS=Homo sapiens GN=WDR72 PE=4 SV=1	1.00E+08	1.37E+08	0.00E+00	-1.37E+00
Q16531	DNA damage-binding protein 1 OS=Homo sapiens GN=DDB1 PE=1 SV=1	8.43E+07	1.54E+08	1.04E+08	-1.83E+00
P13796	Plastin-2 OS=Homo sapiens GN=LCP1 PE=1 SV=6	1.57E+08	8.14E+07	5.34E+07	1.93E+00
Q5T9A4	ATPase family AAA domain-containing protein 3B OS=Homo sapiens GN=ATAD3B PE=1 SV=1	1.30E+08	1.11E+08	7.33E+07	1.17E+00
F5GZJ1	Condensin complex subunit 1 OS=Homo sapiens GN=NCAPD2 PE=3 SV=1	6.54E+07	1.78E+08	5.27E+07	-2.72E+00
B4DP11	Prostaglandin E synthase 3 OS=Homo sapiens GN=PTGES3 PE=2 SV=1	1.22E+08	1.22E+08	1.51E+08	1.00E+00
J3QT28	Mitotic checkpoint protein BUB3 (Fragment) OS=Homo sapiens GN=BUB3 PE=4 SV=1	0.00E+00	2.44E+08	0.00E+00	-1.00E+01

Q14165	Malectin OS=Homo sapiens GN=MLEC PE=1 SV=1	1.45E+08	9.94E+07	7.23E+07	1.46E+00
B2REB8	Protein SET OS=Homo sapiens GN=SET PE=3 SV=1	1.24E+08	1.24E+08	1.27E+08	1.00E+00
Q15056-2	Isoform Short of Eukaryotic translation initiation factor 4H OS=Homo sapiens GN=EIF4H	1.38E+08	1.10E+08	1.47E+08	1.25E+00
P11586	C-1-tetrahydrofolate synthase, cytoplasmic OS=Homo sapiens GN=MTHFD1 PE=1 SV=3	1.11E+08	1.39E+08	1.24E+08	-1.25E+00
Q9BXJ9	N-alpha-acetyltransferase 15, NatA auxiliary subunit OS=Homo sapiens GN=NAA15 PE=1 SV=1	1.35E+08	1.15E+08	5.37E+07	1.17E+00
P09622	Dihydrolipoyl dehydrogenase, mitochondrial OS=Homo sapiens GN=DLD PE=1 SV=2	1.01E+08	1.50E+08	4.98E+07	-1.48E+00
P16615-2	Isoform 2 of Sarcoplasmic/endoplasmic reticulum calcium ATPase 2 OS=Homo sapiens GN=ATP2A2	1.06E+08	1.45E+08	1.20E+08	-1.36E+00
O75340-2	Isoform 2 of Programmed cell death protein 6 OS=Homo sapiens GN=PDCD6	9.99E+07	1.52E+08	9.09E+07	-1.52E+00
B0QY89	Eukaryotic translation initiation factor 3 subunit L OS=Homo sapiens GN=EIF3EIP PE=4 SV=1	1.57E+08	9.86E+07	8.46E+07	1.59E+00
Q9NUN5-3	Isoform 3 of Probable lysosomal cobalamin transporter OS=Homo sapiens GN=LMBRD1	1.28E+08	1.28E+08	0.00E+00	1.00E+00
P10620	Microsomal glutathione S-transferase 1 OS=Homo sapiens GN=MGST1 PE=1 SV=1	1.11E+08	1.46E+08	9.07E+07	-1.32E+00
P62745	Rho-related GTP-binding protein RhoB OS=Homo sapiens GN=RHOB PE=1 SV=1	1.15E+08	1.45E+08	8.08E+07	-1.26E+00
P52569	Low affinity cationic amino acid transporter 2 OS=Homo sapiens GN=SLC7A2 PE=1 SV=2	1.41E+08	1.19E+08	8.39E+07	1.18E+00

Q99714	3-hydroxyacyl-CoA dehydrogenase type-2 OS=Homo sapiens GN=HSD17B10 PE=1 SV=3	1.26E+08	1.35E+08	7.25E+07	-1.07E+00
P41091	Eukaryotic translation initiation factor 2 subunit 3 OS=Homo sapiens GN=EIF2S3 PE=1 SV=3	1.25E+08	1.37E+08	1.34E+08	-1.09E+00
Q9NVP1	ATP-dependent RNA helicase DDX18 OS=Homo sapiens GN=DDX18 PE=1 SV=2	2.62E+08	0.00E+00	0.00E+00	1.00E+01
Q96CX2	BTB/POZ domain-containing protein KCTD12 OS=Homo sapiens GN=KCTD12 PE=1 SV=1	9.44E+07	1.68E+08	1.95E+08	-1.78E+00
F5H6P0	Protein-glutamine gamma-glutamyltransferase 2 OS=Homo sapiens GN=TGM2 PE=3 SV=1	5.88E+07	2.05E+08	8.27E+07	-3.48E+00
P50502	Hsc70-interacting protein OS=Homo sapiens GN=ST13 PE=1 SV=2	1.33E+08	1.31E+08	2.95E+08	1.02E+00
O14818-2	Isoform 2 of Proteasome subunit alpha type-7 OS=Homo sapiens GN=PSMA7	1.28E+08	1.36E+08	1.55E+08	-1.06E+00
Q16576	Histone-binding protein RBBP7 OS=Homo sapiens GN=RBBP7 PE=1 SV=1	1.46E+08	1.19E+08	1.07E+08	1.23E+00
P26196	Probable ATP-dependent RNA helicase DDX6 OS=Homo sapiens GN=DDX6 PE=1 SV=2	1.50E+08	1.15E+08	2.22E+08	1.30E+00
Q9UIG8-2	Isoform 2 of Solute carrier organic anion transporter family member 3A1 OS=Homo sapiens GN=SLCO3A1	1.32E+08	1.33E+08	0.00E+00	-1.01E+00
P56192	Methionine--tRNA ligase, cytoplasmic OS=Homo sapiens GN=MARS PE=1 SV=2	1.40E+08	1.26E+08	1.41E+08	1.10E+00
P33947	ER lumen protein retaining receptor 2 OS=Homo sapiens GN=KDELR2 PE=1 SV=1	1.29E+08	1.39E+08	1.03E+08	-1.08E+00
P01116-2	Isoform 2B of GTPase KRas OS=Homo sapiens GN=KRAS	1.55E+08	1.13E+08	6.15E+07	1.37E+00
Q99497	Protein DJ-1 OS=Homo sapiens GN=PARK7 PE=1 SV=2	1.40E+08	1.28E+08	1.85E+08	1.09E+00

O75367-2	Isoform 1 of Core histone macro-H2A.1 OS=Homo sapiens GN=H2AFY	9.74E+07	1.71E+08	1.27E+08	-1.75E+00
P28074	Proteasome subunit beta type-5 OS=Homo sapiens GN=PSMB5 PE=1 SV=3	1.30E+08	1.39E+08	1.35E+08	-1.08E+00
Q01995	Transgelin OS=Homo sapiens GN=TAGLN PE=1 SV=4	1.26E+08	1.43E+08	1.79E+08	-1.13E+00
O15067	Phosphoribosylformylglycinamidine synthase OS=Homo sapiens GN=PFAS PE=1 SV=4	1.13E+08	1.57E+08	1.58E+08	-1.39E+00
G5E9B6	Protein arginine N-methyltransferase 1 OS=Homo sapiens GN=PRMT1 PE=4 SV=1	1.31E+08	1.40E+08	7.53E+07	-1.07E+00
P22102	Trifunctional purine biosynthetic protein adenosine-3 OS=Homo sapiens GN=GART PE=1 SV=1	9.57E+07	1.76E+08	4.72E+08	-1.84E+00
Q10472	Polypeptide N-acetylgalactosaminyltransferase 1 OS=Homo sapiens GN=GALNT1 PE=1 SV=1	9.11E+07	1.82E+08	1.09E+08	-2.00E+00
P49755	Transmembrane emp24 domain-containing protein 10 OS=Homo sapiens GN=TMED10 PE=1 SV=2	1.20E+08	1.54E+08	1.01E+08	-1.28E+00
P09874	Po	1.66E+08	1.09E+08	1.21E+08	1.51E+00
Q09028-3	Isoform 3 of Histone-binding protein RBBP4 OS=Homo sapiens GN=RBBP4	1.46E+08	1.29E+08	1.17E+08	1.13E+00
P54289-4	Isoform 4 of Voltage-dependent calcium channel subunit alpha-2/delta-1 OS=Homo sapiens GN=CACNA2D1	1.37E+08	1.39E+08	1.15E+08	-1.02E+00
C9JD32	60S ribosomal protein L23 (Fragment) OS=Homo sapiens GN=RPL23 PE=3 SV=1	1.25E+08	1.51E+08	1.27E+08	-1.20E+00
A8MXQ1	Pituitary tumor-transforming gene 1 protein-interacting protein OS=Homo sapiens GN=PTTG1IP PE=4 SV=1	1.21E+08	1.56E+08	1.14E+08	-1.29E+00
Q96IX5	Up-regulated during skeletal muscle growth protein 5 OS=Homo sapiens GN=USMG5 PE=1 SV=1	8.97E+07	1.87E+08	1.32E+08	-2.09E+00

P61158	Actin-related protein 3 OS=Homo sapiens GN=ACTR3 PE=1 SV=3	1.51E+08	1.27E+08	1.29E+08	1.19E+00
O43795	Unconventional myosin-Ib OS=Homo sapiens GN=MYO1B PE=2 SV=3	1.08E+08	1.71E+08	7.22E+07	-1.59E+00
P00403	Cytochrome c oxidase subunit 2 OS=Homo sapiens GN=MT-CO2 PE=1 SV=1	1.37E+08	1.43E+08	7.28E+07	-1.05E+00
P50395	Rab GDP dissociation inhibitor beta OS=Homo sapiens GN=GDI2 PE=1 SV=2	1.35E+08	1.45E+08	1.48E+08	-1.08E+00
P10599	Thioredoxin OS=Homo sapiens GN=TXN PE=1 SV=3	1.60E+08	1.21E+08	1.34E+08	1.32E+00
P60866	40S ribosomal protein S20 OS=Homo sapiens GN=RPS20 PE=1 SV=1	1.49E+08	1.33E+08	2.10E+08	1.11E+00
H0Y5K5	Endoplasmic reticulum-Golgi intermediate compartment protein 3 (Fragment) OS=Homo sapiens GN=ERGIC3 PE=4 SV=1	1.04E+08	1.81E+08	2.46E+08	-1.73E+00
E9PN11	Rho-related GTP-binding protein RhoC (Fragment) OS=Homo sapiens GN=RHOC PE=3 SV=1	1.17E+08	1.72E+08	4.97E+07	-1.48E+00
P42765	3-ketoacyl-CoA thiolase, mitochondrial OS=Homo sapiens GN=ACAA2 PE=1 SV=2	1.37E+08	1.53E+08	1.20E+08	-1.11E+00
P51649	Succinate-semialdehyde dehydrogenase, mitochondrial OS=Homo sapiens GN=ALDH5A1 PE=1 SV=2	0.00E+00	2.91E+08	3.69E+08	-1.00E+01
Q92973-2	Isoform 2 of Transportin-1 OS=Homo sapiens GN=TNPO1	1.48E+08	1.43E+08	1.68E+08	1.04E+00
P30837	Aldehyde dehydrogenase X, mitochondrial OS=Homo sapiens GN=ALDH1B1 PE=1 SV=3	1.30E+08	1.62E+08	0.00E+00	-1.24E+00
Q9Y3U8	60S ribosomal protein L36 OS=Homo sapiens GN=RPL36 PE=1 SV=3	1.35E+08	1.57E+08	2.08E+08	-1.16E+00

O75110	Probable phospholipid-transporting ATPase IIA OS=Homo sapiens GN=ATP9A PE=1 SV=3	1.98E+08	9.74E+07	9.49E+07	2.03E+00
P21266	Glutathione S-transferase Mu 3 OS=Homo sapiens GN=GSTM3 PE=1 SV=3	4.63E+07	2.51E+08	5.50E+07	-5.43E+00
Q07617	Sperm-associated antigen 1 OS=Homo sapiens GN=SPAG1 PE=1 SV=3	5.99E+07	2.39E+08	5.30E+07	-3.99E+00
Q92900-2	Isoform 2 of Regulator of nonsense transcripts 1 OS=Homo sapiens GN=UPF1	0.00E+00	3.00E+08	0.00E+00	-1.00E+01
O60343	TBC1 domain family member 4 OS=Homo sapiens GN=TBC1D4 PE=1 SV=2	2.50E+08	5.01E+07	2.64E+08	5.00E+00
P46778	60S ribosomal protein L21 OS=Homo sapiens GN=RPL21 PE=1 SV=2	1.14E+08	1.88E+08	1.88E+08	-1.65E+00
Q01518	Adenylyl cyclase-associated protein 1 OS=Homo sapiens GN=CAP1 PE=1 SV=5	1.68E+08	1.36E+08	5.12E+08	1.23E+00
P18669	Phosphoglycerate mutase 1 OS=Homo sapiens GN=PGAM1 PE=1 SV=2	1.58E+08	1.46E+08	1.76E+08	1.08E+00
Q9NZ01	Very-long-chain enoyl-CoA reductase OS=Homo sapiens GN=TECR PE=1 SV=1	1.30E+08	1.74E+08	1.51E+08	-1.34E+00
P20700	Lamin-B1 OS=Homo sapiens GN=LMNB1 PE=1 SV=2	1.92E+08	1.14E+08	1.14E+08	1.69E+00
P11166	Solute carrier family 2, facilitated glucose transporter member 1 OS=Homo sapiens GN=SLC2A1 PE=1 SV=2	1.58E+08	1.49E+08	3.62E+07	1.06E+00
F8W914	Reticulon-4 OS=Homo sapiens GN=RTN4 PE=4 SV=1	1.28E+08	1.79E+08	1.24E+08	-1.39E+00
Q02790	Peptidyl-prolyl cis-trans isomerase FKBP4 OS=Homo sapiens GN=FKBP4 PE=1 SV=3	1.59E+08	1.48E+08	1.25E+08	1.08E+00
P50914	60S ribosomal protein L14 OS=Homo sapiens GN=RPL14 PE=1 SV=4	1.25E+08	1.84E+08	1.78E+08	-1.47E+00

P49588	Alanine--tRNA ligase, cytoplasmic OS=Homo sapiens GN=AARS PE=1 SV=2	1.51E+08	1.59E+08	3.55E+08	-1.05E+00
P51991	Heterogeneous nuclear ribonucleoprotein A3 OS=Homo sapiens GN=HNRNPA3 PE=1 SV=2	1.54E+08	1.56E+08	1.70E+08	-1.01E+00
O14979-3	Isoform 3 of Heterogeneous nuclear ribonucleoprotein D-like OS=Homo sapiens GN=HNRPDL	1.60E+08	1.52E+08	1.56E+08	1.05E+00
K7ELH1	Partitioning defective 6 homolog gamma (Fragment) OS=Homo sapiens GN=PARD6G PE=4 SV=1	3.12E+08	0.00E+00	0.00E+00	1.00E+01
Q99733	Nucleosome assembly protein 1-like 4 OS=Homo sapiens GN=NAP1L4 PE=1 SV=1	1.39E+08	1.74E+08	2.66E+08	-1.25E+00
Q15029-2	Isoform 2 of 116 kDa U5 small nuclear ribonucleoprotein component OS=Homo sapiens GN=EFTUD2	1.52E+08	1.62E+08	2.87E+08	-1.07E+00
P34897-3	Isoform 3 of Serine hydroxymethyltransferase, mitochondrial OS=Homo sapiens GN=SHMT2	1.47E+08	1.67E+08	1.27E+08	-1.13E+00
P50454	Serpin H1 OS=Homo sapiens GN=SERPINH1 PE=1 SV=2	1.20E+08	1.96E+08	1.05E+08	-1.63E+00
P31153	S-adenosylmethionine synthase isoform type-2 OS=Homo sapiens GN=MAT2A PE=1 SV=1	9.19E+07	2.26E+08	1.02E+08	-2.45E+00
O75947-2	Isoform 2 of ATP synthase subunit d, mitochondrial OS=Homo sapiens GN=ATP5H	1.41E+08	1.77E+08	1.04E+08	-1.25E+00
B4DZI8	Coatomer protein complex, subunit beta 2 (Beta prime), isoform CRA_b OS=Homo sapiens GN=COPB2 PE=2 SV=1	1.10E+08	2.09E+08	1.14E+08	-1.90E+00
P40926	Malate dehydrogenase, mitochondrial OS=Homo sapiens GN=MDH2 PE=1 SV=3	1.29E+08	1.90E+08	1.97E+08	-1.47E+00

P63244	Guanine nucleotide-binding protein subunit beta-2-like 1 OS=Homo sapiens GN=GNB2L1 PE=1 SV=3	1.68E+08	1.53E+08	1.86E+08	1.10E+00
P23526	Adenosylhomocysteinase OS=Homo sapiens GN=AHCY PE=1 SV=4	1.60E+08	1.61E+08	1.84E+08	-1.00E+00
O75955	Flotillin-1 OS=Homo sapiens GN=FLOT1 PE=1 SV=3	1.88E+08	1.33E+08	9.47E+07	1.41E+00
Q9Y287	Integral membrane protein 2B OS=Homo sapiens GN=ITM2B PE=1 SV=1	1.64E+08	1.58E+08	2.54E+08	1.04E+00
P42330	Aldo-keto reductase family 1 member C3 OS=Homo sapiens GN=AKR1C3 PE=1 SV=4	1.81E+08	1.41E+08	2.74E+08	1.28E+00
P17812	CTP synthase 1 OS=Homo sapiens GN=CTPS1 PE=1 SV=2	1.32E+08	1.90E+08	1.63E+08	-1.43E+00
Q9BXS4	Transmembrane protein 59 OS=Homo sapiens GN=TMEM59 PE=1 SV=1	2.07E+08	1.17E+08	1.04E+08	1.78E+00
F8W1R7	Myosin light polypeptide 6 OS=Homo sapiens GN=MYL6 PE=4 SV=1	1.23E+08	2.01E+08	1.62E+08	-1.63E+00
P42677	40S ribosomal protein S27 OS=Homo sapiens GN=RPS27 PE=1 SV=3	1.75E+08	1.51E+08	1.13E+08	1.16E+00
P46060	Ran GTPase-activating protein 1 OS=Homo sapiens GN=RANGAP1 PE=1 SV=1	1.49E+08	1.78E+08	1.26E+08	-1.20E+00
H3BLW6	Transmembrane protein 63B (Fragment) OS=Homo sapiens GN=TMEM63B PE=4 SV=1	2.68E+08	5.99E+07	0.00E+00	4.47E+00
H3BQZ7	HCG2044799 OS=Homo sapiens GN=hCG_2044799 PE=4 SV=1	1.34E+08	1.94E+08	1.90E+08	-1.46E+00
J3KNF8	Cytochrome b5 type B OS=Homo sapiens GN=CYB5B PE=3 SV=1	1.57E+08	1.72E+08	1.37E+08	-1.09E+00
Q14160	Protein scribble homolog OS=Homo sapiens GN=SCRIB PE=1 SV=4	1.98E+08	1.33E+08	1.24E+08	1.49E+00
P12004	Proliferating cell nuclear antigen OS=Homo sapiens GN=PCNA PE=1 SV=1	3.30E+08	0.00E+00	2.55E+08	1.00E+01

Q15233	Non-POU domain-containing octamer-binding protein OS=Homo sapiens GN=NONO PE=1 SV=4	9.94E+07	2.31E+08	3.33E+08	-2.33E+00
P62280	40S ribosomal protein S11 OS=Homo sapiens GN=RPS11 PE=1 SV=3	1.86E+08	1.45E+08	1.58E+08	1.28E+00
Q9UQ80	Proliferation-associated protein 2G4 OS=Homo sapiens GN=PA2G4 PE=1 SV=3	1.76E+08	1.56E+08	1.75E+08	1.13E+00
P82909	28S ribosomal protein S36, mitochondrial OS=Homo sapiens GN=MRPS36 PE=1 SV=2	1.61E+08	1.71E+08	1.27E+08	-1.06E+00
P35221	Catenin alpha-1 OS=Homo sapiens GN=CTNNA1 PE=1 SV=1	1.60E+08	1.73E+08	4.06E+08	-1.08E+00
P18077	60S ribosomal protein L35a OS=Homo sapiens GN=RPL35A PE=1 SV=2	1.65E+08	1.69E+08	0.00E+00	-1.03E+00
F5H3W1	Podocalyxin OS=Homo sapiens GN=PODXL PE=4 SV=1	1.53E+08	1.82E+08	1.42E+08	-1.20E+00
O76021	Ribosomal L1 domain-containing protein 1 OS=Homo sapiens GN=RSL1D1 PE=1 SV=3	2.21E+08	1.15E+08	8.76E+07	1.93E+00
P35232	Prohibitin OS=Homo sapiens GN=PHB PE=1 SV=1	1.48E+08	1.90E+08	1.13E+08	-1.28E+00
P31689	DnaJ homolog subfamily A member 1 OS=Homo sapiens GN=DNAJA1 PE=1 SV=2	2.21E+08	1.17E+08	1.28E+08	1.89E+00
P08559-3	Isoform 3 of Pyruvate dehydrogenase E1 component subunit alpha, somatic form, mitochondrial OS=Homo sapiens GN=PDHA1	1.52E+08	1.87E+08	1.50E+08	-1.23E+00
P63000	Ras-related C3 botulinum toxin substrate 1 OS=Homo sapiens GN=RAC1 PE=1 SV=1	1.81E+08	1.60E+08	4.10E+07	1.13E+00
P40429	60S ribosomal protein L13a OS=Homo sapiens GN=RPL13A PE=1 SV=2	1.44E+08	2.00E+08	2.06E+08	-1.39E+00
Q92499	ATP-dependent RNA helicase DDX1 OS=Homo sapiens GN=DDX1 PE=1 SV=2	1.67E+08	1.79E+08	9.86E+07	-1.07E+00

P61106	Ras-related protein Rab-14 OS=Homo sapiens GN=RAB14 PE=1 SV=4	1.59E+08	1.88E+08	1.12E+08	-1.18E+00
Q5VV89	Microsomal glutathione S-transferase 3 OS=Homo sapiens GN=MGST3 PE=2 SV=1	1.64E+08	1.84E+08	1.93E+08	-1.12E+00
Q99460-2	Isoform 2 of 26S proteasome non-ATPase regulatory subunit 1 OS=Homo sapiens GN=PSMD1	2.58E+08	9.07E+07	1.82E+08	2.84E+00
P30153	Serine/threonine-protein phosphatase 2A 65 kDa regulatory subunit A alpha isoform OS=Homo sapiens GN=PPP2R1A PE=1 SV=4	1.84E+08	1.65E+08	1.70E+08	1.11E+00
Q99439	Calponin-2 OS=Homo sapiens GN=CNN2 PE=1 SV=4	2.67E+08	8.42E+07	4.40E+07	3.17E+00
P38919	Eukaryotic initiation factor 4A-III OS=Homo sapiens GN=EIF4A3 PE=1 SV=4	1.86E+08	1.65E+08	1.96E+08	1.13E+00
Q9BW60	Elongation of very long chain fatty acids protein 1 OS=Homo sapiens GN=ELOVL1 PE=1 SV=1	2.92E+08	6.01E+07	1.14E+08	4.87E+00
P17858	6-phosphofructokinase, liver type OS=Homo sapiens GN=PFKL PE=1 SV=6	1.05E+08	2.52E+08	6.97E+07	-2.41E+00
Q8TB61-2	Isoform 2 of Adenosine 3'-phospho 5'-phosphosulfate transporter 1 OS=Homo sapiens GN=SLC35B2	1.59E+08	1.98E+08	2.00E+08	-1.24E+00
P00505	Aspartate aminotransferase, mitochondrial OS=Homo sapiens GN=GOT2 PE=1 SV=3	1.60E+08	1.99E+08	1.45E+08	-1.24E+00
O00232	26S proteasome non-ATPase regulatory subunit 12 OS=Homo sapiens GN=PSMD12 PE=1 SV=3	2.33E+08	1.27E+08	6.33E+07	1.83E+00
Q9NZI8	Insulin-like growth factor 2 mRNA-binding protein 1 OS=Homo sapiens GN=IGF2BP1 PE=1 SV=2	1.52E+08	2.09E+08	2.13E+08	-1.38E+00

J3QQT2	60S ribosomal protein L17 (Fragment) OS=Homo sapiens GN=RPL17 PE=3 SV=1	1.45E+08	2.17E+08	2.73E+08	-1.49E+00
P61586	Transforming protein RhoA OS=Homo sapiens GN=RHOA PE=1 SV=1	1.52E+08	2.11E+08	7.21E+07	-1.39E+00
Q96KR1	Zinc finger RNA-binding protein OS=Homo sapiens GN=ZFR PE=1 SV=2	3.64E+08	0.00E+00	1.26E+08	1.00E+01
Q8NCG7	Sn1-specific diacylglycerol lipase beta OS=Homo sapiens GN=DAGLB PE=1 SV=2	1.26E+08	2.39E+08	1.44E+08	-1.90E+00
P11388-3	Isoform 3 of DNA topoisomerase 2-alpha OS=Homo sapiens GN=TOP2A	2.53E+08	1.12E+08	0.00E+00	2.26E+00
Q8N6M3	Fat storage-inducing transmembrane protein 2 OS=Homo sapiens GN=FITM2 PE=2 SV=1	0.00E+00	3.73E+08	0.00E+00	-1.00E+01
F5H667	Aspartyl/asparaginyl beta-hydroxylase OS=Homo sapiens GN=ASPH PE=4 SV=1	7.27E+07	3.01E+08	6.14E+07	-4.14E+00
P25398	40S ribosomal protein S12 OS=Homo sapiens GN=RPS12 PE=1 SV=3	2.02E+08	1.72E+08	1.77E+08	1.18E+00
O76094	Signal recognition particle 72 kDa protein OS=Homo sapiens GN=SRP72 PE=1 SV=3	3.75E+08	0.00E+00	0.00E+00	1.00E+01
P40939	Trifunctional enzyme subunit alpha, mitochondrial OS=Homo sapiens GN=HADHA PE=1 SV=2	1.66E+08	2.09E+08	1.47E+08	-1.26E+00
P98082-3	Isoform 3 of Disabled homolog 2 OS=Homo sapiens GN=DAB2	0.00E+00	3.76E+08	1.24E+08	-1.00E+01
Q9Y6C9	Mitochondrial carrier homolog 2 OS=Homo sapiens GN=MTCH2 PE=1 SV=1	1.57E+08	2.19E+08	8.03E+07	-1.40E+00
Q6PKG0	La-related protein 1 OS=Homo sapiens GN=LARP1 PE=1 SV=2	3.79E+08	0.00E+00	5.61E+08	1.00E+01
P22234	Multifunctional protein ADE2 OS=Homo sapiens GN=PAICS PE=1 SV=3	1.81E+08	1.98E+08	1.74E+08	-1.09E+00
P13797	Plastin-3 OS=Homo sapiens GN=PLS3 PE=1 SV=4	1.73E+08	2.08E+08	1.71E+08	-1.21E+00

P15328	Folate receptor alpha OS=Homo sapiens GN=FOLR1 PE=1 SV=3	1.85E+08	1.97E+08	2.03E+08	-1.06E+00
C9J9K3	40S ribosomal protein SA (Fragment) OS=Homo sapiens GN=RPSA PE=3 SV=1	1.81E+08	2.02E+08	1.75E+08	-1.11E+00
P34932	Heat shock 70 kDa protein 4 OS=Homo sapiens GN=HSPA4 PE=1 SV=4	1.87E+08	1.97E+08	1.68E+08	-1.05E+00
O00567	Nucleolar protein 56 OS=Homo sapiens GN=NOP56 PE=1 SV=4	0.00E+00	3.85E+08	0.00E+00	-1.00E+01
P62854	40S ribosomal protein S26 OS=Homo sapiens GN=RPS26 PE=1 SV=3	2.28E+08	1.57E+08	1.86E+08	1.45E+00
Q07960	Rho GTPase-activating protein 1 OS=Homo sapiens GN=ARHGAP1 PE=1 SV=1	2.01E+08	1.87E+08	2.35E+08	1.07E+00
P04179	Superoxide dismuta	2.96E+08	9.34E+07	1.01E+08	3.17E+00
H0Y6E7	RNA-binding motif protein, X chromosome, N-terminally processed (Fragment) OS=Homo sapiens GN=RBMX PE=4 SV=2	5.83E+07	3.32E+08	3.27E+08	-5.69E+00
F8VZX2	Poly(rC)-binding protein 2 OS=Homo sapiens GN=PCBP2 PE=4 SV=1	2.00E+08	1.91E+08	2.36E+08	1.05E+00
P61604	10 kDa heat shock protein, mitochondrial OS=Homo sapiens GN=HSPE1 PE=1 SV=2	1.94E+08	2.02E+08	2.57E+08	-1.04E+00
K7ESG5	Proteasome activator complex subunit 3 OS=Homo sapiens GN=PSME3 PE=4 SV=1	6.93E+07	3.26E+08	4.80E+07	-4.71E+00
P25705	ATP synthase subunit alpha, mitochondrial OS=Homo sapiens GN=ATP5A1 PE=1 SV=1	1.63E+08	2.33E+08	1.46E+08	-1.43E+00
P12277	Creatine kinase B-type OS=Homo sapiens GN=CKB PE=1 SV=1	2.27E+08	1.69E+08	1.95E+08	1.35E+00
P31939	Bifunctional purine biosynthesis protein PURH OS=Homo sapiens GN=ATIC PE=1 SV=3	1.37E+08	2.60E+08	1.27E+08	-1.90E+00

P61247	40S ribosomal protein S3a OS=Homo sapiens GN=RPS3A PE=1 SV=2	1.85E+08	2.14E+08	1.60E+08	-1.16E+00
Q9H3Z4	DnaJ homolog subfamily C member 5 OS=Homo sapiens GN=DNAJC5 PE=1 SV=1	1.84E+08	2.17E+08	2.54E+08	-1.18E+00
P25786	Proteasome subunit alpha type-1 OS=Homo sapiens GN=PSMA1 PE=1 SV=1	6.25E+07	3.40E+08	8.66E+08	-5.43E+00
P08574	Cytochrome c1, heme protein, mitochondrial OS=Homo sapiens GN=CYC1 PE=1 SV=3	2.10E+08	1.93E+08	1.92E+08	1.09E+00
E9PF10	Nuclear pore complex protein Nup155 OS=Homo sapiens GN=NUP155 PE=4 SV=1	1.68E+08	2.36E+08	1.00E+08	-1.40E+00
P43490	Nicotinamide phosphoribosyltransferase OS=Homo sapiens GN=NAMPT PE=1 SV=1	2.14E+08	1.90E+08	4.22E+07	1.12E+00
P52895	Aldo-keto reductase family 1 member C2 OS=Homo sapiens GN=AKR1C2 PE=1 SV=3	2.68E+08	1.37E+08	2.38E+08	1.95E+00
Q9NR30	Nucleolar RNA helicase 2 OS=Homo sapiens GN=DDX21 PE=1 SV=5	1.84E+08	2.21E+08	8.16E+07	-1.20E+00
P46776	60S ribosomal protein L27a OS=Homo sapiens GN=RPL27A PE=1 SV=2	1.97E+08	2.13E+08	2.69E+08	-1.08E+00
P04083	Annexin A1 OS=Homo sapiens GN=ANXA1 PE=1 SV=2	1.92E+08	2.20E+08	1.99E+08	-1.14E+00
P57678	Gem-associated protein 4 OS=Homo sapiens GN=GEMIN4 PE=1 SV=2	6.14E+07	3.51E+08	4.13E+08	-5.72E+00
Q66LE6	Serine/threonine-protein phosphatase 2A 55 kDa regulatory subunit B delta isoform OS=Homo sapiens GN=PPP2R2D PE=1 SV=1	4.13E+08	0.00E+00	0.00E+00	1.00E+01
P62851	40S ribosomal protein S25 OS=Homo sapiens GN=RPS25 PE=1 SV=1	1.49E+08	2.68E+08	1.01E+08	-1.80E+00
P14923	Junction plakoglobin OS=Homo sapiens GN=JUP PE=1 SV=3	2.03E+08	2.16E+08	2.74E+08	-1.07E+00

P47914	60S ribosomal protein L29 OS=Homo sapiens GN=RPL29 PE=1 SV=2	1.79E+08	2.41E+08	2.52E+08	-1.35E+00
P54886-2	Isoform Short of Delta-1-pyrroline-5-carboxylate synthase OS=Homo sapiens GN=ALDH18A1	2.25E+08	1.98E+08	9.38E+07	1.14E+00
Q13838	Spliceosome RNA helicase DDX39B OS=Homo sapiens GN=DDX39B PE=1 SV=1	2.33E+08	1.90E+08	2.16E+08	1.23E+00
O00264	Membrane-associated progesterone receptor component 1 OS=Homo sapiens GN=PGRMC1 PE=1 SV=3	2.03E+08	2.23E+08	6.95E+07	-1.10E+00
Q7L1Q6-3	Isoform 3 of Basic leucine zipper and W2 domain-containing protein 1 OS=Homo sapiens GN=BZW1	1.75E+08	2.52E+08	1.79E+08	-1.44E+00
O00148	ATP-dependent RNA helicase DDX39A OS=Homo sapiens GN=DDX39A PE=1 SV=2	2.37E+08	1.90E+08	2.32E+08	1.25E+00
P31942-2	Isoform 2 of Heterogeneous nuclear ribonucleoprotein H3 OS=Homo sapiens GN=HNRNPH3	1.92E+08	2.37E+08	6.12E+07	-1.24E+00
Q9H2H9	Sodium-coupled neutral amino acid transporter 1 OS=Homo sapiens GN=SLC38A1 PE=1 SV=1	2.18E+08	2.11E+08	1.10E+08	1.04E+00
P02545	Prelamin-A/C OS=Homo sapiens GN=LMNA PE=1 SV=1	2.05E+08	2.25E+08	1.85E+08	-1.10E+00
Q15365	Poly(rC)-binding protein 1 OS=Homo sapiens GN=PCBP1 PE=1 SV=2	2.17E+08	2.14E+08	2.23E+08	1.01E+00
Q9Y277	Voltage-dependent anion-selective channel protein 3 OS=Homo sapiens GN=VDAC3 PE=1 SV=1	1.62E+08	2.69E+08	1.01E+08	-1.66E+00
P17655	Calpain-2 catalytic subunit OS=Homo sapiens GN=CAPN2 PE=1 SV=6	8.23E+07	3.50E+08	5.21E+07	-4.25E+00

P24752	Acetyl-CoA acetyltransferase, mitochondrial OS=Homo sapiens GN=ACAT1 PE=1 SV=1	4.90E+07	3.85E+08	5.20E+08	-7.85E+00
G3V325	Pentatricopeptide repeat-containing protein 1, mitochondrial OS=Homo sapiens GN=ATP5J2-PTCD1 PE=4 SV=1	1.31E+08	3.05E+08	1.43E+08	-2.33E+00
O95373	Importin-7 OS=Homo sapiens GN=IPO7 PE=1 SV=1	2.00E+08	2.37E+08	2.07E+08	-1.18E+00
P40227	T-complex protein 1 subunit zeta OS=Homo sapiens GN=CCT6A PE=1 SV=3	2.11E+08	2.33E+08	2.00E+08	-1.10E+00
Q13247	Serine/arginine-rich splicing factor 6 OS=Homo sapiens GN=SRSF6 PE=1 SV=2	3.86E+08	5.97E+07	7.73E+07	6.47E+00
P52565	Rho GDP-dissociation inhibitor 1 OS=Homo sapiens GN=ARHGDIA PE=1 SV=3	2.42E+08	2.06E+08	3.10E+08	1.18E+00
P26639	Threonine--tRNA ligase, cytoplasmic OS=Homo sapiens GN=TARS PE=1 SV=3	2.08E+08	2.40E+08	2.47E+08	-1.16E+00
Q02543	60S ribosomal protein L18a OS=Homo sapiens GN=RPL18A PE=1 SV=2	1.98E+08	2.55E+08	2.38E+08	-1.28E+00
P42704	Leucine-rich PPR motif-containing protein, mitochondrial OS=Homo sapiens GN=LRPPRC PE=1 SV=3	2.95E+08	1.59E+08	1.40E+08	1.85E+00
O75533	Splicing factor 3B subunit 1 OS=Homo sapiens GN=SF3B1 PE=1 SV=3	9.64E+07	3.58E+08	2.39E+08	-3.72E+00
O43143	Putative pre-mRNA-splicing factor ATP-dependent RNA helicase DHX15 OS=Homo sapiens GN=DHX15 PE=1 SV=2	3.07E+08	1.49E+08	1.71E+08	2.07E+00
Q00325-2	Isoform B of Phosphate carrier protein, mitochondrial OS=Homo sapiens GN=SLC25A3	2.07E+08	2.49E+08	1.82E+08	-1.20E+00

Q8NFJ5	Retinoic acid-induced protein 3 OS=Homo sapiens GN=GPRC5A PE=1 SV=2	2.18E+08	2.39E+08	2.15E+08	-1.09E+00
O00571	ATP-dependent RNA helicase DDX3X OS=Homo sapiens GN=DDX3X PE=1 SV=3	3.04E+08	1.54E+08	1.57E+08	1.98E+00
P46779	60S ribosomal protein L28 OS=Homo sapiens GN=RPL28 PE=1 SV=3	2.17E+08	2.41E+08	2.50E+08	-1.11E+00
Q9BTW9	Tubulin-specific chaperone D OS=Homo sapiens GN=TBCD PE=1 SV=2	0.00E+00	4.59E+08	2.07E+08	-1.00E+01
P36542	ATP synthase subunit gamma, mitochondrial OS=Homo sapiens GN=ATP5C1 PE=1 SV=1	2.69E+08	1.90E+08	7.52E+07	1.41E+00
O43657	Tetraspanin-6 OS=Homo sapiens GN=TSPAN6 PE=1 SV=1	2.14E+08	2.46E+08	2.11E+08	-1.15E+00
P08133	Annexin A6 OS=Homo sapiens GN=ANXA6 PE=1 SV=3	1.76E+08	2.84E+08	1.08E+08	-1.61E+00
O14828	Secretory carrier-associated membrane protein 3 OS=Homo sapiens GN=SCAMP3 PE=1 SV=3	2.26E+08	2.40E+08	2.68E+08	-1.06E+00
P61224	Ras-related protein Rap-1b OS=Homo sapiens GN=RAP1B PE=1 SV=1	1.87E+08	2.80E+08	0.00E+00	-1.49E+00
F5H4R6	Nucleosome assembly protein 1-like 1 OS=Homo sapiens GN=NAP1L1 PE=3 SV=1	2.63E+08	2.04E+08	1.64E+08	1.29E+00
P37837	Transaldolase OS=Homo sapiens GN=TALDO1 PE=1 SV=2	1.45E+08	3.22E+08	1.58E+08	-2.22E+00
P46781	40S ribosomal protein S9 OS=Homo sapiens GN=RPS9 PE=1 SV=3	2.39E+08	2.30E+08	1.92E+08	1.04E+00
O15118	Niemann-Pick C1 protein OS=Homo sapiens GN=NPC1 PE=1 SV=2	2.10E+08	2.62E+08	2.20E+08	-1.25E+00
F5H1A7	Radixin OS=Homo sapiens GN=RDX PE=4 SV=1	2.57E+08	2.16E+08	3.18E+08	1.19E+00
Q13423	NAD(P) transhydrogenase, mitochondrial OS=Homo sapiens GN=NNT PE=1 SV=3	3.75E+08	1.00E+08	7.77E+07	3.74E+00

P26599	Polypyrimidine tract-binding protein 1 OS=Homo sapiens GN=PTBP1 PE=1 SV=1	2.56E+08	2.20E+08	5.38E+08	1.16E+00
Q96QK1	Vacuolar protein sorting-associated protein 35 OS=Homo sapiens GN=VPS35 PE=1 SV=2	1.47E+08	3.29E+08	5.47E+07	-2.24E+00
Q9UHD1-2	Isoform 2 of Cysteine and histidine-rich domain-containing protein 1 OS=Homo sapiens GN=CHORDC1	4.32E+08	4.50E+07	8.12E+07	9.60E+00
O75643	U5 small nuclear ribonucleoprotein 200 kDa helicase OS=Homo sapiens GN=SNRNP200 PE=1 SV=2	4.16E+08	6.21E+07	2.15E+08	6.70E+00
P58107	Epiplakin OS=Homo sapiens GN=EPPK1 PE=1 SV=2	2.46E+08	2.34E+08	1.72E+08	1.05E+00
P18124	60S ribosomal protein L7 OS=Homo sapiens GN=RPL7 PE=1 SV=1	3.01E+08	1.79E+08	1.56E+08	1.68E+00
Q8N3U4	Cohesin subunit SA-2 OS=Homo sapiens GN=STAG2 PE=1 SV=3	0.00E+00	4.80E+08	0.00E+00	-1.00E+01
P35998	26S protease regulatory subunit 7 OS=Homo sapiens GN=PSMC2 PE=1 SV=3	9.25E+07	3.89E+08	1.25E+08	-4.20E+00
Q8NBN3	Transmembrane protein 87A OS=Homo sapiens GN=TMEM87A PE=1 SV=3	1.57E+08	3.26E+08	0.00E+00	-2.08E+00
Q92945	Far upstream element-binding protein 2 OS=Homo sapiens GN=KHSRP PE=1 SV=4	4.13E+08	7.14E+07	8.49E+07	5.78E+00
P15291	Beta-1,4-galactosyltransferase 1 OS=Homo sapiens GN=B4GALT1 PE=1 SV=5	2.27E+08	2.58E+08	2.13E+08	-1.14E+00
Q14126	Desmoglein-2 OS=Homo sapiens GN=DSG2 PE=1 SV=2	2.08E+08	2.79E+08	3.73E+08	-1.34E+00
P22087	rRNA 2'-O-methyltransferase fibrillarin OS=Homo sapiens GN=FBL PE=1 SV=2	3.14E+08	1.74E+08	2.11E+08	1.80E+00
Q13616	Cullin-1 OS=Homo sapiens GN=CUL1 PE=1 SV=2	4.25E+08	6.35E+07	4.40E+08	6.70E+00
P50991	T-complex protein 1 subunit delta OS=Homo sapiens GN=CCT4 PE=1 SV=4	1.67E+08	3.24E+08	1.60E+08	-1.93E+00

E7EPK1	Septin-7 OS=Homo sapiens GN=SEPT7 PE=3 SV=1	3.28E+08	1.66E+08	6.05E+07	1.97E+00
Q14980-2	Isoform 2 of Nuclear mitotic apparatus protein 1 OS=Homo sapiens GN=NUMA1	2.45E+08	2.54E+08	2.64E+08	-1.04E+00
P07814	Bifunctional glutamate/proline--tRNA ligase OS=Homo sapiens GN=EPRS PE=1 SV=5	1.38E+08	3.62E+08	3.63E+08	-2.63E+00
P30050	60S ribosomal protein L12 OS=Homo sapiens GN=RPL12 PE=1 SV=1	2.08E+08	2.93E+08	2.46E+08	-1.41E+00
P62906	60S ribosomal protein L10a OS=Homo sapiens GN=RPL10A PE=1 SV=2	2.53E+08	2.51E+08	2.26E+08	1.01E+00
P63173	60S ribosomal protein L38 OS=Homo sapiens GN=RPL38 PE=1 SV=2	1.60E+08	3.49E+08	3.24E+08	-2.18E+00
G5E9B2	Chaperonin containing TCP1, subunit 8 (Theta), isoform CRA_a OS=Homo sapiens GN=CCT8 PE=3 SV=1	2.44E+08	2.68E+08	2.32E+08	-1.10E+00
Q99832	T-complex protein 1 subunit eta OS=Homo sapiens GN=CCT7 PE=1 SV=2	2.23E+08	2.92E+08	2.40E+08	-1.31E+00
Q9BQG0	Myb-binding protein 1A OS=Homo sapiens GN=MYBBP1A PE=1 SV=2	3.12E+08	2.06E+08	1.07E+08	1.52E+00
P23246	Splicing factor, proline- and glutamine-rich OS=Homo sapiens GN=SFPQ PE=1 SV=2	2.52E+08	2.66E+08	2.91E+08	-1.06E+00
P08758	Annexin A5 OS=Homo sapiens GN=ANXA5 PE=1 SV=2	2.56E+08	2.63E+08	3.45E+08	-1.03E+00
P48643	T-complex protein 1 subunit epsilon OS=Homo sapiens GN=CCT5 PE=1 SV=1	2.51E+08	2.70E+08	2.44E+08	-1.08E+00
P21796	Voltage-dependent anion-selective channel protein 1 OS=Homo sapiens GN=VDAC1 PE=1 SV=2	2.32E+08	2.90E+08	1.59E+08	-1.25E+00
F8W181	60S ribosomal protein L6 (Fragment) OS=Homo sapiens GN=RPL6 PE=3 SV=1	2.33E+08	2.89E+08	2.80E+08	-1.24E+00
P32119	Peroxiredoxin-2 OS=Homo sapiens GN=PRDX2 PE=1 SV=5	2.96E+08	2.28E+08	3.16E+08	1.30E+00

P47712	Cytosolic phospholipase A2 OS=Homo sapiens GN=PLA2G4A PE=1 SV=2	1.48E+08	3.79E+08	4.13E+08	-2.56E+00
Q9Y4L1	Hypoxia up-regulated protein 1 OS=Homo sapiens GN=HYOU1 PE=1 SV=1	1.88E+08	3.39E+08	8.81E+07	-1.80E+00
A8K3Z3	26S protease regulatory subunit 8 OS=Homo sapiens GN=PSMC5 PE=2 SV=1	3.87E+08	1.41E+08	1.10E+08	2.74E+00
O60506	Heterogeneous nuclear ribonucleoprotein Q OS=Homo sapiens GN=SYNCRIP PE=1 SV=2	3.12E+08	2.22E+08	2.38E+08	1.40E+00
P26038	Moesin OS=Homo sapiens GN=MSN PE=1 SV=3	2.79E+08	2.54E+08	3.30E+08	1.10E+00
P55809	Succinyl-CoA:3-ketoacid coenzyme A transferase 1, mitochondrial OS=Homo sapiens GN=OXCT1 PE=1 SV=1	3.48E+08	1.92E+08	1.20E+08	1.81E+00
P62701	40S ribosomal protein S4, X isoform OS=Homo sapiens GN=RPS4X PE=1 SV=2	2.65E+08	2.78E+08	2.45E+08	-1.05E+00
Q9BSJ8	Extended synaptotagmin-1 OS=Homo sapiens GN=ESYT1 PE=1 SV=1	4.27E+08	1.19E+08	5.09E+08	3.59E+00
P26373	60S ribosomal protein L13 OS=Homo sapiens GN=RPL13 PE=1 SV=4	2.61E+08	2.85E+08	2.66E+08	-1.09E+00
P15311	Ezrin OS=Homo sapiens GN=EZR PE=1 SV=4	2.79E+08	2.69E+08	3.30E+08	1.04E+00
P49411	Elongation factor Tu, mitochondrial OS=Homo sapiens GN=TUFM PE=1 SV=2	2.22E+08	3.32E+08	1.57E+08	-1.50E+00
E5RI99	60S ribosomal protein L30 (Fragment) OS=Homo sapiens GN=RPL30 PE=3 SV=1	2.52E+08	3.01E+08	2.22E+08	-1.19E+00
P11940	Polyadenylate-binding protein 1 OS=Homo sapiens GN=PABPC1 PE=1 SV=2	2.14E+08	3.42E+08	2.67E+08	-1.60E+00
Q16658	Fascin OS=Homo sapiens GN=FSCN1 PE=1 SV=3	2.93E+08	2.64E+08	3.34E+08	1.11E+00
P08670	Vimentin OS=Homo sapiens GN=VIM PE=1 SV=4	3.63E+08	1.94E+08	3.25E+08	1.87E+00

P52597	Heterogeneous nuclear ribonucleoprotein F OS=Homo sapiens GN=HNRNPF PE=1 SV=3	2.64E+08	2.95E+08	3.47E+08	-1.12E+00
Q14974	Importin subunit beta-1 OS=Homo sapiens GN=KPNB1 PE=1 SV=2	2.02E+08	3.62E+08	2.33E+08	-1.79E+00
P46940	Ras GTPase-activating-like protein IQGAP1 OS=Homo sapiens GN=IQGAP1 PE=1 SV=1	3.45E+08	2.19E+08	1.92E+08	1.57E+00
Q9H0U4	Ras-related protein Rab-1B OS=Homo sapiens GN=RAB1B PE=1 SV=1	2.23E+08	3.45E+08	1.71E+08	-1.55E+00
P17844	Probable ATP-dependent RNA helicase DDX5 OS=Homo sapiens GN=DDX5 PE=1 SV=1	2.18E+08	3.52E+08	2.14E+08	-1.61E+00
B5MCQ5	Protein disulfide-isomerase A6 OS=Homo sapiens GN=PDIA6 PE=3 SV=1	2.13E+08	3.57E+08	4.33E+08	-1.68E+00
F5H157	Ras-related protein Rab-35 (Fragment) OS=Homo sapiens GN=RAB35 PE=3 SV=1	3.57E+08	2.16E+08	1.83E+08	1.65E+00
P18206-2	Isoform 1 of Vinculin OS=Homo sapiens GN=VCL	2.29E+08	3.44E+08	1.61E+08	-1.50E+00
Q9H3N1	Thioredoxin-related transmembrane protein 1 OS=Homo sapiens GN=TMX1 PE=1 SV=1	2.80E+08	2.94E+08	1.88E+08	-1.05E+00
P28070	Proteasome subunit beta type-4 OS=Homo sapiens GN=PSMB4 PE=1 SV=4	2.54E+08	3.20E+08	1.42E+08	-1.26E+00
P31948	Stress-induced-phosphoprotein 1 OS=Homo sapiens GN=STIP1 PE=1 SV=1	2.77E+08	2.98E+08	2.63E+08	-1.07E+00
F5H2A9	Very long-chain-specific acyl-CoA dehydrogenase, mitochondrial OS=Homo sapiens GN=ACADVL PE=3 SV=1	2.26E+08	3.53E+08	3.66E+08	-1.56E+00
P62753	40S ribosomal protein S6 OS=Homo sapiens GN=RPS6 PE=1 SV=1	2.58E+08	3.30E+08	2.57E+08	-1.28E+00

P23919	Thymidylate kinase OS=Homo sapiens GN=DTYMK PE=1 SV=4	2.93E+08	2.95E+08	3.38E+08	-1.01E+00
P14866	Heterogeneous nuclear ribonucleoprotein L OS=Homo sapiens GN=HNRNPL PE=1 SV=2	3.04E+08	2.92E+08	3.18E+08	1.04E+00
Q5M775-4	Isoform 4 of Cytospin-B OS=Homo sapiens GN=SPECC1	4.59E+08	1.39E+08	3.38E+08	3.31E+00
B4DJV2	Citrate synthase OS=Homo sapiens GN=CS PE=2 SV=1	3.09E+08	2.89E+08	2.61E+08	1.07E+00
E7ERF4	Adenylosuccinate lyase OS=Homo sapiens GN=ADSL PE=4 SV=1	3.18E+08	2.81E+08	2.68E+08	1.13E+00
P11387	DNA topoisomerase 1 OS=Homo sapiens GN=TOP1 PE=1 SV=2	2.84E+08	3.16E+08	1.76E+08	-1.11E+00
P63241	Eukaryotic translation initiation factor 5A-1 OS=Homo sapiens GN=EIF5A PE=1 SV=2	3.07E+08	2.93E+08	3.68E+08	1.05E+00
Q9UBT2	SUMO-activating enzyme subunit 2 OS=Homo sapiens GN=UBA2 PE=1 SV=2	2.66E+08	3.35E+08	2.41E+08	-1.26E+00
P35268	60S ribosomal protein L22 OS=Homo sapiens GN=RPL22 PE=1 SV=2	2.88E+08	3.14E+08	2.97E+08	-1.09E+00
F5H698	Leucine--tRNA ligase, cytoplasmic OS=Homo sapiens GN=LARS PE=3 SV=1	3.02E+08	3.01E+08	3.72E+08	1.00E+00
Q14697	Neutral alpha-glucosidase AB OS=Homo sapiens GN=GANAB PE=1 SV=3	2.62E+08	3.42E+08	2.55E+08	-1.31E+00
O60701	UDP-glucose 6-dehydrogenase OS=Homo sapiens GN=UGDH PE=1 SV=1	2.97E+08	3.13E+08	3.65E+08	-1.06E+00
P36776	Lon protease homolog, mitochondrial OS=Homo sapiens GN=LONP1 PE=1 SV=2	3.63E+08	2.48E+08	7.32E+07	1.46E+00
Q12906-5	Isoform 5 of Interleukin enhancer-binding factor 3 OS=Homo sapiens GN=ILF3	2.73E+08	3.43E+08	1.42E+08	-1.26E+00
F8VPD4	CAD protein OS=Homo sapiens GN=CAD PE=3 SV=1	2.51E+08	3.69E+08	1.89E+08	-1.47E+00

P53675	Clathrin heavy chain 2 OS=Homo sapiens GN=CLTCL1 PE=1 SV=2	3.08E+08	3.13E+08	2.97E+08	-1.02E+00
P07237	Protein disulfide-isomerase OS=Homo sapiens GN=P4HB PE=1 SV=3	2.87E+08	3.37E+08	2.07E+08	-1.17E+00
P42167	Lamina-associated polypeptide 2, isoforms beta/gamma OS=Homo sapiens GN=TMPO PE=1 SV=2	3.85E+08	2.42E+08	1.33E+08	1.59E+00
H7BXY3	Putative ATP-dependent RNA helicase DHX30 OS=Homo sapiens GN=DHX30 PE=4 SV=1	3.16E+08	3.13E+08	1.04E+08	1.01E+00
P04843	Dolichyl-diphosphooligosaccharide--protein glycosyltransferase subunit 1 OS=Homo sapiens GN=RPN1 PE=1 SV=1	2.77E+08	3.56E+08	4.01E+08	-1.29E+00
Q9BUP3-3	Isoform 3 of Oxidoreductase HTATIP2 OS=Homo sapiens GN=HTATIP2	2.16E+08	4.25E+08	0.00E+00	-1.97E+00
Q96QD8	Sodium-coupled neutral amino acid transporter 2 OS=Homo sapiens GN=SLC38A2 PE=1 SV=2	3.26E+08	3.19E+08	2.99E+08	1.02E+00
Q9Y5B9	FACT complex subunit SPT16 OS=Homo sapiens GN=SUPT16H PE=1 SV=1	5.47E+08	1.06E+08	1.06E+08	5.18E+00
Q96S97	Myeloid-associated differentiation marker OS=Homo sapiens GN=MYADM PE=1 SV=2	3.15E+08	3.44E+08	1.91E+08	-1.09E+00
A8MXP9	Matrin-3 OS=Homo sapiens GN=MATR3 PE=4 SV=1	3.18E+08	3.43E+08	6.94E+08	-1.08E+00
P09972	Fructose-bisphosphate aldolase C OS=Homo sapiens GN=ALDOC PE=1 SV=2	4.39E+08	2.21E+08	3.97E+08	1.99E+00
Q07021	Complement component 1 Q subcomponent-binding protein, mitochondrial OS=Homo sapiens GN=C1QBP PE=1 SV=1	2.93E+08	3.68E+08	2.14E+08	-1.25E+00

P62263	40S ribosomal protein S14 OS=Homo sapiens GN=RPS14 PE=1 SV=3	3.24E+08	3.46E+08	3.27E+08	-1.07E+00
P15880	40S ribosomal protein S2 OS=Homo sapiens GN=RPS2 PE=1 SV=2	2.85E+08	3.93E+08	3.03E+08	-1.38E+00
P06576	ATP synthase subunit beta, mitochondrial OS=Homo sapiens GN=ATP5B PE=1 SV=3	3.42E+08	3.47E+08	7.96E+08	-1.01E+00
P41440	Folate transporter 1 OS=Homo sapiens GN=SLC19A1 PE=1 SV=3	6.91E+08	0.00E+00	0.00E+00	1.00E+01
G5EA52	Protein disulfide isomerase family A, member 3, isoform CRA_b OS=Homo sapiens GN=PDIA3 PE=3 SV=1	2.60E+08	4.36E+08	3.68E+08	-1.68E+00
P23284	Peptidyl-prolyl cis-trans isomerase B OS=Homo sapiens GN=PPIB PE=1 SV=2	5.09E+08	1.90E+08	1.42E+08	2.67E+00
Q9NZM1-6	Isoform 6 of Myoferlin OS=Homo sapiens GN=MYOF	3.77E+08	3.22E+08	3.91E+08	1.17E+00
P17980	26S protease regulatory subunit 6A OS=Homo sapiens GN=PSMC3 PE=1 SV=3	8.46E+07	6.16E+08	6.69E+07	-7.28E+00
Q92616	Translational activator GCN1 OS=Homo sapiens GN=GCN1L1 PE=1 SV=6	3.48E+08	3.55E+08	2.08E+08	-1.02E+00
Q03135	Caveolin-1 OS=Homo sapiens GN=CAV1 PE=1 SV=4	3.80E+08	3.28E+08	3.11E+08	1.16E+00
Q9UJS0	Calcium-binding mitochondrial carrier protein Aralar2 OS=Homo sapiens GN=SLC25A13 PE=1 SV=2	3.17E+07	6.78E+08	1.57E+09	-1.00E+01
P14868	Aspartate--tRNA ligase, cytoplasmic OS=Homo sapiens GN=DARS PE=1 SV=2	3.40E+08	3.71E+08	4.71E+08	-1.09E+00
P55084	Trifunctional enzyme subunit beta, mitochondrial OS=Homo sapiens GN=HADHB PE=1 SV=3	3.13E+08	4.03E+08	3.78E+08	-1.29E+00
Q14103-3	Isoform 3 of Heterogeneous nuclear ribonucleoprotein D0 OS=Homo sapiens GN=HNRNPD	3.49E+08	3.81E+08	2.76E+08	-1.09E+00

P45880-2	Isoform 2 of Voltage-dependent anion-selective channel protein 2 OS=Homo sapiens GN=VDAC2	3.05E+08	4.31E+08	1.93E+08	-1.41E+00
Q9H078-2	Isoform 2 of Caseinolytic peptidase B protein homolog OS=Homo sapiens GN=CLPB	3.24E+08	4.14E+08	0.00E+00	-1.28E+00
P20674	Cytochrome c oxidase subunit 5A, mitochondrial OS=Homo sapiens GN=COX5A PE=1 SV=2	5.10E+08	2.38E+08	2.57E+08	2.15E+00
P04792	Heat shock protein beta-1 OS=Homo sapiens GN=HSPB1 PE=1 SV=2	4.75E+08	2.73E+08	1.14E+09	1.74E+00
P05783	Keratin, type I cytoskeletal 18 OS=Homo sapiens GN=KRT18 PE=1 SV=2	4.71E+08	2.91E+08	2.63E+08	1.62E+00
E9PEJ4	Dihydrolipoyllysine-residue acetyltransferase component of pyruvate dehydrogenase complex, mitochondrial OS=Homo sapiens GN=DLAT PE=3 SV=1	0.00E+00	7.63E+08	0.00E+00	-1.00E+01
P35579	Myosin-9 OS=Homo sapiens GN=MYH9 PE=1 SV=4	3.04E+08	4.63E+08	3.06E+08	-1.52E+00
P62424	60S ribosomal protein L7a OS=Homo sapiens GN=RPL7A PE=1 SV=2	3.34E+08	4.41E+08	6.51E+08	-1.32E+00
Q01844-3	Isoform 3 of RNA-binding protein EWS OS=Homo sapiens GN=EWSR1	4.15E+08	3.65E+08	4.30E+08	1.14E+00
P46782	40S ribosomal protein S5 OS=Homo sapiens GN=RPS5 PE=1 SV=4	2.57E+08	5.24E+08	1.99E+08	-2.04E+00
Q6P2Q9	Pre-mRNA-processing-splicing factor 8 OS=Homo sapiens GN=PRPF8 PE=1 SV=2	3.94E+08	3.89E+08	2.87E+08	1.01E+00
F5GWX5	Chromodomain-helicase-DNA-binding protein 4 OS=Homo sapiens GN=CHD4 PE=4 SV=1	6.72E+08	1.15E+08	2.06E+08	5.86E+00
Q63HN8	E3 ubiquitin-protein ligase RNF213 OS=Homo sapiens GN=RNF213 PE=1 SV=3	3.77E+08	4.16E+08	2.30E+08	-1.10E+00

D6RIA2	Matrin-3 (Fragment) OS=Homo sapiens GN=MATR3 PE=4 SV=1	5.35E+08	2.61E+08	3.15E+08	2.05E+00
P19338	Nucleolin OS=Homo sapiens GN=NCL PE=1 SV=3	3.56E+08	4.48E+08	3.77E+08	-1.26E+00
P15531	Nucleoside diphosphate kinase A OS=Homo sapiens GN=NME1 PE=1 SV=1	4.28E+08	3.77E+08	4.17E+08	1.13E+00
P53396-2	Isoform 2 of ATP-citrate synthase OS=Homo sapiens GN=ACLY	4.03E+08	4.03E+08	4.37E+08	1.00E+00
Q7KZF4	Staphylococcal nuclease domain-containing protein 1 OS=Homo sapiens GN=SND1 PE=1 SV=1	3.77E+08	4.31E+08	5.16E+08	-1.14E+00
P29144	Tripeptidyl-peptidase 2 OS=Homo sapiens GN=TPP2 PE=1 SV=4	6.64E+08	1.46E+08	0.00E+00	4.54E+00
J3KQ42	Tetraspanin-4 OS=Homo sapiens GN=TSPAN4 PE=4 SV=1	3.74E+08	4.37E+08	4.83E+08	-1.17E+00
P13010	X-ray repair cross-complementing protein 5 OS=Homo sapiens GN=XRCC5 PE=1 SV=3	2.98E+08	5.13E+08	1.96E+09	-1.72E+00
P22392-2	Isoform 3 of Nucleoside diphosphate kinase B OS=Homo sapiens GN=NME2	4.36E+08	3.77E+08	4.17E+08	1.16E+00
Q86VP6	Cullin-associated NEDD8-dissociated protein 1 OS=Homo sapiens GN=CAND1 PE=1 SV=2	1.21E+08	6.98E+08	8.64E+07	-5.79E+00
P60842	Eukaryotic initiation factor 4A-I OS=Homo sapiens GN=EIF4A1 PE=1 SV=1	4.53E+08	3.71E+08	3.94E+08	1.22E+00
P14174	Macrophage migration inhibitory factor OS=Homo sapiens GN=MIF PE=1 SV=4	4.46E+08	3.79E+08	5.26E+08	1.18E+00
Q92841-1	Isoform 2 of Probable ATP-dependent RNA helicase DDX17 OS=Homo sapiens GN=DDX17	4.34E+08	3.97E+08	1.84E+08	1.09E+00
O75369-2	Isoform 2 of Filamin-B OS=Homo sapiens GN=FLNB	4.65E+08	3.72E+08	7.67E+08	1.25E+00

Q8IZY2	ATP-binding cassette sub-family A member 7 OS=Homo sapiens GN=ABCA7 PE=1 SV=3	8.39E+08	0.00E+00	0.00E+00	1.00E+01
O00410	Importin-5 OS=Homo sapiens GN=IPO5 PE=1 SV=4	2.63E+08	5.78E+08	2.63E+08	-2.20E+00
P37802	Transgelin-2 OS=Homo sapiens GN=TAGLN2 PE=1 SV=3	4.50E+08	3.97E+08	5.63E+08	1.13E+00
P12236	ADP/ATP translocase 3 OS=Homo sapiens GN=SLC25A6 PE=1 SV=4	3.96E+08	4.57E+08	3.43E+08	-1.15E+00
O15371	Eukaryotic translation initiation factor 3 subunit D OS=Homo sapiens GN=EIF3D PE=1 SV=1	7.06E+08	1.48E+08	1.33E+08	4.77E+00
P23528	Cofilin-1 OS=Homo sapiens GN=CFL1 PE=1 SV=3	4.34E+08	4.26E+08	8.09E+08	1.02E+00
Q16777	Histone H2A type 2-C OS=Homo sapiens GN=HIST2H2AC PE=1 SV=4	3.50E+08	5.10E+08	4.09E+08	-1.46E+00
P62244	40S ribosomal protein S15a OS=Homo sapiens GN=RPS15A PE=1 SV=2	4.02E+08	4.66E+08	4.02E+08	-1.16E+00
P05141	ADP/ATP translocase 2 OS=Homo sapiens GN=SLC25A5 PE=1 SV=7	3.96E+08	4.72E+08	5.32E+08	-1.19E+00
Q14566	DNA replication licensing factor MCM6 OS=Homo sapiens GN=MCM6 PE=1 SV=1	2.69E+08	6.00E+08	8.28E+07	-2.23E+00
P62826	GTP-binding nuclear protein Ran OS=Homo sapiens GN=RAN PE=1 SV=3	4.44E+08	4.27E+08	5.20E+08	1.04E+00
E5KLJ6	Dynamin-like 120 kDa protein, mitochondrial OS=Homo sapiens GN=OPA1 PE=3 SV=1	4.20E+08	4.53E+08	5.00E+08	-1.08E+00
Q07065	Cytoskeleton-associated protein 4 OS=Homo sapiens GN=CKAP4 PE=1 SV=2	5.91E+08	2.90E+08	5.19E+08	2.04E+00
P78527	DNA-dependent protein kinase catalytic subunit OS=Homo sapiens GN=PRKDC PE=1 SV=3	7.31E+08	1.54E+08	4.76E+08	4.74E+00
P38646	Stress-70 protein, mitochondrial OS=Homo sapiens GN=HSPA9 PE=1 SV=2	4.30E+08	4.64E+08	3.45E+08	-1.08E+00

Q9H0A0	N-acetyltransferase 10 OS=Homo sapiens GN=NAT10 PE=1 SV=2	4.29E+08	4.69E+08	1.55E+08	-1.09E+00
P26641	Elongation factor 1-gamma OS=Homo sapiens GN=EEF1G PE=1 SV=3	4.55E+08	4.49E+08	4.90E+08	1.01E+00
P31943	Heterogeneous nuclear ribonucleoprotein H OS=Homo sapiens GN=HNRNPH1 PE=1 SV=4	3.05E+08	6.01E+08	3.39E+08	-1.97E+00
P39023	60S ribosomal protein L3 OS=Homo sapiens GN=RPL3 PE=1 SV=2	5.25E+08	3.91E+08	5.36E+08	1.34E+00
Q9H3U1	Protein unc-45 homolog A OS=Homo sapiens GN=UNC45A PE=1 SV=1	8.64E+08	6.07E+07	5.28E+07	1.00E+01
P52272-2	Isoform 2 of Heterogeneous nuclear ribonucleoprotein M OS=Homo sapiens GN=HNRNPM	6.63E+08	2.62E+08	2.87E+08	2.53E+00
Q01813	6-phosphofructokinase type C OS=Homo sapiens GN=PFKP PE=1 SV=2	6.02E+08	3.26E+08	3.64E+08	1.85E+00
K7EIG1	Protein CLUH OS=Homo sapiens GN=CLUH PE=4 SV=1	0.00E+00	9.35E+08	0.00E+00	-1.00E+01
Q13813	Spectrin alpha chain, non-erythrocytic 1 OS=Homo sapiens GN=SPTAN1 PE=1 SV=3	6.59E+08	2.88E+08	2.52E+08	2.29E+00
P31040	Succinate dehydrogena	6.19E+08	3.37E+08	5.82E+08	1.84E+00
P78371	T-complex protein 1 subunit beta OS=Homo sapiens GN=CCT2 PE=1 SV=4	4.85E+08	4.74E+08	4.82E+08	1.02E+00
P09211	Glutathione S-transferase P OS=Homo sapiens GN=GSTP1 PE=1 SV=2	6.39E+08	3.35E+08	4.69E+08	1.91E+00
P23921	Ribonucleoside-diphosphate reductase large subunit OS=Homo sapiens GN=RRM1 PE=1 SV=1	5.57E+08	4.22E+08	6.88E+08	1.32E+00
P12956	X-ray repair cross-complementing protein 6 OS=Homo sapiens GN=XRCC6 PE=1 SV=2	5.00E+08	4.85E+08	4.71E+08	1.03E+00

P46063	ATP-dependent DNA helicase Q1 OS=Homo sapiens GN=RECQL PE=1 SV=3	4.42E+08	5.52E+08	4.13E+08	-1.25E+00
Q13263	Transcription intermediary factor 1-beta OS=Homo sapiens GN=TRIM28 PE=1 SV=5	6.20E+08	3.87E+08	6.41E+08	1.60E+00
C9JAB2	Serine/arginine-rich-splicing factor 7 OS=Homo sapiens GN=SRSF7 PE=4 SV=1	7.67E+08	2.58E+08	2.58E+08	2.98E+00
P23396	40S ribosomal protein S3 OS=Homo sapiens GN=RPS3 PE=1 SV=2	4.50E+08	5.80E+08	4.96E+08	-1.29E+00
Q9UQE7	Structural maintenance of chromosomes protein 3 OS=Homo sapiens GN=SMC3 PE=1 SV=2	5.07E+08	5.27E+08	1.57E+09	-1.04E+00
P05388	60S acidic ribosomal protein P0 OS=Homo sapiens GN=RPLP0 PE=1 SV=1	4.93E+08	5.42E+08	4.34E+08	-1.10E+00
P22314	Ubiquitin-like modifier-activating enzyme 1 OS=Homo sapiens GN=UBA1 PE=1 SV=3	6.73E+08	3.65E+08	3.73E+08	1.85E+00
P01891	HLA class I histocompatibility antigen, A-68 alpha chain OS=Homo sapiens GN=HLA-A PE=1 SV=4	3.57E+08	6.89E+08	2.72E+08	-1.93E+00
P06744	Glucose-6-phosphate isomerase OS=Homo sapiens GN=GPI PE=1 SV=4	5.91E+08	4.57E+08	6.34E+08	1.29E+00
P49368	T-complex protein 1 subunit gamma OS=Homo sapiens GN=CCT3 PE=1 SV=4	5.91E+08	4.98E+08	6.76E+08	1.19E+00
P07355	Annexin A2 OS=Homo sapiens GN=ANXA2 PE=1 SV=2	4.74E+08	6.24E+08	4.84E+08	-1.32E+00
O00411	DNA-directed RNA polymerase, mitochondrial OS=Homo sapiens GN=POLRMT PE=1 SV=2	1.01E+09	8.97E+07	1.08E+09	1.00E+01
P61978	Heterogeneous nuclear ribonucleoprotein K OS=Homo sapiens GN=HNRNPK PE=1 SV=1	5.47E+08	5.56E+08	6.02E+08	-1.01E+00
O00299	Chloride intracellular channel protein 1 OS=Homo sapiens GN=CLIC1 PE=1 SV=4	1.72E+08	9.31E+08	1.94E+08	-5.41E+00

P02538	Keratin, type II cytoskeletal 6A OS=Homo sapiens GN=KRT6A PE=1 SV=3	7.46E+08	3.59E+08	1.93E+08	2.08E+00
P11216	Glycogen phosphorylase, brain form OS=Homo sapiens GN=PYGB PE=1 SV=5	1.11E+09	0.00E+00	5.39E+07	1.00E+01
Q01082	Spectrin beta chain, non-erythrocytic 1 OS=Homo sapiens GN=SPTBN1 PE=1 SV=2	6.16E+08	5.00E+08	5.63E+08	1.23E+00
Q92598	Heat shock protein 105 kDa OS=Homo sapiens GN=HSPH1 PE=1 SV=1	5.82E+08	5.34E+08	4.08E+08	1.09E+00
P31327	Carbamoyl-phosphate syntha	5.32E+08	5.96E+08	6.21E+08	-1.12E+00
Q14152	Eukaryotic translation initiation factor 3 subunit A OS=Homo sapiens GN=EIF3A PE=1 SV=1	3.57E+08	7.72E+08	6.52E+08	-2.16E+00
P05787	Keratin, type II cytoskeletal 8 OS=Homo sapiens GN=KRT8 PE=1 SV=7	8.87E+08	2.41E+08	2.63E+08	3.68E+00
Q04941	Proteolipid protein 2 OS=Homo sapiens GN=PLP2 PE=1 SV=1	5.19E+08	6.10E+08	4.81E+08	-1.18E+00
Q00610-2	Isoform 2 of Clathrin heavy chain 1 OS=Homo sapiens GN=CLTC	5.47E+08	5.88E+08	4.67E+08	-1.07E+00
Q10471	Polypeptide N-acetylgalactosaminyltransferase 2 OS=Homo sapiens GN=GALNT2 PE=1 SV=1	5.38E+08	6.05E+08	4.88E+08	-1.12E+00
P00558	Phosphoglycerate kinase 1 OS=Homo sapiens GN=PGK1 PE=1 SV=3	6.31E+08	5.12E+08	6.02E+08	1.23E+00
P61160	Actin-related protein 2 OS=Homo sapiens GN=ACTR2 PE=1 SV=1	6.06E+08	5.55E+08	5.36E+08	1.09E+00
P61163	Alpha-centractin OS=Homo sapiens GN=ACTR1A PE=1 SV=1	5.75E+08	5.87E+08	7.41E+08	-1.02E+00
P27797	Calreticulin OS=Homo sapiens GN=CALR PE=1 SV=1	5.10E+08	6.54E+08	4.71E+08	-1.28E+00
P17987	T-complex protein 1 subunit alpha OS=Homo sapiens GN=TCP1 PE=1 SV=1	7.44E+08	4.28E+08	5.48E+08	1.74E+00

Q09666	Neuroblast differentiation-associated protein AHNAK OS=Homo sapiens GN=AHNAK PE=1 SV=2	3.93E+08	7.82E+08	4.56E+08	-1.99E+00
Q99613	Eukaryotic translation initiation factor 3 subunit C OS=Homo sapiens GN=EIF3C PE=1 SV=1	3.13E+08	8.67E+08	0.00E+00	-2.77E+00
Q14204	Cytoplasmic dynein 1 heavy chain 1 OS=Homo sapiens GN=DYNC1H1 PE=1 SV=5	7.67E+08	4.27E+08	4.85E+08	1.80E+00
P60174	Triosephosphate isomerase OS=Homo sapiens GN=TPI1 PE=1 SV=3	5.70E+08	6.39E+08	8.25E+08	-1.12E+00
P21333-2	Isoform 2 of Filamin-A OS=Homo sapiens GN=FLNA	6.29E+08	5.93E+08	6.50E+08	1.06E+00
P31947	14-3-3 protein sigma OS=Homo sapiens GN=SFN PE=1 SV=1	6.32E+08	5.95E+08	7.11E+08	1.06E+00
P61981	14-3-3 protein gamma OS=Homo sapiens GN=YWHAG PE=1 SV=2	6.32E+08	5.95E+08	7.11E+08	1.06E+00
P31946-2	Isoform Short of 14-3-3 protein beta/alpha OS=Homo sapiens GN=YWHAB	6.32E+08	5.95E+08	7.11E+08	1.06E+00
P27348	14-3-3 protein theta OS=Homo sapiens GN=YWHAQ PE=1 SV=1	6.32E+08	5.95E+08	7.49E+08	1.06E+00
P62937	Peptidyl-prolyl cis-trans isomerase A OS=Homo sapiens GN=PPIA PE=1 SV=2	6.65E+08	5.62E+08	1.05E+09	1.18E+00
O00161	Synaptosomal-associated protein 23 OS=Homo sapiens GN=SNAP23 PE=1 SV=1	6.13E+08	6.18E+08	6.23E+08	-1.01E+00
O95573	Long-chain-fatty-acid--CoA ligase 3 OS=Homo sapiens GN=ACSL3 PE=1 SV=3	1.09E+09	1.64E+08	1.13E+09	6.63E+00
Q00839	Heterogeneous nuclear ribonucleoprotein U OS=Homo sapiens GN=HNRNPU PE=1 SV=6	5.96E+08	6.60E+08	7.25E+08	-1.11E+00
P06703	Protein S100-A6 OS=Homo sapiens GN=S100A6 PE=1 SV=1	6.23E+08	6.46E+08	6.91E+08	-1.04E+00
P62258	14-3-3 protein epsilon OS=Homo sapiens GN=YWHAE PE=1 SV=1	6.51E+08	6.23E+08	7.25E+08	1.04E+00

P14625	Endoplasmin OS=Homo sapiens GN=HSP90B1 PE=1 SV=1	5.75E+08	7.20E+08	5.68E+08	-1.25E+00
P57053	Histone H2B type F-S OS=Homo sapiens GN=H2BFS PE=1 SV=2	4.45E+08	8.59E+08	5.52E+08	-1.93E+00
P09651-3	Isoform 2 of Heterogeneous nuclear ribonucleoprotein A1 OS=Homo sapiens GN=HNRNPA1	6.43E+08	7.36E+08	7.09E+08	-1.15E+00
P14678	Small nuclear ribonucleoprotein-associated proteins B and B' OS=Homo sapiens GN=SNRPB PE=1 SV=2	9.23E+08	4.57E+08	7.94E+08	2.02E+00
P13647	Keratin, type II cytoskeletal 5 OS=Homo sapiens GN=KRT5 PE=1 SV=3	7.46E+08	6.36E+08	2.50E+08	1.17E+00
P62805	Histone H4 OS=Homo sapiens GN=HIST1H4A PE=1 SV=2	6.99E+08	7.04E+08	5.67E+08	-1.01E+00
Q9Y490	Talin-1 OS=Homo sapiens GN=TLN1 PE=1 SV=3	5.35E+08	8.83E+08	2.84E+08	-1.65E+00
Q9H4M9	EH domain-containing protein 1 OS=Homo sapiens GN=EHD1 PE=1 SV=2	3.04E+08	1.12E+09	4.61E+08	-3.67E+00
P36578	60S ribosomal protein L4 OS=Homo sapiens GN=RPL4 PE=1 SV=5	7.22E+08	7.12E+08	7.43E+08	1.02E+00
F5H8E5	Ubiquitin carboxyl-terminal hydrolase OS=Homo sapiens GN=USP7 PE=3 SV=1	9.40E+08	4.97E+08	8.06E+07	1.89E+00
P13645	Keratin, type I cytoskeletal 10 OS=Homo sapiens GN=KRT10 PE=1 SV=6	9.88E+08	4.50E+08	4.65E+08	2.20E+00
Q15758	Neutral amino acid transporter B(0) OS=Homo sapiens GN=SLC1A5 PE=1 SV=2	6.54E+08	7.97E+08	6.02E+08	-1.22E+00
P63104	14-3-3 protein zeta/delta OS=Homo sapiens GN=YWHAZ PE=1 SV=1	7.73E+08	7.37E+08	8.67E+08	1.05E+00
P49327	Fatty acid synthase OS=Homo sapiens GN=FASN PE=1 SV=3	9.46E+08	5.89E+08	4.55E+08	1.61E+00

Q96RQ3	Methylcrotonoyl-CoA carboxylase subunit alpha, mitochondrial OS=Homo sapiens GN=MCCC1 PE=1 SV=3	7.99E+08	7.46E+08	7.83E+08	1.07E+00
Q96FX8	p53 apoptosis effector related to PMP-22 OS=Homo sapiens GN=PERP PE=2 SV=1	7.23E+08	8.51E+08	3.48E+08	-1.18E+00
P12814-2	Isoform 2 of Alpha-actinin-1 OS=Homo sapiens GN=ACTN1	7.60E+08	8.47E+08	8.01E+08	-1.11E+00
Q9BUF5	Tubulin beta-6 chain OS=Homo sapiens GN=TUBB6 PE=1 SV=1	8.23E+08	8.31E+08	9.80E+08	-1.01E+00
P55060-3	Isoform 3 of Exportin-2 OS=Homo sapiens GN=CSE1L	7.90E+08	8.68E+08	4.08E+08	-1.10E+00
Q06830	Peroxiredoxin-1 OS=Homo sapiens GN=PRDX1 PE=1 SV=1	7.94E+08	8.73E+08	9.82E+08	-1.10E+00
F5H897	Heat shock protein 75 kDa, mitochondrial OS=Homo sapiens GN=TRAP1 PE=3 SV=1	8.31E+08	8.49E+08	7.56E+08	-1.02E+00
Q04637-6	Isoform E of Eukaryotic translation initiation factor 4 gamma 1 OS=Homo sapiens GN=EIF4G1	8.53E+08	8.82E+08	8.36E+08	-1.03E+00
E7EPA7	Transketolase OS=Homo sapiens GN=TKT PE=4 SV=1	9.99E+08	7.43E+08	1.04E+09	1.34E+00
Q96P70	Importin-9 OS=Homo sapiens GN=IPO9 PE=1 SV=3	7.42E+07	1.68E+09	7.58E+07	-1.00E+01
P22626	Heterogeneous nuclear ribonucleoproteins A2/B1 OS=Homo sapiens GN=HNRNPA2B1 PE=1 SV=2	8.86E+08	8.97E+08	9.27E+08	-1.01E+00
P62070	Ras-related protein R-Ras2 OS=Homo sapiens GN=RRAS2 PE=1 SV=1	1.78E+09	9.37E+07	4.32E+07	1.00E+01
O43707	Alpha-actinin-4 OS=Homo sapiens GN=ACTN4 PE=1 SV=2	8.18E+08	1.07E+09	1.04E+09	-1.31E+00
Q15046-2	Isoform Mitochondrial of Lysine--tRNA ligase OS=Homo sapiens GN=KARS	9.47E+08	9.59E+08	7.42E+08	-1.01E+00
P13639	Elongation factor 2 OS=Homo sapiens GN=EEF2 PE=1 SV=4	8.71E+08	1.08E+09	1.21E+09	-1.24E+00

A6NNI4	CD9 antigen OS=Homo sapiens GN=CD9 PE=4 SV=1	9.09E+08	1.04E+09	9.74E+08	-1.14E+00
P05165	Propionyl-CoA carboxylase alpha chain, mitochondrial OS=Homo sapiens GN=PCCA PE=1 SV=4	9.98E+08	1.00E+09	9.46E+08	-1.01E+00
P04075	Fructose-bisphosphate aldolase A OS=Homo sapiens GN=ALDOA PE=1 SV=2	1.08E+09	9.20E+08	1.23E+09	1.18E+00
P16070-11	Isoform 11 of CD44 antigen OS=Homo sapiens GN=CD44	9.53E+08	1.11E+09	8.83E+08	-1.16E+00
P07195	L-lactate dehydrogenase B chain OS=Homo sapiens GN=LDHB PE=1 SV=2	1.05E+09	1.02E+09	1.12E+09	1.02E+00
Q01628	Interferon-induced transmembrane protein 3 OS=Homo sapiens GN=IFITM3 PE=1 SV=2	9.45E+08	1.13E+09	9.69E+08	-1.20E+00
P08107	Heat shock 70 kDa protein 1A/1B OS=Homo sapiens GN=HSPA1A PE=1 SV=5	1.02E+09	1.08E+09	1.11E+09	-1.06E+00
P07737	Profilin-1 OS=Homo sapiens GN=PFN1 PE=1 SV=2	1.04E+09	1.09E+09	2.27E+09	-1.05E+00
P08779	Keratin, type I cytoskeletal 16 OS=Homo sapiens GN=KRT16 PE=1 SV=4	1.29E+09	8.47E+08	1.13E+09	1.52E+00
P11021	78 kDa glucose-regulated protein OS=Homo sapiens GN=HSPA5 PE=1 SV=2	1.08E+09	1.17E+09	8.91E+08	-1.08E+00
P14618	Pyruvate kinase isozymes M1/M2 OS=Homo sapiens GN=PKM PE=1 SV=4	9.93E+08	1.28E+09	1.43E+09	-1.29E+00
Q01650	Large neutral amino acids transporter small subunit 1 OS=Homo sapiens GN=SLC7A5 PE=1 SV=2	9.70E+08	1.31E+09	1.02E+09	-1.35E+00
P55072	Transitional endoplasmic reticulum ATPase OS=Homo sapiens GN=VCP PE=1 SV=4	2.02E+09	3.67E+08	2.70E+08	5.49E+00
P08195-2	Isoform 2 of 4F2 cell-surface antigen heavy chain OS=Homo sapiens GN=SLC3A2	1.11E+09	1.29E+09	8.26E+08	-1.16E+00
P35637-2	Isoform Short of RNA-binding protein FUS OS=Homo sapiens GN=FUS	1.28E+09	1.24E+09	8.43E+07	1.03E+00

P04264	Keratin, type II cytoskeletal 1 OS=Homo sapiens GN=KRT1 PE=1 SV=6	2.22E+09	3.12E+08	3.17E+08	7.11E+00
Q04695	Keratin, type I cytoskeletal 17 OS=Homo sapiens GN=KRT17 PE=1 SV=2	1.40E+09	1.15E+09	1.56E+09	1.21E+00
P27105	Erythrocyte band 7 integral membrane protein OS=Homo sapiens GN=STOM PE=1 SV=3	1.14E+09	1.41E+09	8.46E+08	-1.24E+00
P06748-2	Isoform 2 of Nucleophosmin OS=Homo sapiens GN=NPM1	1.30E+09	1.26E+09	1.21E+09	1.04E+00
P62979	Ubiquitin-40S ribosomal protein S27a OS=Homo sapiens GN=RPS27A PE=1 SV=2	1.31E+09	1.28E+09	7.75E+08	1.02E+00
E9PEZ3	Protein diaphanous homolog 1 OS=Homo sapiens GN=DIAPH1 PE=4 SV=1	6.45E+08	2.04E+09	2.91E+09	-3.15E+00
P15924	Desmoplakin OS=Homo sapiens GN=DSP PE=1 SV=3	9.73E+08	1.79E+09	2.71E+09	-1.84E+00
P00338	L-lactate dehydrogenase A chain OS=Homo sapiens GN=LDHA PE=1 SV=2	1.38E+09	1.41E+09	1.47E+09	-1.02E+00
P02786	Transferrin receptor protein 1 OS=Homo sapiens GN=TFRC PE=1 SV=2	1.23E+09	1.57E+09	1.39E+09	-1.27E+00
Q14344	Guanine nucleotide-binding protein subunit alpha-13 OS=Homo sapiens GN=GNA13 PE=1 SV=2	1.29E+09	1.56E+09	1.24E+09	-1.21E+00
P11142	Heat shock cognate 71 kDa protein OS=Homo sapiens GN=HSPA8 PE=1 SV=1	1.37E+09	1.50E+09	1.38E+09	-1.09E+00
Q10589	Bone marrow stromal antigen 2 OS=Homo sapiens GN=BST2 PE=1 SV=1	1.34E+09	1.64E+09	1.43E+09	-1.22E+00
Q13085	Acetyl-CoA carboxylase 1 OS=Homo sapiens GN=ACACA PE=1 SV=2	1.79E+09	1.33E+09	1.74E+09	1.34E+00
P07900	Heat shock protein HSP 90-alpha OS=Homo sapiens GN=HSP90AA1 PE=1 SV=5	1.72E+09	1.68E+09	1.47E+09	1.02E+00
K7ENY1	Titin OS=Homo sapiens GN=TTN PE=4 SV=1	1.79E+09	1.67E+09	1.58E+09	1.07E+00

F8VWK8	CD63 antigen (Fragment) OS=Homo sapiens GN=CD63 PE=4 SV=1	1.63E+09	1.86E+09	1.81E+09	-1.15E+00
P68371	Tubulin beta-4B chain OS=Homo sapiens GN=TUBB4B PE=1 SV=1	1.72E+09	1.90E+09	1.90E+09	-1.10E+00
P06733	Alpha-enolase OS=Homo sapiens GN=ENO1 PE=1 SV=2	1.82E+09	1.82E+09	2.24E+09	-1.00E+00
P68366	Tubulin alpha-4A chain OS=Homo sapiens GN=TUBA4A PE=1 SV=1	1.81E+09	1.83E+09	1.96E+09	-1.01E+00
P46926	Glucosamine-6-phosphate isomerase 1 OS=Homo sapiens GN=GNPDA1 PE=1 SV=1	1.74E+09	1.97E+09	0.00E+00	-1.13E+00
F8VW92	Tubulin beta chain OS=Homo sapiens GN=TUBB PE=3 SV=1	1.82E+09	1.90E+09	1.90E+09	-1.04E+00
P08238	Heat shock protein HSP 90-beta OS=Homo sapiens GN=HSP90AB1 PE=1 SV=4	1.62E+09	2.14E+09	1.49E+09	-1.32E+00
P10809	60 kDa heat shock protein, mitochondrial OS=Homo sapiens GN=HSPD1 PE=1 SV=2	1.81E+09	2.18E+09	1.48E+09	-1.21E+00
Q71U36	Tubulin alpha-1A chain OS=Homo sapiens GN=TUBA1A PE=1 SV=1	1.99E+09	2.05E+09	1.90E+09	-1.03E+00
Q9BQE3	Tubulin alpha-1C chain OS=Homo sapiens GN=TUBA1C PE=1 SV=1	2.11E+09	2.05E+09	1.96E+09	1.03E+00
P0CG38	POTE ankyrin domain family member I OS=Homo sapiens GN=POTEI PE=3 SV=1	2.42E+09	2.77E+09	2.79E+09	-1.15E+00
P52209	6-phosphogluconate dehydrogenase, decarboxylating OS=Homo sapiens GN=PGD PE=1 SV=3	5.37E+09	1.40E+08	1.40E+08	1.00E+01
Q13151	Heterogeneous nuclear ribonucleoprotein A0 OS=Homo sapiens GN=HNRNPA0 PE=1 SV=1	1.50E+08	5.53E+09	1.58E+08	-1.00E+01
P41252	Isoleucine--tRNA ligase, cytoplasmic OS=Homo sapiens GN=IARS PE=1 SV=2	2.49E+09	3.44E+09	3.64E+08	-1.39E+00
P27824	Calnexin OS=Homo sapiens GN=CANX PE=1 SV=2	3.15E+09	3.57E+09	2.69E+09	-1.13E+00

Q9Y6D5	Brefeldin A-inhibited guanine nucleotide-exchange protein 2 OS=Homo sapiens GN=ARFGEF2 PE=1 SV=3	0.00E+00	7.28E+09	6.89E+08	-1.00E+01
P11498	Pyruvate carboxylase, mitochondrial OS=Homo sapiens GN=PC PE=1 SV=2	4.30E+09	5.42E+09	5.31E+09	-1.26E+00
P68032	Actin, alpha cardiac muscle 1 OS=Homo sapiens GN=ACTC1 PE=1 SV=1	5.82E+09	6.06E+09	6.18E+09	-1.04E+00
Q15149	Plectin OS=Homo sapiens GN=PLEC PE=1 SV=3	7.42E+09	9.73E+09	7.76E+09	-1.31E+00

BIBLIOGRAPHY

Alto, N. M., & Dixon, J. E. (2008). Analysis of Rho-GTPase mimicry by a family of bacterial type III effector proteins. *Methods Enzymol, 439*, 131-143.

Alto, N. M., & Orth, K. (2012). Subversion of cell signaling by pathogens. *Cold Spring Harb Perspect Biol, 4*(9), a006114. doi: 10.1101/cshperspect.a006114

Alto, N. M., Shao, F., Lazar, C. S., Brost, R. L., Chua, G., Mattoo, S., . . . Dixon, J. E. (2006). Identification of a bacterial type III effector family with G protein mimicry functions. *Cell, 124*(1), 133-145. doi: 10.1016/j.cell.2005.10.031

Andreeva, A. V., Kutuzov, M. A., Evans, D. E., & Hawes, C. R. (1998). The structure and function of the Golgi apparatus: a hundred years of questions. *Journal of Experimental Botany, 49*(325), 1281-1291. doi: DOI 10.1093/jexbot/49.325.1281

Ashida, H., Ogawa, M., Mimuro, H., Kobayashi, T., Sanada, T., & Sasakawa, C. (2011). Shigella are versatile mucosal pathogens that circumvent the host innate immune system. *Curr Opin Immunol, 23*(4), 448-455. doi: 10.1016/j.coi.2011.06.001

Auerbuch, V., Lenz, L. L., & Portnoy, D. A. (2001). Development of a competitive index assay to evaluate the virulence of Listeria monocytogenes actA mutants during primary and secondary infection of mice. *Infect Immun, 69*(9), 5953-5957.

Baay, M., Brouwer, A., Pauwels, P., Peeters, M., & Lardon, F. (2011). Tumor cells and tumor-associated macrophages: secreted proteins as potential targets for therapy. *Clin Dev Immunol, 2011*, 565187. doi: 10.1155/2011/565187

Bachert, C., & Linstedt, A. D. (2010). Dual anchoring of the GRASP membrane tether promotes trans pairing. *Journal of Biological Chemistry, 285*(21), 16294-16301. doi: 10.1074/jbc.M110.116129

Barr, F. A., Nakamura, N., & Warren, G. (1998). Mapping the interaction between GRASP65 and GM130, components of a protein complex involved in the stacking of Golgi cisternae. *EMBO J, 17*(12), 3258-3268. doi: 10.1093/emboj/17.12.3258

Barr, F. A., Puype, M., Vandekerckhove, J., & Warren, G. (1997). GRASP65, a protein involved in the stacking of Golgi cisternae. *Cell, 91*(2), 253-262.

Bhatnagar, R. S., Futterer, K., Farazi, T. A., Korolev, S., Murray, C. L., Jackson-Machelski, E., . . . Waksman, G. (1998). Structure of N-myristoyltransferase with bound myristoylCoA and peptide substrate analogs. *Nat Struct Biol, 5*(12), 1091-1097. doi: 10.1038/4202

Bhatnagar, R. S., Schall, O. F., Jackson-Machelski, E., Sikorski, J. A., Devadas, B., Gokel, G. W., & Gordon, J. I. (1997). Titration calorimetric analysis of AcylCoA recognition by myristoylCoA:protein N-myristoyltransferase. *Biochemistry, 36*(22), 6700-6708. doi: 10.1021/bi970311v

Black, D. S., & Bliska, J. B. (2000). The RhoGAP activity of the Yersinia pseudotuberculosis cytotoxin YopE is required for antiphagocytic function and virulence. *Mol Microbiol, 37*(3), 515-527.

Bunkenborg, J., Garcia, G. E., Paz, M. I., Andersen, J. S., & Molina, H. (2010). The minotaur proteome: avoiding cross-species identifications deriving from bovine serum in cell culture models. *Proteomics, 10*(16), 3040-3044. doi: 10.1002/pmic.201000103

Burdette, D. L., & Vance, R. E. (2013). STING and the innate immune response to nucleic acids in the cytosol. *Nat Immunol, 14*(1), 19-26. doi: 10.1038/ni.2491

Buysse, J. M., Dunyak, D. S., Hartman, A. B., & Venkatesan, M. M. (1997a). Identification and molecular characterization of a 27 kDa Shigella flexneri invasion plasmid antigen, IpaJ. *Microbial Pathogenesis, 23*(6), 357-369. doi: DOI 10.1006/mpat.1997.0164

Buysse, J. M., Dunyak, D. S., Hartman, A. B., & Venkatesan, M. M. (1997b). Identification and molecular characterization of a 27 kDa Shigella flexneri invasion plasmid antigen, IpaJ. *Microb Pathog, 23*(6), 357-369. doi: 10.1006/mpat.1997.0164

Capmany, A., & Damiani, M. T. (2010). Chlamydia trachomatis intercepts Golgi-derived sphingolipids through a Rab14-mediated transport required for bacterial development and replication. *PLoS One, 5*(11), e14084. doi: 10.1371/journal.pone.0014084

Carabeo, R. A., Mead, D. J., & Hackstadt, T. (2003). Golgi-dependent transport of cholesterol to the Chlamydia trachomatis inclusion. *Proc Natl Acad Sci U S A, 100*(11), 6771-6776. doi: 10.1073/pnas.1131289100

Castaneda, J. A., Lim, M. J., Cooper, J. D., & Pearce, D. A. (2008). Immune system irregularities in lysosomal storage disorders. *Acta Neuropathol, 115*(2), 159-174. doi: 10.1007/s00401-007-0296-4

Chardin, P., & McCormick, F. (1999). Brefeldin A: the advantage of being uncompetitive. *Cell, 97*(2), 153-155.

Charron, G., Zhang, M. M., Yount, J. S., Wilson, J., Raghavan, A. S., Shamir, E., & Hang, H. C. (2009). Robust fluorescent detection of protein fatty-acylation with chemical reporters. *J Am Chem Soc, 131*(13), 4967-4975. doi: 10.1021/ja810122f

Chockalingam, A., Brooks, J. C., Cameron, J. L., Blum, L. K., & Leifer, C. A. (2009). TLR9 traffics through the Golgi complex to localize to endolysosomes and respond to CpG DNA. *Immunology and Cell Biology, 87*(3), 209-217. doi: Doi 10.1038/Icb.2008.101

Choy, A., Dancourt, J., Mugo, B., O'Connor, T. J., Isberg, R. R., Melia, T. J., & Roy, C. R. (2012). The Legionella effector RavZ inhibits host autophagy through irreversible Atg8 deconjugation. *Science, 338*(6110), 1072-1076. doi: 10.1126/science.1227026

Christian, J. G., Heymann, J., Paschen, S. A., Vier, J., Schauenburg, L., Rupp, J., . . . Heuer, D. (2011). Targeting of a chlamydial protease impedes intracellular bacterial growth. *PLoS Pathog, 7*(9), e1002283. doi: 10.1371/journal.ppat.1002283

Colbert, J. D., Matthews, S. P., Miller, G., & Watts, C. (2009). Diverse regulatory roles for lysosomal proteases in the immune response. *Eur J Immunol, 39*(11), 2955-2965. doi: 10.1002/eji.200939650

D'Souza-Schorey, C., Li, G., Colombo, M. I., & Stahl, P. D. (1995). A regulatory role for ARF6 in receptor-mediated endocytosis. *Science, 267*(5201), 1175-1178.

Datsenko, K. A., & Wanner, B. L. (2000). One-step inactivation of chromosomal genes in Escherichia coli K-12 using PCR products. *Proc Natl Acad Sci U S A, 97*(12), 6640-6645.

Donaldson, J. G., & Jackson, C. L. (2011). ARF family G proteins and their regulators: roles in membrane transport, development and disease. *Nat Rev Mol Cell Biol, 12*(6), 362-375. doi: 10.1038/nrm3117

Dong, N., Zhu, Y., Lu, Q., Hu, L., Zheng, Y., & Shao, F. (2012). Structurally distinct bacterial TBC-like GAPs link Arf GTPase to Rab1 inactivation to counteract host defenses. *Cell, 150*(5), 1029-1041. doi: 10.1016/j.cell.2012.06.050

Farazi, T. A., Waksman, G., & Gordon, J. I. (2001). The biology and enzymology of protein N-myristoylation. *J Biol Chem, 276*(43), 39501-39504. doi: 10.1074/jbc.R100042200

Ge, J., & Shao, F. (2011). Manipulation of host vesicular trafficking and innate immune defence by Legionella Dot/Icm effectors. *Cell Microbiol, 13*(12), 1870-1880. doi: 10.1111/j.1462-5822.2011.01710.x

Goldberg, J. (1998). Structural basis for activation of ARF GTPase: mechanisms of guanine nucleotide exchange and GTP-myristoyl switching. *Cell, 95*(2), 237-248.

Hackstadt, T., Rockey, D. D., Heinzen, R. A., & Scidmore, M. A. (1996). Chlamydia trachomatis interrupts an exocytic pathway to acquire endogenously synthesized sphingomyelin in transit from the Golgi apparatus to the plasma membrane. *EMBO J, 15*(5), 964-977.

Hang, H. C., Geutjes, E. J., Grotenbreg, G., Pollington, A. M., Bijlmakers, M. J., & Ploegh, H. L. (2007). Chemical probes for the rapid detection of Fatty-acylated proteins in Mammalian cells. *J Am Chem Soc, 129*(10), 2744-2745. doi: 10.1021/ja0685001

Hansen, K., Prabakaran, T., Laustsen, A., Jorgensen, S. E., Rahbaek, S. H., Jensen, S. B., . . . Paludan, S. R. (2014). Listeria monocytogenes induces IFNbeta expression through an IFI16-, cGAS- and STING-dependent pathway. *EMBO J, 33*(15), 1654-1666. doi: 10.15252/embj.201488029

Hardiman, C. A., & Roy, C. R. (2014). AMPylation is critical for Rab1 localization to vacuoles containing Legionella pneumophila. *MBio, 5*(1), e01035-01013. doi: 10.1128/mBio.01035-13

Havarstein, L. S., Diep, D. B., & Nes, I. F. (1995). A family of bacteriocin ABC transporters carry out proteolytic processing of their substrates concomitant with export. *Mol Microbiol, 16*(2), 229-240.

Havarstein, L. S., Holo, H., & Nes, I. F. (1994). The leader peptide of colicin V shares consensus sequences with leader peptides that are common among peptide bacteriocins produced by gram-positive bacteria. *Microbiology, 140 (Pt 9)*, 2383-2389.

Herman, P. K., Stack, J. H., DeModena, J. A., & Emr, S. D. (1991). A novel protein kinase homolog essential for protein sorting to the yeast lysosome-like vacuole. *Cell, 64*(2), 425-437.

Heuer, D., Rejman Lipinski, A., Machuy, N., Karlas, A., Wehrens, A., Siedler, F., . . . Meyer, T. F. (2009). Chlamydia causes fragmentation of the Golgi compartment to ensure reproduction. *Nature, 457*(7230), 731-735. doi: 10.1038/nature07578

Hornef, M. W., Frisan, T., Vandewalle, A., Normark, S., & Richter-Dahlfors, A. (2002). Toll-like receptor 4 resides in the Golgi apparatus and colocalizes with internalized lipopolysaccharide in intestinal epithelial cells. *Journal of Experimental Medicine, 195*(5), 559-570. doi: Doi 10.1084/Jem.20011788

Hsu, F., Zhu, W., Brennan, L., Tao, L., Luo, Z. Q., & Mao, Y. (2012). Structural basis for substrate recognition by a unique Legionella phosphoinositide phosphatase. *Proc Natl Acad Sci U S A, 109*(34), 13567-13572. doi: 10.1073/pnas.1207903109

Huang, Z., Sutton, S. E., Wallenfang, A. J., Orchard, R. C., Wu, X., Feng, Y., . . . Alto, N. M. (2009). Structural insights into host GTPase isoform selection by a family of bacterial GEF mimics. *Nat Struct Mol Biol, 16*(8), 853-860. doi: 10.1038/nsmb.1647

Ingmundson, A., Delprato, A., Lambright, D. G., & Roy, C. R. (2007). Legionella pneumophila proteins that regulate Rab1 membrane cycling. *Nature, 450*(7168), 365-369. doi: 10.1038/nature06336

Isberg, R. R., O'Connor, T. J., & Heidtman, M. (2009). The Legionella pneumophila replication vacuole: making a cosy niche inside host cells. *Nat Rev Microbiol, 7*(1), 13-24. doi: 10.1038/nrmicro1967

Ishikawa, H., Ma, Z., & Barber, G. N. (2009). STING regulates intracellular DNA-mediated, type I interferon-dependent innate immunity. *Nature, 461*(7265), 788-792. doi: 10.1038/nature08476

Islam, D., Veress, B., Bardhan, P. K., Lindberg, A. A., & Christensson, B. (1997). In situ characterization of inflammatory responses in the rectal mucosae of patients with shigellosis. *Infect Immun, 65*(2), 739-749.

Jube, S., Rivera, Z. S., Bianchi, M. E., Powers, A., Wang, E., Pagano, I., . . . Yang, H. (2012). Cancer cell secretion of the DAMP protein HMGB1 supports progression in malignant mesothelioma. *Cancer Res, 72*(13), 3290-3301. doi: 10.1158/0008-5472.CAN-11-3481

Kahn, R. (2009). Diabetes technology--now and in the future. *Lancet, 373*(9677), 1741-1743. doi: 10.1016/S0140-6736(09)60960-0

Kall, L., Storey, J. D., MacCoss, M. J., & Noble, W. S. (2008). Assigning significance to peptides identified by tandem mass spectrometry using decoy databases. *J Proteome Res, 7*(1), 29-34. doi: 10.1021/pr700600n

Kamps, M. P., Buss, J. E., & Sefton, B. M. (1985). Mutation of NH2-terminal glycine of p60src prevents both myristoylation and morphological transformation. *Proc Natl Acad Sci U S A, 82*(14), 4625-4628.

Kelleher, N. L. (2004). Top-down proteomics. *Anal Chem, 76*(11), 197A-203A.

Kenny, B., Ellis, S., Leard, A. D., Warawa, J., Mellor, H., & Jepson, M. A. (2002). Co-ordinate regulation of distinct host cell signalling pathways by multifunctional enteropathogenic Escherichia coli effector molecules. *Mol Microbiol, 44*(4), 1095-1107.

Knodler, L. A., & Steele-Mortimer, O. (2003). Taking possession: biogenesis of the Salmonella-containing vacuole. *Traffic, 4*(9), 587-599.

Kuai, J., Boman, A. L., Arnold, R. S., Zhu, X. J., & Kahn, R. A. (2000). Effects of activated ADP-ribosylation factors on Golgi morphology require neither activation of phospholipase D1 nor recruitment of coatomer. *Journal of Biological Chemistry, 275*(6), 4022-4032. doi: DOI 10.1074/jbc.275.6.4022

Kuai, J., & Kahn, R. A. (2000). Residues forming a hydrophobic pocket in ARF3 are determinants of GDP dissociation and effector interactions. *FEBS Lett, 487*(2), 252-256. doi: Doi 10.1016/S0014-5793(00)02325-5

Landstrom, A. H., Westman, J., & Borg, L. A. (1988). Lysosomes and pancreatic islet function. Time course of insulin biosynthesis, insulin secretion, and lysosomal transformation after rapid changes in glucose concentration. *Diabetes, 37*(3), 309-316.

Latz, E., Visintin, A., Lien, E., Fitzgerald, K. A., Monks, B. G., Kurt-Jones, E. A., . . . Espevik, T. (2002). Lipopolysaccharide rapidly traffics to and from the golgi apparatus with the toll-like receptor 4-MD-2-CD14 complex in a process that is distinct from the initiation of signal transduction. *Journal of Biological Chemistry, 277*(49), 47834-47843. doi: DOI 10.1074/jbc.M207873200

Lauer, P., Chow, M. Y., Loessner, M. J., Portnoy, D. A., & Calendar, R. (2002). Construction, characterization, and use of two Listeria monocytogenes site-specific phage integration vectors. *J Bacteriol, 184*(15), 4177-4186.

Li, H., Xu, H., Zhou, Y., Zhang, J., Long, C., Li, S., . . . Shao, F. (2007). The phosphothreonine lyase activity of a bacterial type III effector family. *Science, 315*(5814), 1000-1003. doi: 10.1126/science.1138960

Liu, M., Ren, Z., Lei, C., Wen, Y., Yan, W., & Zheng, Z. (2002). Sequence analysis and characterization of plasmid pSFD10 from Salmonella choleraesuis. *Plasmid, 48*(1), 59-63.

Luo, R. B., Jacques, K., Ahvazi, B., Stauffer, S., Premont, R. T., & Randazzo, P. A. (2005). Mutational analysis of the Arf1 center dot GTP/Arf GAP interface reveals an Arf1 mutant that selectively affects the Arf GAP ASAP1. *Current Biology, 15*(23), 2164-2169. doi: DOI 10.1016/j.cub.2005.10.065

Machner, M. P., & Isberg, R. R. (2006). Targeting of host Rab GTPase function by the intravacuolar pathogen Legionella pneumophila. *Dev Cell, 11*(1), 47-56. doi: 10.1016/j.devcel.2006.05.013

Manderson, A. P., Kay, J. G., Hammond, L. A., Brown, D. L., & Stow, J. L. (2007). Subcompartments of the macrophage recycling endosome direct the differential secretion of IL-6 and TNF alpha. *Journal of Cell Biology, 178*(1), 57-69. doi: DOI 10.1083/jcb.200612131

Manzanillo, P. S., Shiloh, M. U., Portnoy, D. A., & Cox, J. S. (2012). Mycobacterium tuberculosis activates the DNA-dependent cytosolic surveillance pathway within macrophages. *Cell Host Microbe, 11*(5), 469-480. doi: 10.1016/j.chom.2012.03.007

Maurer-Stroh, S., Gouda, M., Novatchkova, M., Schleiffer, A., Schneider, G., Sirota, F. L., . . . Eisenhaber, F. (2004). MYRbase: analysis of genome-wide glycine

myristoylation enlarges the functional spectrum of eukaryotic myristoylated proteins. *Genome Biol, 5*(3), R21. doi: 10.1186/gb-2004-5-3-r21

McLaughlin, S., & Aderem, A. (1995). The myristoyl-electrostatic switch: a modulator of reversible protein-membrane interactions. *Trends Biochem Sci, 20*(7), 272-276.

McLoughlin, R. M., Jenkins, B. J., Grail, D., Williams, A. S., Fielding, C. A., Parker, C. R., . . . Jones, S. A. (2005). IL-6 trans-signaling via STAT3 directs T cell infiltration in acute inflammation. *Proceedings of the National Academy of Sciences of the United States of America, 102*(27), 9589-9594. doi: DOI 10.1073/pnas.0501794102

Michiels, J., Dirix, G., Vanderleyden, J., & Xi, C. (2001). Processing and export of peptide pheromones and bacteriocins in Gram-negative bacteria. *Trends Microbiol, 9*(4), 164-168.

Mittal, R., Peak-Chew, S. Y., & McMahon, H. T. (2006). Acetylation of MEK2 and I kappa B kinase (IKK) activation loop residues by YopJ inhibits signaling. *Proc Natl Acad Sci U S A, 103*(49), 18574-18579. doi: 10.1073/pnas.0608995103

Mounier, J., Boncompain, G., Senerovic, L., Lagache, T., Chretien, F., Perez, F., . . . Sauvonnet, N. (2012). Shigella Effector IpaB-Induced Cholesterol Relocation Disrupts the Golgi Complex and Recycling Network to Inhibit Host Cell Secretion. *Cell Host Microbe, 12*(3), 381-389. doi: 10.1016/j.chom.2012.07.010

Mukherjee, S., Keitany, G., Li, Y., Wang, Y., Ball, H. L., Goldsmith, E. J., & Orth, K. (2006). Yersinia YopJ acetylates and inhibits kinase activation by blocking phosphorylation. *Science, 312*(5777), 1211-1214. doi: 10.1126/science.1126867

Mukherjee, S., Liu, X., Arasaki, K., McDonough, J., Galan, J. E., & Roy, C. R. (2011). Modulation of Rab GTPase function by a protein phosphocholine transferase. *Nature, 477*(7362), 103-106. doi: 10.1038/nature10335

Neunuebel, M. R., Chen, Y., Gaspar, A. H., Backlund, P. S., Jr., Yergey, A., & Machner, M. P. (2011). De-AMPylation of the small GTPase Rab1 by the pathogen Legionella pneumophila. *Science, 333*(6041), 453-456. doi: 10.1126/science.1207193

Neunuebel, M. R., Mohammadi, S., Jarnik, M., & Machner, M. P. (2012). Legionella pneumophila LidA affects nucleotide binding and activity of the host GTPase Rab1. *J Bacteriol, 194*(6), 1389-1400. doi: 10.1128/JB.06306-11

Orchard, R. C., Kittisopikul, M., Altschuler, S. J., Wu, L. F., Suel, G. M., & Alto, N. M. (2012). Identification of F-actin as the dynamic hub in a microbial-induced GTPase polarity circuit. *Cell, 148*(4), 803-815. doi: 10.1016/j.cell.2011.11.063

Orth, K., Palmer, L. E., Bao, Z. Q., Stewart, S., Rudolph, A. E., Bliska, J. B., & Dixon, J. E. (1999). Inhibition of the mitogen-activated protein kinase kinase superfamily by a Yersinia effector. *Science, 285*(5435), 1920-1923.

Paludan, S. R., & Bowie, A. G. (2013). Immune sensing of DNA. *Immunity, 38*(5), 870-880. doi: 10.1016/j.immuni.2013.05.004

Pan, X., Luhrmann, A., Satoh, A., Laskowski-Arce, M. A., & Roy, C. R. (2008). Ankyrin repeat proteins comprise a diverse family of bacterial type IV effectors. *Science, 320*(5883), 1651-1654. doi: 10.1126/science.1158160

Pei, J., & Grishin, N. V. (2009). The Rho GTPase inactivation domain in Vibrio cholerae MARTX toxin has a circularly permuted papain-like thiol protease fold. *Proteins, 77*(2), 413-419. doi: 10.1002/prot.22447

Pei, J., Kim, B. H., & Grishin, N. V. (2008). PROMALS3D: a tool for multiple protein sequence and structure alignments. *Nucleic Acids Res, 36*(7), 2295-2300. doi: 10.1093/nar/gkn072

Peters, P. J., Hsu, V. W., Ooi, C. E., Finazzi, D., Teal, S. B., Oorschot, V., . . . Klausner, R. D. (1995). Overexpression of wild-type and mutant ARF1 and ARF6: distinct perturbations of nonoverlapping membrane compartments. *Journal of Cell Biology, 128*(6), 1003-1017.

Pistor, S., Chakraborty, T., Niebuhr, K., Domann, E., & Wehland, J. (1994). The ActA protein of Listeria monocytogenes acts as a nucleator inducing reorganization of the actin cytoskeleton. *EMBO J, 13*(4), 758-763.

Puertollano, R., Randazzo, P. A., Presley, J. F., Hartnell, L. M., & Bonifacino, J. S. (2001). The GGAs promote ARF-dependent recruitment of clathrin to the TGN. *Cell, 105*(1), 93-102.

Rejman Lipinski, A., Heymann, J., Meissner, C., Karlas, A., Brinkmann, V., Meyer, T. F., & Heuer, D. (2009). Rab6 and Rab11 regulate Chlamydia trachomatis development and golgin-84-dependent Golgi fragmentation. *PLoS Pathog, 5*(10), e1000615. doi: 10.1371/journal.ppat.1000615

Ren, X. F., Farias, G. G., Canagarajah, B. J., Bonifacino, J. S., & Hurley, J. H. (2013). Structural Basis for Recruitment and Activation of the AP-1 Clathrin Adaptor Complex by Arf1. *Cell, 152*(4), 755-767. doi: DOI 10.1016/j.cell.2012.12.042

Rivera, V. M., Wang, X., Wardwell, S., Courage, N. L., Volchuk, A., Keenan, T., . . . Clackson, T. (2000). Regulation of protein secretion through controlled aggregation in the endoplasmic reticulum. *Science, 287*(5454), 826-830.

Roth, M. J., Plymire, D. A., Chang, A. N., Kim, J., Maresh, E. M., Larson, S. E., & Patrie, S. M. (2011). Sensitive and reproducible intact mass analysis of complex protein mixtures with superficially porous capillary reversed-phase liquid chromatography mass spectrometry. *Anal Chem, 83*(24), 9586-9592. doi: 10.1021/ac202339x

Saitoh, T., Fujita, N., Hayashi, T., Takahara, K., Satoh, T., Lee, H., . . . Akira, S. (2009). Atg9a controls dsDNA-driven dynamic translocation of STING and the innate immune response. *Proc Natl Acad Sci U S A, 106*(49), 20842-20846. doi: 10.1073/pnas.0911267106

Salcedo, S. P., & Holden, D. W. (2003). SseG, a virulence protein that targets Salmonella to the Golgi network. *EMBO J, 22*(19), 5003-5014. doi: 10.1093/emboj/cdg517

Sauer, J. D., Sotelo-Troha, K., von Moltke, J., Monroe, K. M., Rae, C. S., Brubaker, S. W., . . . Vance, R. E. (2011). The N-ethyl-N-nitrosourea-induced Goldenticket mouse mutant reveals an essential function of Sting in the in vivo interferon response to Listeria monocytogenes and cyclic dinucleotides. *Infect Immun, 79*(2), 688-694. doi: 10.1128/IAI.00999-10

Schmidt, G., Selzer, J., Lerm, M., & Aktories, K. (1998). The Rho-deamidating cytotoxic necrotizing factor 1 from Escherichia coli possesses transglutaminase activity.

Cysteine 866 and histidine 881 are essential for enzyme activity. *Journal of Biological Chemistry, 273*(22), 13669-13674.

Selyunin, A. S., Reddick, L. E., Weigele, B. A., & Alto, N. M. (2014). Selective protection of an ARF1-GTP signaling axis by a bacterial scaffold induces bidirectional trafficking arrest. *Cell Rep, 6*(5), 878-891. doi: 10.1016/j.celrep.2014.01.040

Selyunin, A. S., Sutton, S. E., Weigele, B. A., Reddick, L. E., Orchard, R. C., Bresson, S. M., . . . Alto, N. M. (2011). The assembly of a GTPase-kinase signalling complex by a bacterial catalytic scaffold. *Nature, 469*(7328), 107-111. doi: 10.1038/nature09593

Shao, F., Merritt, P. M., Bao, Z., Innes, R. W., & Dixon, J. E. (2002). A Yersinia effector and a Pseudomonas avirulence protein define a family of cysteine proteases functioning in bacterial pathogenesis. *Cell, 109*(5), 575-588.

Shiba, T., Kawasaki, M., Takatsu, H., Nogi, T., Matsugaki, N., Igarashi, N., . . . Wakatsuki, S. (2003). Molecular mechanism of membrane recruitment of GGA by ARF in lysosomal protein transport. *Nat Struct Biol, 10*(5), 386-393. doi: 10.1038/nsb920

Shima, D. T., Haldar, K., Pepperkok, R., Watson, R., & Warren, G. (1997). Partitioning of the Golgi apparatus during mitosis in living HeLa cells. *Journal of Cell Biology, 137*(6), 1211-1228.

Shorter, J., Watson, R., Giannakou, M. E., Clarke, M., Warren, G., & Barr, F. A. (1999). GRASP55, a second mammalian GRASP protein involved in the stacking of Golgi cisternae in a cell-free system. *EMBO J, 18*(18), 4949-4960. doi: 10.1093/emboj/18.18.4949

Shurety, W., Merino-Trigo, A., Brown, D., Hume, D. A., & Stow, J. L. (2000). Localization and post-Golgi trafficking of tumor necrosis factor-alpha in macrophages. *Journal of Interferon and Cytokine Research, 20*(4), 427-438. doi: Doi 10.1089/107999000312379

Silva, J. C., Gorenstein, M. V., Li, G. Z., Vissers, J. P., & Geromanos, S. J. (2006). Absolute quantification of proteins by LCMSE: a virtue of parallel MS acquisition. *Mol Cell Proteomics, 5*(1), 144-156. doi: 10.1074/mcp.M500230-MCP200

Slagowski, N. L., Kramer, R. W., Morrison, M. F., LaBaer, J., & Lesser, C. F. (2008). A functional genomic yeast screen to identify pathogenic bacterial proteins. *PLoS Pathog, 4*(1), e9.

Smyth, D., McKay, C. M., Gulbransen, B. D., Phan, V. C., Wang, A., & McKay, D. M. (2012). Interferon-gamma signals via an ERK1/2-ARF6 pathway to promote bacterial internalization by gut epithelia. *Cell Microbiol, 14*(8), 1257-1270. doi: 10.1111/j.1462-5822.2012.01796.x

Soding, J., Biegert, A., & Lupas, A. N. (2005). The HHpred interactive server for protein homology detection and structure prediction. *Nucleic Acids Res, 33*(Web Server issue), W244-248. doi: 10.1093/nar/gki408

Stanley, P. (2011). Golgi glycosylation. *Cold Spring Harb Perspect Biol, 3*(4). doi: 10.1101/cshperspect.a005199

Stumpo, D. J., Graff, J. M., Albert, K. A., Greengard, P., & Blackshear, P. J. (1989). Molecular cloning, characterization, and expression of a cDNA encoding the "80- to 87-kDa" myristoylated alanine-rich C kinase substrate: a major cellular substrate for protein kinase C. *Proc Natl Acad Sci U S A, 86*(11), 4012-4016.

Sun, Q., Fan, W., Chen, K., Ding, X., Chen, S., & Zhong, Q. (2008). Identification of Barkor as a mammalian autophagy-specific factor for Beclin 1 and class III phosphatidylinositol 3-kinase. *Proc Natl Acad Sci U S A, 105*(49), 19211-19216. doi: 10.1073/pnas.0810452105

Sze, S. K., Ge, Y., Oh, H., & McLafferty, F. W. (2002). Top-down mass spectrometry of a 29-kDa protein for characterization of any posttranslational modification to within one residue. *Proc Natl Acad Sci U S A, 99*(4), 1774-1779. doi: 10.1073/pnas.251691898

Tan, Y., Arnold, R. J., & Luo, Z. Q. (2011). Legionella pneumophila regulates the small GTPase Rab1 activity by reversible phosphorylcholination. *Proc Natl Acad Sci U S A, 108*(52), 21212-21217. doi: 10.1073/pnas.1114023109

Travier, L., Guadagnini, S., Gouin, E., Dufour, A., Chenal-Francisque, V., Cossart, P., . . . Lecuit, M. (2013). ActA promotes Listeria monocytogenes aggregation, intestinal colonization and carriage. *PLoS Pathog, 9*(1), e1003131. doi: 10.1371/journal.ppat.1003131

Volpicelli-Daley, L. A., Li, Y., Zhang, C. J., & Kahn, R. A. (2005). Isoform-selective effects of the depletion of ADP-ribosylation factors 1-5 on membrane traffic. *Mol Biol Cell, 16*(10), 4495-4508. doi: 10.1091/mbc.E04-12-1042

Von Pawel-Rammingen, U., Telepnev, M. V., Schmidt, G., Aktories, K., Wolf-Watz, H., & Rosqvist, R. (2000). GAP activity of the Yersinia YopE cytotoxin specifically targets the Rho pathway: a mechanism for disruption of actin microfilament structure. *Mol Microbiol, 36*(3), 737-748.

Wajant, H., Pfizenmaier, K., & Scheurich, P. (2003). Tumor necrosis factor signaling. *Cell Death Differ, 10*(1), 45-65. doi: 10.1038/sj.cdd.4401189

Wang, D., Lou, J., Ouyang, C. A., Chen, W. L., Liu, Y. Q., Liu, X. Y., . . . Lu, L. R. (2010). Ras-related protein Rab10 facilitates TLR4 signaling by promoting replenishment of TLR4 onto the plasma membrane. *Proceedings of the National Academy of Sciences of the United States of America, 107*(31), 13806-13811. doi: DOI 10.1073/pnas.1009428107

Way, S. S., Borczuk, A. C., Dominitz, R., & Goldberg, M. B. (1998). An essential role for gamma interferon in innate resistance to Shigella flexneri infection. *Infect Immun, 66*(4), 1342-1348.

Wilson, J. P., Raghavan, A. S., Yang, Y. Y., Charron, G., & Hang, H. C. (2011). Proteomic analysis of fatty-acylated proteins in mammalian cells with chemical reporters reveals S-acylation of histone H3 variants. *Mol Cell Proteomics, 10*(3), M110 001198. doi: 10.1074/mcp.M110.001198

Witte, C. E., Archer, K. A., Rae, C. S., Sauer, J. D., Woodward, J. J., & Portnoy, D. A. (2012). Innate immune pathways triggered by Listeria monocytogenes and their role in the induction of cell-mediated immunity. *Adv Immunol, 113*, 135-156. doi: 10.1016/B978-0-12-394590-7.00002-6

Wu, M., Lu, L., Hong, W., & Song, H. (2004). Structural basis for recruitment of GRIP domain golgin-245 by small GTPase Arl1. *Nat Struct Mol Biol, 11*(1), 86-94. doi: 10.1038/nsmb714

Yewdell, J. W., & Bennink, J. R. (1989). Brefeldin A specifically inhibits presentation of protein antigens to cytotoxic T lymphocytes. *Science, 244*(4908), 1072-1075.

Zhang, Q., Cox, D., Tseng, C. C., Donaldson, J. G., & Greenberg, S. (1998). A requirement for ARF6 in Fcgamma receptor-mediated phagocytosis in macrophages. *J Biol Chem, 273*(32), 19977-19981.

Zychlinsky, A., Thirumalai, K., Arondel, J., Cantey, J. R., Aliprantis, A. O., & Sansonetti, P. J. (1996). In vivo apoptosis in Shigella flexneri infections. *Infect Immun, 64*(12), 5357-5365.